

9  
MIT

22

# EARTH RESOURCES TECHNOLOGY SATELLITE FINAL REPORT

## 5. DATA COLLECTION SYSTEM

PREPARED FOR

GODDARD SPACE FLIGHT CENTER  
NATIONAL AERONAUTICS  
AND SPACE ADMINISTRATION

UNDER CONTRACT NAS5 11260



Reproduced by  
**NATIONAL TECHNICAL  
INFORMATION SERVICE**  
Springfield Va 22151

FACILITY FORM 602	<b>N70-34413</b>	
	(ACCESSION NUMBER)	(THRU)
	265	
	(PAGES)	
	CR-109911	31
	(NASA CR OR TMX OR AD NUMBER)	(CATEGORY)

EARTH RESOURCES TECHNOLOGY SATELLITE

FINAL REPORT

Volume 5. Data Collection System

February 11, 1970

prepared for  
National Aeronautics and Space Administration  
Goddard Space Flight Center

Contract NAS5-11260  
item 3c

TRW Systems Group  
One Space Park Redondo Beach  
Los Angeles County  
California 90278

## PREFACE

The final report for the ERTS Phase B/C study consists of the 12 volumes that are submitted now and additional volumes to be delivered in April covering the results of the study of the Ground Data Handling System for ERTS. The contents of the first volumes of the report are as follows

### Volume

1. (to be completed in April). Summarizes all significant conclusions of the study and indicates where the supporting analyses are presented. The system specification is included as an appendix.
2. (to be completed in April). Contains all system interface studies.
3. Describes the design of ERTS resulting from the study, to a block diagram level of detail.
4. Presents the detailed results of the study supporting the design in Volume 3, including backup tradeoffs and analyses.
5. Presents both the design of the data collection system and the supporting analyses.
- 6-12. Present the plans prepared for the ERTS Phase D program on the Phase B/C program.

## CONTENTS

	Page
1. INTRODUCTION AND SUMMARY	1-1
2. SYSTEM CONCEPT DEVELOPMENT	2-1
2.1 Visibility Time and Coverage	2-1
2.2 Message Structure	2-6
2.3 Error Detection Coding	2-10
2.4 Link Analysis	2-14
2.5 Random Emission Capacity	2-18
2.6 Radio Frequency Interference	2-34
2.7 Platform Deployment	2-38
2.8 Platform Power Sources	2-44
2.9 Applicable Standard Antennas	2-51
2.10 Pulse Repetition Frequency	2-53
3. HARDWARE DESIGN	3-1
3.1 Data Collection Platform	3-1
3.2 Spacecraft Receiver	3-16
3.3 Ground Signal Recovery	3-24
4. MESSAGE COLLISION ANALYSIS	4-1
4.1 Time Domain	4-1
4.2 Random Emission Multiple Access With Replication	4-13
4.3 Dual Random Time and Frequency Mode	4-36
4.4 Computer Simulation	4-43
5. DATA TRANSMISSION TO GSFC	5-1
APPENDIX A - DERIVATION OF $P(K = \text{ODD})$	A-1
APPENDIX B - SECOND-ORDER TERMS OF $P(K = \text{EVEN})$	B-1
APPENDIX C - FORTRAN IV MONTE CARLO PROGRAM	C-1
APPENDIX D - PRELIMINARY SPECIFICATION	D-1





## CONTENTS

	Page
1. INTRODUCTION AND SUMMARY	1~1

## 1. INTRODUCTION AND SUMMARY

The concept for the data collection system defined by TRW Systems, and illustrated in Figure 1-1, provides for a large number of simple, low cost data collection platforms dispersed throughout the United States connected to appropriate sensors. The platforms assemble short digital messages (110 bits) and transmit them approximately every 2 minutes. The polar-orbiting ERTS collects all incident signals from the platforms with a 100 kHz band at approximately 400 MHz and relays these signals, without further processing, to the NASA ground tracking stations via the spacecraft unified S-band downlink. The resulting signals acquired by the Fairbanks, Corpus Christi, and Goddard stations are combined and centrally processed to recover the original sensed information for the end user agencies, such as the Department of Agriculture or the U.S. Geological Survey.

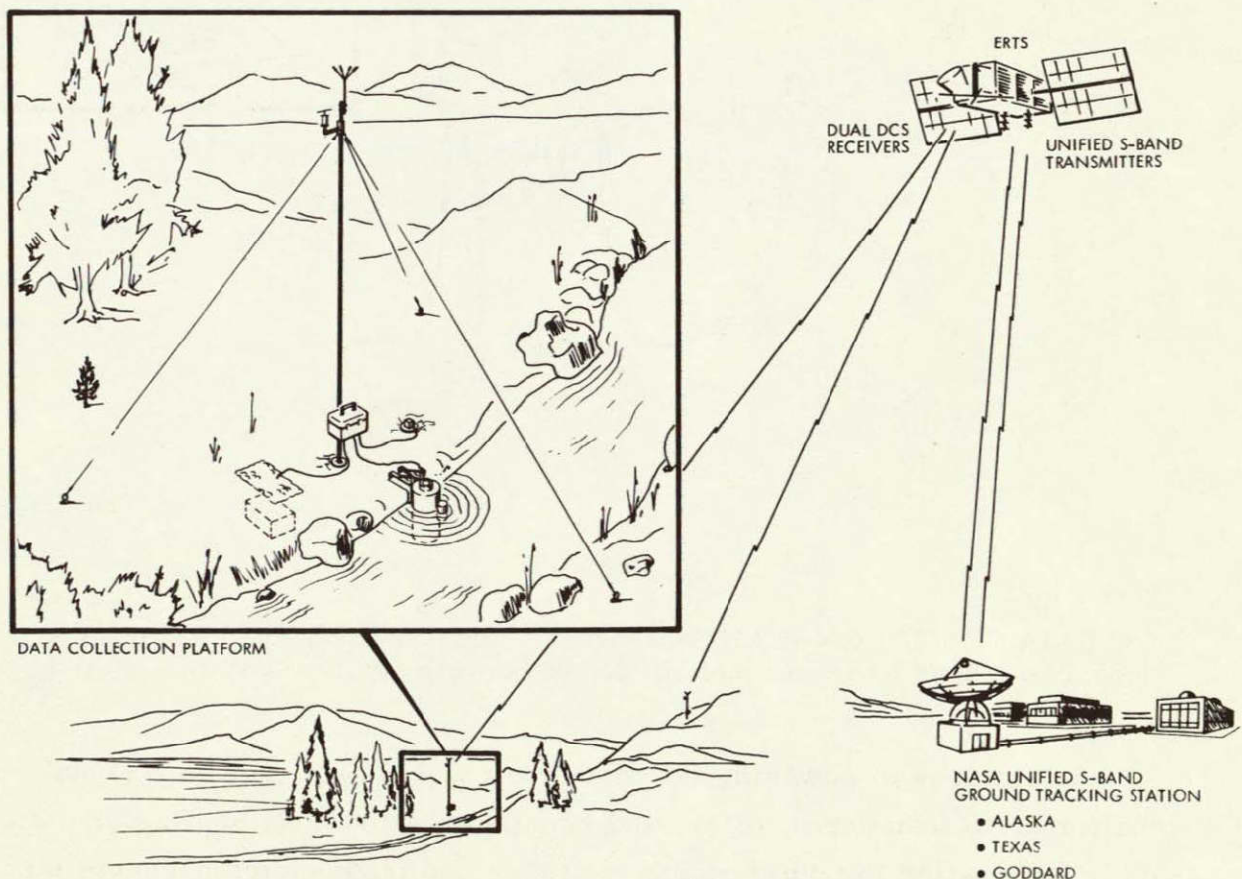


Figure 1-1

DATA FROM AS MANY AS EIGHT SENSORS IS COLLECTED and processed on each platform and transmitted to ERTS. The DCS receiver in ERTS collects this data from all platforms in view and feeds it to the unified S-band link for relay to the ground

TRW proposes a simple, versatile platform design capable of handling eight sensor inputs and operating over the same range of environmental conditions as the sensors with which it is associated. The platform is a small, lightweight, portable unit, self-contained except for the battery and antenna (see Figure 1-2).

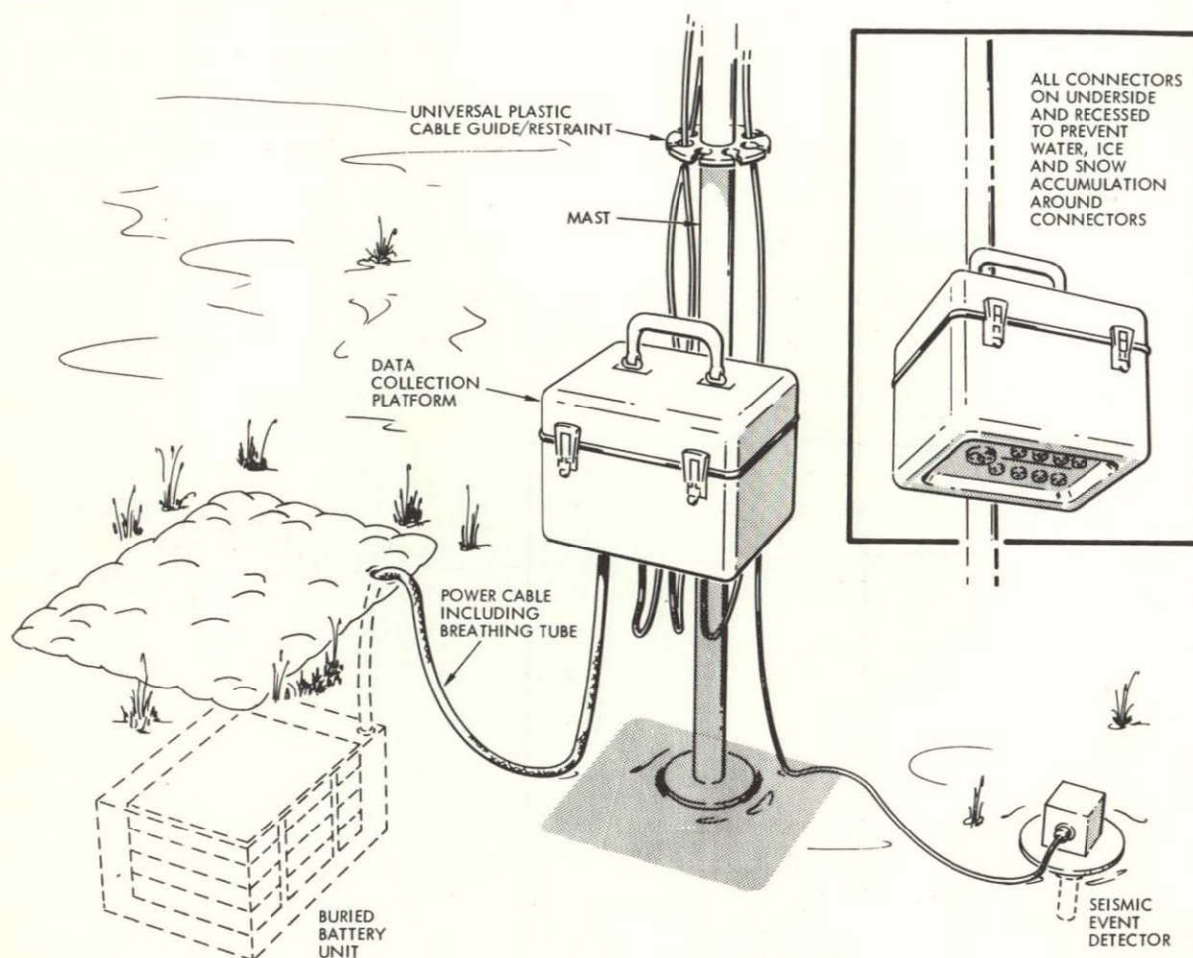


Figure 1-2

THE DATA COLLECTION PLATFORM includes data processing equipment and the transmitter. Batteries for the platform can be buried for thermal control

Two modes of powering the platform are offered: 1) a line signal conditioner to transform, filter, and regulate the 117-volt 60-Hz domestic supply (adaptation for other supply voltages and frequencies presents no problem), or 2) a commercial grade of storage battery housed in a low-cost plastic protective box and buried approximately 6 feet in the ground

adjacent to the platform. The radiating antenna for the platforms is a standard commercial item consisting of a crossed dipole arrangement of vee elements. Where the associated sensors include a mast-mounted anemometer or wind vane, the antenna would be mounted to such a mast (Figure 1-3). For other temporary applications, a low-cost fiberglass pole, available from fishing rod manufacturers, is suggested. A ground spike secures its base, and guy wires provide the requisite stability. For more permanent sites, a conventional protective housing of wood, wood and metal, or brick, depending on application and location is recommended

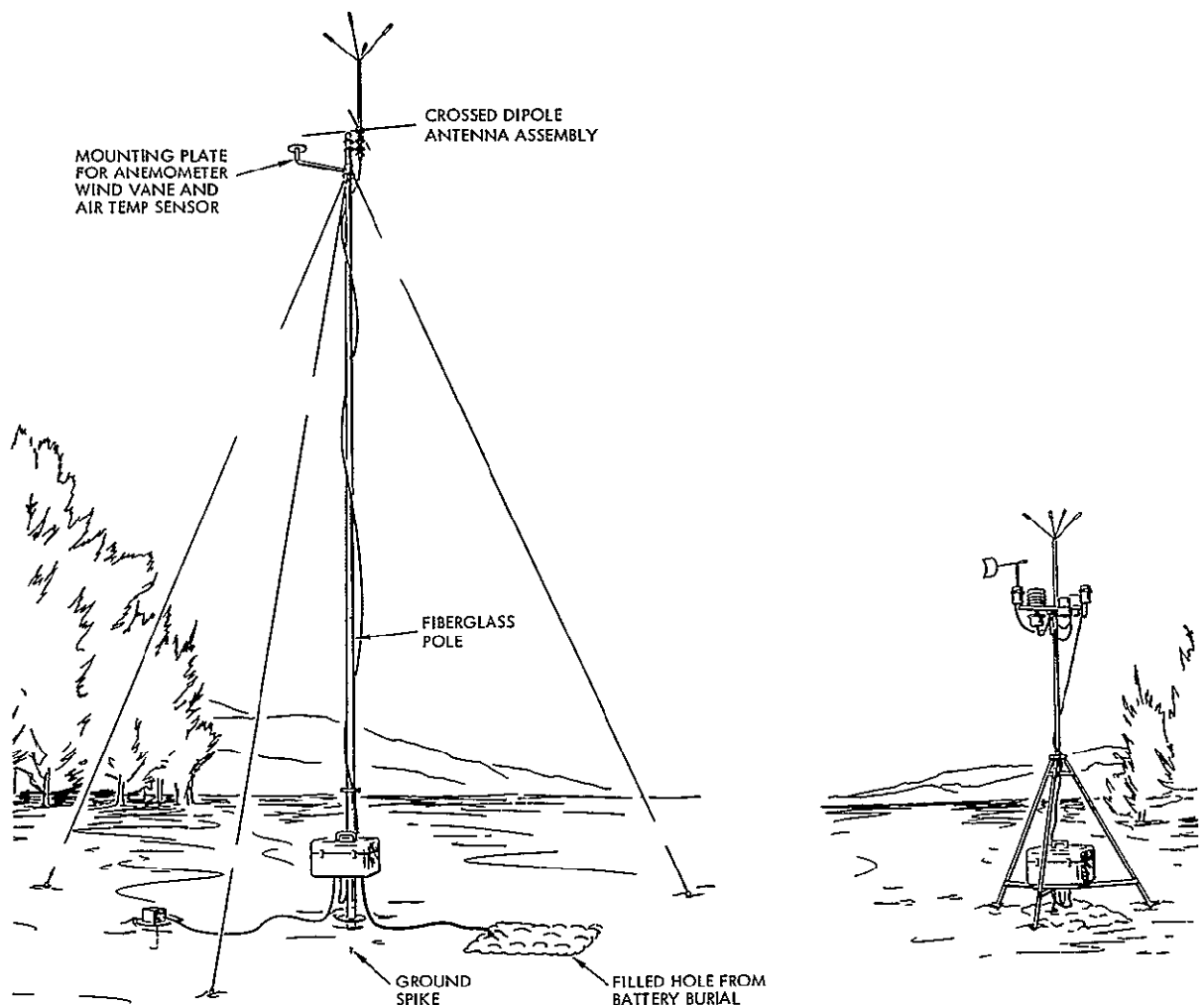


Figure 1-3

COMMERCIAL ANTENNAS MOUNTED ON EXISTING ANEMOMETER POLES can serve the platform or an inexpensive tripod mount can be provided



Before the present study TRW Systems performed detailed systems analyses covering the performance of various data collection systems. The results of this work have been presented to NASA in a series of briefings and in the TRW Phase B/C proposal. Our initial work started with a study of the relative merits of the four basic approaches to a data collection system:

- Interrogation or transponder mode
- Externally-timed platforms using a common clock
- Internally-timed platforms with precision individual clocks
- Random-emission modes

From these studies we concluded that the random mode was the most attractive from the standpoint of minimizing the cost and complexity.

At that time we assumed a system operating mode in which the wideband signals from dispersed platforms would be processed within the satellite and stored on a tape recorder.

Equipped with the basic system parameters, efforts were then turned to analyzing the performance of a random emission system. A random emission system is characterized by finite message collision probabilities; the first task, therefore, involved developing mathematical models from which statistical relationships could be derived. The initial results were not very encouraging, indicating that about 18 platforms could use the same frequency, emitting 256-bit messages in a 12-minute time slot (visibility time), which was far from the desired capacity of 1000, and implied a need for many contiguous channels and an extensive spectrum allocation.

It was determined that the number of users could be increased about 50 percent by message replication, but that after this, the multiple messages resulted in saturation in the time domain, for the particular parameters used, and eventually a reduction in performance. At that time the replication enhanced capacity was estimated as 30 platforms.

In this initial application of the replication concept, however, we were considering the probability of obtaining one good copy of each

message within one of the replicated subsets. Subsequently we determined that this was an unnecessary restriction, since the one good copy of each message could be derived from any combination of messages from all the replicated subsets during the satellite pass. Revision of the equations to reflect this mode of accumulating good message copies resulted in a capacity of more than 80 platforms for a replication factor  $M = 3$ , and over 90 platforms for  $M = 4$ , based on a standard 256-bit message and 12-minute visibility period. The system characteristics are shown in Figure 1-4.

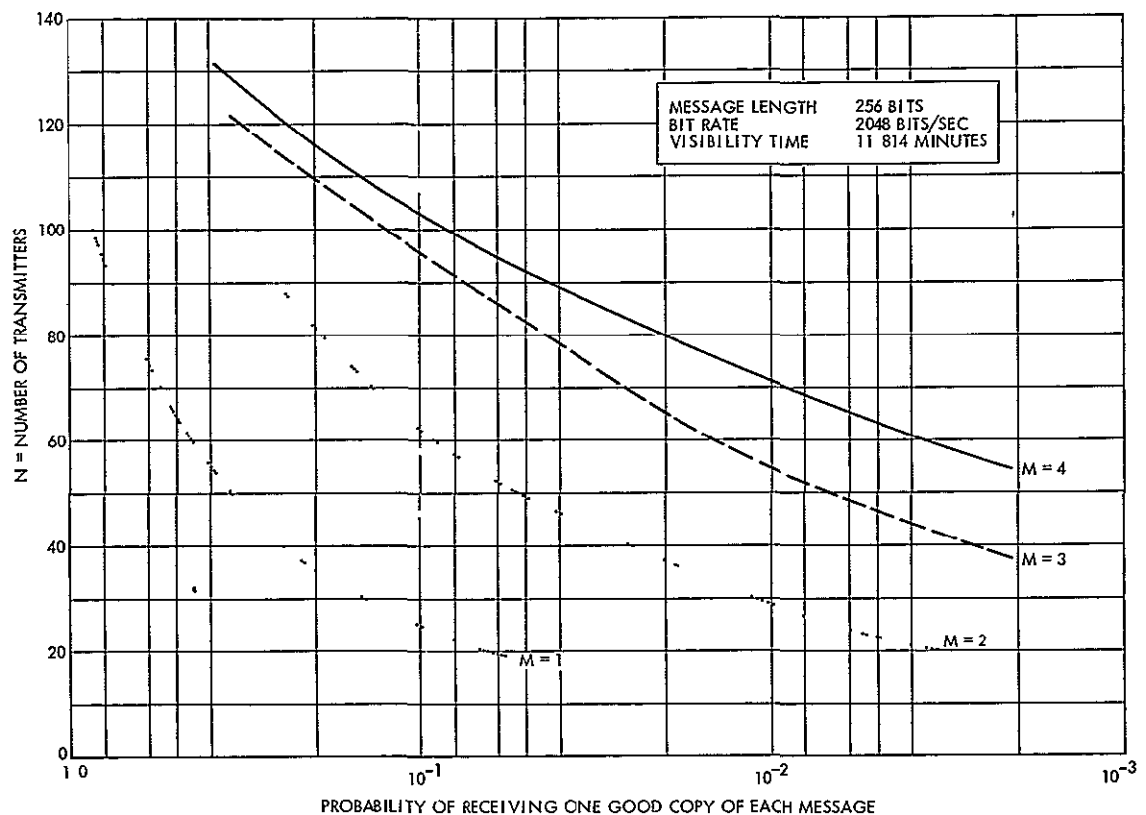


Figure 1-4

#### SYSTEM CAPACITY VERSUS MESSAGE LOSS Random emission in time domain

Up to the time of contract award, TRW had been concerned with a system concept which involved platform regimentation in the frequency domain. Our work showed that a temperature-compensated crystal oscillator could be designed to exhibit a substantial stability improvement over a conventional crystal for a modest cost increase. For such an

arrangement, the total channel bandwidth was determined to be 23 kHz, thus four independent frequency channels, each with a time domain capacity of about 100 platforms could be supported in each 100 kHz of RF allocation a total of 400 ground platforms.

Considerable thought was devoted to the use of "gross timers" to regiment the transmission of geographic subgroups of platforms. This entailed allocating each platform to one of the three useful orbits in a 12-hour period. The scheme effectively reduced the mutual interference by a factor of three and extended the total national capacity for the continental U S to some 1200 units. During the initial phases of this contract, however, it was decided that such a mode was undesirable because it required a complex precision timer, having a long-term stability over many months. Although future large volume production of ground platforms using LSI techniques could employ an ultra-miniature low cost digital logic chip to perform this function, because the timing must be preset for each location, preventing interchangeable platforms, this feature has been abandoned as an inappropriate Phase D concept. Since local geographic features will prevent effective visibility for some orbits, it is necessary to provide for data collection by the spacecraft on at least two of the three useful orbits per 12-hour period. We concluded that the simplest mode of operation is to allow all platforms to transmit continuously at a low duty cycle.

During Phase B/C the study has adapted the system design concept to accommodate two constraints requested by GSFC

- No precision oscillators or frequency regimentation are permissible
- No on-board signal processing in the spacecraft

The configurations of both the platform and spacecraft equipment have been determined, and specific design recommendations are presented including power sources for the platform. Preferred antenna designs are described. A compromise shaped beam is recommended for the spacecraft.



Our Monte Carlo message collision synthesis program has been converted to CDC 6500 compatible Fortran IV and a number of runs made to investigate the system capacity statistics. Data has been obtained on time random, frequency random, and combined random time and frequency modes of system operation. These results are presented in Section 2.5, and Section 4 presents associated theoretical analyses and discussions. The system link analysis is presented in Section 2.4, showing a 7 db overall system performance margin. The 1 db excess over the normal 6 db used for good design practice has been allocated to proximity effects related to the spacecraft antenna.

It is required that the final design for the data collection platforms be capable of proper operation over a wide temperature range. The temperatures encountered in the U.S. pose a major design problem. As discussed in Section 2.7, TRW has determined that relatively shallow burial of the battery can adequately reduce the temperature excursions encountered and allow a conventional battery to be used. The total platform power consumption determines the battery size, weight, and cost. Unless design care is exercised, the PRF timing circuit, which is 'on' continuously, can become the major power user. TRW has investigated this aspect in detail, and offers an approach which provides simplicity of design, high reliability, and entails a drain of only 10 milliwatts. The preliminary system specification is contained in Appendix D.



## CONTENTS

	Page
2 SYSTEM CONCEPT DEVELOPMENT	2-1
2 1 Visibility Time and Coverage	2-1
2 2 Message Structure	2-6
2 2 1 Carrier Preamble	2-7
2.2.2 Bit and Word Synchronization	2-8
2 2.3 Platform Address	2-8
2 2.4 Data Message	2-8
2.2 5 Calibration	2-10
2.2 6 Error Detection Coding	2-10
2 3 Error Detection Coding	2-10
2 3.1 Coding Techniques	2-11
2 3.2 Special Implementation	2-12
2 3.3 Other Approaches	2-14
2 4 Link Analysis	2-14
2 5 Random Emission Capacity	2-18
2 5 1 Frequency Domain	2-19
2.5 2 Time Domain	2-27
2 5 3 Combined Random Time and Frequency	2-29
2 6 Radio Frequency Interference	2-34
2.7 Platform Deployment	2-38
2 8 Platform Power Sources	2-44
2 8 1 Batteries	2-44
2 8 2 Fuel Cells	2-48
2 8.3 Solar Cells	2-48
2 8 4 Thermoelectric Generators	2-50
2 8.5 Wind Generators	2-50
2 9 Applicable Standard Antennas	2-51
2.10 Pulse Repetition Frequency	2-53

## 2 SYSTEM CONCEPT DEVELOPMENT

### 2 1 VISIBILITY TIME AND COVERAGE

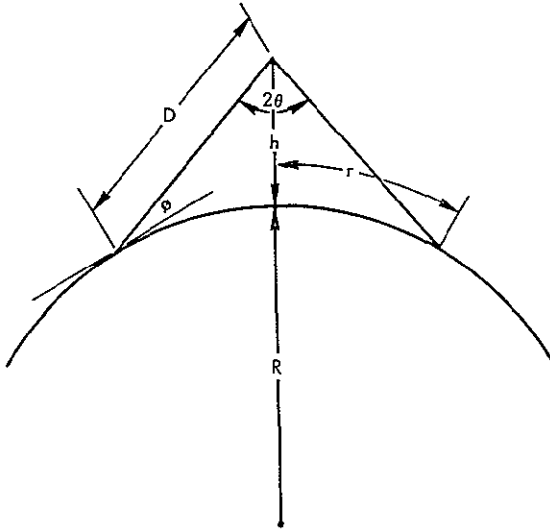


Figure 2-1  
SATELLITE CONE COVERAGE AT  
EARTH SURFACE

The extent of the earth which can be seen from orbit is directly proportional to the satellite altitude and inversely proportional to the permissible elevation angle on earth. Thus, to receive the maximum number of platform transmissions, the satellite must provide an antenna pattern with a cone coverage of  $2\theta$ , as shown in Figure 2-1

As can be seen in Figure 2-1, the maximum communication distance as a function of elevation angle is given by

$$D = \frac{R + h}{\cos \phi} \cos (\theta + \phi)$$

and the maximum radius of visibility for fixed altitude and elevation angle is

$$r = \frac{2\pi}{360} (90 - \theta - \phi) R$$

where  $r$  is the distance from the subsatellite point on earth.

For ERTS,  $h = 496$  nautical miles,  $R = 3444$  nautical miles, and the following values apply

	<u>Elevation Angle (Deg)</u>			
	<u>0</u>	<u>5</u>	<u>7 5</u>	<u>10</u>
Visibility angle, $2\theta$ (deg)	121 9	121.1	120 3	118.9
Maximum communication distance, $D$ (n mi)	1913.8	1637 0	1510 9	1405 0
Radius of visibility, $r$ (n mi)	1746	1470	1342	1238

If the elevation angle of the platform antenna is limited to 10 degrees, the maximum width on earth from which the satellite is visible is only 2476 nautical miles. This means that if the platforms are located within the 214 nautical mile zones disposed about the satellite's ground trace, they will be in view no more than once per each 12 hours. However, if the platforms are in the shaded area of Figure 2-2, they will have the probability of being in view more than once per each 12 hours.

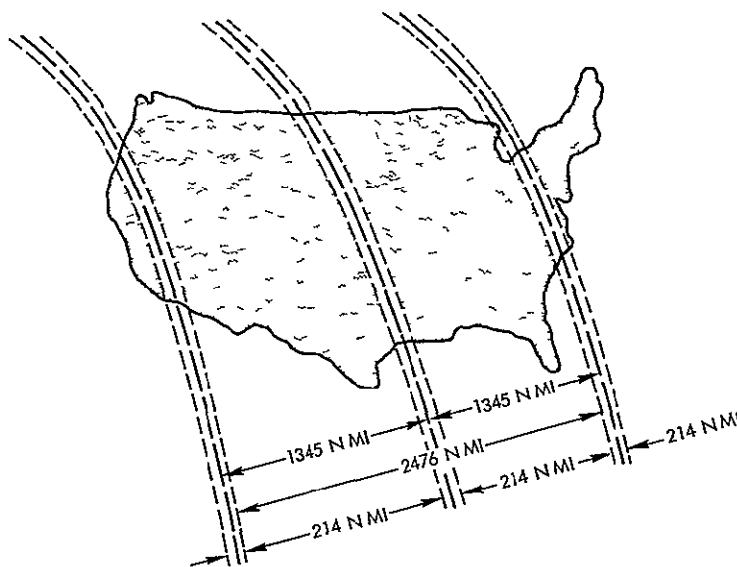


Figure 2-2

#### PLATFORM VISIBILITY FOR 10-DEGREE ELEVATION ANGLE

As a compromise between low elevation angle (5 degrees) which may introduce severe multipath problems and high elevation angle (10 degrees) which does not provide sufficient coverage, a choice of 7.5 degrees as the elevation angle limit appears proper, both for the platform and unified S-band tracking station. This selection entails that the satellite antenna have nominal coverage of 120 degrees and the platform antenna of 165 degrees.

For the relay mode of satellite use we are concerned with the mutual visibility time between any platform and any one of the three NASA unified S-band tracking stations designated for ERTS support, Fairbanks, Alaska, Greenbelt, Maryland, and Corpus Christi, Texas. The coverage areas

for the three unified S-band tracking stations are illustrated in Figure 2-3. The coverage for a representative platform, located centrally in the U.S., is shown in Figure 2-4.

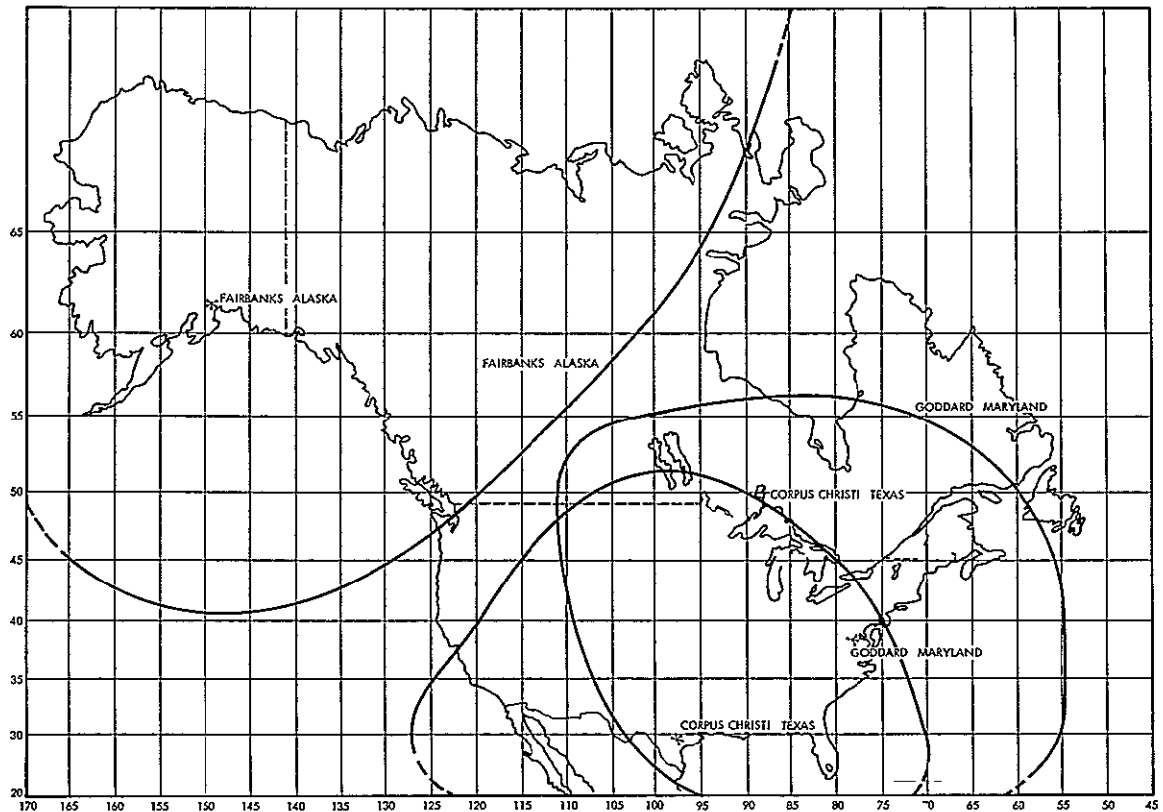


Figure 2-3

#### COVERAGE AREAS OF NASA UNIFIED S-BAND GROUND STATIONS

Since the actual deployment of the data collection platforms is not known, visibility time can be derived only by postulating a distribution model. A uniform distribution, i.e., a chessboard array, is convenient for analysis although in practice sensors will be deployed in clusters to cover areas of concern such as the following

- River basins for water quantity
- Inland and coastal waterways for pollution
- Mountain runoffs for flash flood warning
- Gulf coastal regions for hurricane monitoring
- Alaska for earthquake tremors.

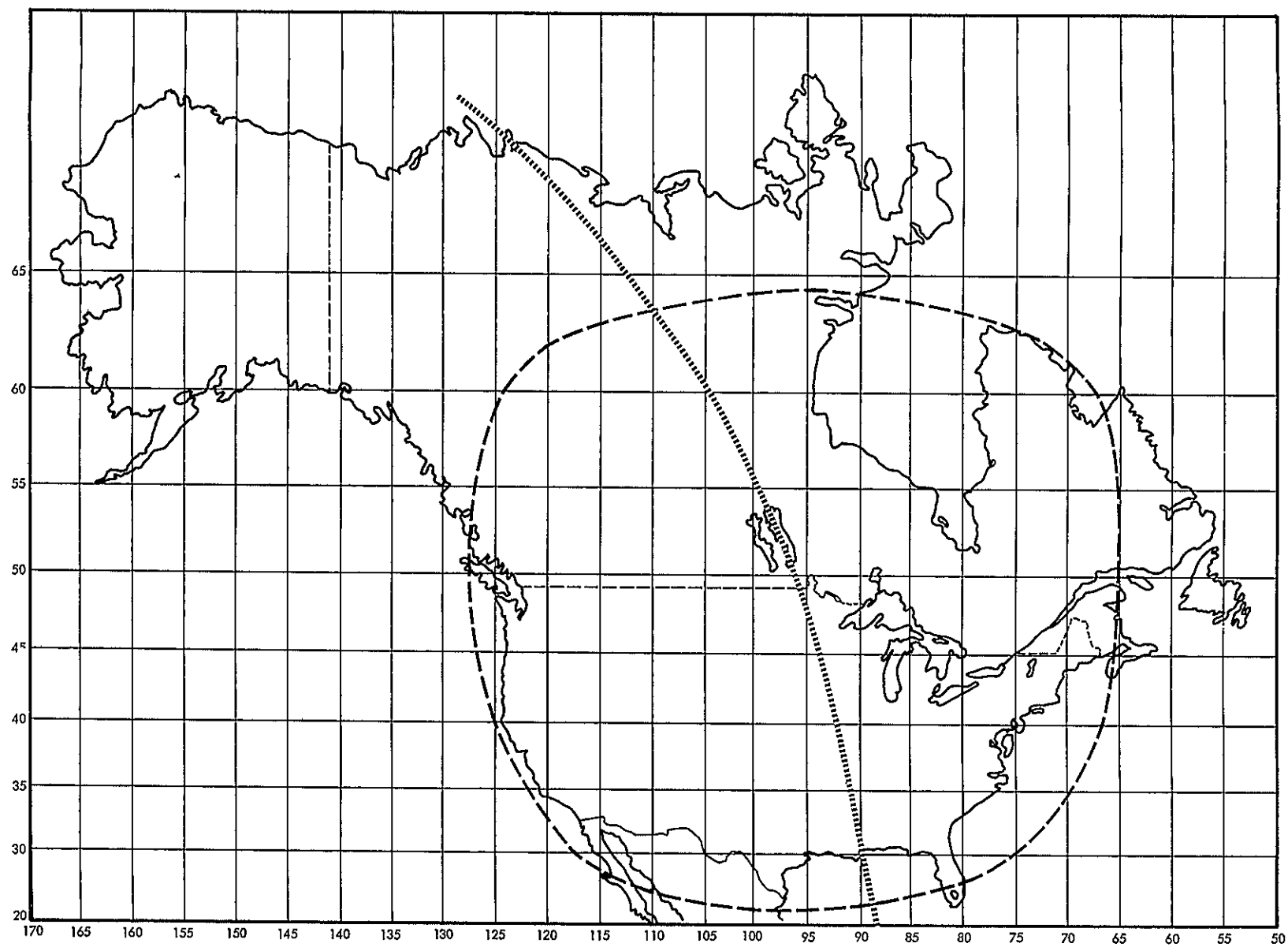


Figure 2-4

COVERAGE FOR A REPRESENTATIVE PLATFORM LOCATED CENTRALLY IN THE U S

The evaluation of those factors needed to arrive at a more realistic geographic distribution is outside the scope of our current work, and we fell back on the arbitrary assumption of a linear distribution of platforms.

TRW has performed an analysis of the mutual visibility period as a function of platform location. Our results, and those reported by Computer Sciences Corporation, who have made an independent study of this topic, indicate that an acceptable visibility is available for most regions of the United States.

The approximate visible times for gross geographic sectors of the United States are shown in Figure 2-5. These figures are the average values for ascending and descending orbital passes, ascending and descending passes in fact provide different visibility characteristics. The coverage data must be considered in the light of the general requirements for monitoring, particularly the relevance of a satellite-based collection network. Poor visibility is indicated for the west coast, but this is not considered serious for the following reasons:

- The temperate climate allows wire-line transmission
- Fast highly reliable warnings for hurricanes are not required
- Supplementary monitoring facilities exist
- A fourth unified S-band receiving site in California seems a reasonable assumption for the near future.

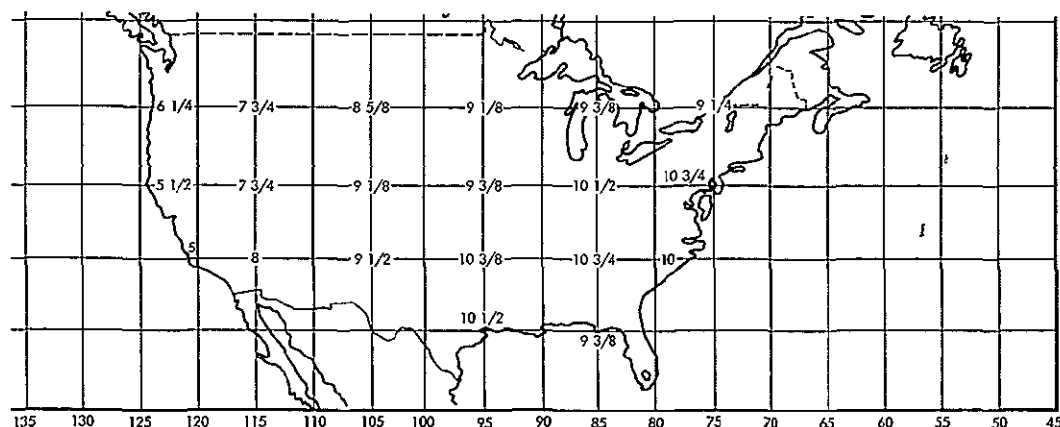


Figure 2-5

APPROXIMATE MUTUAL VISIBILITY TIMES FOR GROSS GEOGRAPHIC SECTIONS OF THE U.S. (Values are in minutes)



On the foregoing basis we believe it reasonable to assume a typical visibility time of 8 minutes. Our further analyses of message performance are based on this value for the time slot

## 2.2 MESSAGE STRUCTURE

The basic parameters which control the message design are listed in Table 2-1.

Table 2-1. Message Design Parameters

Parameters	Value	Comments
Nominal carrier frequency	401.9 MHz	Specified
Data rate	2 kbit/sec	Selected
Modulation	PSK	Selected for optimum SNR performance
Message length	110 bits	Selected
Platform data coherence	None	Fast bit synch and word synch
Probability of nondetection of error	1% or less	BCH error detection coding (see Section 2.3)

At the present state of conceptual development, implementation of the data collection system involves transmitting platform messages consisting of five contiguous sections

- Carrier preamble
- Bit-word synchronization
- Platform address
- The actual data message
- Error correction postamble

The preferred format incorporates a 110-bit message, with 8 bits devoted to error detection. The first 25 bits are used for signal acquisition by the ground data recovery equipment, they constitute a preamble to the regular message and are transmitted as an unbroken sequence of 1's

This portion of the platform transmission and the 3-bit synchronization bits immediately following are not encoded by the error detection logic, but are transmitted as a string of 1's followed by the 010 synchronization transitions (28 bits total). The subsequent message, in its entirety, comprising the platform address and quantized sensor data, (74 bits maximum) is routed to the error detection encoder shift-register. The message structure is presented in Table 2-2

Table 2-2. Revised Message Structure

Function	No of Bits Proposed	Comments
Carrier preamble	25	All 1's hinges on spacecraft antenna
Bit and word synch	3	1010 pattern (first '1' is last bit of preamble)
Platform address	10	Binary code 1023 capacity
Sensor quantization	7 or 8 each	Under review
Error detection	8	Preliminary value

#### 2 2 1 Carrier Preamble

The purpose of the carrier preamble is to allow the phase-lock loop of the ground-based receiver to attain lock. The length of the preamble necessary depends on the required acquisition time for the ground receiver and the number of phase-lock loop detectors we are prepared to implement. Based on conservative link analysis, we have assumed that about 25 bits of the message are devoted to this function.

We are currently investigating alternative demodulation and data recovery approaches without phase-lock loops, and the attendant problems of complexity, acquisition time, and message bit wastage. If the phase-lock loop is indicated as the optimum design approach, the preamble will comprise a string of all 1's to facilitate carrier acquisition

## 2.2.2 Bit and Work Synchronization

The approach proposed makes use of two known data transitions arranged to occur immediately after the carrier preamble. These transitions permit the ground signal processing circuitry to correct the frequency and phase of a local (ground) reference oscillator running at the bit rate. Once the phase and frequency had been set by the bit synchronization transitions they would not be updated for the remainder of the 110 bit message. Our analysis shows no need for periodic recorection during the message period. Use of the two falling-edge zero crossings of the sequence 1010 are proposed. The word synchronization is obtained directly from the bit synch

## 2.2.3 Platform Address

For the initial implementation there will be no more than 1000 platforms. Thus, a 10-bit binary code having a capacity of 1023 will suffice

## 2.2.4 Data Message

For the actual quantized sensor readings maximum flexibility is necessary. To gain some idea of the information capacity per message let us assume that the platforms are set up for 7-bit quantization and that we are employing a 256-bit message length. For these constraints we could provide the following sensor message plan

No. 1 time slot ident = 5 bits	}	Total Bits = 183
channels B through H at 7 bits = 42 bits		
No. 2 time slot ident = 5 bits		
channels D through H at 7 bits = 35 bits		
No. 3 time slot ident = 5 bits	}	
channels B through H at 7 bits = 42 bits		
No. 4 time slot ident = 5 bits		
channels D through H at 7 bits = 35 bits	}	
channel A only at 9 bits = 9 bits		

The above calculation is purely illustrative. The present design concept for the platform provides for individual programming of the analog-to-digital converter and multiplexer functions, this approach maximizes the flexibility. For the Phase D platform design there will be no internal message storage, and the plan is to specify a total of 64 bits for sensor data.

An 8-bit analog-to-digital quantization provides 255 quantization levels. Since decisions are made at the half level threshold, the uncertainty will be  $\pm 1/2$  level or  $\pm 1/510$ , i.e., a resolution of 0.2 percent.

For a relatively simple, low cost platform design, required to operate over a very wide range of environmental conditions, this performance will be difficult to match in the analog processing. Our conclusion is that 7-bit quantization is more appropriate. This decision is keyed to the anticipated sensor accuracy, and the general guideline that the system not degrade the sensor information. On the basis of our present knowledge we believe a resolution of  $\pm 1/254$  or  $\pm 0.4$  percent satisfies that criteria. Such a resolution entails a maximum of 7 bits per sensor and a total of 56 bits.

For sensors requiring more than 8 bits, delta transmission or split messages are proposed. Delta involves transmitting only the change in reading. Split format allows the sensor to be quantized in two parts of up to 8 bits each.

If stored messages are implemented (perhaps as a future optional feature), station date and time can be correlated with the end data word to identify the time of the last data word. It follows that it is only necessary to identify the times at which the earlier data words were quantized that day (i.e., to resolve an uncertainty span of 12 hours). This function can be performed by assigning a 5-bit relative-time word as an appendix to the quantized sensor data of each prior word.

Such an arrangement will provide 30-minute quantization of data timing, which seems adequate at this time. If greater accuracy is needed more bits can be assigned to this function and correspondingly less to the

quantized data words, although we see no requirement for such enhanced time tagging accuracy.

Although it appears desirable that, for a future data collection system, we collect data at different times during the 12-hour periods, there seems no basis now for choosing different times for each sensor. Considerable economy in the number of bits assigned to time words can be effected by defining a versatile interrogation timer and prefacing all the sensors read during that interval by a single time code word (a headed listing concept). Assuming we might wish to take as many as four readings during a 12-hour period we would require only four time words, one to preface each group of sensor readings. By contrast, the use of personal time codes associated with each data value, for eight sensors and four times, entails 32 time words.

## 2 2.5 Calibration

Incorporating the capability for calibration of the sensors has been rejected as not cost effective for the Phase D units

## 2.2 6 Error Detection Coding

The NASA system specifications call for a data collection system in which the probability of a message error being undetected is less than 1 percent. Using the random emission mode the actual probability of message collision will substantially exceed 5 percent, consequently error detection coding is proposed. The basic coding approach consists of adding a BCH code checking postamble to the data message. This method requires only eight additional bits to exceed the specified system performance requirement. This maximizes the fractional number of message bits available for quantized data transmission, and minimizes the message length and time domain interference. See Section 2 3.

## 2 3 ERROR DETECTION CODING

The most likely source of errors, for the proposed mode of operation, is that associated with message collisions in the time or frequency domain. A message collision implies that one message overlaps another. Such an overlap causes a burst of interference in the head or

tail of the messages affected, and it is this disturbance we wish to detect via an encoding and decoding procedure. The design goal is that the probability of failure to recognize the occurrence of errors in the decoded message is less than 1 percent.

### 2.3.1 Coding Techniques

Encoding consists of adding a fixed number,  $P$ , of parity bits to the  $M$  bit length message. These are generated via a  $P$  stage shift register to form code words of a  $(M + P, M)$  cyclic or shortened cyclic code of the BCH type.\* If all bursts are equally probable, the probability of undetected burst errors is reduced to  $2^{-P}$ , conditioned on a burst occurring. In general, the probability of an undetected burst error is the product of the probability of a burst occurring multiplied by the probability that such an error is undetected.

Burst error detection coding will detect all single bursts of length  $r < P$ . Random error detection performance is a function of the Hamming distance  $d$  of the code and will detect up to  $(d - 1)$  errors in an algebraic decoding procedure.

Theorem If the  $P$  parity checks form a cyclic or shortened cyclic code of length  $M + P$  and dimension  $M$ , then for equiprobable bursts, the probability of burst of any length  $r$  getting undetected is  $2^{-P}$  in any cyclic or shortened cyclic  $(M + P, M)$  code.

Proof Let the length of the burst be  $r$ . Note if  $r < P$ , then any detection will work and the probability of an undetected burst is zero. A burst of length  $r < P$  looks like

000 1, x, x, . . . , x, 1 000

with  $x$  any value. There are  $2^{r-2}$  possible bursts, all of which are equiprobable in the case treated. Of these there are only  $2^{r-2-P}$  which are

---

\*W. W. Peterson, Error Correcting Codes, New York, Wiley and Sons, 1965.

possible code words. Thus for a burst to be undetected, it must be a code word and thus the probability of no detection for any burst of length  $r$  is simply the ratio of bursts that are codewords to all possible bursts, giving the value  $2^{-P}$ .

To achieve a probability of undetected single burst error of  $2^{-P}$  for the case of equiprobable bursts, we adjoin  $P$  parity checks to the  $M$  message bits to be protected to form a  $(M + P, M)$  cyclic or shortened cyclic code. To achieve the design goal of  $2^{-P} \leq 10^{-2}$ , we would select a design with  $P = 8$ .

Encoding for the  $(M + P, M)$  cyclic code generated by  $g(x)$ , a polynomial of degree  $P$  can be accomplished by using a  $P$  stage division shift register. However, to have a systematic code (a code vector consists of the  $M$  unaltered information bits followed by  $P$  check bits), we employ the following procedure. Let  $f(x)$  be a polynomial in which the  $M$  coefficient of terms involving  $x^{M+P-1}, x^{M+P-2}, \dots, x^P$  are arbitrary information symbols and the coefficient of terms of degree less than  $P$  is 0. Then by the division algorithm

$$f(x) = g(x) q(x) + r(x)$$

where  $r(x)$  is the remainder with degree less than  $P$ . The  $[f(x) - r(x)]$  forms a code vector whose higher order terms are the information symbols unaltered and the lower terms are the check symbols unaltered.

### 2.3.2 Special Implementation

From the above discussion, we need to calculate the remainder after dividing a polynomial  $f(x)$  by  $g(x)$ . This can be done by a simple binary division circuit. The  $f(x)$  that has information symbols as its  $M$  high order coefficients and 0's as its  $P$  low order coefficient is shifted into the circuit. This requires a total of  $M + P$  shifts,  $M$  for information symbols and  $P$  for the low order 0's. The remainder  $r(x)$ , which is the additive inverse of the check symbols, is held in the shift register. These check symbols can then replace the low order symbols of  $f(x)$  to form a code vector, appended to the information portion of the message.

For  $M = 74$  bits, we may put  $P = 8$  to obtain the  $(82, 82-8)$  shortened version of the  $(127, 127-8)$  BCH code. The code generator  $g(x)$ , a polynomial of degree 8 can be formed from Peterson's table, as

$$g(x) = x^8 + x^4 + x^3 + x^2 + 1$$

A circuit for dividing  $g(x)$  and calculating  $r(x)$  is shown in Figure 2-6. This approach results effectively in multiplying the symbols automatically by  $x^8$  as they are added into the shift register. The coding proceeds as follows

- The binary information symbols are shifted into the feedback division register as shown in Figure 2-6. At the same time, the  $M$  information symbols are fed into the communication channel through S-1.
- After the  $M$  information symbols have entered the register, the contents of the register become the remainder, that is, the negative of the  $P$  check symbols.
- As soon as the  $M$  symbols have entered the register, the feedback circuit is disabled by gating.
- The content of the shift register is then shifted out by clock pulses, and the negative of the symbols sent into the communication channel through S-1. The  $P$  check symbols together with the  $M$  information symbols make a complete code vector.

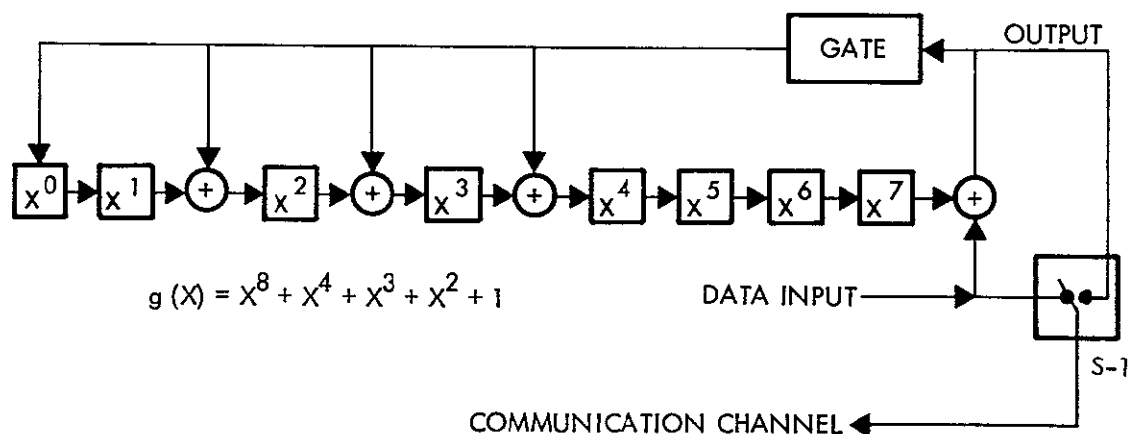


Figure 2-6  
FEEDBACK SHIFT REGISTER FOR  $(82, 74)$  ERROR DETECTION ENCODING



The received code vector can be checked for parity failure by simply entering the entire vector or input to the circuit of Figure 2-6 with all storage elements initially set at zero. The contents after the vector has been entered will be the remainder after division by  $g(x)$  and therefore zero if and only if the vector was a code vector

### 2.3.3 Other Approaches

Convolutional coding has been rejected as a candidate. It doubles the number of bits to be transmitted, which doubles either the message length or data rate, and increases the chances of message collision. Increased ground processing complexity is entailed. The primary advantage of this coding mode is its message security, and for earth resources applications this has no immediately apparent advantage

If the coding mode were able to prevent the retransmission of unwanted (free-loading and RFI) signals through the spacecraft, there would be some real merit to it, but this is not the case. To the best of our knowledge there are no cases of commercial or civil systems using convolutional encoded signal, which would justify NASA adopting it for a simple low cost data link, since the simpler 8-bit BCH block code will comfortably achieve the desired performance at low cost.

## 2.4 LINK ANALYSIS

The UHF transmitter in the platform will feed a nearly omnidirectional antenna and transmit a narrowband PSK signal. PSK modulation is selected since it provides the lowest bit error rate for the order of SNR involved and its energy distribution optimizes the random emission performance in the frequency domain.

The satellite receiver will perform double conversion of the uplink signals and relay them to the ground data collection stations at Alaska, Goddard or Corpus Christi via the unified S-band transmitter on the spacecraft and corresponding unified S-band receiving equipment at the ground stations. The uplink carrier is centered at a nominal 401.9 MHz and is directly biphase modulated by the semi-random binary signals comprising the platform message. At the unified S-band ground stations,

differential phase-coherent techniques will be employed for covering the individual signals in real time, and recording them for later data reduction

Link parameters are as follows

- Platform transmitter power is 5 watts RF, as specified by NASA, i.e., +37 dbm.
- Platform transmitter antenna gain, an elliptically polarized beam with some 165 degree sky coverage, providing 0 db above an isotropic radiator
- Spacecraft receiving antenna is a crossed dipole over a ground plane to provide an elliptically polarized earth coverage with half power beamwidth of 120 degrees, having an on-axis gain of -1 db with respect to isotropic radiator and off-axis gain of +2.5 db ( $\pm 60$  degrees).
- Platform transmission circuit loss, - combining the transmission line loss, VSWR loss and radiation efficiency, estimated to be 1 db
- Free space transmission loss, for a 496 nautical mile orbit and communication range from 496 to 1511 nautical miles for the proposed 7.5 degree limit elevation angle, at 401.9 MHz, 143.79 and 153.5 db, respectively.
- Polarization loss is obtained by considering the axial ratio performance for both the transmitting and receiving antennas. The assumed value of axial ratio for the spacecraft receiving antenna is 2 db on-axis and 6 db at  $\pm 60$  degrees off-axis and for the platform antenna 0 and 5 db, respectively. The combination of these two implies a loss of 0.8 db on-axis and 1.7 db off-axis.
- Spacecraft receiving circuit loss, the feedline and coupling losses, estimated to be about 1 db
- Receiving system noise power spectral density is based on the noise power per unit bandwidth,  $KT_{(syst)}$ , where  $K$  = Boltzmann's constant and  $T_{(syst)}$  is the effective system noise temperature in  $^{\circ}K$ . The effective noise temperature is obtained from

$$T_{(syst)} = (F - 1) T_o + \frac{T_s}{L_R} + T_o \left( 1 - \frac{1}{L_R} \right)$$

where

$T_o$  = thermal equilibrium noise temperature,  $290^{\circ}\text{K}$   
with cold sky

$F$  = receiver noise figure, 2 db

$T_s$  = source noise temperature,  $660^{\circ}\text{K}^*$

$L_R$  = receiver feedline loss ratio, 1.26

The nominal  $T_{(\text{syst})}$  is  $753.3^{\circ}\text{K}$  and noise power spectral density is  $169.8 \text{ dbm/Hz}$ .

- Detection noise bandwidth, the bandwidth required to recover the data, is 1.2 times data rate, i.e., 2.4 kHz. The excess bandwidth, 20 percent over the theoretical minimum of 50 percent of the bit rate, is used to reduce the intersymbol interference. It represents initial optimization of the carrier SNR, the intersymbol interference and the frequency domain spectral width.
- Detection SNR threshold is defined by the permissible bit error probability. The NASA specifications call for a 95 percent probability of receiving one good message from each platform. We desire to fully utilize this allowance in maximizing time domain density. TRW has therefore assumed that only 10 percent of this allowance is applied to the effect of noise on the bit error rate. On that basis, for a message length of 110 bits, the bit error probability must be less than or equal to  $5 \times 10^{-5}$ . Using differentially PSK demodulation technique, this entails a threshold SNR +9.6 db.
- Demodulation and filter degradation, due to filter performance and imperfection of the demodulator hardware, assessed to contribute 1.5 db.
- Downlink performance degradation, for which the additive noise  $N_2$  of the S-band downlink must be combined with that of the uplink noise  $N_1$  to give the final SNR as below:

$$\text{SNR} = \frac{aS}{aN_1 + N_2}$$

---

\*A. J. Mallinckrodt, "The UHF Noise Temperature of the Earth as Seen from Space," Communication Research Laboratories, Santa Ana, Calif., Contract NAS5-1009

where  $a$  is a downlink factor. For the proposed design, the downlink power budget will provide a SNR of  $(S + N_1)/N_2 \approx 16$  db in the 600 kHz predetection bandwidth. This corresponds to a less than 0.5 db degradation of uplink performance, and is based on the worst case combination of unified S-band and system noise temperature.

On the basis of the parameter values enumerated, the power budget for the data collection system is presented in Table 2-3. The overall system performance is shown in Figure 2-7 in the form of system error SNR versus selected data rate. It assumes the detector filter bandwidth value is correspondingly adjusted to suite the data rate.

Table 2-3 Communication Power Budget

	<u>Platform on Subtrack</u>	<u>Platform off Subtrack</u>
Platform transmitter power, dbm	+37	+37
Platform transmission circuit loss, db	-1	-1
Platform antenna gain, db	0	0
Space loss, db	-143.7	-153.3
Polarization loss, db	-0.5	-1.6
Spacecraft antenna gain, db	-1	+2.5
Spacecraft receiving circuit loss, db	<u>-1</u>	<u>-1</u>
Total Received Power, dbm	-110.2	-117.4
Spacecraft receiver noise spectral density, dbm, $T_{\text{system}} = 753.3$ deg	-169.8	-169.8
Detection noise bandwidth (2.4 kHz), db	+33.8	+33.8
Threshold SNR (including 1.5 db degradation), db, $P_e = 5 \times 10^{-5}$	+11.1	+11.1
Downlink performance degradation, db	-0.5	-0.5
Threshold signal power, db	<u>-124.4</u>	<u>-124.4</u>
Performance margin, db	+14.2	+7.0

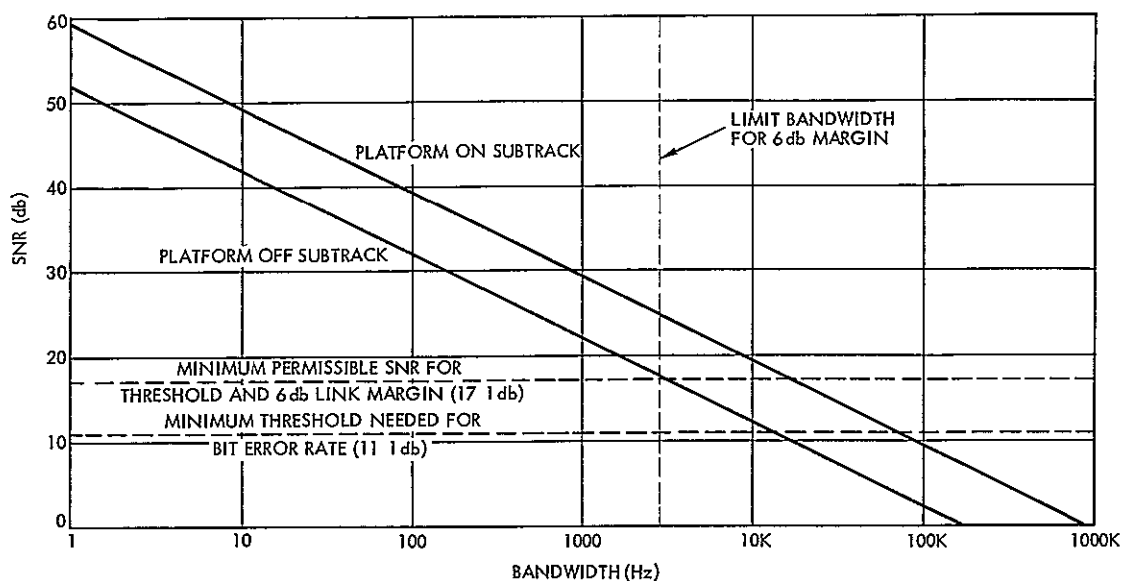


Figure 2-7

## LINK SIGNAL-TO-NOISE RATIO VERSUS DATA BANDWIDTH

The link analysis indicates that the proposed system configuration will provide reliable operation out to the maximum slant range with an excess of 1 db available over the normal 6 db system design margin. This 1 db excess has been assigned to the proximity loss associated with mounting the data collection system crossed dipole antenna on the spacecraft rather than in free space.

The link calculation confirms that 2 kHz is the correct order of data rate. In the analysis a detection filter bandwidth of 2.4 kHz is postulated. Energy loss considerations alone would allow a width of under half the bit rate, but excessive narrowness mutilates the data stream wave shapes causing intersymbol interference. A value of about 60 percent of the data rate (1,200 Hz) is about the optimum. The corresponding noise bandwidth is twice this (2.4 kHz).

## 2.5 RANDOM EMISSION CAPACITY

The random emission capacity for the data collection system results from the combination of the collision statistics in both the time and frequency domains.

## 2 5 1 Frequency Domain

The message collision analyses performed thus far have dealt with applying the random emission concept to the time domain only, and have assumed that the platforms are regimented into a series of discrete frequency channels. We shall now consider the application of the random mode to the frequency domain rather than the time

The first step involves defining a model for the system performance from which statistical equations can be developed to describe that performance in terms of the basic variables

The model for frequency domain performance is shown in Figure 2-8, where the rectangle "A" represents the acceptance bandwidth of the ground data recovery equipment (not the unified S-band receiver). The dimension "F" represents the total permissible system bandwidth allocated to the data collection system, 100 kHz

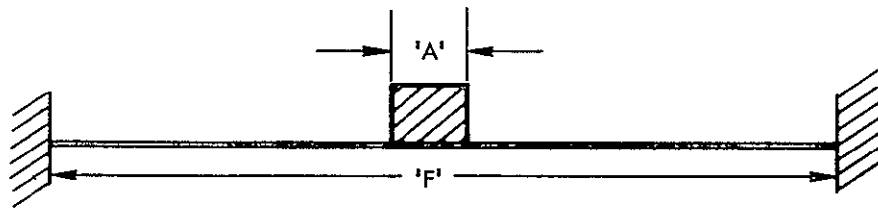


Figure 2-8  
FREQUENCY DOMAIN MODEL

We define the characteristics of this model such that if a signal falls within the rectangle "A", an unacceptable level of damage results to the message already occupying the bandwidth "A". By contrast, all signals falling outside the region "A" produce no significant damage to the signal within bandwidth "A". All platform signals fall within the total assignment "F". The manner in which interference occurs, and the numerical value obtained for the equivalent rectangular bandwidth "A" depend on the form of signal detection and data recovery used. First we consider the case of a narrowband phase-lock loop and filter arrangement (Figure 2-9)

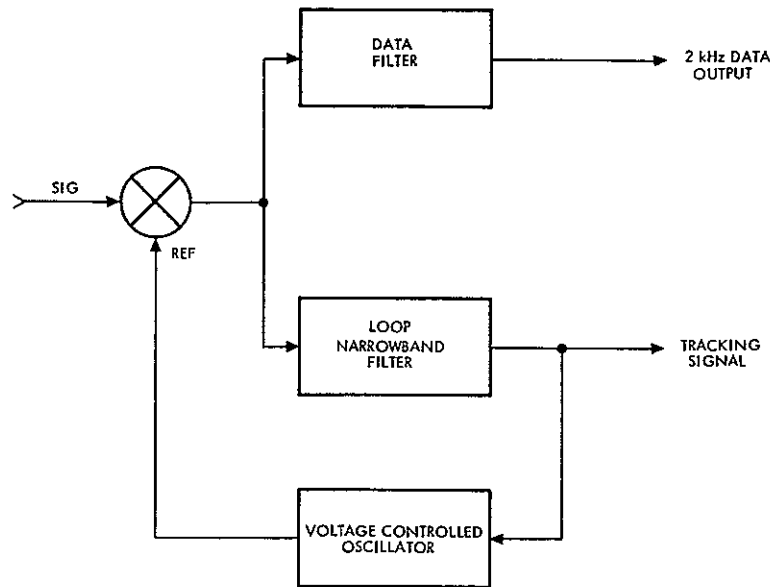


Figure 2-9  
PHASE-LOCK LOOP CONFIGURATION

The maximum doppler-induced rate of change for the platform carrier frequency is approximately 70 Hz/sec. If  $f_d$  is the carrier frequency

$$f_d = V_r f_t, \quad V_r = V \cos \phi$$

Then

$$f_d = -\frac{f_r}{C} V \sin \phi \frac{d\phi}{dt}$$

$$f_d \Big|_{\max} = \frac{f_t V}{C} \left[ \frac{V}{D} - \frac{V}{D+R} \right] = \frac{f_t}{C} V^2 \left[ \frac{1}{D} - \frac{1}{D+R} \right]$$

Substituting  $V = 24247 \text{ ft/sec} = 39906 \text{ n m/sec}$ ,  $f_t = 401.9 \times 10^6 \text{ Hz}$ ,  
 $D = 496 \text{ n m}$ , and  $R = 3444 \text{ n m}$ ,

$$\begin{aligned} f_d \Big|_{\max} &= \frac{401.9 \times 10^6}{3 \times 10^8 \times 3281} 24247^2 \left[ \frac{1}{496} - \frac{1}{3940} \right] \frac{1}{6076} \\ &= \frac{401.9 \times 24247^2}{300 \times 3281} \frac{0.00175}{6076} = 69.65 \approx 70 \text{ Hz/sec} \end{aligned}$$

The minimum loop noise bandwidth ( $W_n$ ) is related to the sweep rate by

$$f = K_o(W_n)^2$$

for  $K = 0.2$ ,  $0.2(W_n)^2 = 70$ , whence  $W_n \approx 20$  Hz

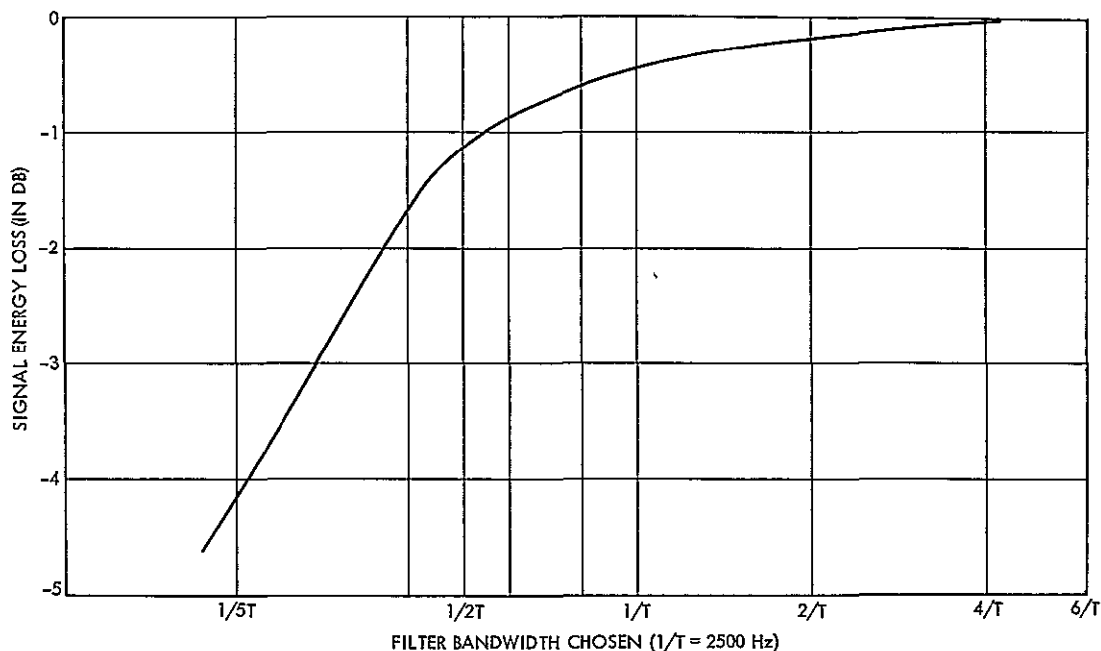


Figure 2-10

SIGNAL LOSS VERSUS FILTER BANDWIDTH (2048 bits/sec data)

The signal loss as a function of the data filter bandwidth is illustrated in Figure 2-10. For 2 kHz data the low pass data filter can have a bandwidth of 1 kHz, from the standpoint of signal loss since for this width there is only about a -1 db penalty. Intersymbol interference increases sharply as a result of the waveform distortion from excessive band limiting. This topic has been very thoroughly treated in the literature,\* and there is general agreement that band limiting of PCM beyond 0.6 of the bit rate causes an unacceptable increase in intersymbol interference with only a

\*See, for example, J. H. Park, "Effects of Band Limiting on the Detection of Binary Signals," IEEE Trans AES, September 1969, p. 867.



minor improvement in SNR. As with previous similar systems, TRW has adopted a nominal 0.6 factor, implying a low pass data filter cutoff at 1.2 kHz.

A second-order, critically-damped, high-gain active design is assumed for the 20 Hz carrier tracking filter. A linear phase filter is assumed for the data, since this will provide optimum transient performance for the digital information stream.

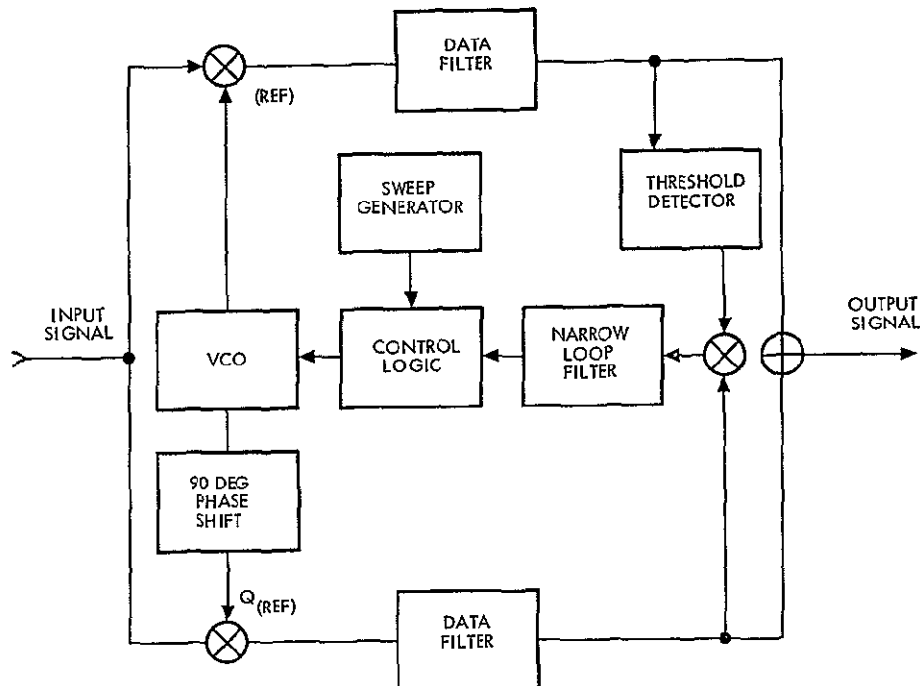


Figure 2-11  
I-Q PHASE-LOCK LOOP DEMODULATOR

The calculated uplink power budget indicates a carrier-to-noise power ratio of approximately 52 db, allowing a 20 kHz sweep bandwidth and a +6 db loop SNR during acquisition. After acquisition, while tracking the carrier, the worst case loop SNR will be 52 db (C/N), less 13 db for 20 Hz bandwidth, i.e., an effective SNR of +39 db. An I-Q loop type of phase-lock loop demodulator is recommended because this avoids the compromise involved in arranging for a residual carrier component (less than  $\pm\pi$  radians PSK modulation) to allow carrier tracking. The configuration is shown in Figure 2-11. Since signals from either side of the reference carrier can enter the data filter and loop carrier tracking loop filter,

from an interference standpoint the input acceptance bandwidths are 2.4 kHz and 40 Hz, respectively.

For the proposed mode of operation the preamble consists of carrier only (a string of ones) for about 12.5 milliseconds, followed by a biphase modulated data stream. When the carrier is modulated by the data stream a symmetrical side band structure is developed with the amplitude of the components decreasing outward from the carrier. If the modulating data takes the form of a continuous bit stream, with a constant bit pattern (e.g., 101010 ----, or 10011001100), then the spectral power distribution can be derived from superimposing the Fourier series components corresponding to two on-off keyed carriers with carrier phases differing by  $\pi$  radians, which results in the familiar  $\sin x/x$  amplitude and  $(\sin x/x)^2$  energy distribution.

In practice the transmitter will be modulated by a binary code representing the quantified sensor data, which is pseudorandom in character. The power spectral density for this condition has been analyzed by Matson\*, who derived the following expression

$$G_3(f) = G_3(f)_1 + G_3(f)_2 = \frac{V^2}{2} \left\{ \frac{\sin^2 \Delta\phi}{H} \left[ \frac{\sin^2 \left( \frac{\omega - \omega_0}{2H} \right)}{2 \left( \frac{\omega - \omega_0}{2H} \right)} + \frac{\sin^2 \left( \frac{\omega - \omega_0}{2H} \right)}{2 \left( \frac{\omega - \omega_0}{2H} \right)} \right] \right. \\ \left. + \cos^2 \Delta\phi \left[ \frac{\delta(f - f_0)}{2} + \frac{\delta(f + f_0)}{2} \right] \right\}$$

A plot of the power density based on the above equation is presented in Figure 2-12. Fortunately it has approximately the same form as that for the much simpler expression  $(\sin x/x)^2$ .

---

\* D. Matson, "Tracking, Telemetry, and Command Studies of Ground and Satellite Subsystems," Aerospace Corporation, May 1964.

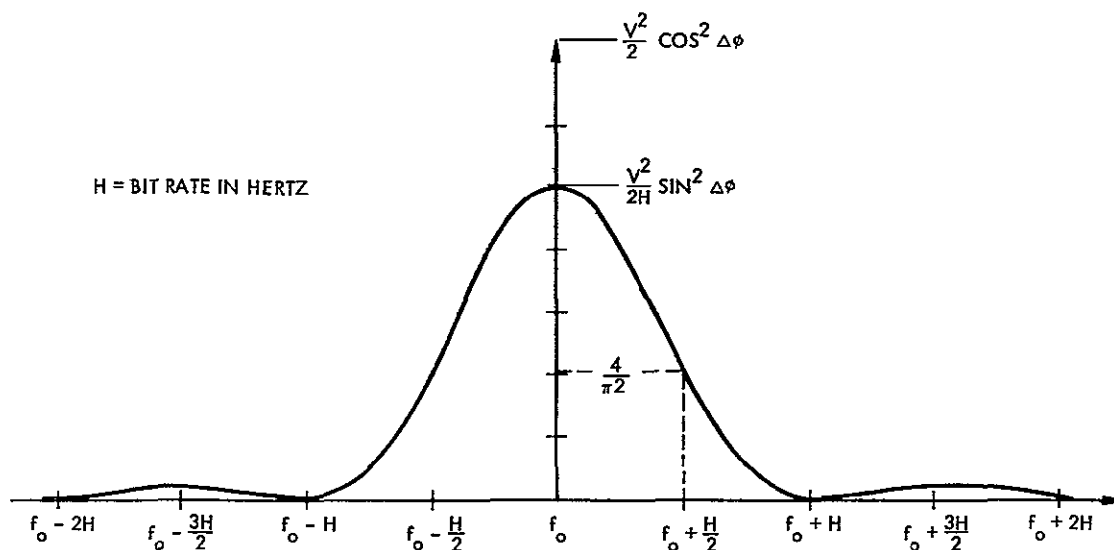


Figure 2-12

# POWER SPECTRAL DENSITY OF A CARRIER BIPHASE MODULATED BY A RANDOM BINARY WAVEFORM

Consider the situation when the phase-lock loop has acquired carrier lock, is tracking the carrier, and demodulated data is exiting the data filter. If the carrier of an interfering signal occurs at an adjacent frequency, those components of its spectral output that fall within the loop or data filter passbands will cause interference. For the theoretical case of rectangular filters the magnitude of the interfering signals in each filter can be determined by simply integrating the spectral power of the interfering carriers frequency components between the frequency limits of the two filters involved.

Two quite different situations are possible. The interfering signal can be an unmodulated carrier, corresponding to the preamble period of a message emission, or it can be the biphase modulated data portion. For the purpose of quantifying the disruptive effect of either condition we assume that the undesired signal can be treated as a noise component insofar as the loop performance is concerned.

When a previously locked loop is subjected to a steadily worsening signal-to-noise ratio, the data SNR deteriorates and the loop partially loses lock (cycle skipping) until it falls below its threshold and drops out.

of lock semi-permanently Laboratory tests indicate that semi-permanent dropout corresponds to a zero SNR in the phase-lock loop The message error rate is a function of the basic bit error rate and can be derived therefrom

The NASA specification requires that the system exhibit a 95 percent probability of receiving one good message from each platform, each 12-hour period Message errors may be caused by time-frequency domain collisions and receiver noise To maximize the time-frequency domain platform density, 90 percent of the 5 percent allowance is utilized for this purpose and only 10 percent is assigned to the effect of noise on the message error rate

A message is in error if one or more of the 110 message bits is in error Let  $P_e$  be the bit error rate and  $P_m$  be the message error rate Then the probability that one or more bits are in error is given by

$$P_m = \sum_{r=1}^{110} \frac{110}{r} P_e^r (1 - P_e)^{110-r}$$

This can be rewritten as

$$P_m = 1 - (1 - P_e)^{110}$$

Using  $P_m = 0.005$ , we have

$$P_e = 1 - 0.995^{1/110} = 1 - 0.99995443 = 0.00004557 \approx 5 \times 10^{-5}$$

So we see that the bit error rate must not exceed  $5 \times 10^{-5}$  if noise is to be an order less important than signal collision statistics in producing lost messages. The SNR required in the data bandwidth to provide the specified maximum value of error depends on the type of modulation adopted. Representative curves covering PSK and FSK forms are shown

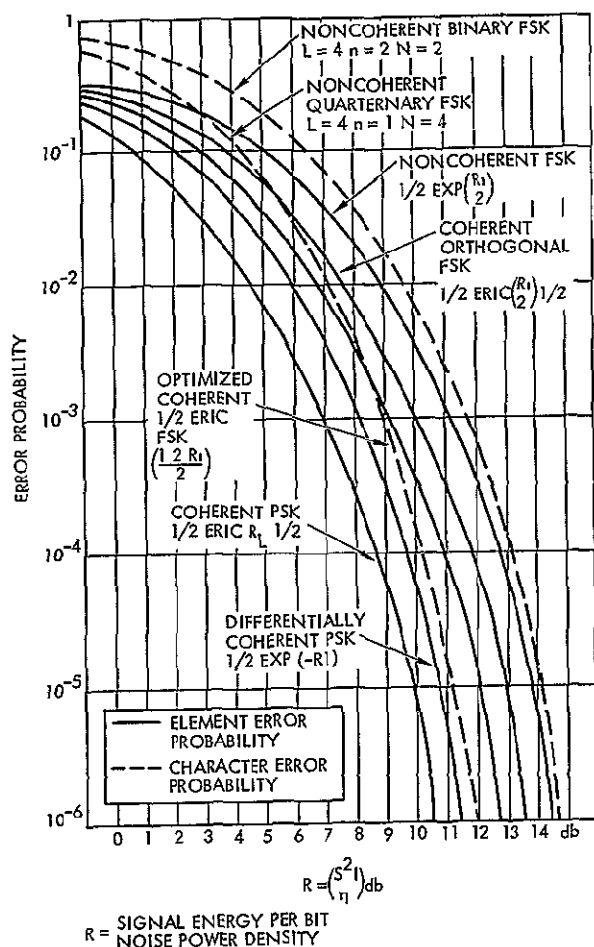


Figure 2-13  
BIT ERROR RATE AS A FUNCTION OF SNR  
FOR SEVERAL MODULATION FORMS\*

- If the total power due to interference signal components in the data bandwidth causes the data SNR to fall below  $\approx 11$  db

To determine the interference levels in both filters as a function of the intercarrier spacing of a pair of transmitters we must integrate the power spectrum distribution equation, between limits which differ by the magnitude of the bandwidths of a) the narrowband carrier tracking filter,

in Figure 2-13. From the curve corresponding to differentially coherent PSK, the selected mode for the data collection system, we see that an SNR of  $\approx 9.6$  db is indicated to ensure a message error rate that is less than 10 percent of the total allowance (5 percent)

The message error rate changes very rapidly with the SNR (see Figure 2-14) and therefore the level we adopt as our criteria for unacceptable performance need not be very precise. For the purposes of our further analyses we use a nominal figure of 11 db.

We have now established two separate criteria for interference, thus

- If the total power due to interference signal components in the carrier tracking loop bandwidth causes the loop SNR to become zero

\* N E Hveding, "Comparison of Digital Modulation and Detection Techniques for a Low-Capacity Transportable Troposcatter System," Report AD-461599, Shape Technical Centre

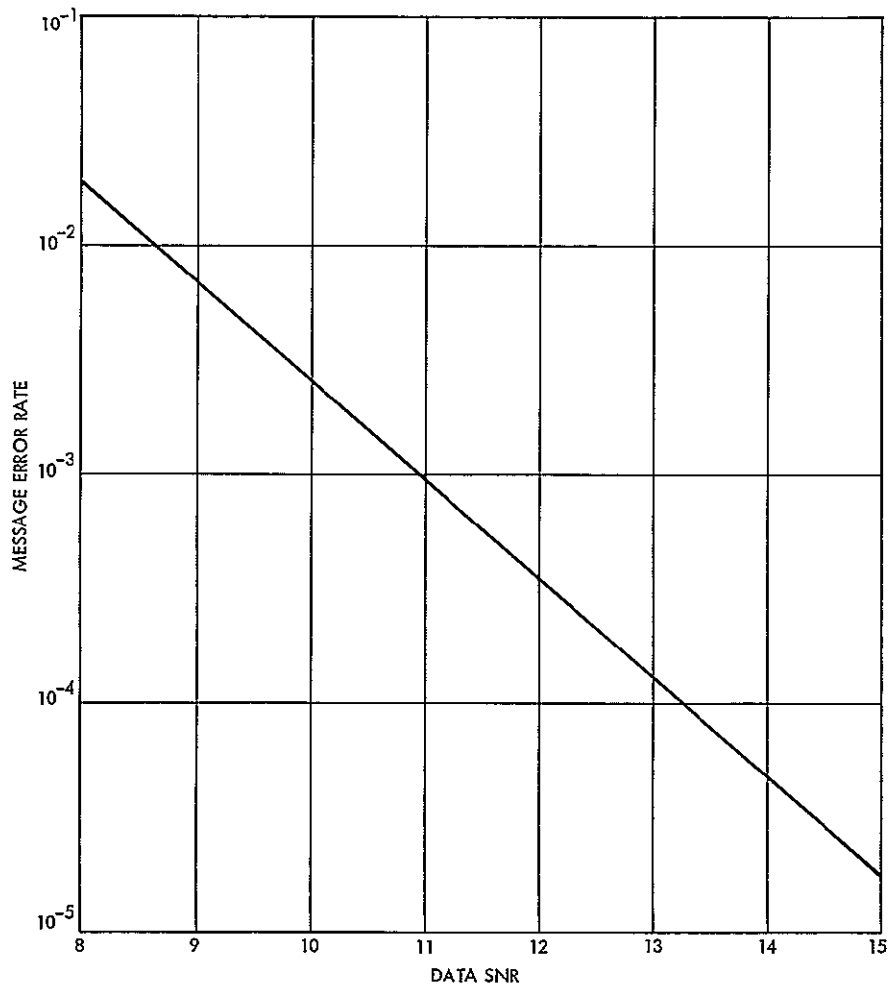


Figure 2-14  
MESSAGE ERROR RATE FOR 110-BIT MESSAGES VERSUS SNR

and b) the medium bandwidth data filter. The integration must be repeated while the spacing between the filter center frequency and offending carrier is varied to derive the interference power versus spacing.

For the initial analysis, rectangular filter cutoff shapes were assumed, with widths equal to the calculated filter cutoff frequencies. The results are shown in Figure 2-15, based on the model of the frequency domain depicted in Figure 2-16.

## 2.5.2 Time Domain

The system capacity in the time domain had been quantified only for messages of 256-bit length. The decision to delete storage in the platform

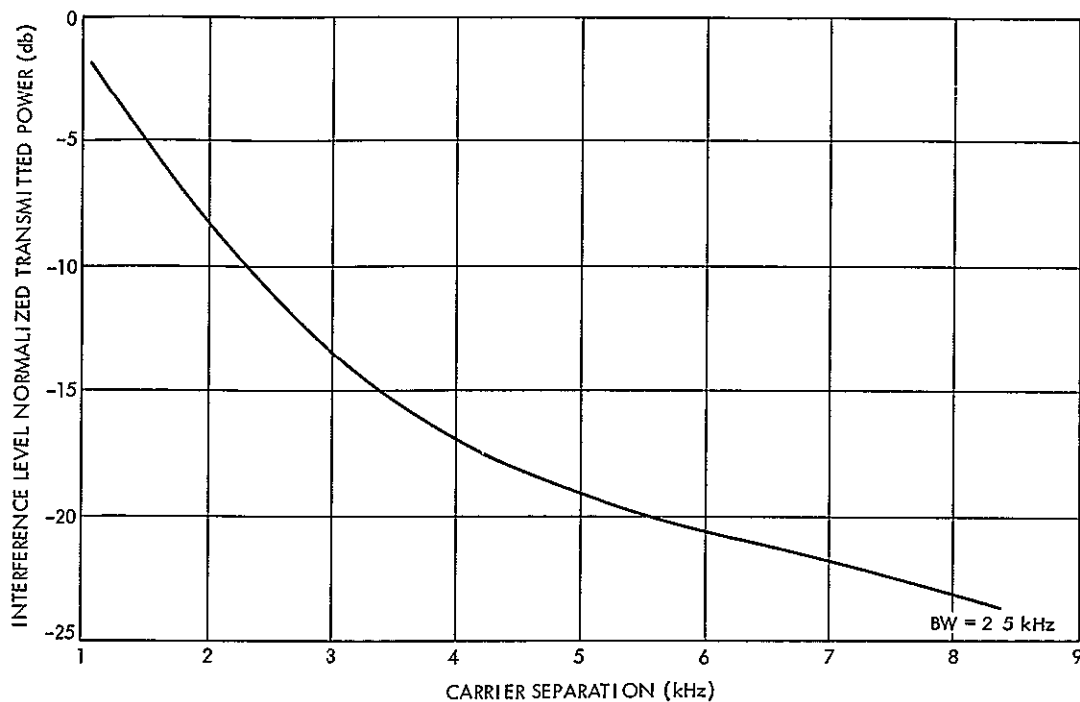


Figure 2-15

### INTERFERENCE TO SIGNAL RATIO VERSUS CARRIER SEPARATION

The calculations assume a squarewave data filter and a transmitter power envelope following  $(\sin x/x)^2$

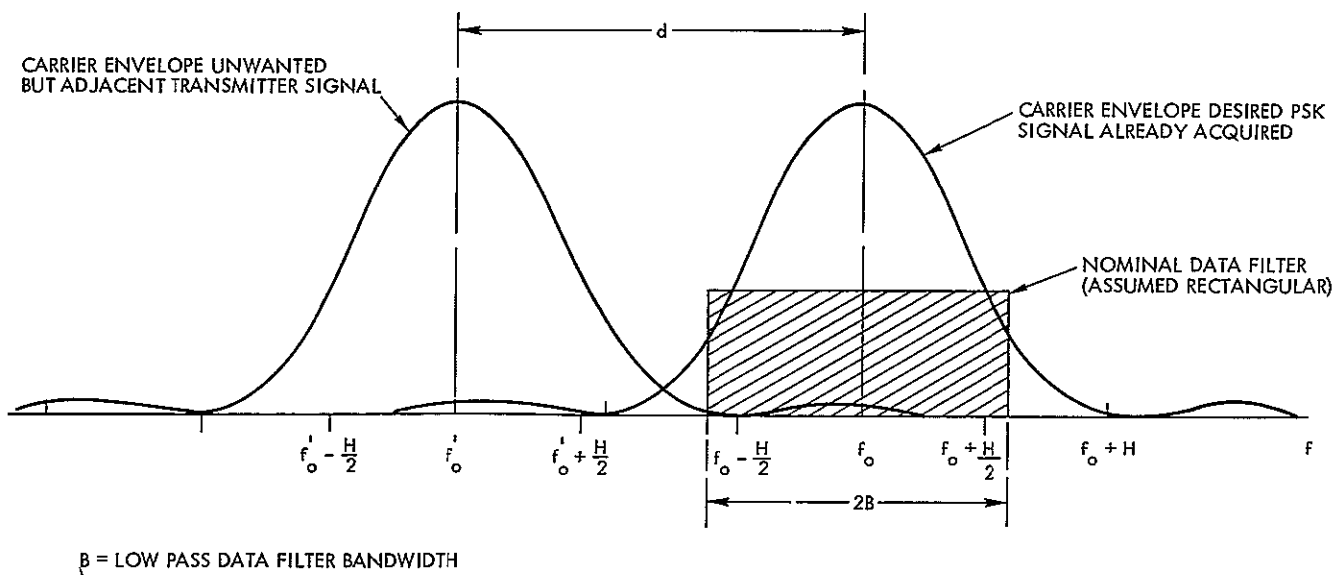


Figure 2-16

### FREQUENCY DOMAIN INTERFERENCE

changes the message to 110 bits or 0.054 second at the 2 048 kbit data rate Figure 2-17 illustrates the message reception statistics anticipated for the 110-bit message length for messages transmitted on the same carrier frequency, at the same 2048 bits/sec rate, and for a time slot value of 8 minutes The effect of increasing replication factor is clearly shown in Figure 2-18 from which it is evident that  $M = 7$  is near the optimum value

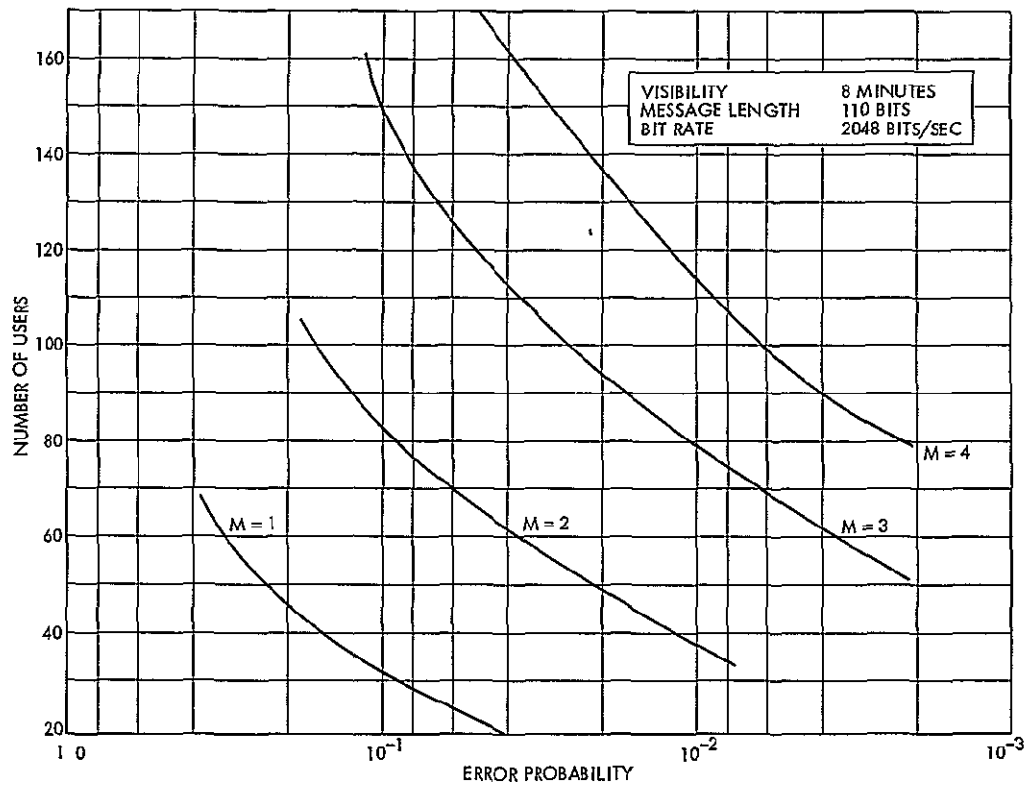


Figure 2-17  
MESSAGE STATISTICS FOR 110-BIT MESSAGE

### 2.5 3 Combined Random Time and Random Frequency

So far we have considered the performance of the system with and without replication in the time domain. In both cases, we assumed that all the transmitters used the same carrier frequency. However, in the combined time-frequency system, we allow the  $N$  transmitters to choose any frequency within a certain interval. For our study we assume that each transmitter picks at random a frequency anywhere within a 100 kHz



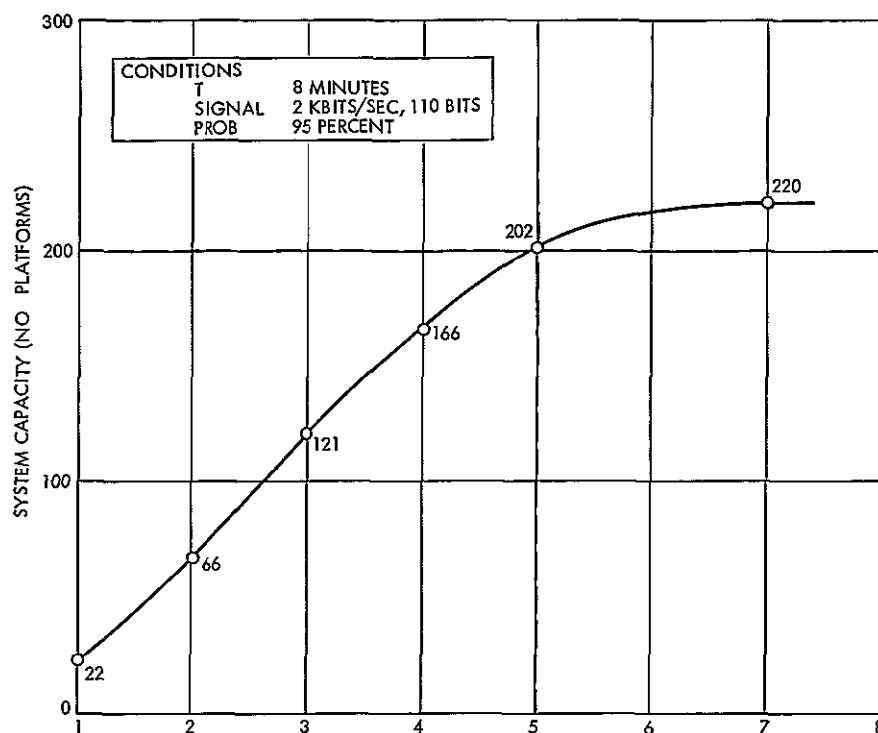


Figure 2-18  
PLATFORM CAPACITY FOR RANDOM TIME MODE DCS

bandwidth. The probability density of the randomly chosen carrier frequency is assumed to be uniform over the interval

A preliminary examination of the combined time-frequency system shows that the analysis becomes very tedious and difficult when we allow replication, and unfortunately in only few cases can we obtain a closed form expression. Using the combined time-frequency, we estimated that for  $M = 1$  we would be able to accommodate as many as 250 users when the error probability is near 0.05. For more exact results we have written a Monte Carlo computer simulation program for use with the CDC computer. This program and its results are discussed in considerable detail in Section 4.

When there is no signal replication an error occurs if two or more signals are not distinguishable in both the time and frequency domains at any instant during the entire transmission interval. Using simple illustrative sketches we can show the several different modes of interference. If messages A and B with nominal individual bandwidths of 2.5 kHz each, and

carrier frequencies as shown in Figure 2-19, arrive at the satellite receiver at  $t_1$  and  $t_2$ , we have no interference. In this case, the two messages do not interfere in the time domain, although they are overlapping in the frequency domain.

Similarly in the second case (Figure 2-20) there is no interference because the two messages A and B are distinguishable in the frequency domain, though they are overlapping in time.

In the situation illustrated in Figure 2-21, however, there is interference because the two messages interfere in both the time and frequency domains. Only when there is such interference in the two domains do we have error from message collision. In order to have a clean copy of all  $N$  messages, each of the  $\binom{N}{2}$  pairs must be free of interference either in the time or the frequency domain.

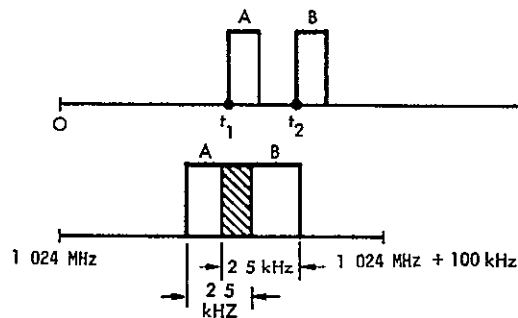


Figure 2-19  
TWO NONINTERFERING MESSAGES,  
WITH FREQUENCY OVERLAP

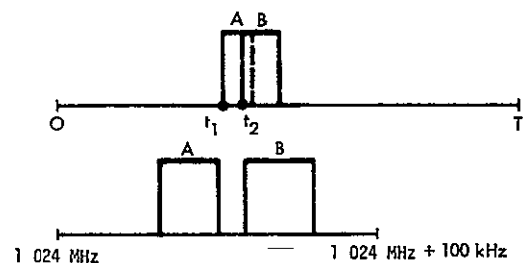


Figure 2-20  
TWO NONINTERFERING MESSAGES,  
WITH TIME OVERLAP

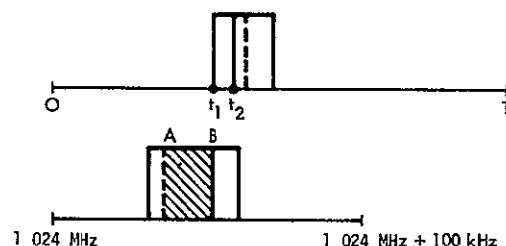


Figure 2-21  
TWO INTERFERING MESSAGES

With replication an error occurs if any message is lost throughout the M subintervals. Unlike the case where there is no replication, a message may be lost in one subinterval as long as it is not lost M times.

There are three levels at which we can examine the combined time-frequency system

- 1)  $\binom{N}{2} d^{(1)}/T \ll 1$  and message pair collision losses dominate
- 2)  $\binom{N}{2} d^{(1)}/T \ll 1$  even number of messages are lost, and  $K/2$  distinct-pair interferences dominate
- 3)  $\binom{N}{2} d^{(1)}/T \gtrsim 1$

where  $d^{(1)}/T$  = ratio of the duration of a message to the visibility time of the satellite, and  $M = 1$

In the first case, we can show that the overall error probability ( $P_o$ ) is given by

$$P_o = P_{(T)} \times P_{(f)}$$

where

$P_{(T)}$  = probability of any interference in the time domain

$P_{(f)}$  = probability of any interference in the frequency domain

where

$$P_o \approx \binom{N}{2} \frac{d^{(1)}}{T} \cdot \frac{2(\text{bandwidth of the signal})}{\text{total bandwidth available}}$$

We observe that the total probability is the product of an error probability in the time domain and another in the frequency domain. Unfortunately this simple multiplication does not occur in other cases, although the overall error probability will always be larger than the product of the error probabilities in the time and frequency domain.

In the second case, we can assume that whenever there is any interference  $K/2$ -pair-interference dominates and that only two messages interfere in the time domain at any instant. For the K messages (which

interfered in time) to be error-free in the frequency domain, these messages must not interfere  $K/2$  times in the frequency domain. The probability that  $K$  messages are free of error is given by

$$P = \left[ 1 - \frac{2(\text{bandwidth of signal})}{100 \text{ kHz}} \right]^{K/2}$$

and

$$P(\text{error}) \approx \sum_{K=2}^N P(K \text{ messages are lost in time}) \left[ 1 - \frac{2(\text{bandwidth})}{100} \right]^{K/2}$$

In the third case, the task of computing the overall probability of error becomes difficult for the following reasons

- We must consider how messages are lost. For example, if three messages are lost then all three messages may overlap at any instant, or only two overlap at any instant
- We must study the probability of interference in the frequency domain if more than two messages arrive at the same time. Unfortunately, the ratio of the bandwidth of a message to the 100 kHz allocation is only 0.05 and we cannot readily compute the interference probability when, say, four signals arrive at once

However, we can approximate how well the combined time-frequency system performs. We assume that whenever  $K$  messages are lost,  $K/2$  distinct-pair-interferences are the dominant form of interference. Of course this is an optimistic approximation, because at times we may have  $K$  messages colliding in the same interval.

With this assumption, we have the same expression for the probability of error as in the second case. The result shows that 40 to 60 more users can be accommodated than for a simple random time mode, assuming a desired system message error probability around 0.05. Similarly, if we allow a replication of two, we can accommodate close to 150 users for the same error probability. The improvement we can obtain for higher replication is discussed in Section 4. The simulation discussed there

- Obtains the performance of the time-frequency system when there is replication and  $\left(\frac{N}{2}\right) d/T$  approaches a value of unity
- Examines the tradeoff between the increase in the PRF and the subsequent increase in the bandwidth of the signal

Synthesis of the combined time and frequency mode has only been performed for replication factors of one and two. For  $M = 2$ , the system capacity is 550 platforms, using 110-bit messages

The magnitude of this capacity, combined with the increase obtained by going from  $M = 1$  to  $M = 2$  makes it clear that such a mode will support a total of 1000 platforms for  $M = 3$ . Extensions of the Monte Carlo simulation for  $M = 3$  is planned at the outset of Phase D. It is interesting that the calculated capacity for a multiple random time system using buried oscillators appears to be usefully larger than for the random time-frequency ( $M = 2$ ) case.

## 2 6 RADIO FREQUENCY INTERFERENCE

Interference signals originating from military and commercial transmitters could adversely affect the performance of the ERTS data collection system. Four types of RF interference are recognized

- 1) Co-channel Some portion of the link overlaps another emitter
- 2) Adjacent channel Emitter outside passband of the link receiver injects a significant signal due to poor selectivity, frequency proximity, or high power
- 3) Harmonic components Emitters operating on submultiples of the frequency of the link can yield spurious outputs Problem aggravated when final (PA) overdriven or overmodulated
- 4) Intermodulation Both the fundamental and harmonics from all spectrum users combine to form new intermodulation components at mixer (or nonlinear element) of link receiver

For a communications path involving a spacecraft-to-ground link some special factors are involved that are not encountered in conventional ground to ground links.

- Terrain is a factor only at low elevations
- For a synchronous satellite, the range loss can be assumed to be approximately equal for all terrestrial emitters on hemisphere
- A very large number of emitters will be in view for any reasonable antenna size
- Spectrum density changes slowly as a function of spacecraft position
- Subsattellite point provides reference for signal analysis

For many types of interference the degree of interference encountered varies with the time of day. Two separate time factors are involved

- 1) A repeating pattern, 24-hour duty cycle, related to local time. This is common to all emitters of a subset. For example, commercial broadcast stations usually do not operate all 24 hours, but follow an operating schedule. Even allowing for equipment maintenance transmission, they exhibit a useful off period each 24 hours. In addition the number of aircraft flights reduces in evening, and falls to a minimum during early morning.
- 2) A statistical variation, which can be defined as a group characteristic for a subset. Mobile radio equipment transmits for short bursts. As a group, their density can be defined by a statistical model. TRW has such data from prior police and fire studies.

Two approaches are commonly used for making an RFI appraisal, a practical field survey using instruments and a theoretical analysis using documented details of sources. Practical measurement involves setting up a spectrum analyzer in the region where the planned system will be installed and observing the power spectral density within the proposed frequency band. In most cases the measuring equipment is partially automated, a swept-frequency receiver is coupled to a pen recorder to provide a permanent record of the energy distribution. In addition to the actual power profile across the band, a secondary analysis is often performed of the signals within certain critical regions to determine the modulation energy distribution.

The theoretical method requires access to data on the performance specifications, geographic locations, and mode of operation of the transmitters controlled by other spectrum users

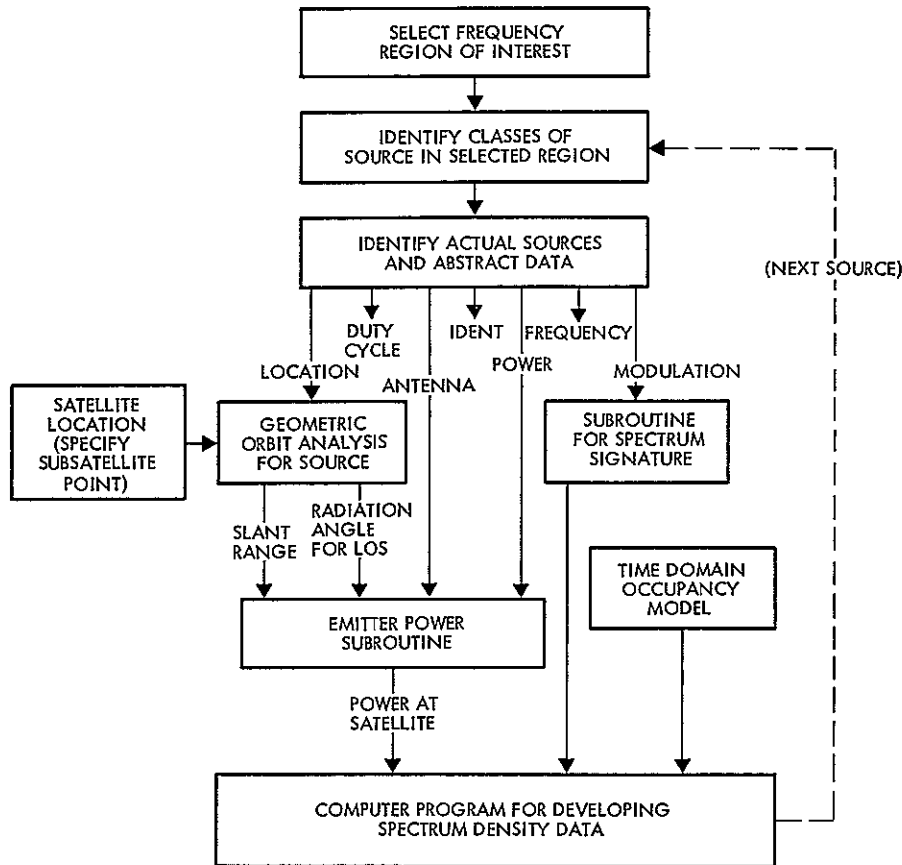


Figure 2-22  
SPECTRUM DENSITY COMPUTATION

Because of the large number of users involved it has become an established practice to store data relating to spectrum users on tape and perform RFI analyses with a fast digital computer. A simplified example of the operations involved in examining such source data, and evaluating potential interference modes, is depicted in Figure 2-22. Several outputs are possible from running an evaluation program of this type. Those more commonly involved are

- Lowest interference signal density for a single frequency slot of specified width

- Preferred mix of frequency slots, each of a specified minimum width, to make up a total specified width
- Interference level for a specified width as a function of satellite location
- Best slot location and time for a specified message time (assumes  $T \ll 24$  hours)

Although a number of industry publications provide limited details on commercial transmitters, by far the most significant data bank is that developed by Illinois Institute of Technology and controlled by the U S Army Electromagnetic Compatibility Analysis Center (ECAC). A partial list of the range of services available from the ECAC is presented in Table 2-4.

Table 2-4 U S Army Electromagnetic Compatibility Analysis Center Services

Electronic Equipment Environmental Listing	Comprehensive description of equipment characteristics, location, and user (approximately 110 line items)
Special Summary Listing	Performed by ECAC staff — extracted subset of entries to suit customer area of interest Can reformat before listing
Punched Cards / Magnetic Tape	Alternative form of electronic equipment environmental listing output
Equipment Characteristics Data Base	Measured spectrum signatures (to MIL-STD-449) and nominal characteristics of equipment (available on magnetic tape)
Index of Spectrum Signatures	Tabulation by equipment nomenclature, serial number, military service, DDC report number, and date taken
Interference Prediction Analyses	ECAC developed models combined with dates from equipment files to establish field environment  Outputs include lists of potential victims, signal density at stated location, interference effects prediction (for given receivers), statistics for pulse interference, and separation versus frequency curves



Normally, the design of a civil or commercial communications system does not convey any 'need to know' which would permit access to classified data of military users. This impasse can be overcome by indicating the planned frequency of operation and asking ECAC to perform the required computer analysis. By this means only the resulting recommendations need be furnished to the system designer, and not the cards or tapes containing the classified data.

If the planned frequency band is relatively narrow, then the co-channel, adjacent channel, and simple harmonic interference can be checked by scanning a tabulation of frequency assignments. Where beacons, radar, and like interference sources are involved, many harmonics are significant and the manual process is tedious.

Intermodulation poses a task of quite a different order of magnitude, and cannot usually be performed without a computer. It involves calculating the various intermodulation products for each source combination. Locating the frequencies of these terms is a straightforward and simple arithmetic operation, but determining the magnitude involves knowledge of the nonlinearity characteristic of the receiver front end for the proposed system. This problem has been studied and reported in detail by several authors (e.g., Burt, Oyer and Truske) and the necessary analytical tools are available.

TRW has not investigated this aspect of the data collection system. An RFI evaluation is recommended for the early part of Phase D.

## 2.7 PLATFORM DEPLOYMENT

The manner in which both the Phase D and subsequent generations of platforms are deployed has a significant effect on the design approach. Particularly affected are the environmental constraints and packaging design.

Field use of the data collection platforms will involve deployment in remote regions where climatic extremes will be experienced. The overall objective is a low-cost, mass-producible unit, this implies a simple design from a mechanical as well as an electrical standpoint. On the

other hand, the extreme climatic conditions indicate the need for complete waterproofing and dust proofing, in fact a hermetically sealed assembly. Existing meteorological and water resource instrumentation suggest a solution; they house their equipments in one of a series of standard structures. These structures range from a small wooden box on stilts (Figure 2-23) to a concrete block room with a floor area of some 144 square feet.

It is desirable, however, that the platform be able to be deposited on the ground, like a lunch box, and operated in an unprotected mode. The packaging design proposed by TRW for the Phase D units is based on a sturdy, lightweight, off-the-shelf, deep drawn aluminum alloy box. It is waterproof, portable, and self-contained except for the battery pack. For acceptable communications, the antenna must be elevated and correctly oriented, implying some form of pole. In all cases, external sensors will be attached by means of cables.

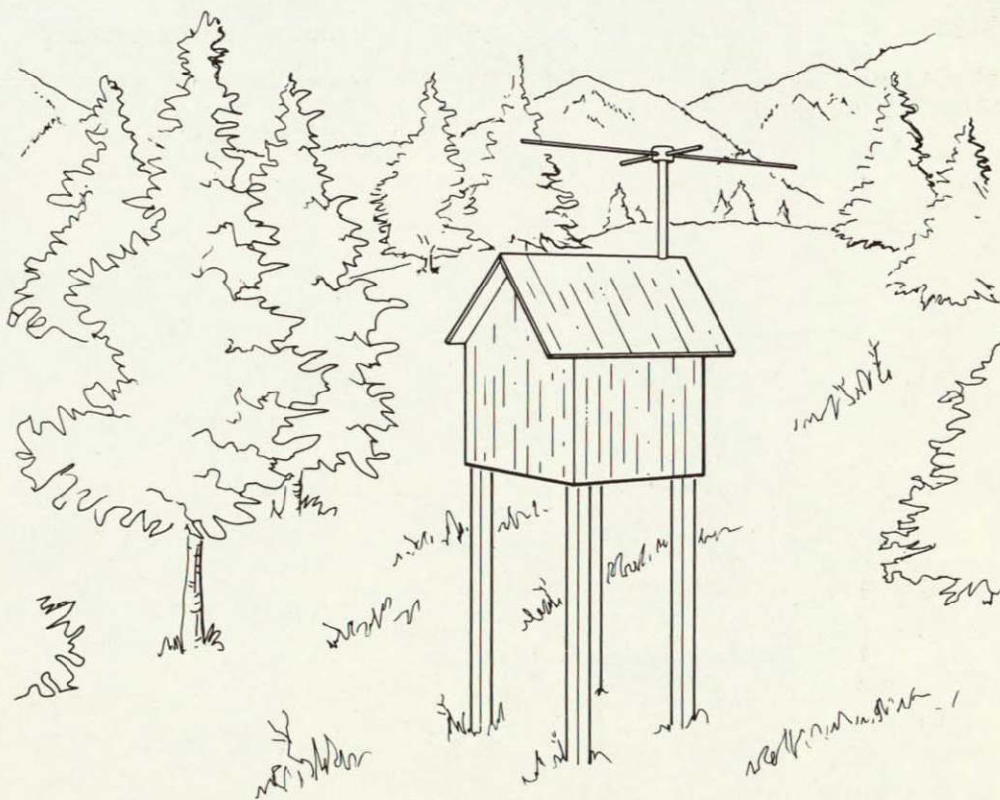


Figure 2-23

TYPICAL WOODEN STILT-MOUNTED INSTRUMENTATION HOUSING

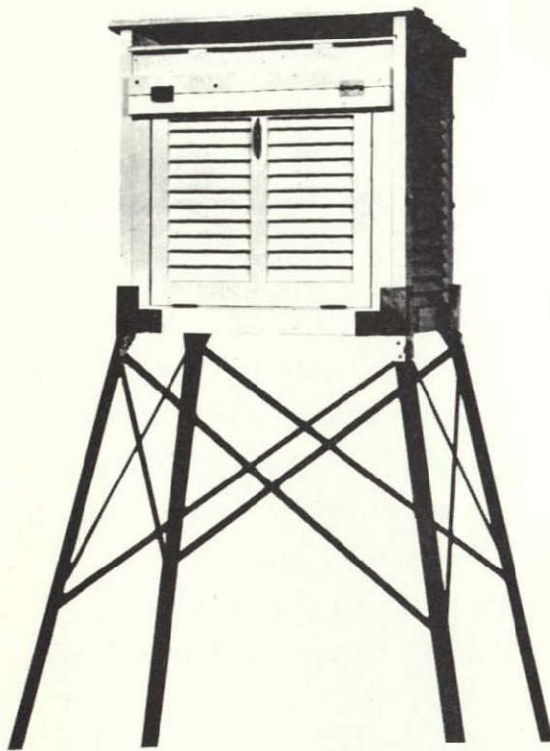


Figure 2-24  
REPRESENTATIVE LOW COST INSTRUMENTATION SHELTER (BELFORT)

TRW believes that both the most practical approach and the one most acceptable to end user is to install the platforms in one of these low cost instrumentation housings. The typical cost of such a unit, as shown in Figure 2-24, is \$100 for single units and appreciably less in large quantities. For the most permanent sites it will be worth using the small brick, stone, or concrete housings already adopted by USGS for stream gauging (Figure 2-25). These two types of housing currently exist at many locations throughout the continental U.S. It seems reasonable to assume that both the initial units and early large quantities will be located at such sites during initial exercising of the system.

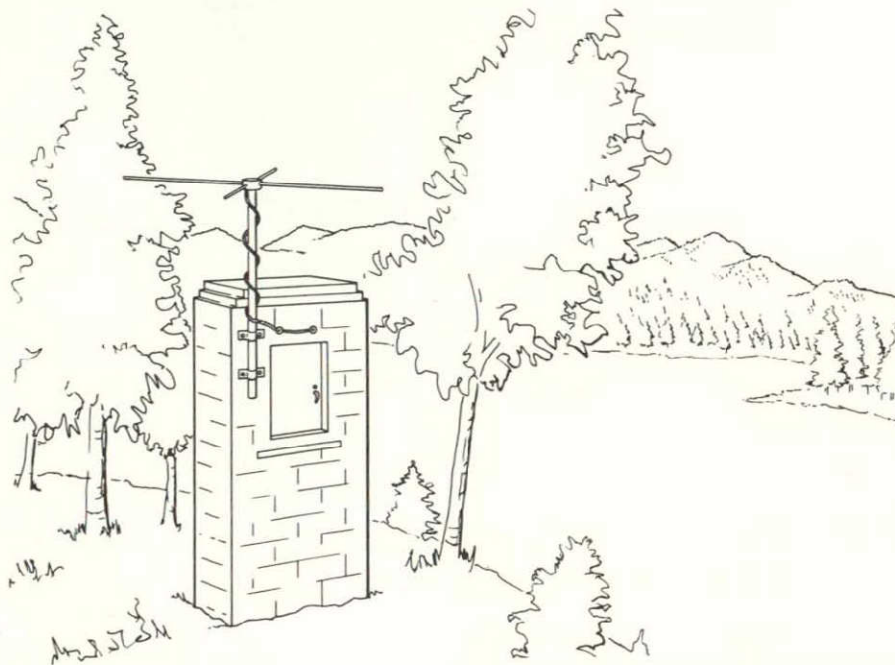


Figure 2-25  
TYPICAL INTERMEDIATE SIZE BRICK INSTRUMENTATION ENCLOSURE

For later system expansion, we believe it reasonable to assume such housings would be supplied by the user. Precedent exists for this conceptual approach in the Alaska environmental telemetry system installed in 1967-68 for monitoring the Salcha, Chena, and Tanana rivers, the Arizona system for the Bill Williams River, and the Connecticut system for the Thames, Blackstone, and Naugatuck rivers.

The wide range of temperatures encountered in the U.S. requires the use of expensive designs and components, if reliable and predictable electrical performance is to be achieved for the platforms. The problem is most severe for the batteries, as discussed in Section 2.8. Conventional air conditioning and heating techniques are unattractive because of the required power, complexity and cost.

A simple means of stabilizing the platform temperature is to bury the critical elements in the ground. TRW has investigated this approach and established that for most locations in the continental U.S., shallow burial (4 to 6 feet) will assure a total annual temperature range of  $\pm 3$  to 5 degrees, and a mean temperature of about  $20^{\circ}\text{C}$ , depending on location.

A typical temperature profile is shown in Figure 2-26. The peak-to-peak temperature range is under  $\pm 3.5$  degrees for the eight probes used, at a depth of 10 feet. A mathematical relationship between the air and subsurface temperature profiles have been established\*. The corresponding air temperature is also shown in Figure 2-26.

The reduction in temperature excursion made possible by this simple deployment technique allows the use of conventional low-cost batteries, such as those intended for automobile and domestic service. Burial will also reduce the likelihood of theft and vandalism. It also prevents direct contact by blown sand and dust, salty spray, ice, and snow.

It is easy to protect the batteries from damage resulting from burial, in a low-cost plastic cast of the type used for pleasure-boat

---

\* M. Jacob and G. Hawkins, Elements of Heat Transfer, New York, Wiley, 1959, p. 1-317.



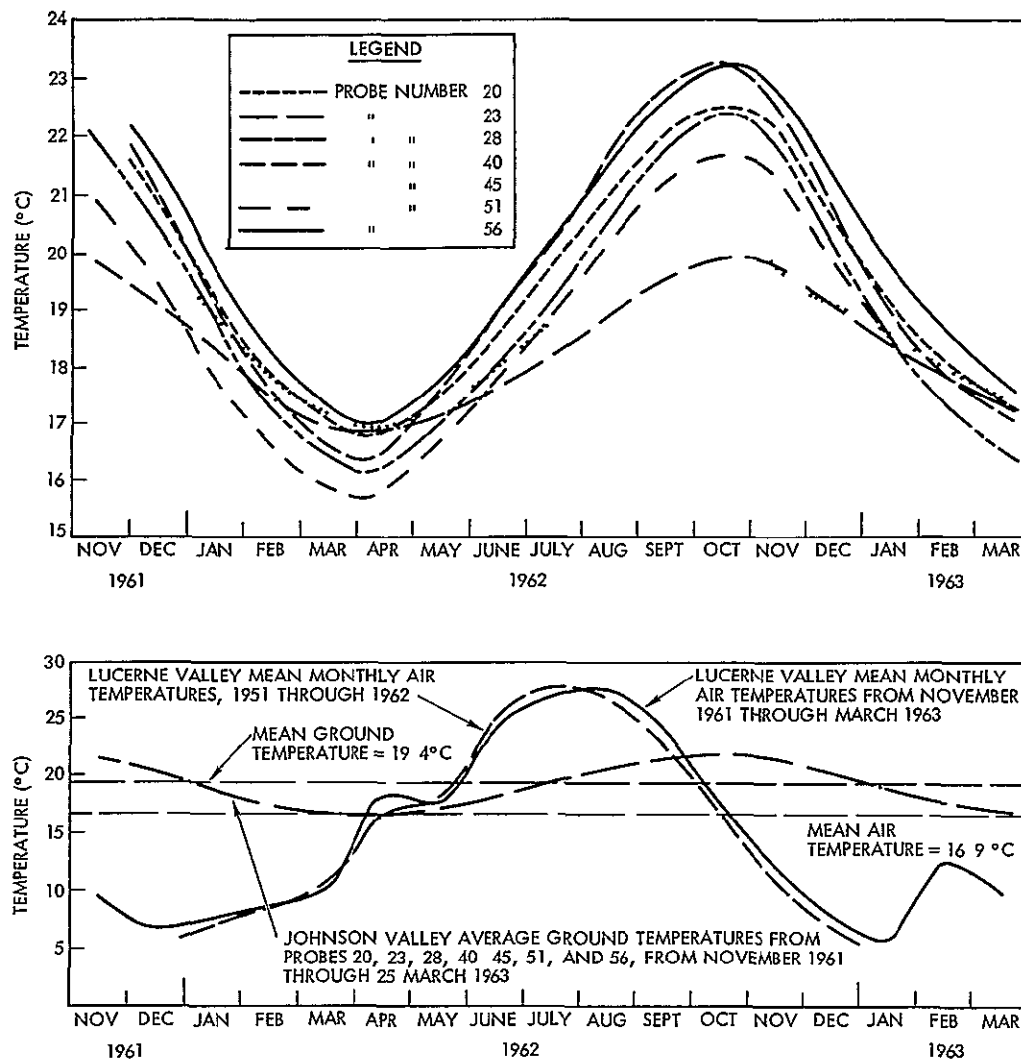


Figure 2-26

LONG-TERM THERMAL PROFILES FOR SEVEN PROBES (10 November 1961 through 25 March 1963, Johnson Valley, California)

batteries A plastic tube, integral with the power cable, allows the battery compartment to exhaust fumes and equalize pressure while preventing ingress of water

TRW next examined the potential advantages of burying the entire platform Our analyses indicate that a dual random frequency and random time mode of operation will provide appreciably less platform capacity than is possible with a channelized approach, and it was with the potential advantages of random time, channelized frequency in mind that we oriented our original approach Unfortunately, such a regimented system requires

precise stabilization of the crystal oscillators associated with each of the platform transmitters. Although the necessary stability is well within the current state of the art it involves additional expense. The temperature compensated crystal oscillator, the preferred design approach, runs about \$50 in quantity for a  $\pm 2$  ppm frequency stability. By burying the crystal oscillator, one can use the lowest cost crystal and components and operate all platforms in an unregimented mode, while gaining most of the advantages of increased total system capacity possible from a channelized mode of system operation.

Uncompensated crystal oscillators exhibit a typical temperature-dependent frequency change of  $\pm 18$  ppm maximum for  $-15$  to  $+80^{\circ}\text{C}$ . For small temperature excursion near the nominal  $+30^{\circ}\text{C}$  design frequency the slope of  $df/dt$  is greatest,  $0.65 \text{ ppm}/^{\circ}\text{C}$ . For a 400-MHz carrier frequency this corresponds to about  $260 \text{ Hz}/^{\circ}\text{C}$ .

The uncontrolled temperature range for the U.S. covers about  $-60^{\circ}\text{F}$  (Alaska) through  $+140^{\circ}\text{F}$  (Arizona, Nevada desert), with a maximum of  $50^{\circ}\text{C}$  variation over 24 hours. For the more temperate regions, and Alaska even, the annual variation in temperature of the oscillator are anticipated to be appreciably less than  $50^{\circ}\text{C}$ . The largest variation in platform temperature is expected between night and day for the desert units, where a worst case change of  $90^{\circ}\text{F}$  ( $50^{\circ}\text{C}$ ) is expected. For a completely uncontrolled crystal oscillator such a range corresponds to a total variation of  $0.65 \times 50$  or  $32.5 \text{ ppm}$ , i.e.,  $\pm 6.5 \text{ kHz}$ .

In addition to the temperature induced variations, the spacecraft motion induces a doppler of  $\pm 8.5 \text{ kHz}$ . Under the worst case conditions, assuming the  $50^{\circ}\text{C}$  daily variation in temperature, the total change in carrier frequency is  $\pm 6.5 \text{ kHz}$  for temperature and  $\pm 8.5 \text{ kHz}$  for doppler, giving a total of  $\pm 15 \text{ kHz}$ . We could thus accommodate three groups of platforms in the  $100 \text{ kHz}$  allocation by crudely tuning all members to one of three evenly spaced group frequencies.

If we adopt a phase-lock loop for the ground data recovery, it will track out the doppler component. For the temperature to equal the doppler rate of  $70 \text{ Hz/sec}$  with a coefficient of  $260 \text{ Hz}/^{\circ}\text{C}$ , the temperature would have to change at a rate of  $(90 \times 60)/260$  or some  $21^{\circ}\text{C}$  per minute.

A relatively small variation in temperature is to be expected during the period of platform visibility. The primary differences will arise from changes in temperature associated with short-term local weather conditions, such as sudden overcast sky, rain squalls, or snow showers. It will be feasible to use the total package as a heat sink to smooth out such variations. It appears the rate of change of frequency due to temperature does not require the allocation of any additional tracking loop bandwidth. Our initial studies indicate that for depths of between 4 and 6 feet the annual temperature change is only  $\pm 3^{\circ}\text{C}$  for most of the U.S. Alaska would entail about 10-foot depth for the same performance.

If we assume a conservative design figure of  $\pm 5^{\circ}\text{C}$  change, the temperature-induced oscillator frequency variation becomes  $\pm 1.3\text{ kHz}$ , and the total variation ( $\pm 8.5$  and  $\pm 1.3$ ) is  $\pm 9.8\text{ kHz}$ . The total group bandwidth including  $4\text{ kHz}$  for data is about  $24\text{ kHz}$  so that five frequency groups are possible within the  $100\text{ kHz}$  allocation. With five such (unregimented) frequency groups we can provide five times the basic time domain capacity derived in Section 1.2, i.e., handle a total U.S. complement of about  $5 \times 160$  or 800 platforms ( $M=4$ ), and tentatively,  $5 \times 220$  or 1100 platforms ( $M=7$ ).

If the entire platform is buried, appreciably lower cost components, and a simpler design became possible. Both digital and analog portions benefit in terms of lowest unit cost and simplified testing throughout the unit.

## 2.8 PLATFORM POWER SOURCES

The primary source of power for the Phase D data collection platforms will be a 117-volt 60-Hz line power conditioner. Because of the extreme temperatures encountered in the U.S., it is difficult to provide power for remote units within the constraints of low cost. Five alternative power sources have been investigated: batteries, fuel cells, solar cells, thermo-electric generators, and wind generators.

### 2.8.1 Batteries

Batteries operate reasonably well over the range of  $0$  to  $30^{\circ}\text{C}$ , but their performance deteriorates rapidly above and below these limits.

The application places restrictions on both size and weight, and implies a battery with both a high specific energy and a high energy density factor. For reasons of schedule, cost, and reliability, we must restrict our consideration to those batteries which have a proven performance and are available off-the-shelf.

Operation at low temperatures presents special problems, the effective capacity is reduced, and the internal resistance increases. At a temperature of  $-40^{\circ}\text{F}$ , the performance of all regular cells is so much reduced that most are virtually unusable, not primarily because of reduced capacity (see Figure 2-27), but more as a result of increased internal resistance. The internal resistance is usually presented in the form of a parametric graph in which the cell plateau voltage is depicted as a function of temperature for various rates of discharge (C and  $10 \times \text{C}$  typically). Representative characteristics for modern silver cadmium and silver-zinc cells are shown in Figure 2-28.

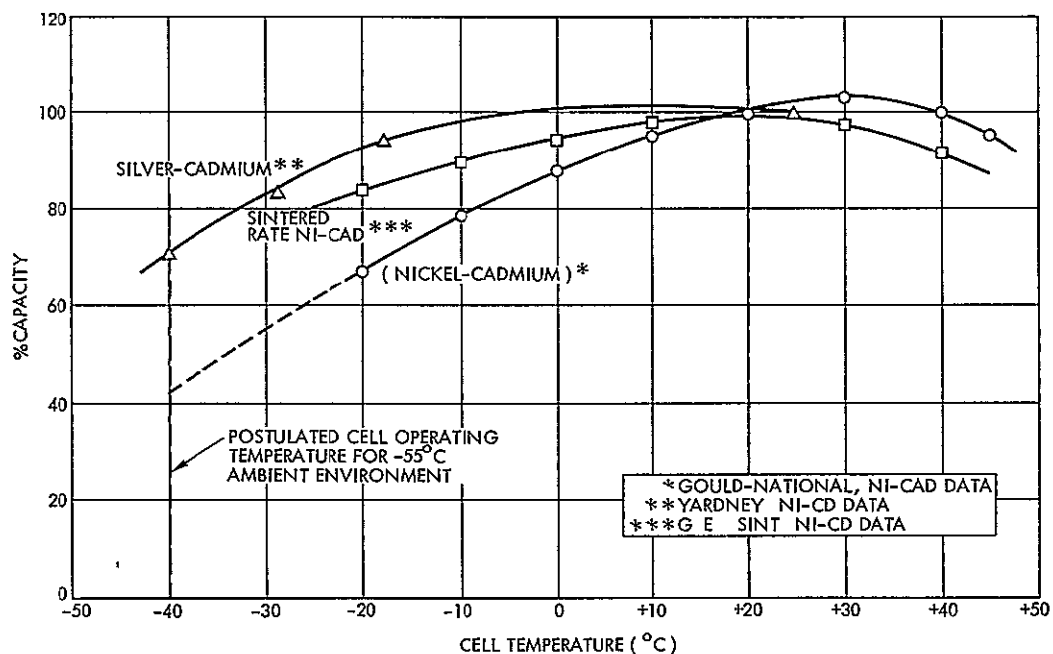


Figure 2-27

AVAILABLE BATTERY CAPACITY VERSUS OPERATING TEMPERATURE (ILLUSTRATIVE)



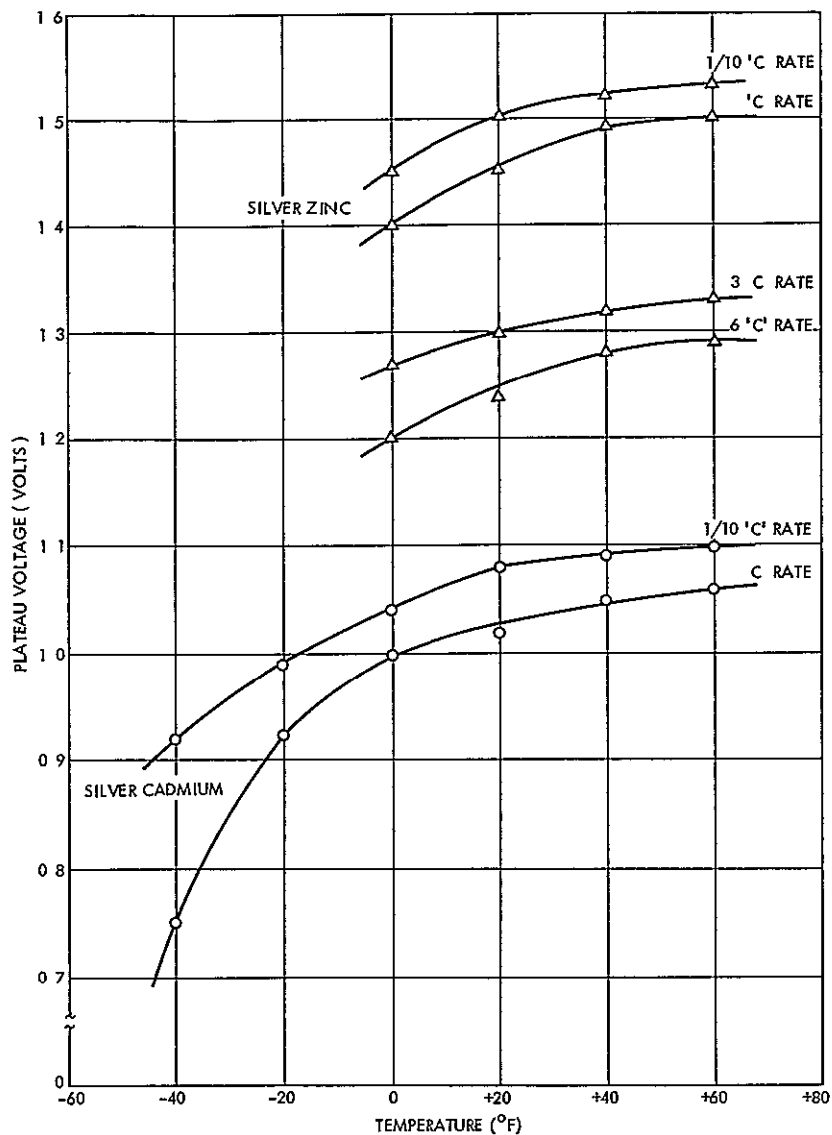


Figure 2-28

EFFECT OF TEMPERATURE ON PLATEAU VOLTAGE FOR REPRESENTATIVE SILVER CADMIUM AND SILVER ZINC CELLS

Our initial estimates for the power consumption of the platform are as follows

Transmitter DC input (5 watts RF)	1.7 watts
Logic subsystem DC input	3 watts
Quiescent power drain of transmitter	10 mw
Quiescent power drain of logic (timer)	10 mw

Thus the platform will have a nominal power drain of 20 watts during transmission. Operating from a 24-volt supply rail, the battery would have to furnish 20/24 or 0.833 ampere of load current

For a data rate of 2048 bits/sec and a message length of 110 bits replicated four times in 8 minutes, the average current drain is

$$0.833 \times \frac{110}{2048} \times \frac{4}{8} \times \frac{1}{60} = 0.4 \text{ milliampere}$$

The total average current drain is

$$0.371 + \frac{10}{24} + \frac{10}{24} = 0.371 + 0.415 + 0.415 = 1.20 \text{ milliamperes}$$

The corresponding energy rate is

$$1.20 \times 10^{-3} \text{ ampere/hr}$$

Nine months of unattended operation correspond to a total of

$$\frac{9}{12} \times 365 \times 24 \text{ or } 6.57 \times 10^3 \text{ hours of use}$$

The total minimum battery capacity required for platform operation is the product of the last two factors

$$1.20 \times 10^{-3} \times 6.57 \times 10^3 = 7.934 \text{ or } \approx 8 \text{ ampere/hr}$$

The requirement to operate at low temperature is greatly aggravated by the impulsive mode of discharge. The load demands power for only 1/20 second. The ratio of the pulse load current to the estimated total capacity is  $0.833/8.0 = 0.105$  and corresponds to  $\approx$  a 1/10 'C' rate of discharge.

The foregoing calculations suggest a silver-zinc battery with a minimum total capacity on the order of 8 ampere/hr. A typical suitable cell of this type is the Yardney Electric type HR-4, the salient details of which are tabulated below.

Nominal Capacity	Peak Discharge Current	Weight (oz)	Height (in.)	Width (in.)	Depth (in.)	Approximate Cost (\$)	
						1-99	500-1000
4.0	24A	3.7	3.36	1.72	0.59	12.75	10.95

This cell will provide satisfactory service down to 0°F, at which temperature the cell output will be 1.45 volts. For a 24-volt nominal supply bus then we would require 24/1.45 or some 17 cells in series. The Phase D cost per platform would be (17 x \$12.75) or approximately \$217 per bank, i.e., \$434 total. This figure is optimistic since it does not allow for charge loss due to cell discharge (typically 15 percent at room temperature over 3 months). It is apparent that a 12 to 15 ampere/hr battery rating should be selected to accommodate the storage degradation.

Operation over the full annual temperature range of -60°F to the +140°F would require heaters and extensive thermal insulation. The heaters would consume power and further increase the required battery capacity and cost.

## 2.8.2 Fuel Cells

Fuel cells are now a well established means of direct energy conversion. TRW investigations have, however, failed to disclose any device which would be acceptable from a unit cost standpoint.

### 2.8.3 Solar Cells

The solar panel is an interesting source of prime power for those locations where adequate sunlight can be expected. The cost of solar panels is relatively high, the cheapest devices are those used to power small portable transistor radios. Representative glass protected devices of this class are those available from the large component parts suppliers.

such as Allied Radio. Table 2-5 lists typical characteristics of such devices

Table 2-5 Commercial Silicon Solar Cells Data

Type	Load Current (ma)	Power (mw)	Price (1-99) (\$)	Size (dim)
200A	60	24	11 50	1 3
200B	90	36	13 50	1 3
200C	120	48	17 50	1 3
200D	150	60	25 50	1 3

Each solar cell unit provides an emf of 0.4 volt on full-load current.

Since continuous operation of the platform is desired even when there is an overcast sky, we must adopt a trickle charge mode in which the fuel cell provides the replacement energy for a local storage battery.

The estimated power consumption is equivalent to an average current demand of under 1.5 milliamperes. If we assume that under the worst conditions there would be an average of 3 hours of useful sunlight per day, then the solar cell during 3/24 of a day must provide in excess of 1.5 milliamperes average current, or  $1.5 \times 24/3$ , or 12 milliamperes minimum. We assume 15 milliamperes for a tentative design. For effective charging, the solar cell array output voltage must exceed that of the battery. If we assume 28 volts, using 0.4 volt solar cell elements, we require 70 cells in series to yield the requisite output voltage. For a charge current of 12 milliamperes we would require a single 60 milli-ampere rated series string. The total array would then comprise one group of 70 cells, at an estimated cost of  $70 \times \$11.50$ , or \$805.

The cost of the reservoir battery must be added to that of the solar cells and ancillary mounting hardware. Because of the high value of peak demand which the battery must provide, the size and cost does not

reduce in proportion to the reduced energy storage needs. TRW concluded that this approach is of limited usefulness, and not a preferred approach.

#### 2.8.4 Thermoelectric Generators

Thermoelectric generators are now quite widely used for railroad signaling and rural carrier telephone equipment. In addition they have been extensively tested as proven as power sources for the VHF radio transceivers on railroads. These devices operate from natural gas, either bottled or from taps on a convenient gas line. The reliability and long term maintenance records on such sources have been thoroughly reported.

At present the prices are too high for consideration for platform primary power. Typical units cost several hundred dollars, and will operate unattended for 6 to 9 months. It is TRW's considered opinion that these devices may well become available by the time that the large-scale deployment of data collection platforms is implemented. It is equally clear that for Phase D such an approach is not appropriate.

#### 2.8.5 Wind Generators

Wind-driven generators have been used for many years as a convenient source of 'almost free' natural power. Generally such units are relatively large and involve step-up gearing from the windmill to the generator.

Since the average power level (1.5 milliamperes x 24 volts) is only 36 milliwatts, it seemed possible that a conventional anemometer might be used as the means of obtaining trickle charging power for a reservoir battery. In many locations there will be an anemometer, serving as a wind speed sensor. Coupling the output to a rectifier and charge regulator would obviously load the sensor and modify its response. Since the planned mode of operation for the platform is real-time sampling at a low frequency, it appears feasible to disconnect the charging circuitry just before commanding the multiplexer gate associated with the anemometer signal. TRW has not yet determined the feasibility of such a mode of operation. Typical anemometer cost is in the range of \$50 to \$100.

## 2.9 APPLICABLE STANDARD ANTENNAS

The ERTS antenna system coverage requirements for the DCS are discussed in Section 2.1. Basically the satellite antenna is required to exhibit a nominal coverage of 120 degrees and the ground platform antenna a coverage of 165 degrees. In this section we review the gain, pattern, and polarization loss that may be expected from various conventional types of antennas that appeared to be potentially relevant to the DCS. Because of size and weight requirements along with interference problems of the satellite body, the types of antennas considered here are dipoles, crossed dipoles, and crossed dipoles with ground planes.

The study has shown that a gain summation, of the satellite and ground antennas at the coverage angles, of +2 dbi and a maximum polarization loss of 3 db can be achieved with conventional antennas such as crossed dipoles over a ground plane. By using array techniques and beam shaping higher gains are possible, and the analyses indicate that it is feasible to effectively compensate for the path loss resulting from range variation by beam shaping.

Figure 2-29 shows a radiation pattern of a dipole antenna. This antenna has a peak gain of approximately 2.0 dbi. As can be seen the gain at  $\pm 60$  degrees is 6 db below the peak gain. Therefore, the gain is -4.0 dbi at  $\pm 60$  degrees. This antenna is linearly polarized. If a similar antenna were used on the ground the gain would be -14.0 dbi at  $\pm 82.5$  degrees. The summation of the gains at the coverage angles would be -18 dbi when the axis of the antennas were aligned. If the dipoles were normal to each other they would be crossed polarized, which would cause a complete loss of signal.

Figure 2-30 is a radiation pattern of a set of crossed dipole antennas fed in phase quadrature and placed above a ground plane. The separation between the crossed dipoles and ground plane is a quarter wavelength. The peak gain of this antenna is approximately 4.0 dbi and the polarization is circular. The gain at  $\pm 82.5$  degrees is -1 dbi. If this antenna were used as a ground platform antenna and the linearly polarized antenna were used on the spacecraft, the sum of the gains of the antennas at the

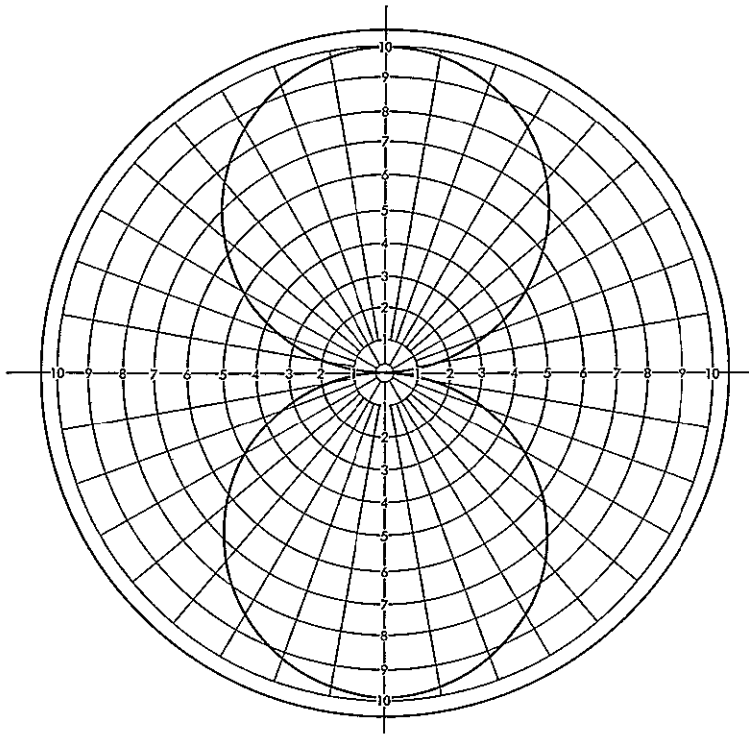


Figure 2-29  
DIPOLE RADIATION PATTERN VOLTAGE PLOT LINEAR POLARIZATION

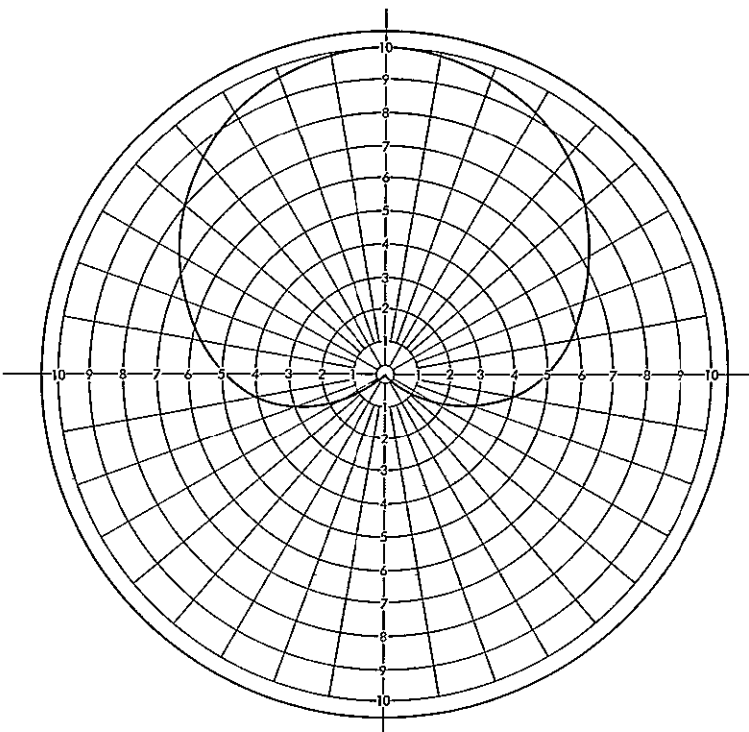


Figure 2-30  
CROSSED DIPOLE OVER GROUND PLANE RADIATION PATTERN VOLTAGE  
PLOT, CIRCULAR POLARIZATION OF  $0.25 \lambda$

coverage angles would be -5.0 dbi. A 6 db (maximum) polarization loss may be present, however, since the ground antenna is elliptically polarized and the satellite antenna is linear, depending on the alignment of the polarization ellipse and the dipole antenna axis.

If the spacecraft antenna were a crossed dipole antenna without a ground plane the sum of the gains at the coverage angles would be the same as the crossed dipole with ground plane for the ground platform antenna and dipole antenna for the satellite. The polarization loss would be less, however, since the antennas are both circularly polarized. Crossed dipoles have an axial ratio of 6 db at  $\pm 60$  degrees off axis and approximately 10 db at  $\pm 82.5$  degrees off axis. Therefore, the polarization loss would be on the order of 3 db maximum depending on the orientation of the polarization ellipse. By placing a ground plane behind the crossed dipoles approximately a quarter wavelength, the gain of the antenna at  $\pm 60$  degrees would be  $\pm 1.0$  dbi. The sums of the gain at the coverage angles would be 0 dbi. The polarization loss would still be 3 db maximum.

By extending the ground plane separation on the ground platform antenna and/or satellite antenna to 0.4 wavelength the pattern would become as depicted in Figure 2-31. The peak gain of this antenna is approximately 1.5 dbi but at approximately  $\pm 82.5$  degrees is 0.5 dbi. The sum of the gains of this antenna if used on the ground and satellite is 2.0 dbi with a maximum polarization loss of 3 db.

Other antennas such as conical log spirals of conventional design would provide radiation patterns similar to that of the crossed dipoles over a ground plane but with better off-axis axial ratios. These antennas seem impractical for the satellite because of their large size and weight. Table 2-6 summarizes the above information.

## 2.10 PULSE REPETITION FREQUENCY

The PRF timer operates continuously to provide the command signals which activate the remaining platform circuitry every 2 minutes. It is desirable to keep the power consumption of the timer at an absolute minimum to prevent this minor item from becoming the dominant factor in determining the capacity, size, and cost of the platform battery.



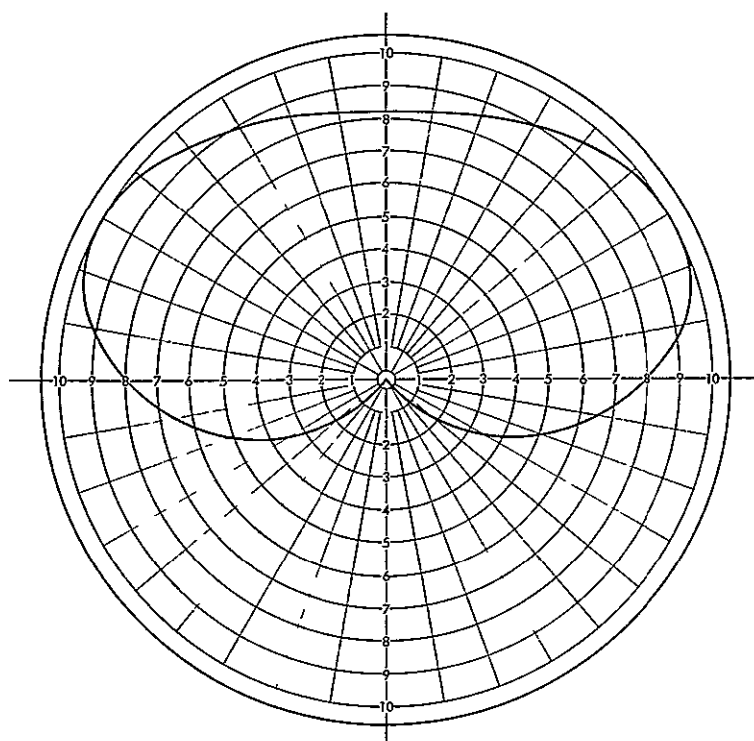


Figure 2-31

ANTENNA PATTERN WITH GROUND PLANE SEPARATION OF  $0.4\lambda$

Table 2-6 Gain Summaries and Polarization Loss

Ground Antenna Type	Satellite Antenna Type	Gain Summation at Coverage Angle (dbi)	Maximum Polarization Loss at $\pm 60^\circ$ (db)
Dipole	Dipole	-14.0	0 - $\infty$
Crossed dipole over ground plane ( $0.25\lambda$ )	Dipole	-5.0	6
Crossed dipole over ground plane ( $0.25\lambda$ )	Crossed dipole	-5.0	3
Crossed dipole over ground plane ( $0.25\lambda$ )	Crossed dipole over ground plane ( $0.25\lambda$ )	0.0	3
Crossed dipole over ground plane ( $0.4\lambda$ )	Crossed dipole over ground plane ( $0.4\lambda$ )	+2.0	3

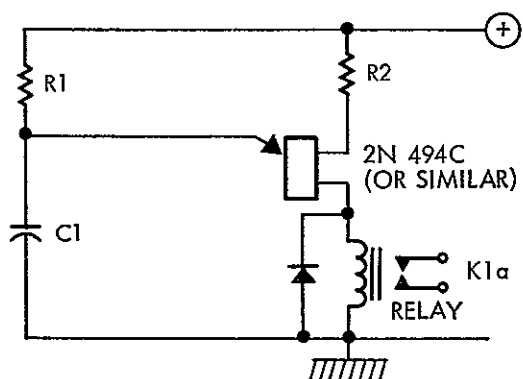


Figure 2-32

### SIMPLE UNIJUNCTION TIMER

the whole cycle repeats. The relay contacts K1a perform the desired external functions, such as initiating the transmitter 'on' circuitry, at the time that C1 discharges and actuates K1

The time between relay operations is the charge time for the resistance-capacitance components R1 and C1. It is not possible to operate this rudimentary timer with charge times on the order of 2 minutes, as required for the platform. The emitter electrode of the unijunction transistor requires a small current at its peak point for it to trigger. Values of current range from 1 to 25 microamperes, and 2 microamperes is a reasonable figure for production versions of the 2N494C. If we divide the peak current by this leakage current, we arrive at a value for the equivalent resistance ( $R_u$ ) of the transistor. This resistance is effectively in parallel with C1 and thus forms a potential divider with R1 across the supply. It is clear that C1 can never charge to a voltage greater than the  $R_u / (R_u + R1)$  fraction of the supply bus. Practical capacitors are also endowed with a shunt resistance component ( $R_c$ ) corresponding to their DC insulation quality and terminal leakage.  $R_c$  and  $R_u$  are effectively connected in parallel. In addition, most transistor circuits are assembled on printed circuit boards which introduce further leakage components, the magnitude of which depend on the skill of the designer. For these reasons the available maximum delay for the simple unijunction circuit is usually limited to 20 to 60 seconds depending on the quality of the particular components, materials, and construction.

The simplest possible timing device is the unijunction transistor, a common arrangement for which is illustrated in Figure 2-32. The circuit operates in the following manner. When power is applied, the capacitor C1 charges towards the positive rail potential via R1. When the voltage across C1 reaches the peak point for the unijunction transistor, the transistor conducts heavily and C1 discharges through the relay K1, following which

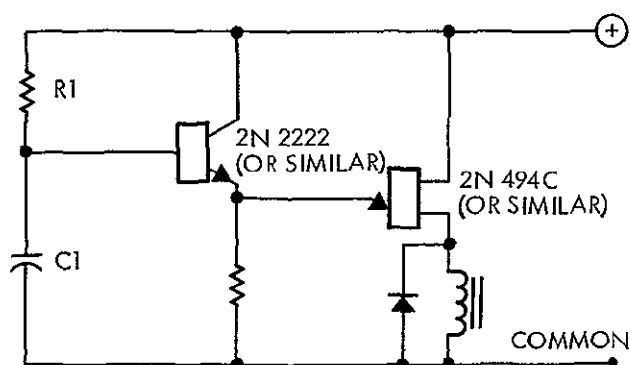


Figure 2-33  
UNI-JUNCTION WITH ISOLATION STAGE

The easiest way to extend the time to that needed for the platform timer is to isolate the leakage resistance of the unijunction emitter from the timing components. This isolation can be attained by interposing a high-quality starvation current silicon transistor, or an FET, between the unijunction and the R1-C1 junction, as depicted in Figure 2-33

The collector cutoff leakage current for the 2N2222 is  $10^{-8}$  ampere (maximum) and the minimum DC  $\beta$ , for a 100-microampere collector current, is 35. At a collector current of about 10 microampere the corresponding DC gain is about 20 (see Figure 2-34). Thus, the base current drive required is 0.5 microampere, a 4:1 improvement over that required for the 2N1671 emitter.

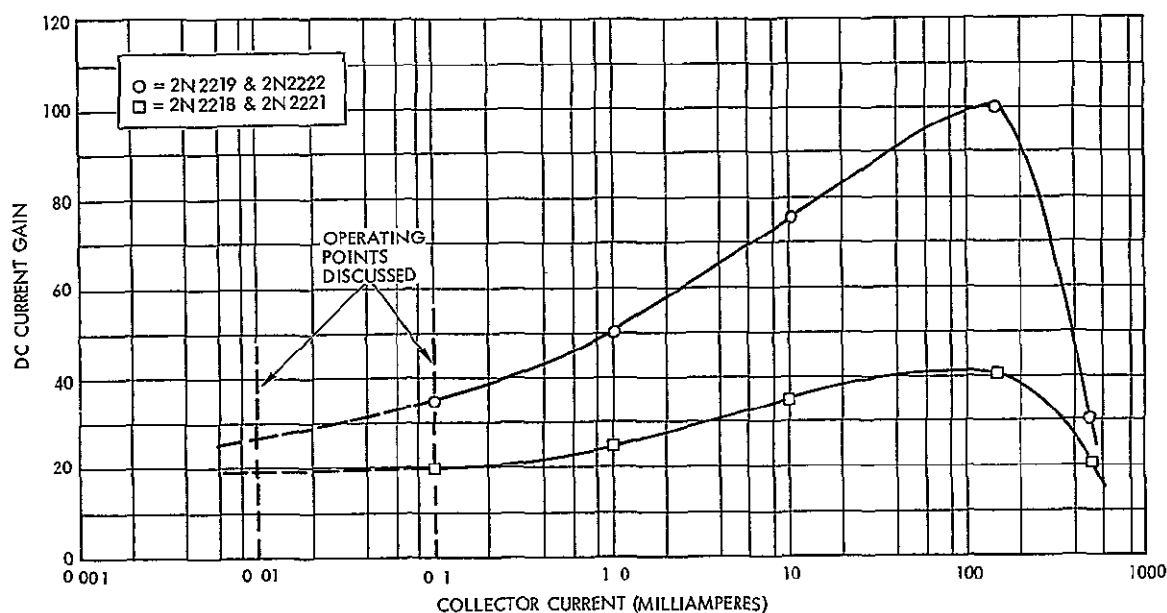


Figure 2-34  
DC CURRENT GAIN VERSUS COLLECTOR CURRENT  
FOR NPN SILICON TRANSISTORS

For a really impressive improvement we must turn to the insulated-gate, field-effect transistor rather than a junction unit operated in a starvation mode.

Typical of such low-cost units is the RCA 3N142 family. Such units exhibit a control gate input resistance of the order of  $10^6$  megohms. By contrast a 2N2222 family silicon junction unit operated at a base current of 0.5 microampere, and a unijunction with a point voltage of 12 volts, would be 12/0.5 or 25 megohms. The FET offers an improvement of 40:1 in shunt loading.

The arrangement illustrated in Figure 2-33 would not work in practice because the unijunction requires a source of energy in its emitter circuit to effect the firing action when the point voltage is attained. For relay load shown in Figure 2-32, the capacitor C1 has a minimum value below which the relay will not pull in. For driving solid state circuitry rather than a relay, K1 is replaced by a resistor. Such external circuits also exhibit shunt capacitance. Reduction in C1 under such circumstances reduces the pulse output amplitude and rise time available. These considerations limit the value of C1, typically, to a minimum of between 0.0003 and 0.001 microfarads. Thus, when an isolation element is interposed between the R1C1 timing components and the unijunction, an appropriate value of energy storage capacitor must be included for the unijunction emitter.

Finally, since the unijunction firing action now discharges this added energy storage capacitor, rather than the timing capacitor (C1), additional means must be provided to discharge C1. Relay contacts of K1, or an FET, shunted across C1 can perform this role.

Yet another solution to the loading problem is to provide a supplementary commutation oscillator arranged to periodically connect the unijunction to the C1. By choosing a low duty cycle for this commutation, the average loading can be reduced by as much as three orders of magnitude. One circuit arrangement for implementing this concept involves a second unijunction transistor to produce the interrogation pulses. A pair of very low reverse leakage current diode gates is inserted between C1R1 and the

unijunction emitter, and back biased from a divider across the main power bus line. Low level pulses from the supplementary unijunction are periodically added to the potential of C1. As C1 nears the point voltage of the unijunction, one such a pulse is just large enough to forward bias the added gate diode, and trigger the emitter

A somewhat different approach to extending the basic performance of the unijunction is to add a counting circuit between the output of the unijunction and the load so that only every nth pulse is used as a command. Since the basic unijunction circuit can provide a time delay of 30 seconds, a simple -4 in cascade would yield a 2-minute PRF

This particular approach is attractive because it involves digital circuitry, which is more tolerant of component aging and as a result more reliable. Most digital logic is not designed for power economy, because of the consequent need for high circuit impedances and in turn low speeds. Since only four transistors are needed for a basic -4 pair of flip-flops, discrete components are a reasonable approach.

In the earlier discussion of the isolation device, data was presented on the 2N2222 family. These devices work well with collector currents well under 100 microamperes. Assuming operation at an  $I_C$  of about 100 microamperes, the base current will be only 3 percent of  $I_C$  and can be neglected. The 'on' limit of each flip-flop will then require 100 microamperes, and the complete counter (for -4) entail a 200-microampere bus demand.

In the preliminary platform design TRW has assumed 10 milliwatts of steady power drain for the timer, corresponding with a 24-volt bus supply to a current of 420 microamperes. This very conservative allowance will permit us to implement as much as a -16 circuit, greatly easing the insulation and component constraints for R1 and C1, and allow the range of available PRF values to be extended to 4 minutes. The divider concept is also a convenient means for providing a wide range of preset PRF values, by selecting the relevant stage tapping points for transmitter control.



## CONTENTS

	Page
3    HARDWARE DESIGN	3-1
3.1    Data Collection Platform	3-1
3 1.1    Configuration Packaging	3-1
3 1.2    Electrical Design	3-3
3 1.3    Analog Signal Conditioning	3-4
3.1 4    Multiplexing, Analog-to-Digital Conversion, and Timing	3-4
3.1 5    Transmitter	3-10
3 1.6    Power	3-12
3 1.7    Antenna	3-14
3 1.8    Packaging	3-16
3.2    Spacecraft Receiver	3-16
3 2.1    Frequency Selection	3-19
3 2.2    Crystal Filter Requirement	3-20
3 2.3    Local Oscillator Chain	3-21
3 2.4    Noise Figure	3-21
3 2.5    AGC versus Limiting	3-22
3 2.6    Gain Distribution	3-22
3.2.7    Power	3-24
3 2.8    Integrated Circuits	3-24
3 3    Ground Signal Recovery	3-24

### 3. HARDWARE DESIGN

This section presents the results of the TRW hardware design efforts. It reflects those changes resulting from recent meetings with NASA. Design tradeoffs have been completed and specific design recommendations are offered.

#### 3.1 DATA COLLECTION PLATFORM

The current design objectives in preparing specifications for the data collection platform are the following:

- So specify the performance that the units are readily producible by U.S. industry
- Call out a simple design that will allow a minimum unit cost compatible with useful field performance
- Maximize the flexibility of the signal processing so that the units can be used with almost any sensors that may be available without redesign or modification
- Strike the most cost-effective balance between environmental performance, cost, and complexity.

##### 3.1.1 Configuration Packaging

Because of the extremely wide range of temperature and general environmental conditions that must be anticipated, design of a low cost platform to operate fully exposed to the weather is difficult. TRW has concluded that in the interest of achieving an acceptably low cost, platforms should be designed for deployment inside the readily available and already widely used instrument shelters described in Section 2.6. It appears that such a compromise will provide the most cost-effective total solution.

Despite the obvious attractions of such a concept and its cost benefits, there will be many situations where such protective facilities do not exist, cannot be economically provided, or are not desired by the end-user. To meet these situations, it is necessary to specify an appropriate packaging configuration. The preferred approach is an attache-case type of outer housing incorporating gasket seals against dust and water. A major problem with such units involves the mechanical performance of



the external electrical connectors for the sensors and prime power inputs. To assure adequately reliable performance under conditions of blown dust, sand, and rain, TRW recommends waterproof connectors with protective boots and an overall plastic bag.

In order to secure the best of both concepts, the off-the-shelf housings and the rugged attache-case, TRW recommends standard printed circuit board circuit elements for the digital and analog portions, such that these can be installed in

- Low-cost, simple casing for controlled environment (if desired)
- Special shock-protected cylindrical case for air drop applications (at a later date, if still of interest)
- Protective attache-case enclosure for unprotected environments (this will be the standard packaging arrangement)

The attache-case enclosure is available as off-the-shelf items from several suppliers, specifically Zero Manufacturing and American Aluminum.

It is apparent that there is little point in designing a platform that works over the complete range of environmental conditions experienced in the U.S. if the associated sensors have a far more restricted performance. Recognizing this problem TRW has made an analysis of the benefits available from a less demanding specification. Table 3-1 presents the original environmental specification and the latest revised version applicable to the unprotected attache-case design.

Table 3-1 Original and Revised Environmental Specifications

	<u>Unprotected</u>	<u>Proposed Lesser Specification</u>
Temperature	-60 to +140°F	-40 to +104°F
Sand and dust	Direct impact	Direct impact
Humidity	Continuous 98% RH	Continuous 80%
Ice storm	2 in ice coating	2 in. ice coating
Wind	Up to 100 mph	Not applicable
Salt spray	Continuous exposure	Continuous exposure
Atmospheric pressure	15 to 32 in Hg	15 to 32 in Hg

It appears that extremes of humidity and the sand and dust can be adequately alleviated by incorporation of conventional (replaceable) desiccants inside the platform casing in association with a good gasket-seal and high quality connectors.

### 3 1 2 Electrical Design

The data handling subsystem for the platform accepts and encodes preconditioned analog sensor data and formats this data, along with preamble and address information, for subsequent transmission. The data handling is based on the following factors

- Acceptance of eight distinct analog signals.
- Conversion of each analog signal into an 8-bit digital word.
- Provision for temporary storage of the encoded digital information (64 bits) and timing for subsequent readout.
- Generation of 25 bits of digital preamble information.
- Generation of 3 bits of digital synchronization.
- Provisions for 10 bits of digital address information to accommodate up to 1023 distinct addresses.
- An 8-bit error correction code for the processed sensor and address information.
- Readout of the resulting 110-bit data message.
- Subsystem power control and processing a rate determined by the PRF oscillator, presently at 4-minute intervals to provide low DCP duty cycles which result in conservation of input energy.

The electrical design for the platform is illustrated in Figure 3-1, from which it can be seen that there are six subsidiary elements

- 1) Analog signal conditioning
- 2) Multiplexing, analog-to-digital conversion and timing
- 3) Error detection encoder
- 4) 400 MHz transmitter
- 5) Power and power control
- 6) Antenna.

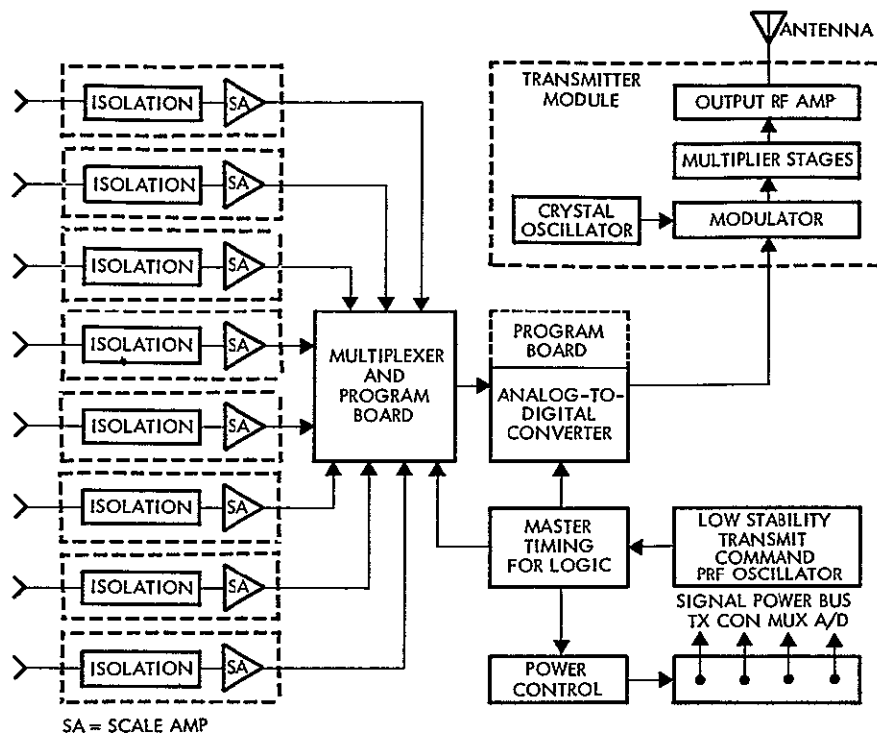


Figure 3-1  
DATA COLLECTION PLATFORM BLOCK DIAGRAM

### 3. 1. 3 Analog Signal Conditioning

Eight channels of input sensor signal conditioning are provided, each channel incorporating capability for amplification, attenuation, filtering (bandwidth limitation), DC offset and common mode isolation. The features use off-the-shelf, low cost, integrated-circuit operational amplifiers. The actual combination of characteristics incorporated in a particular channel will be determined by a "mode plug" which allows substitution of various feedback networks around the operational amplifiers. Balanced input will permit adequate common mode rejection for floating and differential sensor modes.

### 3. 1. 4 Multiplexing, Analog-to-Digital Conversion and Timing

The outputs of the eight signal conditioners are tied to a single input bus associated with the analog-to-digital converter via separate channel gates. These gates are controlled by command logic elements

which form the master timing. The sequence for channel multiplexing is controlled by a small plug, serving as a command patchboard, permitting flexibility in the sensor data acquisition mode, ranging from eight measurements of one sensor through one measurement of each of eight sensors.

The timing of the complete platform is derived from a relatively low stability PRF determining oscillator. The PRF timing oscillator provides a periodic pulse to the master timing logic and an enable command to the power control switch which applies power to the signal conditioner, multiplexer, analog-to-digital converter and transmitter. The pulse applied to the timing logic initiates the preamble, bit synch, and platform identification code, the logic generates the requisite sequential commands to connect the channel amplifiers to the multiplexer, and for each connection, initiates the analog-to-digital quantization cycle. The resultant data is applied to the 8-bit error detection coding register.

The 102 bits are fed to the transmitter modulator and to the coding register via the modulo-two adders associated with a selected encoding polynomial. Following the basic message (102 bits) the modulo-two adder feed is disconnected and eight subsequent shift pulses applied to append the 8-bit BCH error detection code to the message. The completion of the eight shift pulse for the BCH code results in the master timer sending an "off" command to the power control timer.

In the proposed data handling subsystem, Figure 3-2, a two clock system is recommended for the processing functions.

The subsystem master clock (2 kHz) provides timing for the format generator (preamble and synch), the address generator and readout of the 64-bit buffer register. Both clocks operate under control of the subsystem control unit and are initiated by subsystem power turn-on. The dual clocking system provides independent operation of each portion of the subsystem, thereby allowing data continuity that otherwise would not be possible except through design complexity. In addition, the 100 kHz portion of the subsystem can be shut down after analog-to-digital processing and storage, thereby conserving system power since the

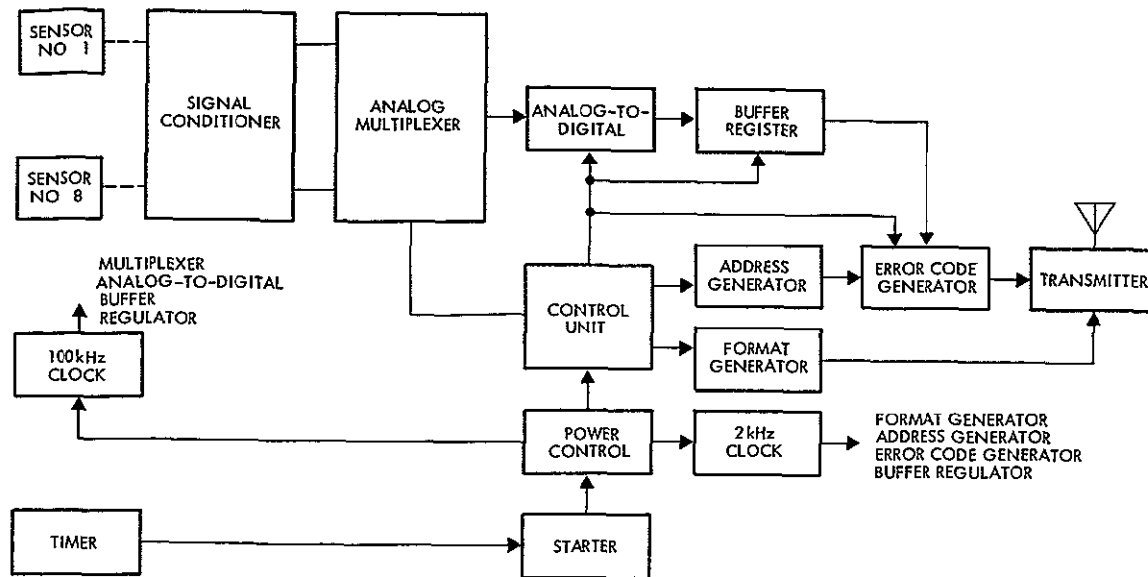


Figure 3-2  
DIGITAL SIGNAL PROCESSING AND TIMER PORTION  
OF THE DATA COLLECTION PLATFORM

multiplexer and analog-to-digital converter are not required during the entire duty cycle.

Both clocks can be implemented as free-running multivibrators. The rate for the data clock was arbitrarily selected to assure processing and storage of analog data within a desirable time frame. Other data clock rates may prove superior for ultimate subsystem processing, the data clock rate will be selected during the equipment design phase. The data clock rate selected will not affect the data handling subsystem within a wide range. An alternate approach is to derive the 2 kHz master clock from control unit programming and a 128 kHz data clock. Such topics will be considered during the detailed DCP design of Phase D.

The message format provided by the data handling subsystem includes the following elements:

- Preamble 25 bits, all 1's
- Synchronization 3 bits, 010
- Sensor data eight 8-bit words, 64 bits

- Platform address, 10 bits
- Error detection, 8 bits

Total 110-bit digital message.

The format generator generates 25 bits of preamble and 3 bits of synchronization under control unit programming. The format generator will be most economically implemented as a five-stage binary counter and associated control and output logic. Upon command, the output logic and counter are enabled via the control unit. Counts 25, 26, and 27 can be used to successively disable, enable and disable the output logic providing the 010 synchronization pattern. Count 28 will disable the counter from the 2 kHz master clock, isolating the format generator from the subsystem communication channel.

The analog multiplexer provides low impedance switching of the eight preconditioned analog sensor inputs into the analog-to-digital converter. Each analog input will be sequentially interrogated under control provided by the output of the analog-to-digital word and the 100 kHz data clock. The sample time of each input is determined by the switching and settling times required for each switched analog input and the analog-to-digital conversion time required.

Eight bit conversion of the multiplexed analog data is provided by an analog-to-digital converter utilizing successive approximation. This approach is recommended to provide the most reasonable tradeoff between available conversion times and hardware complexity.

The successive approximation technique requires one clock time per significant bit of converted data. In this case each analog word conversion will take approximately 80  $\mu$ seconds for the resultant 8-bit digital output. This estimate does not include switching and settling times of the analog multiplexer.

Among the other approaches to analog-to-digital conversion are the counter method and the simultaneous method. The counter method can require up to  $2^n$  counts for an  $n$ -bit digital conversion. The time is variable depending upon the magnitude of the incoming analog voltage

At a 100-kHz clock rate the maximum conversion time would be approximately 2.56 msec per word, so sufficient conversion time for all eight words might not be available during the format generator processing period. (Sensor data is transmitted after the format generator output ) The simultaneous conversion method provides sufficient speed of conversion but hardware complexity increases geometrically with digital word lengths. In order to provide an 8-bit digital word 255 separate voltage comparators would be required.

The successive approximation method uses a single comparator and a feedback-controlled digital-to-analog converter. These elements provide the conversion speed and relative simplicity desired for the platform converter. The conversion is done by successively comparing the incoming analog signal with a voltage generated by the digital-to-analog portion of the converter. The generated voltage is progressively subranged in a direction determined by the previous comparison. The initial subrange decision begins at half of the maximum analog voltage range and proceeds through each subrange which is successively halved in a direction dependent on whether the previous comparison was greater than or less than the generated comparison voltage. At the end of eight approximations the 8-bit digital number is resolved within the magnitude of the least significant bit.

The 64-bit buffer register provides temporary storage of the eight 8-bit converted digital words. Its purpose is to assure data continuity upon subsequent readout. Data processing and storage take place during a portion of the time when the format generator is in operation at the 2 kHz data rate.

The buffer provides data continuity by controlled lock-in and lock-out from the control unit during those periods during the conversion cycle when multiplexer switching and stabilization may be required. After the analog-to-digital data (64-bit) is read into the buffer at the 100 kHz rate the buffer is disabled until data readout is desired. Buffer readout follows the last bit from the format generator and occurs at the 2 kHz clock rate. Buffer register data is processed through the error

code generator concurrently with data transmission. In the absence of the buffer register it would be necessary to convert and process the analog data in real time at the 2-kHz data rate, and uniform periods for the conversion of the significant bits in the resulting digital words would not be available as the result of multiplexer switching and settling times. The requirement for time processing would result in design complexity and problem areas in error code generation since data continuity requires that digital data be immediately available and uniform following the output of the format generator.

The address generator provides a distinct binary address for each of up to 1023 platforms by a 10-bit patchable address plug. The patched address value in each platform occurs in parallel form, thus address is read out by a 10-bit parallel-to-serial converter implemented via a four-stage binary counter. Readout of the address follows analog-to-digital data at the 2 kHz data rate. The address also is processed through the error code generator.

The error code generator provides an 8-bit detection code for the 74 bits of analog-to-digital and address generator data. It is implemented by an eight-stage feedback shift register with exclusive 'or' interstage coupling at four of the stages. The analog-to-digital and address generator data are shifted into the error code generator and into the communication channel for transmission at the same time. After all information bits (74) have entered the feedback register the feedback circuitry is disabled by gating. The remaining contents of the shift register are then clocked out into the communications channel. The 8-bits clocked out after the feedback circuitry has been disabled along with the previous information data provide the complete code signal for subsequent reception and error detection.

The timer initiates a basic 2-minute subsystem operation cycle within which data processing and transmission take place. This value will be preset by a PRF plug. The proposed method for deriving the desired timing interval makes use of an RC relaxation transistor oscillator circuit and a three-stage binary counter. The transistor pulse



generator produces one pulse every 15 seconds and the counter counts eight output pulses, yielding the 2-minute period. This approach is estimated to dissipate < 10 milliwatts and requires only three flip-flops, an oscillator, and RC timing. By use of the counter the timing constant is reduced to 15 megohm microfarads and reliable performance over the temperature range assured. During the circuit design phase this portion of the circuit will be given very detailed consideration since its power is used continuously, and is a major factor in establishing battery capacity. Reliable operation of transistor circuits at very low collection currents has been established over a wide temperature range. Transistors are available, with specially 'doped' emitters to assure adequate current gain at low temperature and minimum current. Operation at 50 to 100 microamperes collector current is feasible with units such as the 2N2222 family. This was discussed in detail in Section 2.10.

The 2-minute timer output pulse operates the power control unit, applying power to all required components during the data processing time. A reset signal from the control unit at the end of the data message disables power until the next timer output pulse occurs.

### 3.1.5 Transmitter

Because the gross timer is no longer proposed, there is no requirement for precise timing of the transmission period. TRW has thus revised the transmitter design to include a crystal oscillator operating at approximately 66.9 MHz, followed by a frequency tripler, a doubler stage, a biphase modulator, and a process amplifier (Figure 3-3). This simple design, with a relatively high basic oscillator frequency, reduces the parts count, cost, and alignment time. The overall DC to RF efficiency is approximately 40 percent. The transmitter is designed for a low duty cycle of less than 0.1 percent.

The selection of crystal oscillator and permissible temperature coefficient depend on the actual temperature range to be experienced by the crystal (see Section 3.1.1).

A 66.9 MHz crystal is chosen to be the operating frequency of the crystal oscillator, because a times-six multiplier produces 401.9

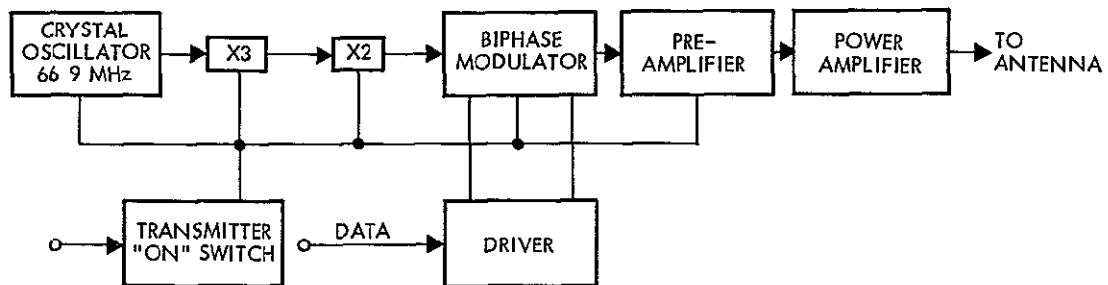


Figure 3-3  
TRANSMITTER FOR DATA COLLECTION PLATFORM

MHz, the desired output frequency. The circuit used excites the crystal in a fifth overtone mode. The circuit is stable throughout the temperature range with good starting characteristics. Output power is easily set with a transformer in the collector circuit which raises the efficiency of the stage.

The times-three multiplier, operated Class C, multiplies the 66.9 MHz signal to 200.9 MHz. Other harmonics are significantly lower in amplitude than the third harmonic. The second and the fourth harmonics are down at least 30 db, with all others down 50 db or more. The times-two stage provides a 401.9 MHz signal to the biphase modulator. The power output to the biphase modulator is one milliwatt in order not to over-drive the modulator.

The biphase modulator uses two hot carrier diodes that are each alternately forward and reverse biased to couple the 401.9 MHz signal through the appropriate output winding on the modulator transformer. By switching windings, a 180-degree phase shift is obtained.

In the driver the data signal is conditioned into a complementary signal by an inverter in order to reverse bias one diode when the other diode in the modulator is conducting. The biphase modulator switching frequency is at the 2 kbits/sec rate.

Since the power out of the modulator is around -10 dbm, two stages of gain are required before the power amplifier stages. These amplifiers have a minimum gain of over 10 db, each with adequate bandwidth to

provide sufficient drive to the Class C power stages. These two stages are controlled by the same power switch which removes power from all other low level stages.

The transmitter on-off switch turns off all low-level stages by removing the collector voltage to keep the power drain on the battery power to a minimum when the transmitter is not used. Also, the complementary signal developed by the driver reverse biases one-half of the biphase modulator while the other half is operative in order to transmit only a CW signal when no data is being sent and the transmitter is on.

Class C operation is used on the power amplifier stages for high efficiency. Three stages of amplification raise the power from 20 milliwatts to 7 watts. The first two stages average a gain of 9.5 db each, with the last stage having a gain of 6.7 db. The 7-watt output is the nominal power at room temperature and nominal 28 vdc in order to provide some margin above a 5-watt minimum requirement.

### 3.1.6 Power

Several different power sources have been investigated, as reported in Section 2.7. Of these only line power and buried batteries appear able to meet the combined requirements of temperature range and low unit cost. Since no dramatic breakthrough in battery technology appears likely before the Phase D fabrication cycle, TRW recommends only these two power sources for the platforms. The potential advantages available by burying conventional low-cost secondary batteries is discussed in Section 2.6.

Off-the-shelf calcium lead acid secondary cells intended for commercial use appear to be quite suitable, depending primarily on their long-term self-discharge characteristics. These cells are relatively inexpensive and readily available. For both convenience and safety of handling by rangers or other installation personnel we propose that such batteries be housed in low-cost thermoplastic boxes such as those in common use for small boats.

To meet the low-cost requirement only a commercially available battery could be considered. The lead-acid type battery is selected since such a battery represents the least expensive type available capable of meeting the electrical requirements. There are two basic types of lead-acid batteries available, antimony lead and calcium lead. The lead alloy type refers to the battery grid metal composition. The common car or truck battery is of the antimony lead type while charge retention and stationary batteries are of the calcium lead type. The calcium lead battery is selected for this application to meet the requirement of at least 6 to 9 months of operation without recharge. The relative charge retention characteristics for a 15 day period are shown in the following table

	<u>Temperature</u>	
	<u>77°F/25°C</u>	<u>92°F/53°C</u>
Antimony lead	9% loss	18% loss
Calcium lead	0.5% loss	1.0% loss

An antimony lead type battery is out of the question because of its self discharge losses. The calcium lead battery costs approximately 15 percent more than the antimony lead.

The cable from the battery platform would be direct buried, and is considered a replacement item in the more severe climates. The line power supply is of conventional design. It incorporates a dual winding power transformer with a grounded isolation shield to assure operational safety along with the requisite line and load regulation to ensure correct performance of the electronic circuitry.

Power consumption for the data handling subsystem is based on the following estimate of anticipated hardware and design complexity.

<u>Component</u>	<u>Power Estimate</u>
100 kHz clock	300 mw
Analog multiplexer	negligible
Analog-to-digital converter	500 mw
64-bit buffer register	160 mw
2 kHz clock	300 mw
Error code generator	46 mw

<u>Component</u>	<u>Power Estimate</u>
Address generator	31 mw
Format generator	28 mw
Power control	160 mw
Starter	2 mw
Timer	10 mw
Control unit	164 mw
Total power during transmission	$\approx 17$ watts
Current demand (from 24 volt bus)	71 milliamperes

Power consumption for the 2 kHz portion of the subsystem will depend in part on the amount of control implemented for each component and the minimum "on" time necessary. This time can vary from that required to generate the 10-bit address (5 milliseconds) up to the time required to generate the entire data message (approximately 55 milliseconds). If it is assumed that the maximum operational time is about 60 milliseconds out of each 4-minute interval the duty cycle will be 0.025 percent.

Based on continuous "on" time for the timer and a 60-millisecond operational time for the remainder of the subsystem, the anticipated energy for the data handling subsystem should be about 28.1 watt-sec/cycle yielding an average power dissipation of 117 milliwatts.

The relative current requirements for the three most significant operations within the platform are illustrated in Figure 3-4.

### 3.1.7 Antenna

The approach selected for the platform antenna is a crossed dipole arrangement based on vee elements. Such an arrangement will provide the following performance:

Frequency	401.9 MHz
Power rating	10 watts
Polarization	RH Circular
VSWR	1.5:1 (ref 50 $\Omega$ )
Minimum gain	0 dbi (down to 7-1/2 deg above horizon)
Axial ratio	5 db max. (down to 7-1/2 deg above horizon)

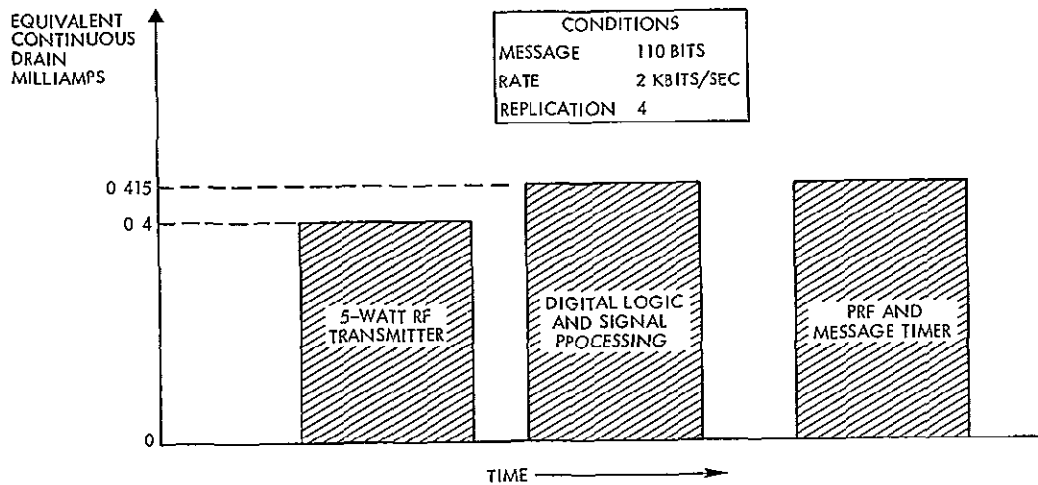


Figure 3-4

RELATIVE OPERATIONS TIME AND POWER CONSUMPTION  
FOR DATA COLLECTION PLATFORM

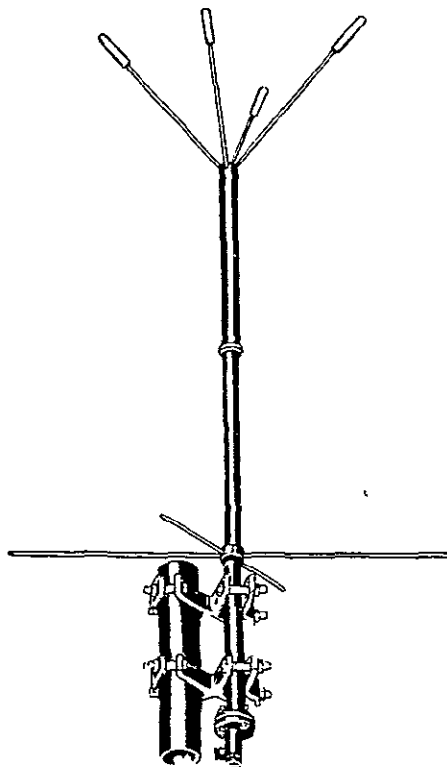


Figure 3-5

GENERAL APPEARANCE OF  
ANDREW ANTENNA MODELS  
54298-2A and 2B

The electrical performance of the ground antenna does not include RF cable losses due to ground environment or multipath. These problems have been considered during the development of the ground platform system. TRW believes the performance of the Andrew antenna (Figure 3-5) to be optimum for the ground platform. The antenna should be mounted as high off the ground as possible on a relatively flat terrain. The antenna will be mounted on a mast which is supported by the ground platform. Low loss coaxial cable, such as helix could be used between the platform and the antenna, but this type of cable is more susceptible to physical damage and for this reason a regular solid dielectric cable is recommended.

The Andrew antenna Model 2A is an omnidirectional hemispherical antenna which

provides a relatively constant gain from horizon to horizon in righthand circular polarization. The minimum gain of the antenna from 7.5 degrees above the horizon is 0 dbi and maximum axial ratio is 5 db. The maximum VSWR of the antenna is 1.3 to 1. The Andrew antenna Model 2B is exactly the same as the 2A except that the minimum gain of the antenna from 7.5 degrees above the horizon is 1 dbi and the maximum axial ratio is 3 db.

### 3.1.8 Packaging

The data collection platform for Phase D will be assembled in standard, lightweight, multipurpose carrying cases. Such units are available off the shelf in a wide range of sizes without tooling changes, from several vendors, aluminum units from American Aluminum (NJ), for example, and fiberglass units from Skydyne, Inc. (NY).

The main advantage of fiberglass lies in its immunity from corrosion and the extreme ease of fabricating internal partitions and assembly attachment features with like material in any small manufacturer's shop. The aluminum case provides electrostatic shielding, a common return (ground) for components and immunity from low temperature embrittlement.

We conclude that the metal case is preferable. The general appearance of these cases and range of sizes available is shown in Figure 3-6.

## 3.2 SPACECRAFT REPEATER

The spacecraft equipment supporting the data collection system will operate as a frequency-translating repeater. The uplink signals at 401.9 MHz are translated to S-band and transmitted to the NASA ground tracking stations via a subcarrier of the unified S-band equipment. The spacecraft equipment complement to support the DCS function (Figure 3-7) includes the antenna, changeover switch, and dual UHF receivers.

The antenna selected for the spacecraft is a turnstile, consisting of a pair of crossed dipoles mounted over a ground plane. The separate dipole elements are fed through a split tube balun and positioned over a ground plane. The time phase quadrature of the turnstile is obtained by

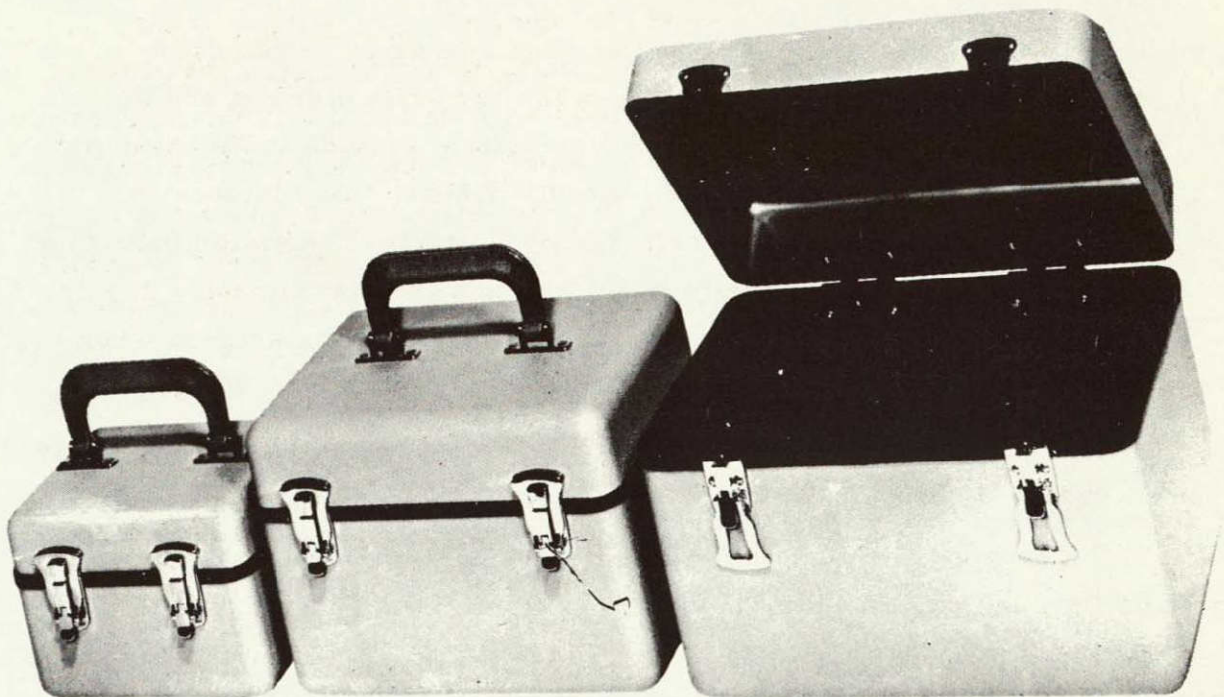


Figure 3-6

AMALCO MULTIPURPOSE ALUMINUM  
CARRYING CASES

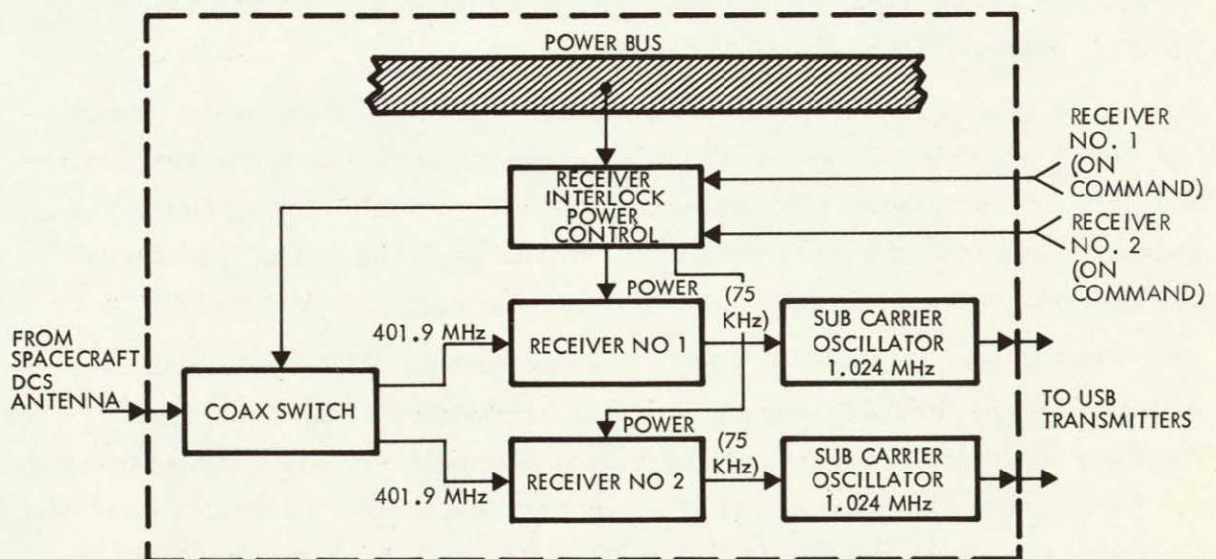


Figure 3-7

DCS RECEIVER IN THE SPACECRAFT, ACTING AS  
FREQUENCY-TRANSLATING REPEATERS



adjusting the lengths of the adjacent elements to give the required 90-degree phase. The spacing between the turnstile element and the ground plane is approximately 0.4 wavelength to provide the maximum gain of the antenna at  $\pm 60$  degrees. At 401.9 MHz, this distance is approximately 12 inches. Figure 3-3 shows a typical radiation pattern of the antenna. The maximum gain of the antenna is approximately 2.5 dbi at approximately  $\pm 60$  degrees off axis. The VSWR of the antenna when matched to 50 ohms resistive is less than 1.3 to 1 at  $401.9 \pm 1$  MHz.

The conductive surface directly below the antenna is approximately 20 inches in diameter centered about the antenna mast.

Because all the signals from the many data collection platforms are routed through the spacecraft, failure of an element in the satellite could result in the loss of all sensor data. For this reason redundant receivers are recommended, as implemented in Figure 3-7. The DCS turnstile antenna feeds a coaxial relay which allows the received signal to be applied to either of the identical receivers.

The output of each receiver is coupled to a separate, identical, 1.024 MHz subcarrier modulator. The modulator outputs are applied to the two identical unified S-band transmitters.

The coaxial switch command signal is interlocked with the power bus feeds so that only the desired receiver, that to which the antenna is coupled, is energized. The selection of receiver is on the ground, via coded commands, the receiver-on command arriving at the interlock power control from the command distribution unit.

The arriving platform signal is a narrowband PSK-modulated carrier. All signals are located within a 100 kHz bandwidth. The spacecraft receiver does not separate the individual platform signals but amplifies the complete band. The front-end of the receiver accepts a 120 kHz band of platform signals in the range 400 to 406 MHz, allowing for the doppler shift of  $\pm 8.5$  kHz. The exact receiver tuned frequency is determined by the frequency of the first local oscillator crystal.

The design is a double conversion arrangement with a first IF frequency of 26 MHz and a second IF of 75 kHz. No automatic gain control

is used, and the output is arranged to limit at 1.0 volt rms when the input signal level equals or exceeds -120 dbm. The output from the receiver is thus a frequency translation of the UHF input spectral segment and consists of a 120 kHz band centered about a 75 kHz IF frequency. This broadband signal frequency modulates a 1.024 MHz subcarrier oscillator using a nominal modulation index of 1.5. The resulting signal is applied to the unified S-band spacecraft transmitter.

### 3.2.1 Frequency Selection

The design of the receiver is influenced by the following requirements:

- Frequency translation without demodulation
- Low frequency of IF output for maximum modulation index SCO
- Image rejection requirements
- Spurious response rejection
- Input frequency and bandwidth specifications

The low output IF frequency of 75 kHz needed to minimize the effect on PRN ranging and other unified S-band services would require a pre-selector ahead of the mixer to attenuate the image ( $2 \times 75 \text{ kHz} \pm 400 \text{ MHz}$ ) if a single conversion receiver were used. Crystal filters are not available at 400 MHz, therefore, at least one conversion is required to reach the frequency range of a practical crystal filter. Crystal filters with a center frequency from 15 to 35 MHz with a 125 kHz bandwidth are, however, perfectly practical. Therefore the first IF frequency is chosen to fall within the range of 15 to 35 MHz.

The second consideration is the image produced from the first mixer. High power ground transmitters operate in the range from 225 to 339.9 MHz, therefore, it is desirable to place the image above the input frequency. Since high-power TV transmitters are located from 470 to 890 MHz, the first IF frequency is limited to  $470 - 406/2 \approx 32 \text{ MHz}$  maximum. Assuming some TV splatter at 470 MHz, a guard of 6 MHz separation from the image is recommended, placing the first IF at 26 MHz. The exact frequency of

the first IF is established by making sure that the harmonics of the second local oscillator do not fall in the RF input band of 400 to 406 MHz

$$400 \text{ MHz} - 15 = 26 \text{ } 65$$

$$406 \text{ MHz} - 16 = 25 \text{ } 35$$

$$26 \text{ } 65 - 25 \text{ } 35 = 1 \text{ } 3 \text{ MHz}$$

Therefore the first IF frequency should be

$$\frac{1 \text{ } 3}{2} + 25 \text{ } 35 = 26 \text{ } 0 \text{ MHz}$$

To produce a 75 kHz IF the second local oscillator must be 25 925 MHz This places the oscillator harmonics at

$$25 \text{ } 925 \times 15 = 388 \text{ } 875 \text{ MHz} \quad ,$$

and

$$25 \text{ } 925 \times 16 = 414 \text{ } 8 \text{ MHz}$$

Crystal filters typically have spurious responses on the high side of their center frequencies The second mixer image should be on the low side since the crystal filter has no spurious responses in that frequency range, and provides the necessary attenuation

The receiver configuration just described produces no troublesome conversion spurious responses in the first mixer The second mixer generates even-order spurious signals, namely,  $2F_2-2F_1$ ,  $3F_2-3F_1$ , and  $4F_2-4F_1$  all of which fall in band Manufacturers' specifications for mixers indicate that these spurs are typically down 50 db from the desired signal, in double-balanced mixers, which is the planned circuit configuration, which places the spurious responses well below the noise level in the output signal

### 3 2 2 Crystal Filter Requirement

The input signals can appear anywhere in the 120 kHz bandwidth The link analysis indicates that at a maximum range there is only 1 db excess over the +6 db "good design practice" margin for system performance For this reason the IF bandwidth was specified in terms of the -1 db points rather than the -3 db points

The required bandpass at the 1 db point is

For broadband data signals = 100 kHz

Worst case doppler ( $\pm 8.5$ ) = 17 kHz

Crystal tolerance ( $\pm 4.0$ ) = 8 kHz

Total bandwidth = 125 kHz

1 db points = 25 9375 to 26 0625 MHz

The lowest IF frequency is

$75 - 62.5 = 12.5$  kHz

Image =  $25.925 - 0.0125 = 25.9125$  MHz

The crystal filter requirements then become

Center frequency	26.0 MHz
1 db bandwidth	25.9375 to 26.0625 MHz
40 db attenuation on low side	25.9125 MHz
High side attenuation	Not critical

At frequencies of 25.9125 MHz and below the filter response must be greater than 40 db down from the center frequency response

### 3.2.3 Local Oscillator Chain

The exact receiver frequency is determined by the first local oscillator frequency. Since the desired input UHF center frequency is 26.0 MHz and the camera frequency is 401.9 MHz, the local oscillator must be  $401.9 + 26.0$ , i.e., 427.9 MHz. To maintain frequency and phase stability and to make a simple and reliable oscillator, the basic crystal frequency should not exceed about 125 MHz. A suitable crystal frequency is 107.25 MHz, which is one quarter of 427.9 MHz. Accordingly, we recommend a first local oscillator chain, a crystal oscillator followed by a quadrupler and culminating in a two-section L-C bandpass filter.

### 3.2.4 Noise Figure

The KMC 5001 transistor is recommended for the RF front-end in the DCS receiver. It has a device noise figure of 1.5 db (typical). Using

two stages of the 5001 with a total gain of 30 db and  $\pm 10$  MHz bandwidth produces less than 2 db noise figure, assuming a conservative 9 db noise figure for the remaining portion of the receiver

### 3 2 5 AGC versus Limiting

The number of signals present at any time in the receiver is variable, best represented as a probability function (see Section 2.4). Since the downlink transmitter requires a constant drive level, either AGC or a limiting receiver must be used. Since the limiting type receiver is less complex and more reliable, it has been selected.

### 3 2 6 Gain Distribution

The basic performance data of the suggested receiver is shown in Figure 3-8. The RF amplifier is a two-stage grounded emitter configuration and provides a minimum of 30 db gain. The receiver noise figure is 2 db when the noise figure from the bandpass filter through the receiver is equal to, or less than 9 db. The 400 MHz bandpass filter has an insertion loss of less than 3 db and the image frequency (455 MHz) is attenuated 76 db.

The single balanced mixer is driven from the local oscillator chain at 0 dbm to provide a conversion loss of 6 db with an 8 db noise figure. Spurious responses in the filtered output from the crystal multiplier chain are more than 40 db down.

The 26 MHz IF amplifier consists of a low noise first-stage, with the overall receiver bandpass characteristics shaped by the crystal filter. Three stages of fixed gain follow the filter, making the total first IF gain 76 db.

The 25 925 MHz crystal oscillator amplifier delivers +10 dbm to the mixer. This injection level and the -23 dbm signal ensures that even order conversion spurious responses are more than 40 db down from the desired signal.

The low pass filter has a cutoff frequency of 150 kHz filtering harmonics of the signal and attenuating the local oscillator. The output level is limited to 1 volt rms across a 600 ohm load.

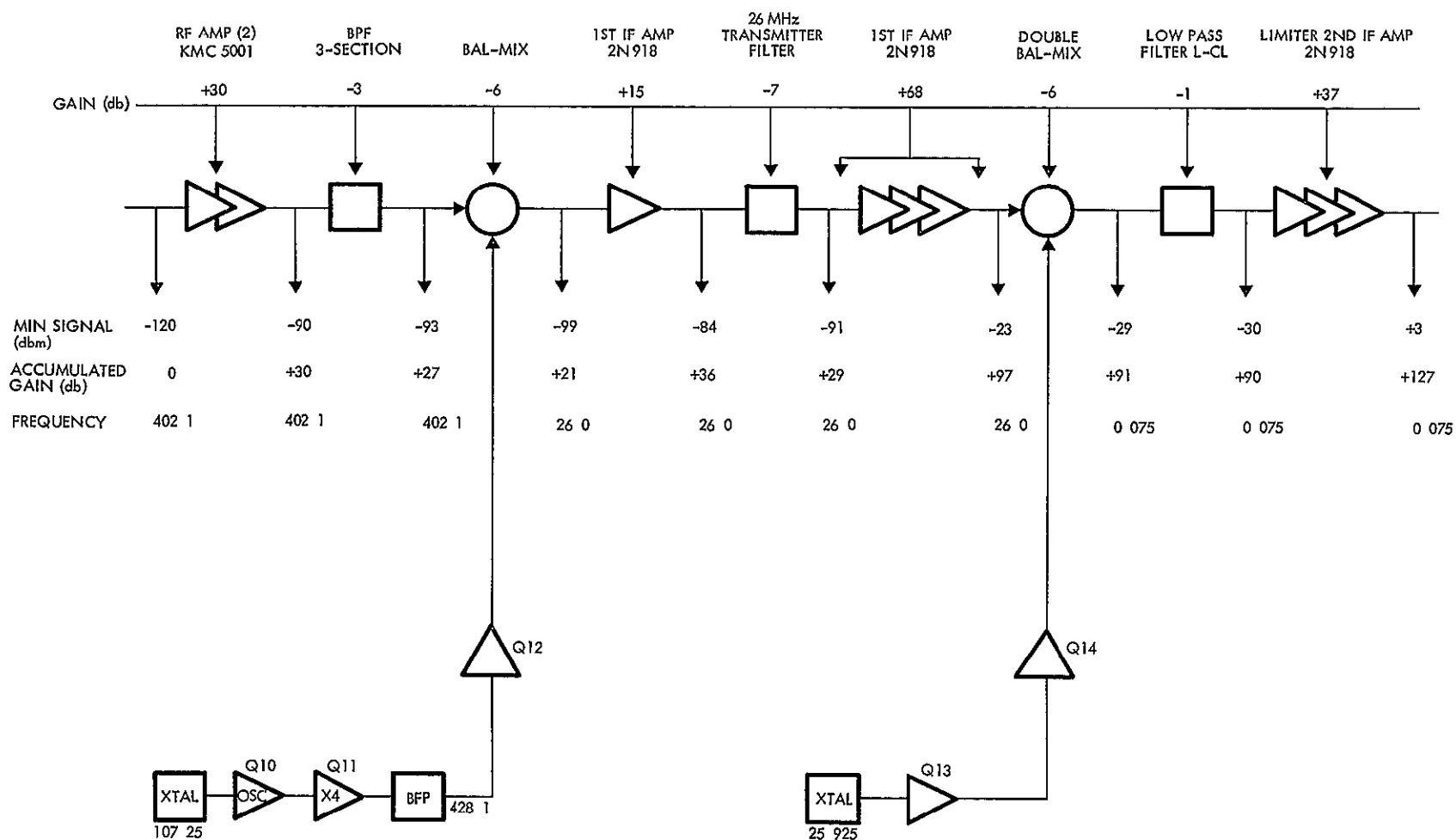


Figure 3-8  
GAIN DISTRIBUTION IN THE DCS RECEIVER

### 3.2.7 Power

The receiver operates from +15 vdc supply. On ERTS a DC-to-DC power converter is necessary for the +28 vdc bus. The series regulator or the DC-to-DC power converter (as required) is contained within the receiver. Separate regulators are provided for each of the two receivers to continue the redundancy and ensure maximum long-term reliability.

### 3.2.8 Integrated Circuits

A tradeoff study is needed early in Phase D to determine whether discrete components or integrated circuits should be used for the IF stages and other sections of the receiver.

## 3.3 GROUND SIGNAL RECOVERY

The composite wideband DSC signal will be derived from the 1 024 MHz subcarrier demodulator of the unified S-band receiver at the NASA ground station. The unified S-band receiver incorporates a narrow-band carrier-tracking phase-lock loop, which will follow the slow excursions of the received signal resulting from the combined effects of doppler on the unified S-band downlink and drifting of the spacecraft's transmitter crystal oscillator. The output available for DSC processing is the 120 kHz spectrum containing periodic and independent PSK signals at spectral locations corresponding to their individual carrier frequencies.

The power budget calculations (see Section 2.4.2) indicate that the carrier-to-noise ratio for unit bandwidth is approximately +50 db. To ensure an acceptable message error rate, the data filter bandwidth must be of the order of 1.2 kHz corresponding to an unfolded subcarrier bandwidth of about 2.5 kHz.

Two methods are commonly employed to acquire dispersed signals, a multiple contiguous filter bank, and multiple phase-lock loops. The contiguous filter bank involves an arrangement of data filters, each having the bandwidth determined by the data rate and message error specifications, but each tuned to a slightly different center frequency. For the DCS design under discussion, 48 filters are needed, each 2.5 kHz wide.

The outputs from the filters are connected to signal presence detectors which, in turn, actuates a demultiplexing (voting) switch

Since more than one signal will occur at any one time, parallel processing is necessary so that the voting commands would direct the demultiplexer to channel data into several output lines. Studies of message arrival statistics indicate that there will seldom be more than five messages present and when there are there is a high probability of message collisions. Five output lines are thus indicated.

The satellite moves during the period of message transmission and, as a result, the carrier experiences doppler change during the message. The worst case doppler rate is about 70 Hz/sec, thus during a message lasting 0.05 second the carrier will change  $0.05 \times 70$  or  $\approx 3.5$  Hz, which is under 0.2 percent of the data bandwidth so that if a signal initially appears within a given filter it will not move significantly during the transmission.





## CONTENTS

	Page
4. MESSAGE COLLISION ANALYSIS	4-1
4.1 Time Domain	4-1
4.1.1 Analysis Model	4-2
4.1.2 Modes of Message Mutilation	4-4
4.1.3 Simulation Results	4-11
4.2 Random Emission Multiple Access With Replication	4-13
4.2.1 Case Where $\binom{N}{2} M_d/T \ll 1$	4-16
4.2.2 Case Where $\binom{N}{2} M_d/T \geq 1$	4-20
4.2.3 Conclusion	4-36
4.3 Dual Random Time and Frequency Mode	4-36
4.3.1 The Frequency Domain	4-38
4.3.2 No Replication	4-41
4.3.3 Replication of Two	4-43
4.3.4 Time-Frequency Tradeoff	4-46
4.4 Computer Simulation	4-48
4.4.1 Simulation on CDC 6500	4-50
4.4.2 Method of Simulation	4-50
4.4.3 Random Number Generators	4-51
4.4.4 Description of the Computer Program	4-51
4.4.5 Recommendations to Reduce Computing Time	4-55
4.4.6 Computer Results	4-56

## 4 MESSAGE COLLISION ANALYSIS

The computer programs developed to validate our statistical analysis of message collision performance has been rewritten in Fortran IV and extensively exercised with the CDC-6500 computer. The conceptual model and criteria for interference in the frequency domain, presented in Section 2.5.1, has been used to generate frequency domain collision statistics. We have also combined the time and frequency models and accumulated system performance message statistics for a fully-random data collection system operation mode, i.e., random in both time and frequency.

### 4.1 TIME DOMAIN

The previously derived equation for the probability of no N-message mutilation was used to determine to what extent N messages can be transmitted without an error. However, there are practical cases where a small percentage of mutilated messages can be tolerated, and these cases are discussed in this section.

If N is the total number of message (as before),  $\alpha$  represents the fraction of total messages, and  $\gamma$  the probability that no more than this fraction is lost, then this situation can be expressed as

$$P(\alpha N) \leq \gamma$$

The first determination will be the upperbound on the number of messages that can be transmitted without exceeding the above statistical relationship.

It is shown that a substantial increase in the number of messages (N) can be obtained. The N increase is more than the system message loss criteria discussed in Section 2.5, although the benefit decreases rapidly as the time domain occupancy approaches unity. A computer program was written to evaluate the probability that exactly K (K=0, 1, 2, ...) messages are lost because of interference. Additional checks were made on these new analytical results by the Monte Carlo simulation program on the Tymshare computer. The results obtained by these two separate methods were in good agreement.

The analysis showed that, under certain circumstances, permitting a finite number of messages to be lost and defining this loss by a statistic results in a system that can accommodate a much larger number of data collection platforms. For comparison, consider a system with the following set of parameters

Message length	256 bits
Data rate.	2048 bits/sec
Visibility time	11.814 minutes
d/T	$3.54 \times 10^{-4}$

The relationship between the number of users and the message loss statistics for values of N between 20 and 100 is shown in Figure 4-1. If  $\alpha = 6$  percent and  $\gamma = 0, 10$ , then we can transmit almost 100 messages. Using the earlier concept for system capacity, the probability of no error was set in the transmission of all messages to be 0.94, under which conditions the system can handle 20 data cycles/sec. At 0.90 probability of correct transmissions, 26 data cycles/sec could be accommodated.

The major results from this section are

- If  $\binom{N}{2} d/T \ll 1$ , the interference is predominantly between pairs of messages, if  $\binom{N}{2} \frac{d}{T} \geq 1$ , then this is no longer true, and there is a distribution of collisions with the highest order forms (involving many messages) occurring least frequently.
- The analysis and conclusions presented in this section have been checked by three computer simulation runs on the Tymshare (see Section 4.1.5). Because of the slow computing time of the Tymshare, more examples were not attempted. The Monte Carlo synthesis program is being translated so that more extensive work in the future can be made on the faster CDC-6400 computer.

#### 4.1.1 Analysis Model

To solve the problem, a statistical model must be assumed, then the probability calculated so that exactly K messages are lost, where  $K = 0, 1, 2, \dots, N$ . Once P is determined (the probability that K messages are lost), then N can be found by solving

$$\sum_{K=0}^{\alpha N} P(K) = 1 - \gamma$$

where  $P(K) = \text{prob}(\text{exactly } K \text{ messages are lost})$ .

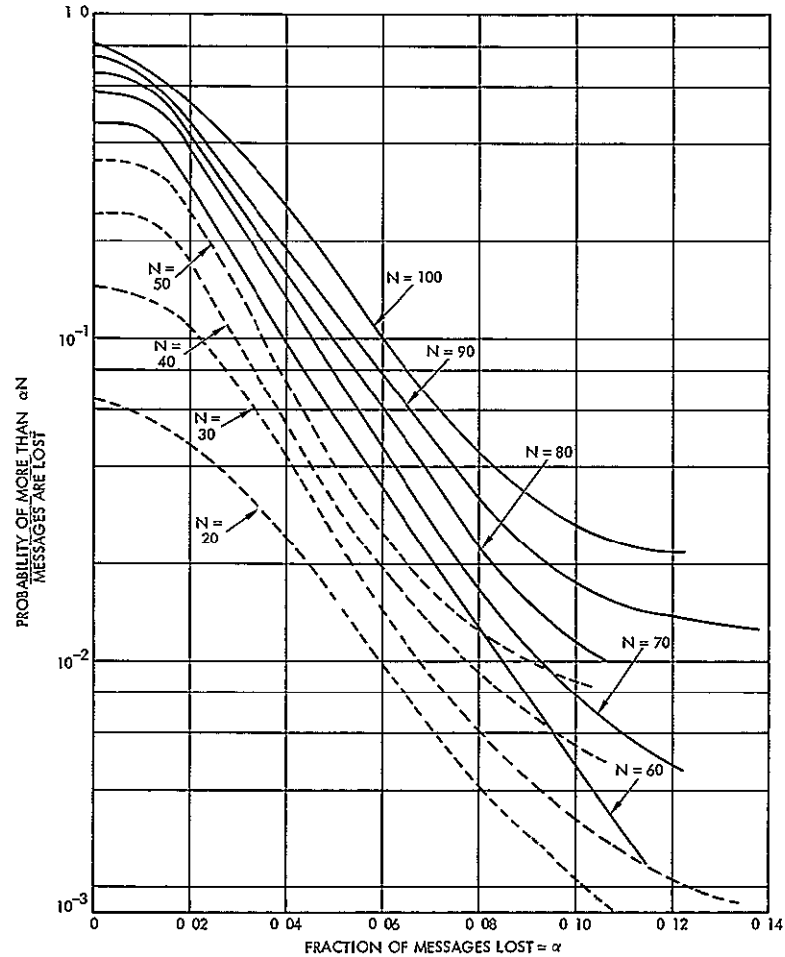


Figure 4-1

PERFORMANCE OF THE MODIFIED SYSTEM ( $d/T = 1.76 \times 10^{-4}$ )

The subsequent analysis is facilitated by using the simplified model discussed in Section 2.5. In particular, it is assumed that

- $Nd/T \ll 1$
- The probability that a message is transmitted during the "edge interval" ( $T-d/2, T$ ) is negligible
- The probability of a message falling in the "forbidden region" discussed in Section 2.5.1 is also negligible.

Without these assumptions, the exact analysis becomes very difficult and tedious. The exact analysis of the simplest case where  $N = 2$  in Section 2.5.1 gives a glimpse of the complexity of calculation. As the analysis

proceeds, references are made frequently to the foregoing three assumptions to simplify our calculations.

#### 4.1 2 Modes of Message Mutilation

In considering the loss of K messages due to interference, the conclusions are

- The probability that an odd number of messages are lost is negligible by comparison with the probability that an even number of messages are lost
- Interference occurs mainly in the form of message pair collisions, i.e., there is a high probability that any one signal receives only one interference.

These conclusions are illustrated and distinct pairs are defined in the following discussion.

If ordered messages, 1, 2, 3, and 4 are lost because of interference, it is very likely that message mutilation occurred in one of three message pairs

$1 \nmid 2$  and  $3 \nmid 4$   
 $1 \nmid 3$  and  $2 \nmid 4$   
 $1 \nmid 4$  and  $2 \nmid 3$

where the symbol  $\nmid$  is used to represent an interference between messages. Under the conditions of four lost messages, one additional state,  $P(1 \nmid 2 \nmid 3 \nmid 4)$ , is added to those listed. However,  $P(1 \nmid 2/3 \nmid 4) \ll P(1 \nmid 2, 3 \nmid 4)$ , etc., since this requires that some signals interfere with two or more signals. The starting times for all four signals must fall in a time interval equal to or less than  $4d$ , out of the total  $T$  interval (and  $d \ll T$ ). In the event of  $1 \nmid 2/3 \nmid 4$ , messages 1 and 2 fall in interval  $d$ , while 3 and 4 can fall in any other interval  $d$  with many possibilities in  $T (>> d)$ . Pair interferences, therefore, are more likely than any other kind of interference.

A group of pairs are distinct if none of the messages are repeated in the group. As an example, consider the three pairs, (1-2, 3-4, 5-6) and (1-2, 1-4, 5-6). By definition, the first group is distinct because none of the six messages are repeated, while the second is not distinct

because message 1 appears twice in the group. Computer simulations justify this conclusion.

#### Case Where K = Even Number

Assume that an even number of K messages are lost because of interference. Since most of the interference occurs in distinct pairs, the number of distinct  $(K/2)$  pairs producing K lost messages must be examined. In total, there are  $\binom{N}{2}$  different pairs from which a choice of  $K/2$  distinct pairs must be made

The  $\binom{N}{2}$  pairs are:

1-2, 1-3, 1-4, 1-5, . . . . .	, 1-N
2-3, 2-4, 2-5,	, 2-N
3-4, 3-5,	, 3-N
4-5, . . . . .	, 4-N
. . . . .	
	, (N-1)-N

First the probability is calculated that a particular group of  $K/2$  distinct pairs interfere. For simplicity of presentation, let  $K = 6$  and consider the case of ordered interfering independent pairs 1/2, 3/5, 4/6, and the remaining  $\binom{N}{2} - 3$  pairs are free of interference. From a standard probability theory, it is known that  $P(1/2, 3/5, 4/6 \text{ others are free of interference}) =$

$$P(1/2|3/5, 4/6, \text{ others are free of interference})$$

$$P(3/5|4/6, \text{ others are free of interference})$$

$$.P(4/6|\text{others are free of interference})$$

$$.P(\text{others are free of interference})$$

Clearly

$$P(1/2|3/5, 4/6, \dots) \neq P(1/2)$$

$$P(3/5|4/6, \dots) \neq P(3/5)$$

$$P(4/6|\text{others are free of interference}) \neq P(4/6)$$

To compute these four terms exactly is a formidable task, however, a few approximations can be made by using the three assumptions presented in Section 4.1.1. As stated in Section 2.5, the assumption is made that whether or not one particular pair interferes depends on what happens to any other pair(s). Thus, the four terms are approximated as follows

$$\begin{aligned} P(1/2|3/5, 4/6, \text{ others are free of interference}) &\approx P(1/2) \approx d/T \\ P(3/5|4/6, \text{ others are free of interference}) &\approx P(3/5) \approx d/T \\ P(4/6|\text{ others are free of interference}) &\approx P(4/6) \approx d/T \\ P\left[\binom{N}{2} - 3 \text{ pairs are free of interference}\right] &\approx \left(1 - \frac{d}{T}\right)\binom{N}{2}^{-3} \end{aligned}$$

where  $d/T \approx P$  (any two messages interfere)

Collecting the four terms,  $P(1/2, 3/5, 4/6, \text{ others are free of interference})$  is obtained

$$\left(\frac{d}{T}\right)^3 \cdot \left(1 - \frac{d}{T}\right) \exp\left(\binom{N}{2}\right)^{-3} \quad (1)$$

Since computing the probability of the loss of exactly six messages is a primary interest, the number of ways three distinct pairs can be chosen from  $\binom{N}{2}$  pairs must be found. When this number is multiplied by Equation (1), the result indicates the desired probability that six messages are lost. In summary, if an even number of messages ( $k$ ) are lost, then the probability of this occurrence is approximately the probability that a particular group of  $K/2$  distinct pairs interfere.

The probability that a particular group of  $K/2$  distinct pairs interfere is

$$\left(\frac{d}{T}\right)^{\frac{K}{2}} \left(1 - \frac{d}{T}\right) \exp\left(\binom{N}{2} - \frac{K}{2}\right) \quad (2)$$

#### Number of $K/2$ Distinct Pairs, $K = \text{Even Number}$

To determine the number of ways  $K/2$  distinct pairs can be chosen is a combinatorial problem. The first pair can be chosen from any one of  $\binom{N}{2}$  pairs. Once the first pair is chosen, there are  $\binom{N-2}{2}$  pairs left from which the second distinct pair can be chosen. After the second choice, there



are  $\binom{N-4}{2}$  pairs to choose from the a third selection. In general, the total number of ways to choose  $K/2$  distinct pairs is given by

$$\binom{N}{2} \binom{N-2}{2} \cdot \cdot \cdot \binom{N-K+2}{2}$$

But the redundancy must be eliminated in this counting procedure because the order in which the  $K/2$  pairs are chosen is not of interest. For example, choosing (1-2), (3-5), (6-8) is the same as choosing (3-5), (6-8), (1-2) as far as the analysis is concerned. There are, in total,  $(K/2)!$  ways to form a group of  $K/2$  pairs. Hence, the total number of different combinations from which  $(K/2)$  distinct pairs can be chosen is given by the formula

$$\frac{1}{(K/2)!} \binom{N}{2} \binom{N-2}{2} \cdot \cdot \cdot \binom{N-K+2}{2}$$

This almost completes the computation of the probability of losing  $K$  messages. Combining the above formula with Equation (2), we have the desired result:

$P$  (exactly even number of  $K$  messages are lost)

$$\begin{aligned} &\approx \frac{1}{(K/2)!} \binom{N}{2} \binom{N-2}{2} \cdot \cdot \cdot \binom{N-K+2}{2} \left(\frac{d}{T}\right)^{\frac{K}{2}} \left(1 - \frac{d}{T}\right)^{\binom{N}{2} - \frac{K}{2}} \\ &= \frac{N!}{(K/2)! (N-K)!} 2^{-K/2} \left(\frac{d}{T}\right)^{\frac{K}{2}} \cdot \left(1 - \frac{d}{T}\right)^{\binom{N}{2} - \frac{K}{2}} \end{aligned} \quad (3)$$

where

$$\binom{N}{2} = \frac{N \cdot (N-1)}{2}$$

A simple computer program was written to permit evaluation of Equation (3) via the Tymshare computer.

Case Where  $\binom{N}{2} d/T \ll 1$

If  $\binom{N}{2} d/T \ll 1$ , when there is any interference among the N messages, it will most likely be an interference of two messages.

From Section 3.5 and Equation (3), it is known that if  $K = 0$ , then  
 $P(\text{no interference among } N \text{ messages}) = P(K = 0)$

$$\approx \left(1 - \frac{d}{T}\right)^{\binom{N}{2}} = \left(1 - \frac{d}{T}\right)^{\frac{N(N-1)}{2}}$$

By using a binomial expansion, we have

$$P(\text{no interference}) \approx 1 - \binom{N}{2} \left(\frac{d}{T}\right) + \left[ \frac{\binom{N}{2}}{2} \right] \left(\frac{d}{T}\right)^2$$

To a first-order of approximation.

$$P(\text{no interference}) \approx 1 - \binom{N}{2} d/T$$

and

$$P(\text{any interference}) \approx \binom{N}{2} d/T \quad (4)$$

But it is known from Equation (3) that  $P(2 \text{ messages are lost})$  is given by

$$\binom{N}{2} \frac{d}{T} \cdot \left(1 - \frac{d}{T}\right)^{\binom{N}{2}} - 1$$

or after a binomial expansion, approximately  $\binom{N}{2} d/T$ , if  $\binom{N}{2} d/T \ll 1$ . Since the expressions in Equations (4) and (5) are equal, it is concluded that if any interference occurs during the transmission of N messages, it is likely to be an interference between two messages. The probability that three or more messages are lost can be easily calculated

$$P(3 \text{ or more messages are lost}) = P(\text{any interference}) - P(k=2)$$

Expanding the expression in Equation (3) in binomial series up to the second-order term gives

$$P(3 \text{ or more messages are lost}) \approx 1/2 \cdot \binom{N}{2}^2 (d/T)^2, \text{ for } \binom{N}{2} \gg 1 \quad (5)$$

Since  $P(K=1)$  was neglected, minimum  $K$  value has to be two because of the second assumption introduced in Section 4.1.1

Now, applying this result to a specific example, assume again that  $\binom{N}{d}d/T \ll 1$  and that mutilation of one or two messages can be tolerated. In addition it is assumed that the probability of three or more messages being lost is less than a predetermined number,  $\gamma$ . The question is how many messages can be transmitted subject to the above constraint? If  $N \gg 1$ , then  $\binom{N}{2} \approx \frac{N^2}{2}$ . After some algebra, the expression is simplified to obtain

$$P(3 \text{ or more messages are lost}) \approx \left(\frac{Nd}{2T}\right)^2$$

It is desirable to set this probability to be no greater than  $\alpha$ . Solving for  $N$  from the above relation

$$N = \frac{2T}{d} \sqrt{\gamma} \quad (6)$$

On the other hand, if no mutilation of messages had been allowed and determination of  $N$  rested upon the probability (subject to constraint that all  $N$  messages be transmitted with an error less than  $1 - P_1$ ), then  $N$  would have been obtained by solving

$$\left(1 - \frac{d}{T}\right) \binom{N}{2} \approx 1 - P_1 \quad (7)$$

An approximate answer is given by

$$N \leq \frac{\sqrt{2P_1 T}}{\sqrt{d}}$$

Clearly, the advantage of allowing up to two messages to be mutilated increases the capacity of the system considerably. In the revised random access system, the total number of transmitters increases linearly with  $d$ , while  $N$  varies as the square root of  $P_1$  and  $d$  in the first system. If  $P_1 = \sqrt{\gamma}$  is set, then

$$N(\text{revised system}) = (N(\text{first system}))^2 \quad (8)$$

For Equation (8) to hold,  $\binom{N}{2}d/T$  must be much less than one. In some practical cases, this constraint may not be met.

#### Case Where $\binom{N}{2}d/T \gtrsim 1$

When  $\binom{N}{2}d/T \gtrsim 1$ , then the probability of any interference is no longer dominated by the  $P(K = 2)$ . For example, set  $N = 80$ ,  $d/T = 1.76 \times 10^{-3}$ , then the following probabilities exist by using Equation (3)

$P(\text{any interference}) = 1 - P(K = 0) =$		0.672
$P(K = 0) =$		0.328
$P(K = 2) =$		0.366
$P(K = 4) =$		0.194
$P(K = 6) =$		0.065
$P(K = 8) =$		0.015

In this case, most interference is not a result of interference between two messages. In the case where  $\binom{N}{2}d/T \ll 1$ ,  $P(K = 2)$  was approximately equal to  $P(\text{any interference})$ . One logical explanation for the two cases is as follows. When  $\binom{N}{2}d/T \ll 1$ , the fraction of time occupied by  $\binom{N}{2}$  pairs (if there is no interference with each other) is approximately  $\binom{N}{2}d/T$ . Since  $\binom{N}{2}d/T \ll 1$ , we have many time slots left to spread the distinct pairs without causing any interference among these pairs. Suppose one particular pair interferes, then the probability that another pair also interferes is small because there are so many time slots left in the interval  $(0, T)$  where the second pair can be placed. On the other hand, the situation is different if  $\binom{N}{2}d/T \gtrsim 1$ . The total time occupied by  $\binom{N}{2}$  noninterfering pairs is greater than  $T$ . Generally, if there is one distinct interfering pair, a second distinct pair is likely to interfere also because there are no longer many time slots that are left for the second pair to be free of interference. As  $N$  increases, the entire transmission time interval  $(0, T)$  becomes so crowded that the second distinct pair will often interfere.

If  $\binom{N}{2}d/T \gg 1$ , then our basic assumptions imposed on the statistical model break down are correct. The conditional probability that one particular pair interferes can be no longer approximated by  $d/T$ , therefore, our analysis must be modified, and Equation (3) is no longer valid.

### 4 1.3 Simulation Results

A computer program was written on the Tymshare to check the analytical results obtained here and in Section 2 5 Section 4 4 presents a detailed explanation of the program and the results applicable to the revised system. Since only three runs were made, these results were preliminary, a more extensive study has since been completed The results of the 3-hour Tymshare run are listed in Table 4-1

Table 4-1 Computer Checks of Message Interference Analysis

		Number of Monte Carlo Tests	Simulation Results = Fraction of Time K Messages are lost	P(K) from Equation ( 3 )
<u>Case I</u>	N = 30 messages $d/T = 1.05 \times 10^{-4}$ $\binom{N}{2} d/T = 0.47$	2107		
	K = 0		0.72	0.71
	K = 2		0.28	0.29
<u>Case II</u>	N = 40 messages $d/T = 1.76 \times 10^{-4}$ $\binom{N}{2} \frac{d}{t} = 0.28$	3056		
	K = 0		0.88	0.87
	K = 2		0.12	0.13
<u>Case III</u>	N = 100 messages $d/T = 3.53 \times 10^{-4}$ $\binom{N}{2} \frac{d}{t} = 1.7$	622		
	K = 0		0.816	0.825
	K = 2		0.281	0.305
	K = 4		0.250	0.255
	K = 6		0.157	0.137

As a practical example, the following set of parameters were chosen to examine the revised system:

$$\text{Visibility time} = 11.814 \text{ min}$$

$$\text{Message length} = 256 \text{ bits}$$

$$\text{Transmission rate} = 2048 \text{ bits/sec}$$

$$N = (20, 100)$$

$$d/T = 3.54 \times 10^{-4}$$

$$\binom{N}{2} \max) d/T = 3.9$$

For the various values of  $\alpha$ , the probability was plotted that more than  $\alpha N$  will interfere. Figure 4-1 showed the capability of the modified random access system for this set of parameters.

The horizontal axis of the graph shows the fraction of the total number of messages lost. As an example, assume that  $N = 20$  is used in the first system by setting the probability of no interference at 0.94. By allowing  $\alpha$  of 0.06 and  $\gamma = 0.10$ , 100 transmitters can be used in the revised system. The performance of the revised random access system depends on  $\gamma$ ,  $(d/T)$ , and  $\alpha$ . As  $d/T$  and  $\alpha$  decreases and  $\gamma$  increases,  $N$  will increase.

The graph was plotted for various values for  $N$ . If  $N$  is greater than 100, it is necessary to modify the analysis that was presented earlier in this section. When  $N > 100$ , then  $\binom{N}{2} \frac{d}{T} \geq 1$  and the probability can longer neglected that an odd number of messages are lost. For example, three messages would be lost if two nondistinct pairs interfere. To a good approximation

$$P(K = 3) \approx P(2 \text{ nondistinct pairs interfere})$$

$$\approx \frac{2(N-2)}{2!} \binom{N}{2} \left(\frac{d}{T}\right)^2 \left(1 - \frac{d}{T}\right)^{\binom{N}{2}-2}$$

$$\approx (N - 2) \frac{d}{T} P(K = 2)$$

Using the different values of  $d$ ,  $T$ , and  $N$ , we have

$$P(K = 2) \approx 0.30$$

$$P(K = 3) \approx 0.011$$

Similarly, the probability of losing five messages can be written

$$P(K = 5) \approx \frac{4}{3} \cdot N\left(\frac{d}{T}\right) \cdot P(K = 4)$$

$$\approx 0.012$$

and

$$P(K = 7) \approx 0.007$$

If  $N = 150$  instead of 100, then probability that odd messages are lost becomes more significant. The computations of such probabilities are lengthy, but may be examined at some future date. Finally, the loss of an odd number of messages becomes significant only if  $\frac{N}{2} \frac{d}{T} \geq 1$

#### 4.2 RANDOM EMISSION MULTIPLE ACCESS WITH REPLICATION

By replicating each of the  $N$  messages, the total number of transmitters can be increased, and by allowing replication, more clean copies of each of the  $N$  messages can possibly be extracted. On the other hand, as  $M$  increases, the probability of an interference will become so large that only a few of the  $N$  messages will be correctly received in any interval. Therefore, for some value of  $M$ ,  $N$  can be maximized, subject to a constraint on the error probability. Whether  $N$  can be increased by increasing  $M$  has not been determined, although it appears possible. If certain conditions are met, it was found that a crude upperbound on the probability of error (when there is replication) can be smaller than  $P(\text{error without replication})$ .

A correct message is obtained at the ground station processor, if an error-free copy from any one of the  $M$  subintervals is extracted. An error is made if all  $N$  messages cannot be produced error-free, for example, if messages 1 and 2 have interfered during the first transmission

interval,  $(0, T/M)$ , while the remaining  $N-2$  messages are transmitted error-free. Assume that during the second subinterval,  $(T/M, 2T/M)$ , only messages 3 and 4 are lost because of interference. The processor can still extract a clean copy of all  $N$  messages by using the two copies of each of the  $N$  messages. Messages 3 and 4 were not damaged during the first subinterval, while messages 1 and 2 are transmitted error-free during the second. This is an example of a clean copy of all  $N$  messages.

The subsequent analysis examines the two cases where

$$\binom{N}{2} Md/T \ll 1$$

and

$$\binom{N}{2} Md/T \gtrsim 1$$

The first step is to find how an error occurs at the processor. Just as there are many ways to lose  $J$  messages in one subinterval, there are many ways to have an error after processing transmissions from the  $M$  subintervals.

In the case where  $\binom{N}{2} Md/T \ll 1$ , the probability of losing only two messages dominates the probability of any error (see Section 4.1). The result is not surprising, since  $\binom{N}{2} Md/T$  represents the average number of interferences among  $N$  messages. Recall that  $Md/T$  is the probability of any interference between two messages, and there are  $\binom{N}{2}$  such possibilities. Because the largest number of messages that can be lost from one interference is two, it can be seen that if  $\binom{N}{2} Md/T \ll 1$ , the likelihood of losing two messages is large whenever there is interference.

During the first subinterval, then, it is possible to lose, at most, two messages if there is interference. Then, the next step is to examine if these two messages are transmitted without error during the next  $(M-1)$  subintervals.

The accounting of an error, however, becomes more complicated when  $\binom{N}{2} Md/T \gtrsim 1$ , since now it is likely that more than two messages are lost in a subinterval. Then, the probability that any number of  $K$  ( $K \leq J$ )



messages are lost in the second interval, and  $L$  of them ( $L \leq K$ ) are lost in the third, etc., must be computed

Throughout the analysis, knowledge of the probability that exactly  $J$  messages ( $J = 0, 1, 2, \dots, N$ ) are lost in one subinterval  $(0, T/M)$  is necessary. Section 4.1 obtains a simple approximation to this probability,  $P(J)$ , when  $\binom{N}{2} d/T \ll 1$ . In particular

$$\begin{aligned} P(J = \text{even number of messages lost}) \\ \approx P(J/2 \text{ distinct pairs interfere}) \end{aligned} \quad (9)$$

and

$$P(J = \text{odd number of messages lost}) \approx 0 \quad (10)$$

These expressions are approximations only to the exact probability, and are called first-order terms of  $P(K)$ . They are sufficient for the case where  $\binom{N}{2} Md/T \ll 1$ , but are not for the case where  $\binom{N}{2} Md/T \gtrsim 1$ . For the latter, a better approximation to  $P(K)$  is necessary. To motivate such a better approximation, consider the example given in Section 4.1 where the probability of losing the odd number of messages is close to 0.05 instead of zero. As  $N$  increases and  $\binom{N}{2} Md/T$  exceeds one, the probability of losing odd messages can easily be as large as 0.20.

With the help of the second-order terms to  $P(K)$  (see Appendixes A and B) the probability of error for the replication cases is computed.

A computer program was written on the Tymshare to evaluate some of the tedious computations. Expressions for the error probability is valid if  $\binom{N}{2} Md/T > 1$ , transmission rate = 2048 bits/sec, and  $M = 1, 2, 3, 4$ .

These examples are applicable to the ERTS project. In comparison, to the case where  $M = 1$ ,  $N$  almost tripled by replicating twice, increased by a factor of five by replicating three times, but did not increase much more by replicating four times.

A preliminary result shows that there are some differences from the random emission multiple access (REMA) system in the time domain. It is desirable to determine the total number of transmitters that can be accommodated if the system is used on both the time and frequency

domains, subject to a constraint on the error probability. This problem involves optimizing the usage of two systems of different characteristics and capacities.

#### 4.2 1 Case Where $\binom{N}{2} Md/T \ll 1$

This paragraph shows the solution to the problem when  $\binom{N}{2} Md/T \ll 1$  and gives an analytical expression for the error probability. An error occurs at the processor when at least one error-free copy of each of the N messages after M subintervals is not obtained. The availability of the storage device on the processor is important, without it, there is no significant gain in the capacity of the system with replication.

Assume that J messages are lost during the first subinterval, I-1. What happens to the remaining (N-J) messages during the subsequent M subintervals is of no concern, since correct copies of these messages have been obtained. However, what happens to the J messages in other subintervals determines whether or not there is an error. Assume that K out of J messages (where  $K \leq J$ ) are lost in the second subinterval I-2. Again, there is no concern in J-K messages already correctly received in I-2, the concern is whether any one of the K messages, if any, are lost in I-3, and so on through the last subinterval, I-M.

In general, an expression for the probability of an error is

$$\begin{aligned}
 P(\text{error}) = & \sum_{J=2}^N P(J \text{ messages are lost in I-1}) \\
 & \sum_{K=4}^J P(K \text{ out of } J \text{ messages are lost in I-2}) \\
 & \sum_{L=1}^K P(L \text{ out of } K \text{ messages are lost in I-3}) \quad (11) \\
 & \cdot \sum_{M=1}^L P(M \text{ out of } L \text{ messages are lost in I-4})
 \end{aligned}$$

... · P(at least one of the messages lost through  
I-1, I-2, ..., I-(M-1) is also lost in  
I-M)

where

$$\begin{aligned} I-1 &= (0, T/M) \\ I-2 &= (1/M, 2T/M) \\ I-3 &= (2T/M, 3T/M) \\ &\vdots \\ I-M &= \left(\frac{M-1}{M} \cdot T, T\right) \end{aligned}$$

For the case where  $\binom{N}{2} Md/T \ll 1$ , Equation (11) simplifies considerably. From Section 4.1, it is probable that any interference is approximately given by P(2 messages are lost). Using Equation (3)

$$\begin{aligned} P(\text{any interference}) &= 1 - P(K = 0) \approx 1 - (1 - Md/T)^{\binom{N}{2}} \\ &\approx \binom{N}{2} Md/T \quad \text{if } \binom{N}{2} (Md/T) \ll 1 \end{aligned}$$

Similarly

$$P(K = 2) = \binom{N}{2} (Md/T)(1 - Md/T)^{\binom{N}{2}-1} *$$

Hence,

$$P(\text{any interference}) \approx P(K = 2) \tag{12}$$

In other words, if there is any interference in I-1, most likely two messages would be lost. In the case where  $\binom{N}{2} Md/T \ll 1$ ,  $P(K)$  is approximated by a Poisson distribution. Let  $\lambda = \binom{N}{2} Md/T$ , the average number of interferences among  $\binom{N}{2}$  pairs. Since the interferences among distinct pairs are the primary causes of loss of K messages, the number of messages lost can be approximated by twice the number of pair-interferences. If  $N \gg 1$  and  $\binom{N}{2} Md/T \ll 1$ , Poisson distribution approximates the binomial distribution. Hence  $P(K) = e^{-\lambda}$ ,  $P(K = 2) = e^{-\lambda} \cdot \lambda$ , and so on.

Using Equation (12), Equation (11) is

$$P(\text{error}) \approx P(2 \text{ messages lost in I-1}) \cdot \sum_{K=1}^2 P(K \text{ out of 2 messages are lost in I-2})$$

· P (at least one of the messages lost throughout I-1, 2, 3, ..., (M-1) is also lost in I-M)

Next, the probability of losing one or two messages (which were lost in I-1) in I-2 must be computed. To compute this probability, consider the  $\binom{N}{2}$  pairs

1-2,	1-3, 1-4, 1-5, 1-6, . . . . . , 1-N
	2-3, 2-4, 2-5, 2-6, . . . . . , 2-N
	3-5, 3-6, . . . . . ,
	·
	·
	·
	·
	·
	(N-1)-N

For convenience, assume that messages 1 and 2 were lost in I-1. As shown in the above diagram, message 1 or 2 (but not both) is lost if any one of the pairs in the shaded area interfere. Noting that  $Md/T$  is the probability that any pair interferes in one subinterval,

$$P(\text{losing messages 1 or 2, but not both, in I-2}) = (2N-4)(Md/T)(1-Md/T)^{2N-5}$$

and  $\approx 2N Md/T$

$$P(\text{losing both messages 1 and 2 in I-2}) \approx Md/T$$

$$\text{if } N \gg 1 \text{ and } \binom{N}{2} Md/T \ll 1$$

After the second subinterval, I-2, most likely only one message is lost, because

$$P(\text{losing both messages 1 and 2 in I-2}) \ll P(\text{losing messages 1 or 2, not both in I-2})$$

Without loss of generality in argument, assume that message 1 is lost in I-2. The probability of losing message 1 again in I-3 is approximately  $N Md/T$ . Similar reasoning can be used for the successive intervals, I-4, I-5, . . . , I-m. Then, Equation (11) can be simplified to

$$P(\text{error}) \approx \binom{N}{2} (Md/T) \cdot [2 N (Md/T)] \cdot [NMd/T]^{M-2} \quad (13)$$

where

$$M = 2, 3, \dots$$

$$N \gg 1$$

and

$$\binom{N}{2} Md/T \ll 1$$

By approximating  $\binom{N}{2}$  by  $N^2/2$ , Equation (13) can be simplified further.

$$P(\text{error}) \approx N^{M+1} (Md/T)^M$$

Solving for N,

$$N_M = \sqrt[M+1]{P(\text{error})(T/Md)^M} \quad M = 2, 3, \dots \quad (14)$$

where the subscript M on N denotes the number of replications. To compare with the case where there is no replication, recall that

$$N_{M=1} = \sqrt{2 P(\text{error}) \cdot T/d} \quad (15)$$

If  $M = 2$ , then

$$N_2 = \sqrt[3]{P(\text{error})(T/2d)^2}$$

Suppose  $P(\text{error}) = 10^{-4}$  and  $d/T = 10^{-7}$

Then Equations (14) and (15) yield

$$N_2 = 10^3 \sqrt[3]{2 \cdot 5}$$

$$N_1 = 10 \sqrt{20}$$

and

$$N_2/N_1 = 29.8$$

The number of transmitters was increased by a factor of almost 30. The significant increase in N is evident. In general, the gain is given by

$$\frac{N_M}{N_1} = \frac{P(\text{error}) (T/Md)^M}{2P(\text{error}) \cdot (T/d)} \quad (16)$$

For Equation (16) to be valid,  $\binom{NM}{2} Md/T \ll 1$ , otherwise the gain in N would be less than one promised by Equation (16)

For this case, a substantial increase in N can still be obtained by using replication. To justify this conclusion, assume that 50 percent of the total number of messages are lost during the first subinterval, 50 percent may be lost (of those already lost in I-1) during the second subinterval and 50 percent (of those already lost in I-1 and I-2) during the third. After sufficiently large M replications, a clean copy of each of the N messages is obtained because it is unlikely that one message is lost M times. The percentage lost, however, also increases as M increases. Therefore, there is an optimum M that gives maximum N for a fixed P (error)

#### 4 2 2 Case Where $\binom{N}{2} Md/T \geq 1$

This section discusses the increase in N achieved by using replication when  $\binom{N}{2} Md/T \geq 1$ . The general equation for the probability of error has already been derived in Equation (11). This section presents the second-order terms to P(K) that are derived in the appendixes. Using the new expression on P(K) and Equation (11), the error probability is derived. Finally, two examples are worked out and the gain in N over the system without replication is plotted in Figures 4-2 and 4-3.

The two examples under consideration have the following parameters

	<u>Example 1</u>	<u>Example 2</u>
Transmission rate	3570 bits/sec	2048 bits/sec
Message length	256 bits	256 bits
or	75 msec	125 msec
Visibility time	11.814 min	11.814 min
P(error)	Order of 0.1	Order of 0.1
$\binom{N}{2} d/T$	Order of 1	Order of 1

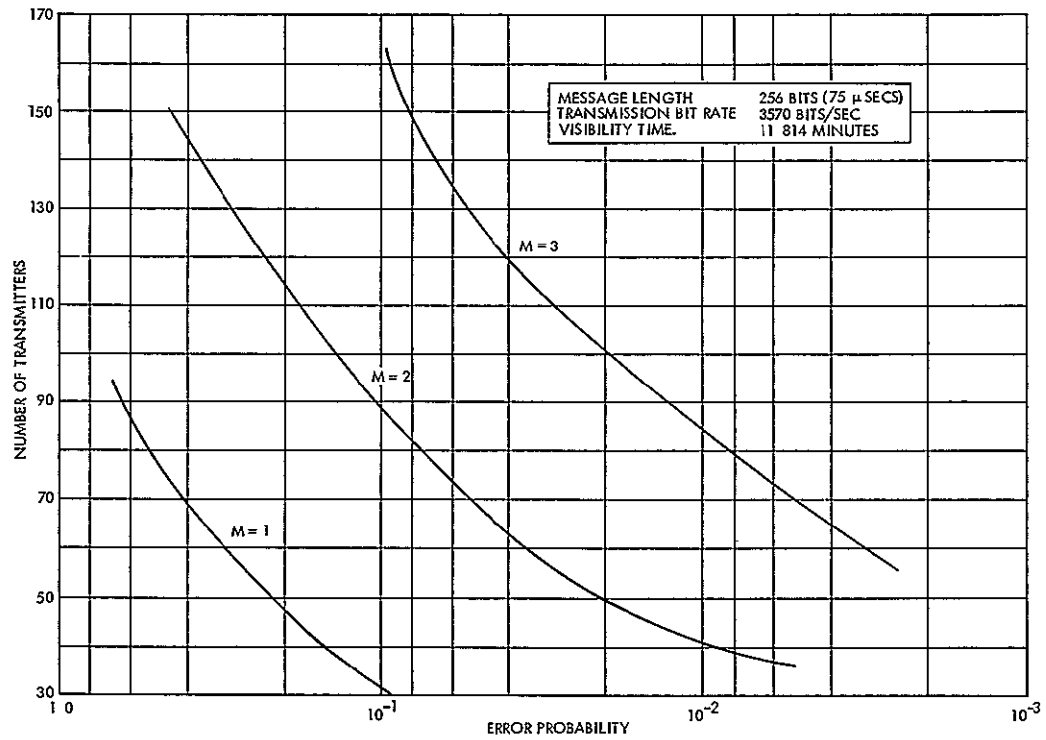


Figure 4-2  
PERFORMANCE OF REMA SYSTEM WITH REPLICATION

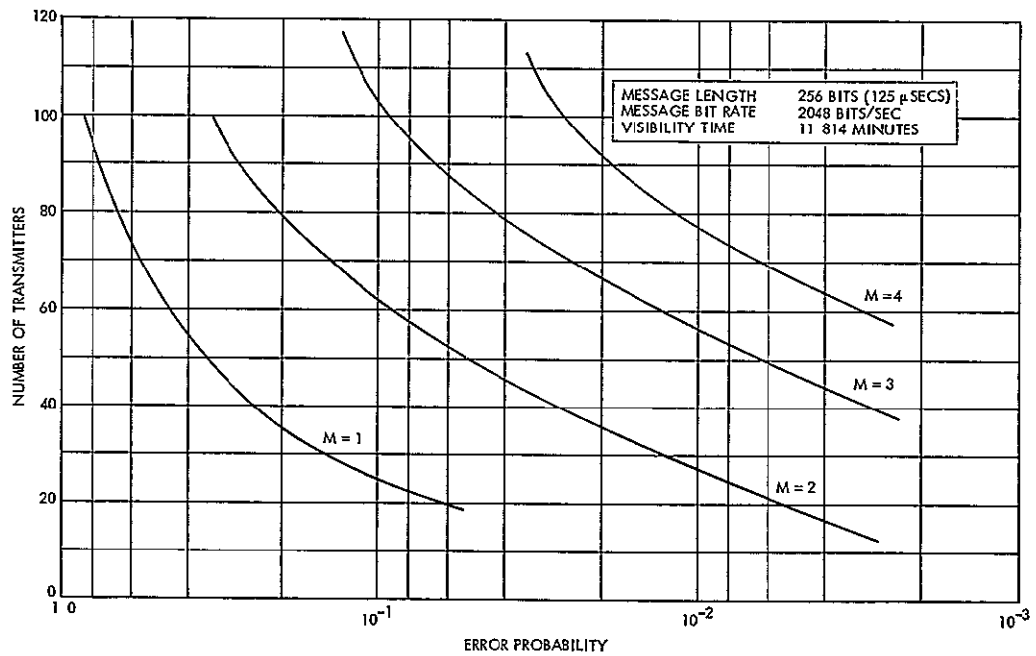


Figure 4-3  
COMPARISON AMONG CASES WHERE  $M = 1$  (NO REPLICATION) AND  $M = 2, 3, 4$

The Tymshare computer was used to evaluate Equation (11) for the cases where  $M = 2, 3, 4$

#### Derivation of $P(K)$

Figure 4-4 presents the general shape of  $P(K)$  for different values of  $\binom{N}{2} d^1/T$ . (See Appendixes A and B.)

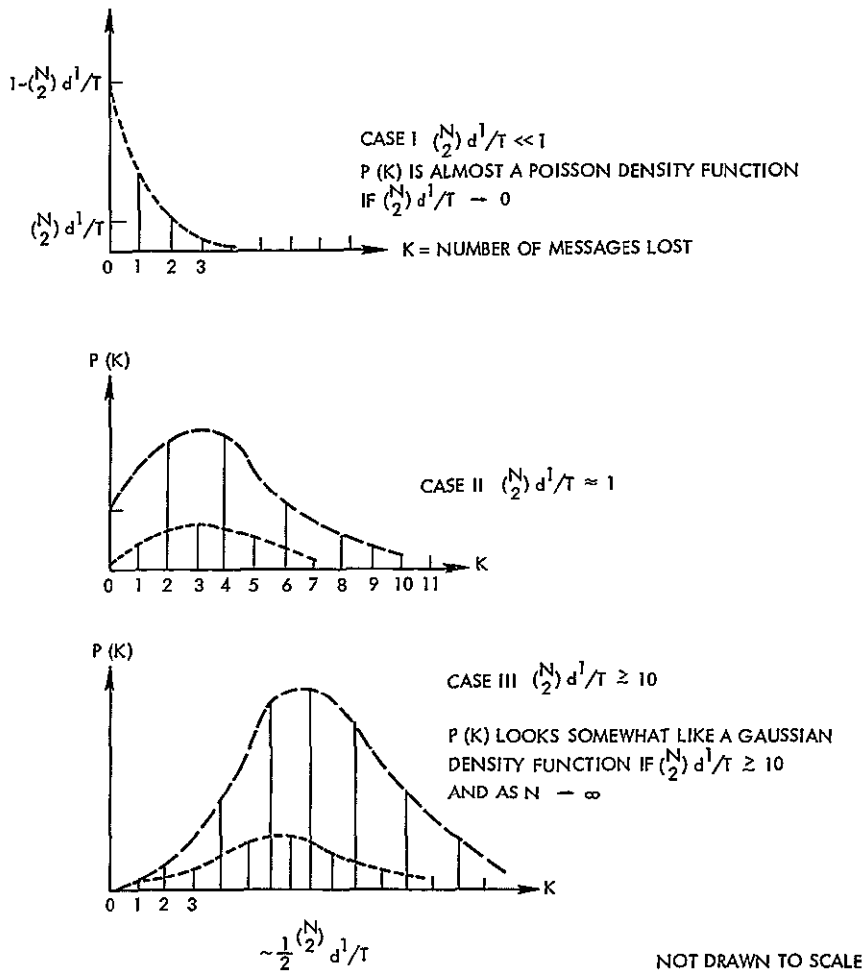


Figure 4-4  
 GENERAL SHAPE OF  $P(K)$

As noted earlier, there are different ways of losing  $K$  messages because of interference(s). However, when  $\binom{N}{2} Md/T \ll 1$ , the event of losing  $K$  messages is dominated by interferences of  $K/2$  distinct pairs. From Section 4.1, the first-order approximation to  $P(K)$  is

$$P(K = \text{odd}) \approx 0 \quad (17)$$



and

$$P(K = \text{even}) \approx \frac{1}{\left(\frac{K}{2}\right)!} \binom{N}{2} \binom{N-2}{2} \cdots \binom{N-K+2}{2} \left(\frac{d^1}{T}\right)^{K/2} \left(1 - \frac{d^1}{T}\right)^{\binom{N}{2} - K/2} \quad (18)$$

where  $d^1 = Md$

However, these expressions are not accurate approximations for  $P(K)$  when  $\binom{N}{2}Md/T \gtrsim 1$ . In a specific example presented in Section 4.1, the sum of  $P(K)$ 's given by Equation (18), instead of being 1.0, is 0.95 for the case where  $N = 100$ , 0.83 when  $N = 150$ , and 0.55 when  $N = 200$ .

Clearly, higher order approximations must be considered for  $P(K)$ , if cases where  $\binom{N}{2}Md/T \gtrsim 1$  are to be examined. Also note that  $\binom{N}{2}d/T$  may be much less than 1, but  $\binom{N}{2}Md/T$  may not be.

From Appendix A,

$$\begin{aligned} \underline{P}(K = \text{odd}) &= \frac{1}{\left(\frac{K-1}{2}\right)!} \binom{N}{2} \binom{N-K+2}{2} \left\{ \frac{(K-1)}{2} (N-K+1) \right\} \\ &\quad \left(\frac{d^1}{T}\right)^{\frac{K+1}{2}} \left(1 - \frac{d^1}{T}\right)^{\binom{N}{2} - \frac{(K+1)}{2}} \end{aligned} \quad (19)$$

or

$$\approx \underline{P}(K-1) \frac{1}{2} (K-1)(N-K+1) \left(\frac{d^1}{T}\right)^{\frac{K+1}{2}}$$

where  $d^1 = Md$ . Similarly, from Appendix B,

$$\begin{aligned} P(K = \text{even}) &\approx \text{first-order terms} + \left[ \binom{N}{2} \cdots \binom{N-K+4}{2} \frac{1}{\left(\frac{K-2}{2}\right)!} \right] \\ &\quad \left[ \frac{1}{8} (N-K+2)(N-KH)(K-2)(K-3) + \frac{(N-1)(N-2)}{6} \right] \\ &\quad \left[ \left(\frac{d^1}{T}\right)^{K+1} \left(1 - \frac{d^1}{T}\right)^{\binom{N}{2} - (K+1)} \right] \\ &+ \frac{1}{\left(\frac{K}{2}\right)!} \binom{N}{2} \binom{N-2}{2} \cdots \binom{N-K+2}{2} \left(\frac{K}{2} - \frac{K}{2}\right) \left(\frac{d^1}{T}\right)^{K+1} \left(1 - \frac{d^1}{T}\right)^{\binom{N}{2} - K - 1} \end{aligned}$$

Using these second-order terms, the sum of  $P(K)$ 's in the example in Section 4.1 yields

$$\begin{aligned} \sum_{K=2}^N P(K) &= 0.999 \text{ when } N = 100 \\ &= 0.995 \text{ when } N = 150 \\ &= 0.975 \text{ when } N = 200 \end{aligned}$$

Without the second-order terms, the sums are 0.95, 0.83, and 0.55 respectively

### Probability of Error

After deriving better approximations for  $P(K)$ 's, the probability of error when there is replication may be computed

#### Case Where $M = 2$

To illustrate how an error occurs at the processor, examine an example where  $M = 2$ . An error is made if no error-free copy of each of  $N$  messages is found either in the first or the second subinterval.

Suppose there is an interference between messages 1 and 2, an error occurs if there is any pair interference(s) in  $I_2$  which mutilates either message 1 or 2

Consider the  $\binom{N}{2}$  pairs again

$$\begin{array}{ll} 1-2, 1-3, 1-4, 1-5, & , 1-N \\ 2-3, 2-4, 2-5, & . \quad . \quad , 2-N \\ 3-4, 3-5, & . \quad , 3-N \\ 4-5, 4-6, 4-7 & . \quad , 4-N \\ 5-6, 5-7 & . \quad , 5-N \\ & (N-1)-N \end{array}$$

Let  $\Omega$  denote the set  $1-3, 1-4, 1-5, \quad , 1-N$   
 $2-3, 2-4, 2-5, \quad , 2-N$

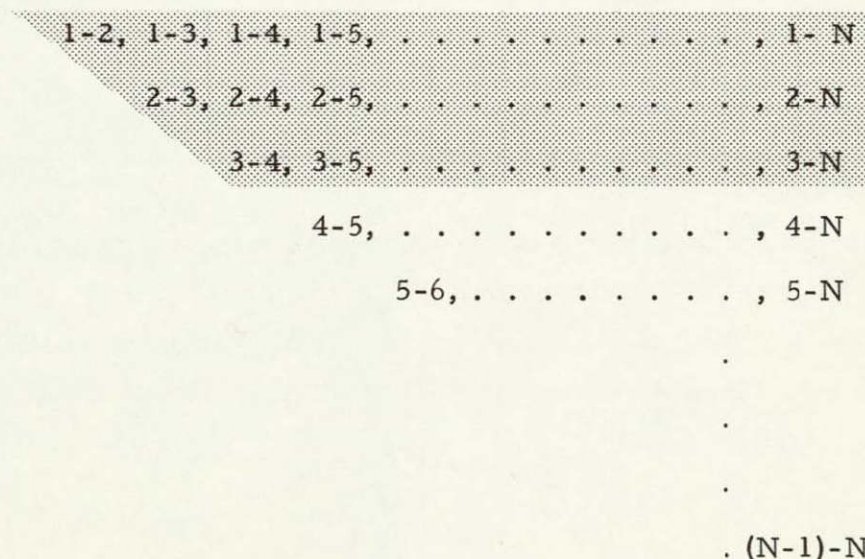
Since messages 1 and 2 were lost in I-1, there would be an error if any pair in  $\Omega$  interferes in I-2. The error probability, given that two messages were lost in I-1, is that at least one of the  $2N-3$  pairs in  $\Omega$  interferes in I-2.

$$\begin{aligned} P(\text{Error} \mid 2 \text{ messages are lost in I-1}) &= P(\text{at least one of } 2N-3 \text{ pairs} \\ &\quad \text{in } \Omega \text{ interferes in I-2}) \\ &= 1 - P(\text{none of } 2N-3 \text{ pairs} \\ &\quad \text{in } \Omega \text{ interfere}) \\ &= 1 - (1 - d^1/T)^{2N-3} \end{aligned}$$

Therefore,

$$P(\text{error, 2 lost in I-1}) = P(J = 2) \left[ 1 - \left( 1 - d^1/T \right)^{2N-3} \right]$$

Now consider the case where three messages are lost in I-1. For convenience, assume that 1/2 and 2/3 and that messages 1, 2, and 3 were lost in I-1. This assumption does not restrict the subsequent analysis, because for any two interferences of one distinct pair and one nondistinct pair, the  $\binom{N}{2}$  triangle can be used similarly.



The triangle shows that an error occurs if any pair in the shaded region interferes in I-2. The probability of such an event is  $1 - \left( 1 - \frac{d^1}{T} \right)^{3N-6}$

Hence,

$$P(\text{error}/3 \text{ messages are lost in I-1}) = 1 - \left(1 - \frac{d^1}{T}\right)^{3N-6}$$

and

$$P(\text{error}, 3 \text{ messages are lost in I-1}) = 1 - \left(1 - \frac{d^1}{T}\right)^{3N-6}$$

A general expression for the probability of error is

$$\begin{aligned} P(\text{error}) = & P(\text{error}, 2 \text{ messages lost in I-1}) \\ & + P(\text{error}, 3 \text{ messages lost in I-1}) \\ & + \dots + P(\text{error}, N \text{ messages} \\ & \text{are lost in I-M}) \end{aligned}$$

or

$$P(\text{error}) = \sum_{J=2}^N P(J \text{ messages are lost in I-1}) P(1 \text{ or more of the } J \text{ messages are lost in I-2})$$

$$= \sum_{J=2}^N P(J) \left[ 1 - \left(1 - \frac{d^1}{T}\right)^{JN - \frac{J+1}{2}} \right]$$

where  $d^1 = 2d$ .

#### Case Where $M = 3$

The case where  $M = 3$  is considered in this paragraph. An error occurs if at least one clean copy of all  $N$  messages is not received by the satellite during the three subintervals. As an example, assume that the following interferences occurred during the three transmission intervals:

I-1	I-2	I-3
1/3	1/4	5/6
2/10		
4/22		

where  $N \geq 22$ . Messages lost in I-1 are 1, 2, 3, 4, 10, 22; 1, 4 in I-2; and 5, 6 in I-3.



In this example, an error-free copy of all messages is obtained since messages 1, 2, 3, 4, 10, 22 are correctly transmitted in I-3 and 5, 6 are correctly transmitted both in I-1 and I-2.

In general, it is assumed that J messages are lost in I-1, K messages in I-2, and L messages in I-3, where  $J = 0, 1, 2, \dots$ ;  $K = 0, 1, 2, \dots$ ; and  $L = 0, 1, 2, \dots, N$ . If any of J, K, or L is 0, then there is no error. To have an error, the minimum number of messages lost in the first subinterval is two. (The loss of messages from the "edge effects" is ignored.) However, the minimum number of messages lost in the subsequent intervals is one, because interest is recent subintervals. For example, only one of the two messages that were already lost in I-1 was lost in I-2.

If messages 1, 2, 3, and 4 were lost in I-1 and 3, 4, 7 were lost in I-2, a search must be made to see if messages 3 and 4 are lost in I-3 (no interest in what happens to messages 1, 2, and 7 in I-3).

Hence, the probability of an error is

$$\begin{aligned}
 P(\text{error}) &= \sum_{J=2}^N P(J \text{ messages are lost in I-1}). \sum_{K=1}^J P(K \text{ out of } J \text{ messages} \\
 &\quad \text{are lost in I-2}) \\
 &= \sum_{L=1}^K P(L \text{ out of } K \text{ messages are lost in I-3}) \\
 &= \sum_{J=2}^N P(J \text{ messages are lost in I-1}). \sum_{K=1}^J \underline{P}(K \text{ out of } J \text{ messages} \\
 &\quad \text{are lost in I-2}). P(\text{at least one of } K \text{ messages is lost in I-3})
 \end{aligned}$$

where  $J \geq K \geq L$

The next task is to derive the various terms in the above expression. Since the last term,  $P(\text{at least one of } K \text{ messages is lost in I-3})$  is simpler of the remaining terms, it is discussed first.

If K messages are still lost after two subintervals, I-1 and I-2, then an error occurs if at least one of the K messages are lost during the last subinterval I-3. The probability that such an event occurs is equal to:

I-P (all K messages are free of interference in I-3). From the previous section,

P (at least one of the K messages is lost in I-3

$$= \left[ 1 - \left( 1 - \frac{d^1}{T} \right)^{KN} - \binom{K+1}{2} \right] \quad (20)$$

The probability that K out of J messages are lost in I-2 can be obtained quite easily with the help of the familiar  $\binom{N}{2}$  triangle:

J columns	N-J-1 columns	
1-2, 1-3, 1-4, 1-5, . . . ., 1-J	1 - (J + 1), . . . ., 1-N	
2-3, 2-4, 2-5, . . . ., 2-J	2 - (J + 1), . . . ., 2-N	
3-4, 3-5, . . . ., 3-J	3 - (J + 1), . . . ., 3-N	
.		
.		
(J - 1) - J, (J - 1) - (J + 1) . . . ., (J - 1) - N		
	J - (J + 1) . . . ., J - N	
	(J + 1) - (J + 2) . . . ., (J + 1) - N	
	.	
	.	
	.	
	.	
	(N - 1) - N	J rows

Assume that J (2, 3, . . . , N) messages are lost in I-1. Assume without loss of generality that messages 1, 2, . . . , J are lost in I-1.

K = 1 If any one of the shaded parts interfere in I-2, one message is lost. Then

$$P \begin{matrix} \text{(exactly 1 message is lost} \\ \text{in I-2/J messages are} \\ \text{lost in I-1, } J > 1) \end{matrix} = (N-1-J) J \left( \frac{d^1}{T} \right) \left( 1 - \frac{d^1}{T} \right)^{N_T' - 1} \quad (21)$$

where  $N_T' = JN - \binom{J+1}{2}$

K = 2 There are several ways to lose two messages in I-2, but only two of them are important. First, if any one of the pair in the nonshaded triangle interferes, two messages are lost in I-2. The probability of this event is

$$\binom{J+1}{2} \left( \frac{d^1}{T} \right) \left( 1 - \frac{d^1}{T} \right)^{N_T' - 1} \quad (22)$$

Another way to lost two messages is to have two nondistinct pairs (in the shaded region in the  $\binom{N}{2}$  - triangle) to interfere. As an example, if  $1 \nmid (J+1)$  and  $2 \nmid N$ , then two messages are lost messages 1 and 2. The probability of such similar event is

$$\frac{1}{2} (N - J - 1)^2 (J - 1) J \left( \frac{d^1}{T} \right)^2 \left( 1 - \frac{d^1}{T} \right)^{N_T' - 2} \quad (23)$$

Adding Equations (22) and (23),

$$P \text{ (2 messages are lost in I-2/J messages are lost in I-1, } J \geq 2)$$

$$= \binom{J+1}{2} \left( \frac{d^1}{T} \right) \left( 1 - \frac{d^1}{T} \right)^{N_T' - 1} + \frac{1}{2} (N - J - 1)^2 (J - 1) J \left( \frac{d^1}{T} \right)^2 \left( 1 - \frac{d^1}{T} \right)^{N_T' - 2}$$

K = 3 Again, there are many ways to lose three messages in I-2. However, two of them contribute significantly to the P (3 out of J messages are lost in I-2/J messages are lost in I-1) and they are

- 1) P (1 distinct pair and 1 nondistinct pair interfere in I-2)
- 2) P (3 nondistinct pairs interfere in I-2)

An example of the first case is an interference between messages 1 and 3 (1/3) and another interference between messages 3 and J + 1 (3/(J + 1)). For the second case, it may be 1/(J + 2), 2/(J + 4), and 4/(J + 3).

After some manipulation, it can be shown that

P (1 distinct pair + 1 nondistinct pair interfere in I-2)

$$= \binom{J+1}{2} (N-J-1)(J-1) \left(\frac{d^1}{T}\right)^2 \left(1 - \frac{d^1}{T}\right)^{N_T^1 - 2}$$

and

$$P (3 \text{ nondistinct pairs interfere in I-2}) \approx \frac{(N-J-1)^3 [(J-1)(J-2)(J-3)]}{3!}$$

$$\left(\frac{d^1}{T}\right) \left(1 - \frac{d^1}{T}\right)^{N_T^1 - 3}$$

Finally, adding these two terms obtains

P (3 out of J messages are lost in I-2/J lost in I-1)

$$\begin{aligned} &\approx \binom{J+1}{2} (N-J-1)(J-1) \left(\frac{d^1}{T}\right)^2 \left(1 - \frac{d^1}{T}\right)^{N_T^1 - 2} \\ &+ (N-J-1)^3 \frac{[(J-1)(J-2)(J-3)]}{3!} \left(\frac{d^1}{T}\right)^3 \\ &\left(1 - \frac{d^1}{T}\right)^{N_T^1 - 3} \end{aligned} \tag{24}$$



K = 4 Three terms contribute significantly to P (4 out of J messages are lost in I-2/J ≥ 4 messages are lost in I-1) and they are

1) P (4 nondistinct pairs interfere)

$$= \frac{(N - J - 1)^4 J \cdot (J - 1)(J - 2)(J - 3)}{4!} \left(\frac{d^1}{T}\right)^4 \left(1 - \frac{d^1}{T}\right)^{N_T^1 - 4}$$

$$2) \quad P (2 \text{ distinct pairs interfere}) = \frac{1}{2!} \binom{J+1}{2} \binom{J-1}{2} \left(\frac{d^1}{T}\right)^2$$

$$\left(1 - \frac{d^1}{T}\right)^{N_T^1 - 2}$$

3) P (1 distinct and 2 nondistinct pairs interfere)

$$= \frac{1}{2} \binom{J+1}{2} (N - J - 1)^2 J (J - 1) \left(\frac{d^1}{T}\right)^3 \left(1 - \frac{d^1}{T}\right)^{N_T^1 - 3}$$

The sum of these expressions gives an approximation to P (4 out of J messages are lost in I-2/J ≥ 4 messages are lost in I-1)

K = 5 Similarly, the probability that 5 messages are lost in I-2 as P (5 out of J messages are lost in I-2/J ≥ 5 messages are lost in I-1) is

$$\approx (N - J - 1)^5 \binom{J}{5} \left(\frac{d^1}{T}\right)^5 \left(1 - \frac{d^1}{T}\right)^{N_T^1 - 5}$$

$$+ \binom{J+1}{2} \binom{J-1}{2} \frac{1}{2!} (N - J - 1) (J) \left(\frac{d^1}{T}\right)^3 \left(1 - \frac{d^1}{T}\right)^{N_T^1 - 3}$$

$$+ \binom{J+1}{2} \cdot \frac{1}{4!} (N - J - 1)^4 \binom{J}{4} \left(\frac{d^1}{T}\right)^4 \left(1 - \frac{d^1}{T}\right)^{N_T^1 - 4}$$

A question rises as to how many terms of  $P(K)$ 's can be used to obtain a reasonable answer to  $P(\text{error})$ . One way to answer this question is to compute the  $P(\text{error})$  with terms up to  $K = 5$  and compare with another run in which the terms up to  $K = 3$  are used. At least for examples, using terms up to  $K = 4$  is sufficient.

#### Case Where $M = 4$

The expression for the error probability is given by

$$\underline{P}(\text{error}) = \sum_{J=2}^N P(J \text{ messages are lost in I-1}). \sum_{K=1}^J P(K \text{ out of } J \text{ messages are lost in I-2}).$$

$$\sum_{L=1}^K P(L \text{ out of } K \text{ messages are lost in I-3}). P(1 \text{ or } \dots \text{ of the } L \text{ messages are lost in I-4}).$$

#### Probability of Error

The probability of error was evaluated with the help of the Tymshare computer. Computer programs were written to evaluate the error probability for the cases  $M = 2, 3$ , and  $4$ . As two examples, the following parameters were chosen

$d/T = 1.76 \times 10^{-4}$	$1.04 \times 10^{-4}$
$T = 11.814 \text{ min}$	$11.814 \text{ min}$
Transmission rate = 2048 bits/sec	3570 bits/sec
Message length 256 bits	256 bits

The performance with replications is presented in Figures 4-2 and 4-3. As evident from the graphs, the advantage of replication is significant.

If interest were in a region of larger probability of error (say  $0.7$ ), the increase in  $N$  would be larger. Unfortunately, as  $M$  increases and  $N$  increases, the approximation to  $P(K)$ 's must be re-examined and further finer approximations with third-order terms must be introduced. In the

second example, cases where  $M = 4$  and  $N \geq 150$  were not run. As a check, the approximations to  $P(K)$ 's were summed for the case where  $M = 4$ , and  $N = 150$  and 0.89 was obtained — a number which is believed to be just above the limit where second-order approximations are still reliable.

We have shown that the probability of error is approximately given by  $\binom{N}{2} d^1/T$  if  $\binom{N}{2} d^1/T \ll 1$ , and if  $M = 1$ . The two cases shown in Figures 4-2 and 4-3 are identical with the exception of the transmission rate. One is almost 60 percent less than the other, and the error probabilities of the two systems are given approximately by

$$\binom{N}{2} d_1/T = \binom{N}{2} 3.54 \times 10^{-4}$$

$$\binom{N}{2} d_2/T = \binom{N}{2} 2.08 \times 10^{-4}$$

$$d_1/d_2 = 1.67$$

The above relation suggests that Figure 4-2 can be obtained from Figure 4-3 by merely scaling the curve for the case where  $M = 1$ . The amount of shift is determined by the ratio between  $d_1$  and  $d_2$ , which is approximately 1.67. To obtain Figure 4-2, pick any  $N$  on the curve in Figure 4-3 and find the error probability. For the corresponding value of error probability, then multiply the error probability by a factor of 1.67 and use the same value of  $N$  for Figure 4-2. Table 4-2 shows how good this approximation is.

Similarly, it can be shown that in the case where  $M = 2$ , the two curves in Figures 4-2 and 4-3 are related to each other by a scaling factor of  $(d_1/d_2)^2$  — a result which follows from the discussion in Section 4.2.1. Again, the translation of one curve to the other gives an excellent result. In the case where  $M = 3$ , the scaling factor is  $(d_1/d_2)^3$ , and for  $M = 4$ ,  $(d_1/d_2)^4$ . If a curve for other values of transmission rate, message length, or visibility time is desired, this technique can be used to obtain the performance of the new system.

Table 4-2 Comparison of Actual and Predicted Values of N

<u>N (Figure 4-2, predicted)</u>	<u>N (Figure 4-2, actual)</u>	<u>P (error, Figure 4-3)</u>	<u>N (Figure 4-3)</u>
<u>M = 1</u> Scaling Factor = $d_1/d_2 = 1.67$			
20	20	$3.8 \times 10^{-2}$	20
30	30	$9.0 \times 10^{-2}$	30
40	40	$1.5 \times 10^{-1}$	40
60	60	$3.0 \times 10^{-1}$	60
69	80	$4.0 \times 10^{-1}$	69
<u>M = 2</u> Scaling Factor = 2.7			
50	50	$2.0 \times 10^{-2}$	50
70	70	$5.2 \times 10^{-2}$	70
88	94	$10^{-1}$	88
100	106	$1.4 \times 10^{-1}$	100
<u>M = 3</u> Scaling Factor = 4.6			
60	60.5	$1.35 \times 10^{-2}$	60
80	80	$4 \times 10^{-2}$	80
100	106	$9 \times 10^{-2}$	100
<u>M = 4</u> Scaling Factor = 7.7			
103.5	98	$2.5 \times 10^{-2}$	103.5
124	118	$4 \times 10^{-2}$	124

Next, if the error probabilities are small enough, the curves can be extrapolated for the cases where  $M = 2, 3, 4$  from the curve of  $M = 1$ . For example,

$$P(\text{error}, M = 1) \approx \binom{N}{2} d/T$$

and

$$P(\text{error}, M = 2) \approx \binom{N}{2} 2d/T (2N)(2d/T)$$

or approximately

$$\approx \left( \frac{8Nd}{T} \right) P(\text{error}, M = 1)$$

This approximation is valid only if  $\left( \frac{N}{2} \right) Md/T$  is small. Using a similar technique, curves can be extrapolated for the cases where  $M = 3, 4$ , etc. However, this method is not much use in the two examples of interest in the error probabilities of the order of  $0.1$ .

### 3.7.4.3 Advantage of Having a Storage Device

This paragraph demonstrates how important it is to have a storage device on the processor on the earth.

Suppose there were no such storage device, then a copy of each of the  $N$  messages could be obtained if and only if the processor receives a clean copy of all  $N$  messages during one of the  $M$  subintervals. The probability of such an event is equal to

$$1 - P(\text{all of the } M \text{ subintervals have errors})$$

or

$$= 1 - \left[ 1 - \left( 1 - \frac{d^1}{T} \right)^{\binom{N}{2}} \right]^M$$

where  $d^1 = Md$

The increase in  $N$  for this system is plotted in Figure 4-5.

By comparing Figures 4-2 and 4-5, the advantage of a storage device is evident. Without any storage at the processor, the system with replication is not beneficial to the user, at least for the two examples chosen. With a storage device, correctly transmitted messages can be extracted from all  $M$  subintervals, while without it, only one out of  $M$  subintervals could be used. A more complicated system would involve retransmission of those messages that have been lost from the first to the most recent subintervals. In effect, this system would be a sequential transmission, while the information gathered up to the most recent subinterval would be used. How much better this system would perform is not known, and this system would require the satellite to be

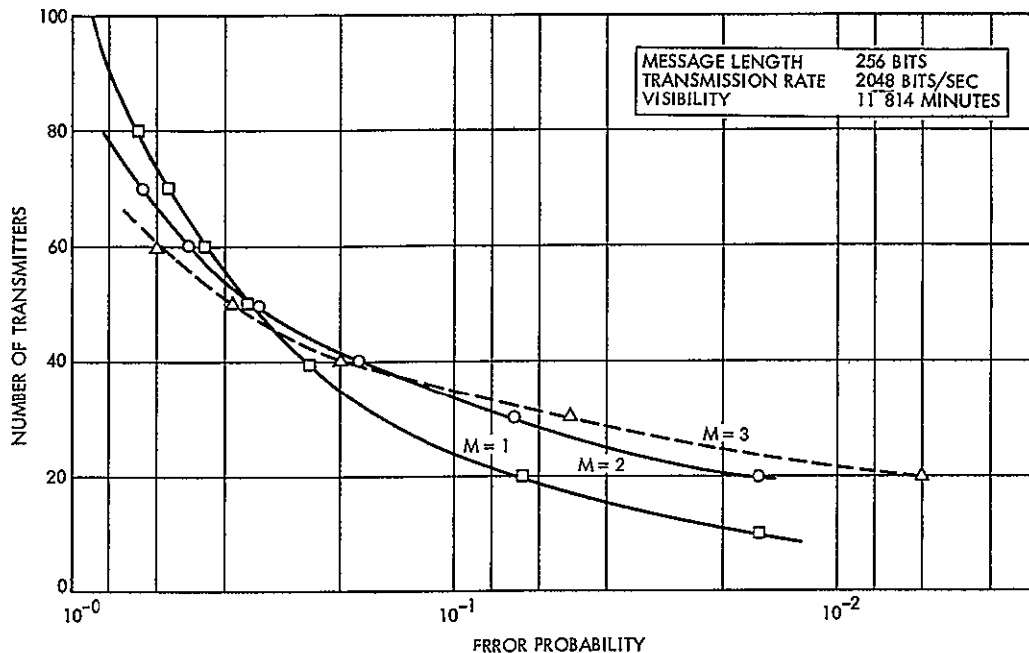


Figure 4-5

PERFORMANCE OF REMA WITH REPLICATION, BUT  
WITHOUT GROUND MESSAGE STORAGE FACILITIES

able to inform each of the  $N$  transmitters whether or not to repeat its message after each subinterval. This topic will be discussed in the TRW final report on ground signal processing and data recovery.

#### 4.2.3 Conclusion

A REMA system with replication can substantially increase the number of transmitters it can accommodate over that of a REMA system without replication. As  $\binom{N}{2}d/T$  decreases, the advantage of using replication increases. The advantage is greatest when  $\binom{N}{2}Md/T \ll 1$ , but when  $\binom{N}{2}Md/T \geq 1$ , as the two examples showed, the gain in system capacity can still be as large as seven or eight.

#### 4.3 DUAL RANDOM TIME AND FREQUENCY MODE

Sections 4.1 and 4.2 discuss the performance of the random emission multiple access (REMA) system in the time domain with and without replication. In both cases, all transmitters were assumed to be using the same carrier frequency. This section discusses the case where

the transmitters can choose any carrier frequency within a predetermined interval. For this case, it is assumed that each transmitter picks, with a uniform probability, a carrier frequency anywhere in the interval  $75 \text{ kHz} - 50 \text{ kHz}$  to  $75 \text{ kHz} + 50 \text{ kHz}$ . Also this section discusses the performance of the REMA system that uses both the time and frequency modes simultaneously. In particular, expressions are derived for the probability of interference (error) for the cases where there is no replication and where there is replication of two. The exact analysis becomes both tedious and difficult with  $M \geq 3$  if

$$\binom{N}{2} d^{1/T} \geq 1$$

This case is of prime interest for the ERTS program.

An error occurs if any message is lost throughout the  $M$  subintervals. With the time-frequency REMA system, a message is lost if it interferes with one or more messages in both the time and the frequency domains for  $M$  successive subintervals. Unlike the case where there is no replication, a loss of a message in any one subinterval does not mean that the message cannot be received in another subinterval. As long as it is not lost throughout the  $M$  subintervals, the message is delivered and is received correctly by the processor on the earth.

Three levels are examined in the proposed time-frequency REMA system.

- 1)  $\binom{N}{2} d^{1/T} \ll 1$  and loss of two messages dominate the event of any interference
- 2)  $\binom{N}{2} d^{1/T} \ll 1$  and an even number of messages are lost, and  $K/2$  distinct-pair interferences dominate the event of any interference.
- 3)  $\binom{N}{2} d^{1/T} \geq 1$

Explicit expressions are obtained for the probability of interference when no replication is allowed and when replication of two ( $M = 2$ ) is allowed

#### 4 3 1 The Frequency Domain

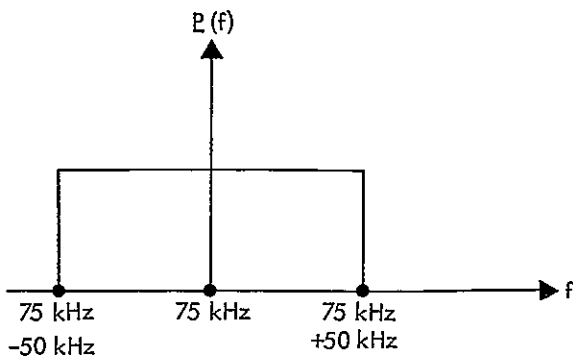


Figure 4-6

UNIFORMITY WHERE  $P(f)$  IS THE PROBABILITY DENSITY FUNCTION OF A RANDOMLY CHOSEN FREQUENCY

Each of the  $N$  transmitters transmits its message to the earth with a carrier frequency that is randomly chosen. In the ERTS Project, it is assumed that the carrier frequency can be any one interval between  $\pm 50$  kHz and about 75 kHz. The density function of this randomly chosen frequency is assumed to be uniformly distributed over the interval (see Figure 4-6)

Assuming a bandwidth of 2.5 kHz for each message, there is an interference if two or more signals collide both in time and in frequency. Hopefully, all the messages that collide in time are free of interference in the frequency domain. Of course, how the collisions take place in the time domain must be known, for example, if six messages are lost in the interval  $(0, T)$ , did these six messages collide simultaneously for any duration. The probability that six messages of different frequencies interfering is much higher than that of only two messages interfering in the frequency domain. On the other hand, perhaps the six messages were lost because three distinct-pair interferences occurred at different instants. In this case, did the two messages interfere in the frequency in any one of the three distinct occasions. This probability may be much smaller than that of six messages of different frequencies interfering.

In this preliminary analysis, a few simplifications must be made to obtain the magnitude of increase in  $N$  that may occur when the time-frequency REMA system is used. Another reason for simplifications is to show how complicated the exact analysis would be without them. A simulation of the frequency-time REMA system on a computer is suggested for a thorough analysis.



#### 4 3 1 1 Definition of Bandwidth and Interference

Each message consists of approximately 110 or more binary digits, each of which may be 1 or 0 with a probability of 1/2. The detection bandwidth required to decode the binary sequence is determined by the PRF of the transmitter and the power spectrum of the binary sequence. For practical purposes, the detection bandwidth can be approximated to be 2.5 kHz when the PRF is set at 2048 bits/sec.

An interference in the frequency occurs if the power of signal A, which slips into the detection bandwidth (2.5 kHz) of B, exceeds -10 db of the total power in message A. The parameter, then, is that an interference occurs whenever the separation of two carriers is less than 5 kHz.

If the PRF is set at 4156, then the separation must at least be 5 kHz to avoid interference.

#### 4 3.1 2 Probability of Interference

This paragraph discusses the probability of an interference of  $K'$  number of messages that are simultaneously received by the satellite. Simultaneous reception means that at one instant  $K'$  messages are being received by the satellite. It is assumed that all  $K'$  messages were tracked by the phase-lock loops and can be decoded if the six carrier frequencies are far enough apart. This assumption may not be practical if a large number of messages, say 10, was received by the satellite receiver at the same time, but it is a practical assumption to determine the best performance to be achieved by using both the time and frequency REMA system.

##### Case $K' = 2$

There is an interference whenever two carriers come within a distance of 5 kHz. An approximate probability of this event is given by  $2(2.5)/100 \approx 0.05$ .

This answer is qualified by saying "approximately" because the odd cases that arise when one of the carrier frequencies is within the intervals (75 kHz + 45 kHz, to 75 kHz + 50 kHz) or 75 kHz - 45 kHz to 75 kHz - 50 kHz).

is yet to be considered For these cases, the probability of interference is not 0.05, it is slightly smaller

#### Case $K' = 3$

This case is similar to  $K' = 2$  and it is concluded that the probability of interference is  $\approx 0.10$ .

#### Case $K' \geq 4$

This case is not analyzed as simply as the previous cases because the frequency range occupied by four or more signals is a considerable portion of 100 kHz. Simulation is necessary to obtain a solution quickly, as the exact analysis is too tedious.

Figure 4-7 shows the result of the simulation on the Tymshare. As is indicated, if there are more than five messages at the same time, the probability of interference is close to 50 percent, with 10 messages, it is up to 90 percent.

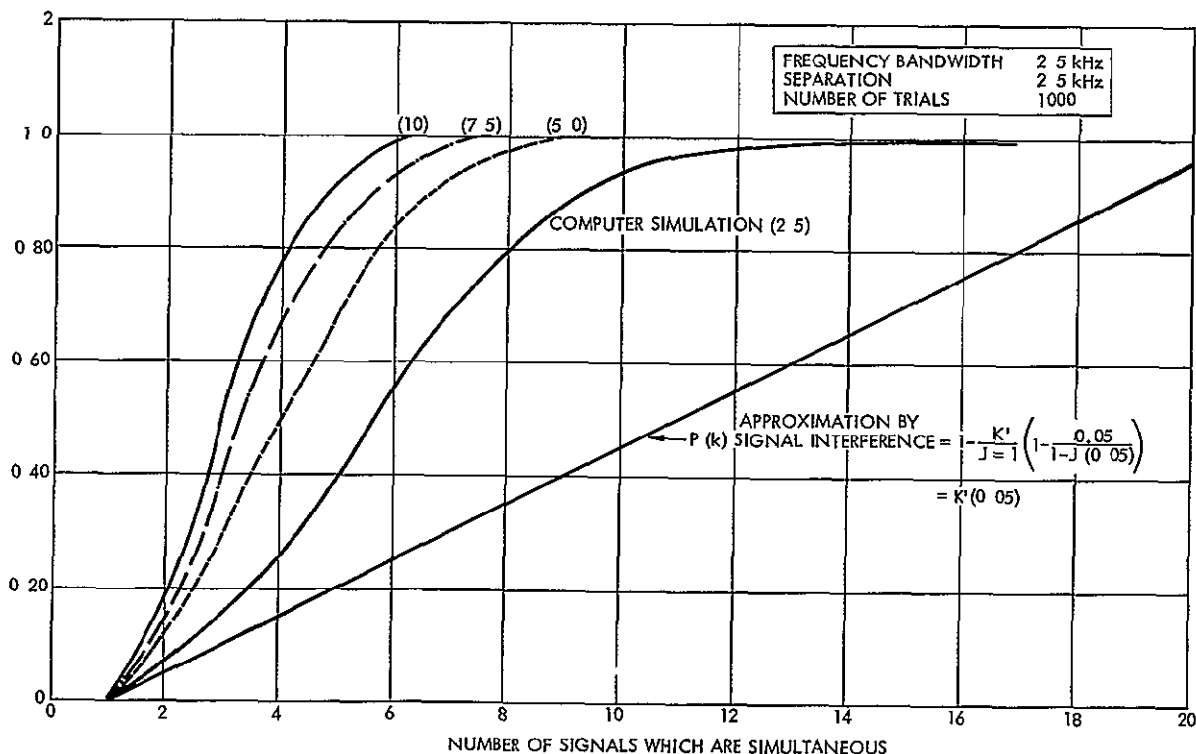


Figure 4-7

PROBABILITY OF INTERFERENCE VERSUS NUMBER OF SIGNALS WHICH ARE ON SIMULTANEOUSLY

#### 4.3.2 No Replication

Case I  $\binom{N}{2} d^1 / T \ll 1$

Section 4.1 approximates the probability of error by  $\binom{N}{2} d^1 / T$ . More important, an interference was defined as a loss of only two messages. An error occurs when these interfering two messages cannot be distinguished in the frequency domain. The probability of two messages (which arrive at the same interval) colliding in the frequency domain is given by approximately  $2f/F$  where  $2f$  = twice the bandwidth of the messages.

The total error probability is simply the product of interfering probability in time and  $2f/T$

$$P(\text{error}) \approx \binom{N}{2} d^1 / T \cdot 2f/F \approx 0.05 \binom{N}{2} d^1 / T \quad (25)$$

For a specific example where  $2f = 0.05$ , the error probability decreases by a factor of 20. The probability of interference is the product of two error probabilities, one in time and another in frequency. This property does not hold when  $\binom{N}{2} d^1 / T \gtrsim 1$ .

To compute the increase in  $N$  offered by the time-frequency REMA system over the time-REMA system,  $N$  can be solved from the expressions of the probability of interference.

From Equation (25)

$$P(\text{error}) \approx \binom{N}{2} d^1 / T \cdot 2f/T$$

and for the time-REMA system

$$P(\text{error}) = P_e \approx \binom{N}{2} d^1 / T$$

Assuming  $\binom{N}{2} \approx N^2/2$  if  $N \gg 1$  the following is obtained

$$N_{T-F} \approx \sqrt{2P_e (T/d^1) (F/2f)} \quad (26)$$

and

$$N_T \approx \sqrt{2P_e (T/d^1)} \quad (27)$$

The ratio of Equations (26) and (27) yields the increase in N

$$\zeta = N_{T-F}/N_T = \sqrt{F/2f}$$

if  $F = 100$  kHz and  $2f = 5$  kHz,  $\zeta = \sqrt{20}$  or approximately 4.5. Hence, it is concluded that, if  $\binom{N}{2} d^1/T \ll 1$  and loss of two messages dominate the interference, the number of users can be increased by 4.5.

Case II Only  $K/2$  Distinct Pairs Interfere,  $\binom{N}{2} d^1/T \ll 1$

This case allows more than two messages to be lost, but still assumes that most of the time interferences are due to loss of messages by  $K/2$  distinct-pair interferences. The probability of losing  $K$  messages in the time domain is given by

$$P(K = \text{even}) \approx \frac{1}{\binom{K}{2}} \binom{N}{2} \binom{N-2}{2} \left(\frac{d^1}{T}\right)^{\frac{K}{2}} \left(1 - \frac{d^1}{T}\right)^{\binom{N}{2} - \frac{K}{2}}$$

The error probability is given by

$$P(\text{error}, T-F) = \sum_{K=2}^N P(K = \text{even}) \left(1 - \frac{2f}{F}\right)^{\frac{K}{2}}$$

An important assumption made here is that at any instant there are at most two messages interfering in the time domain. This assumption is reasonable as long as  $\binom{N}{2} d^1/T \ll 1$

Case III  $\binom{N}{2} d^1/T \lesssim 1$

This case considers the loss of an odd number of messages developed in Section 4.2. However, in using this model, the probabilities of having two messages interfere at one instant, three at a time, four at a time, must be considered. The computation of these probabilities is

difficult. One way to circumvent this problem is to assume that whenever there is an interference in time, it is due to  $K/2$  distinct pairs (only two messages interfere at any time) when an even number of messages are lost, and to assume that  $(K-1)/2$  distinct pairs interfere when an odd number of messages are lost. This is an optimistic approximation since there are cases when more than two messages interfere in time and  $K \geq 2$  messages are lost.

The purpose of this simplification is to obtain the magnitude of improvement by using the time-frequency REMA system.

Using these approximations, the error probability expression is

$$P(\text{error}) = \sum_{K=2}^N \underline{P}(K = \text{even}) \left(1 - \frac{2f}{F}\right)^{\frac{K}{2}} + \sum_{K=3}^N \underline{P}(K = \text{odd}) \left(1 - \frac{2f}{F}\right)^{\frac{K-1}{2}}$$

where  $2f = 5 \text{ kHz}$  and  $F = 100 \text{ kHz}$

Computation of  $P(\text{error})$  was made for the case where the message length was 256 bits, PRF = 2048 bits/sec, and a visibility time of 11.814 minutes. The graph in Figure 4-8 shows the improvement offered by the time-frequency REMA system.

#### 4.3.3 Replication of Two

$$\underline{M} = 2$$

When a replication of two is allowed, a message is lost if any one message is lost both in time and frequency during two successive sub-intervals. The upper bound to the probability of error is written as

$$P(\text{error}) = \sum_{K=2}^N \underline{P}(K \text{ messages are lost in time during the first subinterval, } I-1) \cdot \underline{P}(K^* \text{ messages out of } K \text{ are lost to frequency interference in } I-1) \cdot \sum_{L=1}^{K^*} \underline{P}(\text{Any one of } K^* \text{ messages are lost both in time and frequency during the second subinterval, } I-2)$$

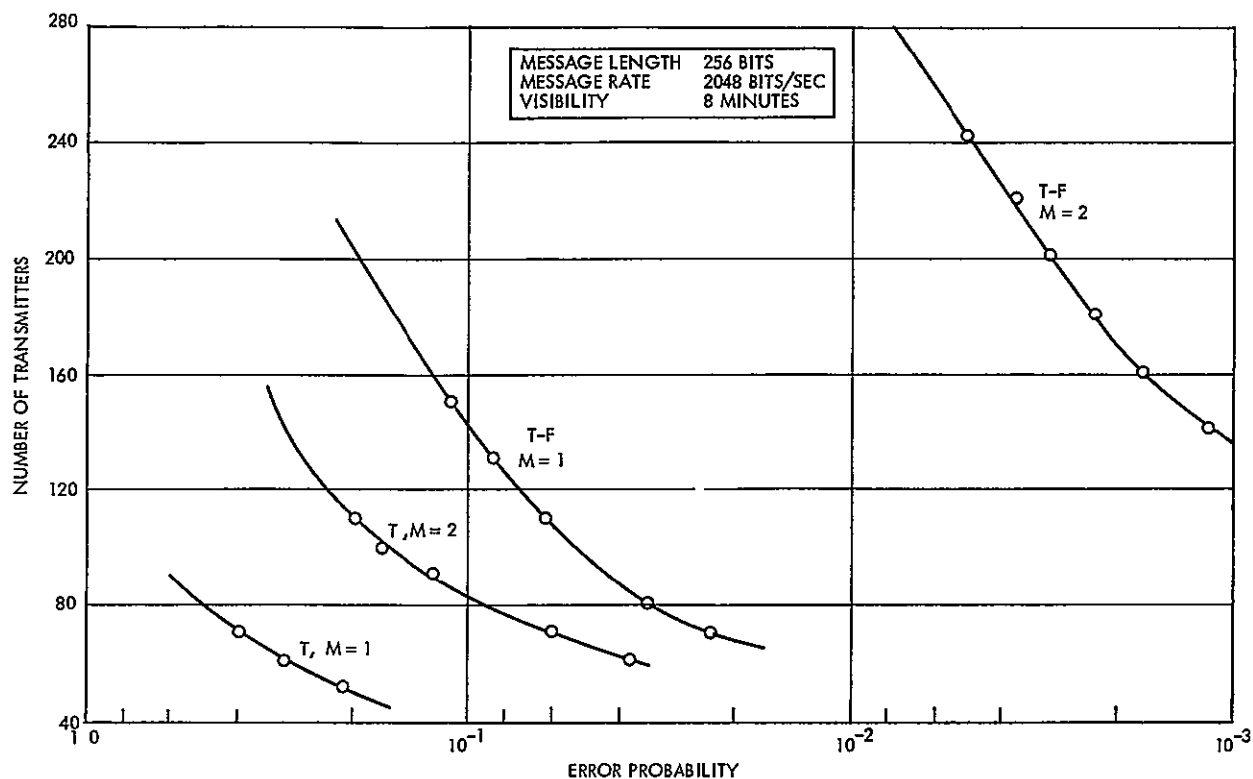


Figure 4-8

COMPARISON BETWEEN TIME-REMA AND TIME-FREQUENCY REMA SYSTEM

where

$$\begin{aligned} & \underline{P} (K^* \text{ messages out of } K \text{ are lost due to frequency interference in I-1}) \\ &= \binom{K^*}{K} P^{K^*} (1-P)^{K-K^*} \end{aligned}$$

and

$$P = \frac{2f}{F}$$

$$\begin{aligned} & \underline{P} (\text{Any one of } K^* \text{ messages are lost both in time and frequency during} \\ & \text{the second subinterval, I-2}) \end{aligned}$$

$$= 1 - P (\text{all } K^* \text{ messages are correctly sent in I-2})$$

For the parameters described previously, the probability of error was analyzed by assuming that at any instant two messages, at most, can interfere in time. The result is plotted in Figure 4-8

### Case Where $\binom{N}{2} d^1/T \geq 1$ With Replication

Several problems must be solved before analyzing the performance of the time-frequency REMA system for this case. A computer simulation was performed to obtain the number of users to be accommodated with the time-frequency REMA system. Though an analysis is much more desirable than a simulation for both accuracy and usefulness, simulation gives a reasonable estimate of the number of users to be accommodated when there is a limited amount of time for study, and was the route taken during the Phase B/C study

By using the time-frequency REMA system, an increase in the number of users,  $N$ , is expected. This phenomenon is evident from the few cases which were described in the preceding paragraph. It appeared that as many as 300 or more users can be accommodated with this system. If  $N = 400$ , then

$$\binom{N}{2} d^1/T = (8 \times 10^4 \times 1.76 \times 10^{-4}) M$$

where  $M$  is the number of replication. If  $M = 2$ , the above expression is nearly 25. This number indicates that all the models developed in Sections 4.1 and 4.2 are no longer valid, since they were restricted to the cases where  $\binom{N}{2} d^1/T =$  order of one. Third-order, perhaps, fourth-order, approximations are needed to describe how an interference occurs.

Whether the binomial probability approach is a valid description of the time-frequency REMA system is another problem when  $N$  and  $M$  increase to a large value. The fraction of time occupied by 400 users over one transmission subinterval will be approximately  $N d^1/T = 0.014$ .

This is much larger than the cases which were examined in Sections 4.1 and 4.2 where  $N d^1/T$  was approximately 0.05 smaller. Even if a refined model of interference is obtained and solved for the probability of error, the result may not describe what really happens if the time-frequency REMA system is used.

#### 4 3 4 Time-Frequency Tradeoff

This section briefly describes the tradeoff between time and frequency as the PRF of the transmitters is increased. It is shown that at least in one case there is no advantage in increasing the PRF, while for other cases the tradeoff cannot be clearly defined without an extensive analysis. This is one reason why a simulation was adopted to explore this problem

##### Case Where $\binom{N}{2} d^1/T \ll 1$ , No Replication

Suppose that a loss of only two messages dominates the cases of interference. Then the probability of error in the time domain is approximately given by  $\binom{N}{2} d^1/T$ . In the frequency domain, the probability that two messages interfere, conditioned on the event that the messages collided in time, is approximately given by  $2(f)/F$  where  $F = 100$  kHz, and  $f$  is the bandwidth. As noted earlier, the bandwidth is related linearly to the PRF. If the PRF increases by a factor of two, then the bandwidth (as defined) increases by two. Assuming that enough power has been made available to the receiver that the entire message is decoded without error, it is observed that the probability of frequency domain interference increases by a factor of two if the PRF increases by a factor of two, while the message duration is halved (for a constant number of data bits). Then,

$$P(\text{error, time}) \approx \binom{N}{2} d^1/2T \quad (28)$$

However,

$$P(\text{error, frequency 2 interfere in time}) = 2 \frac{2f}{F} \quad (29)$$

The product of Equations (28) and (29) yields the probability of error when both the time and the frequency REMA systems are used.

$$P(\text{error}) \approx \binom{N}{2} \frac{d^1}{2T} 2 \left( \frac{2f}{F} \right) = \binom{N}{2} \frac{d^1}{T} \cdot \frac{2f}{F} \quad (30)$$

This equation is identical to Equation (25).



Note that the increase in the PRF (and the corresponding increase in power level) does not change the overall probability of error. Next, other cases when there is replication are examined.

### Replication

If there is a replication of two, then

$$P(\text{error, time}) \approx \binom{N}{2} (d^1/T) \cdot 2N (d^1/T)$$

where  $d^1 = Md$

Incorporating the frequency domain,

$$P(\text{error, frequency}) \approx 2(f)/F$$

If the PRF is increased by a factor of  $m$ ,

$$P(\text{error, time}) \approx \binom{N}{2} (d^1/mT) \cdot 2N (d^1/mT)$$

and

$$P(\text{error, frequency}) = 2(f) m/F$$

and the overall probability of error is given by

$$P(\text{error, } M = 2, T-F) \approx \binom{N}{2} \frac{d^1}{T} \left( \frac{2f}{F} \right) \cdot 2 \frac{Nd^1}{T} \frac{2f}{F}$$

Again, there is no change in the probability of error when the PRF is increased

Of course, by increasing the PRF there is a substantial decrease in the probability of error in the time domain (an increase in  $N$ ) without the frequency-REMA system. Only when the frequency-REMA system is incorporated, is there the cancellation effect.

The PRF cannot be increased without limit and still have the cancellation effect continue. For example, if the PRF is increased too much,

then the probability of error reaches unity in the frequency domain. Then, essentially only the time-REMA without the frequency-REMA is obtained. Theoretically, the overall probability will decrease indefinitely as the PRF increases.

There are other practical problems which arise when the PRF is increased. As the PRF is increased, duration of the message becomes smaller and smaller. Then the phase-lock loops do not have enough time to lock and to start to decode the message. Additional DCP transmitter power is the penalty that must be paid.

On the other hand, if the PRF is decreased too much, then the messages will be interfering in the time domain. Sometimes more than two messages will be interfering at one time. Then the primary assumption that  $\binom{N}{2}d^1/T \ll 1$  will be violated.

#### Case Where $\binom{N}{2}d^1/T \geq 1$

When the above condition holds, it can be assumed that message interference in the time domain occurs in pairs. Similarly, if more than two messages are colliding in the time domain, it is not clear what effect the increase in the PRF has on the overall probability of error. Certainly the probability of collision in the frequency would change if the four messages arrive at one instant and the PRF is varied. Whether the collision probability increases linearly as the PRF increases (when more than two messages arrive in one instant) has not yet been fully explored.

For the ERTS program, it became obvious that additional understanding was needed for a tradeoff when  $\binom{N}{2}d^1/T$  is in the order of one. A simulation approach was used because an exact analysis is too complicated.

#### 4.4 COMPUTER SIMULATION

Basically, the Monte Carlo approach is used to evaluate system performance. This approach utilizes the computer to set up a situation that is analogous to the real system performance. The parameters are varied and the events of interest counted.\*

---

\*S.P. Clarke and R. K. Nisbett, "Low-Cost Random Emission Multiple Access System -- REMA -- for Earth Resources Monitoring via Satellite," TRW Systems Memorandum 7351-06-70, December 4, 1969.

The simulation approach is valuable as an independent check of the results obtained by other methods, such as statistical analyses based on approximation formulas or actual field tests

In the context of the particular problem (mutual interference between multiple transmissions of low duty cycle on the same frequency), the method has been applied in the following manner.

The computer includes a random number generating capability, which permits even the simple Tymshare computer to develop about 100 million different numbers. The magnitude of every number is in the range of from zero to one, and all values are statistically equiprobable, i.e., a uniform and independent distribution. For simulating the random transmissions, a computer program was written that calls for a set of "N" numbers from the random number series. These N numbers are used to define the time locations of the start of each N message associated with the N transmitter situation being simulated.

One program input is the length of message required. The computer program then compares the starting time of each of the N messages with all the N-1 other messages to establish whether, for any pairs, the absolute difference in time is less than the message length  $t$ . A subroutine identifies and counts all message collisions. The program, under control of an iterative loop, repeats this activity for many sets of random numbers, and thereby obtains a statistical measure of the actual number of trials for which one or more messages were mutilated.

Each interference can involve any number of signals. The number of participating signals are recorded for each collision event.

During the course of the Phase B/C study TRW has converted the original Monte Carlo message collision program from the language (appropriate to Tymshare) to Fortran IV. This change has allowed us to perform considerably more comprehensive simulations using the TRW CDC 6500 batch processing computer.

#### 4.4.1 Simulation on CDC 6500

Our simulation shows that with a replication of 2 ( $M = 2$ ), we can accommodate approximately 550 users with the time-frequency REMA

system if the error probability is in the order of 0.05. Unfortunately, this number cannot be verified accurately because of exorbitant computation time, but will be alleviated when our recommendations for a shorter program are incorporated. It is believed that 1000 users can be accommodated by the time-frequency REMA system if  $M = 3$ .

On the other hand, by using frequency channeled REMA system, 800 users can be accommodated if  $M = 4$ , and 1100 users if  $M = 5$ . The channelized REMA system is obtained by channeling the transmitting frequencies of the users on the earth. For this application, we are proposing five different transmitting bands. Burial of the platform's transmitter oscillator is necessary to implement this mode. (See Section 2.7)

#### 4.4.2 Method of Simulation

The general outline of the computer simulation performed is presented below. For the set of input parameters, we need the following information: number of users, data rate, number of replication, whether both time and frequency REMA's or only time-REMA is to be used, and the number of simulations to be carried out.

In the beginning of each simulation run,  $N$  (corresponding to the number of users) random numbers are generated. These pseudo-random numbers are uniformly distributed over the interval  $(0, 1)$ .

Once these numbers are generated, all the possible combinations of pairs among the  $N$  numbers are checked to see whether any two messages are interfering. In general, the following  $\binom{N}{2}$  pairs are considered

1-2	1-3	1-4	1-5	1-6	.....	1-(N-1), 1-N
	2-3	2-4	2-5	2-6	.....	2-(N-1), 2-N
		3-4	3-5	3-6	... ..	3-(N-1), 3-N

If any one of the  $\binom{N}{2}$  pairs is interfering, the checks are made by taking the difference of two random numbers. For example, if the numbers corresponding to messages 1, 2, and 3 are

Message (1) .0013

(2) .185

(3) .950

..

then, to check whether message 1 interferes with message 2, we take the absolute difference between the two numbers (0 0013, 0 185) and see whether the result is smaller than the "normalized" duration of the message. The normalized message duration is given by the formula

$$\frac{(\text{PRF})(\text{Message length in bits})}{(\text{Visibility time in seconds})}$$

For our examples, this duration is approximately  $1.1 \times 10^{-4}$ .

For the examples above, there is clearly no interference among messages 1, 2, and 3

#### 4 4 3 Random Number Generators

Different random number generators (all of which have been thoroughly tested) are available. Three separate routines were tried, but there appears to be little difference in the generation time of the random numbers that are uniformly distributed over the interval (0, 1). For these routines, the possibility of repetition is zero if not more than 100 million of them are consecutively generated.

The time of generation is one of the critical factors in the total computation time. For both of them, the generation time is close to 0.024 msec per number

These routines can be called by the following commands RANK(x), RANDOM(x), and UPR1. Since the last routine is slightly faster than the others, it was used in this program.

#### 4 4 4 Description of the Computer Program

##### Case I Time-REMA, M = 1

To test the time-REMA System, N numbers (corresponding to the number of users) are generated and  $\binom{N}{2}$  pairs are checked if any one of them has interfered. In this program, a counter, ECOUNT, which counts the number of times any interference has occurred during the total number of trials, was started. A5 represents the total number of trials. At the end of the run, ECOUNT is divided by A5 to obtain the fraction of trials that yielded an interference.

## Case II Time-REMA, $M \geq 2$

If the number of replication is greater than two, then a record must be kept of the messages lost during the first interval, I-1, and the second, and so on.

In our Fortran program, this record is made in two arrays, S and S2, each of which has 500 elements. The symbol S(I), stands for the array where the index, I, can range from 1 to N (the number of users). A2 is used in the program to represent N. At any instant, the array S(I) contains the messages that have been lost from the first to the most recent subinterval. Whenever a message, e. g , message 17, is lost during the subintervals, I-1, I-2, . . . I-(next to the most recent), then S(17) is set to 1. Otherwise, S(17) is set to zero. To take another example, messages 1, 2, and 7 are lost during the first subinterval, I-1. Then, at the end of I-1, S(1)=S(2)=S(7)=1, and all other S(I)'s will be 0. Suppose that during the second subinterval, messages 1 and 7 are lost, then S(1) and S(7) will still be equal to one and S(2) will now be set to zero.

The second array, S2(I), contains the information on which messages were lost during the most recent subinterval. For example, during the third interval, messages 1, 2, 7, and 8 are lost. Then S2(2)=S2(1)=S2(7)=S2(8)=1. To determine whether these messages (1, 2, 7, 8) were lost from the first to the previous intervals, to see we check if any of S(1), S(2), S(7), S(8) is one. If S(1)=1 and the others equal zero, then at the end of the third subinterval, we have S(1) = 0 and S2(I) = 0  $\forall I = 1, \dots, A2$ .

All the S2(I)'s are set to zero to be ready for the fourth subinterval. This checking procedure between S2(I)'s and S(I)'s continues until the desired number of replication is completed. The number of replications, represented by IREPL, is compared with a counter that tracks the number of times a set of A2 (or N) random numbers are generated. Each time a set of N random numbers is generated, the counter JOINT increases by 1, until JOINT is equal to IREPL, at which time, that particular trial is finished. Since the array S(I) contains the messages that have been lost during the M subintervals, we check to see if any one of S(I) is one. If so, an interference has been encountered.

Another counter, ICOUNT, keeps track of how many times the trials are carried out. When the ICOUNT equals the number of proposed trials, A5, then the computer program is near completion. The number of trials in which there was an interference is taken from ECOUNT and divided by A5 to obtain the fraction of time in which there was an interference

### Case III Frequency-REMA System

When we have both the time and frequency REMA systems, another set of random numbers is generated to take care of random carrier frequencies. By setting IFREQ=1, the frequency mode of the time-frequency REMA system is activated in the computer simulation program. If IFREQ is anything but one, then only the time-REMA system is operative

In the time-frequency REMA mode, a pair of random numbers (which represents the random carrier frequencies) is generated whenever two messages collide in the time domain. Again, S(I) contains the messages that have been lost (both in the time and frequency domains) from the first to the next to the most recent subinterval. Similarly, S2(I) keeps track of the messages lost during the most recent subinterval.

### Data Format

Two data cards must be fed into the computer to run the computer program. The first card gives the number of separate cases for which simulation runs should be made. The second card includes the following data

IFREQ	one or zero, depending on whether the time-REMA system is used
A1	message lengths in bits
IREPL	number of replications
A2	number of users
FQBAND	frequency bandwidth of one message
A5	number of trials

If additional cases are desired, other cards are fed in after the first case. Of course, the first card, which represents the total number of separate cases (NCASE), must be changed accordingly.

### Number of Trials

To find out how many experiments are needed, the Chernoff bound can be used. Let  $p$  be the desired probability of interference that we would like to estimate by making  $N^*$  experiments. According to our computer program, we add the number of times there was an interference and divide this number by  $N^*$  to obtain the estimate of  $p$ , which we denote by  $\hat{p}$ .

The Chernoff bound states the following

$$p[\hat{p} - p \geq \epsilon] \leq \exp\{-XN^*\}$$

where  $N^* = A5$  in the program and

$$p[p - \hat{p} \geq \epsilon] \leq \exp\{-XN^*\}$$

where

$\epsilon$  = the error

$$\hat{p} = \frac{\text{number of times out of } N^*, \text{ we had interference}}{N^*}$$

$$X = -\ln \left[ \left( \frac{p}{p + \epsilon} \right)^{p + \epsilon} \cdot \left( \frac{1 - p}{1 - p - \epsilon} \right)^{1 - p - \epsilon} \right]$$

If  $\epsilon \ll p$ , we can show that

$$X \approx \frac{\epsilon^2}{p}$$

Using these expressions, we can show that

$$p[|\hat{p} - p| \leq \epsilon] \leq Z \exp\{-XN^*\}$$

If we are interested in the region of  $p = 0.1$  and  $\epsilon = 0.01$ , that is  $p[|\hat{p} - p| \leq \epsilon]$  is close to 0 percent, then we must solve for  $N$  by setting

$$Z \cdot \exp\{-XN^*\} = 0.1$$

For this case, we can show that  $X \approx \epsilon^2/p \approx 0.001$ , and  $N \approx 3000$ . Similarly, if we set  $\epsilon = 0.03$ ,  $N$  is approximately 350.



### Computation Time

The statements used in the revised Fortran IV program are listed in Appendix C. The list below shows typical computations times for both the CDC 3200 and 6500.

	<u>Number of Users</u>	<u>M</u>	<u>Number of Trials</u>	<u>Computation Time</u>
Time-REMA				
	190	4	500	16 minutes
	220	5	500	25 minutes
Time-Frequency REMA				
	650	1	500	60 minutes

### 4 4 5 Recommendations to Reduce Computing Time

Unfortunately, to run the computer program for from 1000 to 3000 experiments, it takes between 1 and 2 hours on the CDC 6500 computer. However, the present programming time can be significantly reduced by making a few major changes to our Fortran IV program.

Whenever there is an interference in one interval, only the messages that are lost should be tracked. In the present system, all N messages during each interval are checked, not just the ones that have been lost from the first up to the most recent subinterval. For example, consider the case in which  $N=500$  and  $M=5$ . Assume that 100 messages are lost during the first subinterval, I-1. What happens to the 100 messages during the second subinterval, I-2, should concern us then so that 500 of them won't have to be checked. Perhaps 50 or more messages out of 100 will be lost again during I-2, and 20 out of 50 during the I-3, and so on.

Considerable computer processing time is wasted in unnecessary computation in the present program, however, not enough engineering time was available to completely overhaul the present computer program. Projected savings in computation time may run as much as a factor of four when M is large, and even more if both time and frequency REMA systems are being simulated together.

The present program gives an estimate of the error probabilities of a REMA system. For example, it is unlikely that the curves obtained by runs of 600 to 700 differ much in the second significant figure of the error probability if  $p \geq 0.1$  as our analysis indicates.

#### 4.4 6 Computer Results

On the basis of the determination in the previous section that the number of experiments needed for  $P_e$ , of the order of 0.05 is over 1000 and that the computation time for such a run will take 60 min on the CDC 6500, we ran cases in which  $P_e$  was greater than 0.10 and extrapolated the graph for the cases in which  $P_e = 0.05$ .

Figures 4-9 through 4-11 show the results of our simulation. These results from the computer simulation agree closely with those of the analyses in the regions in which the analysis was applicable.

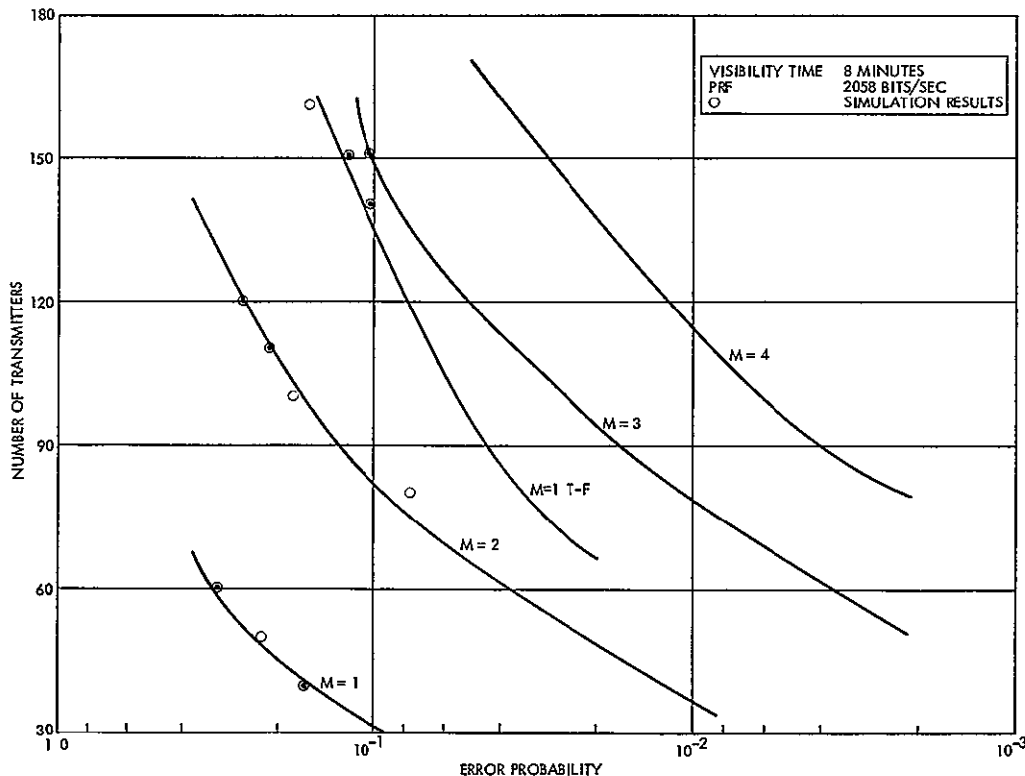


Figure 4-9  
NUMBER OF TRANSMITTERS VERSUS ERROR PROBABILITY

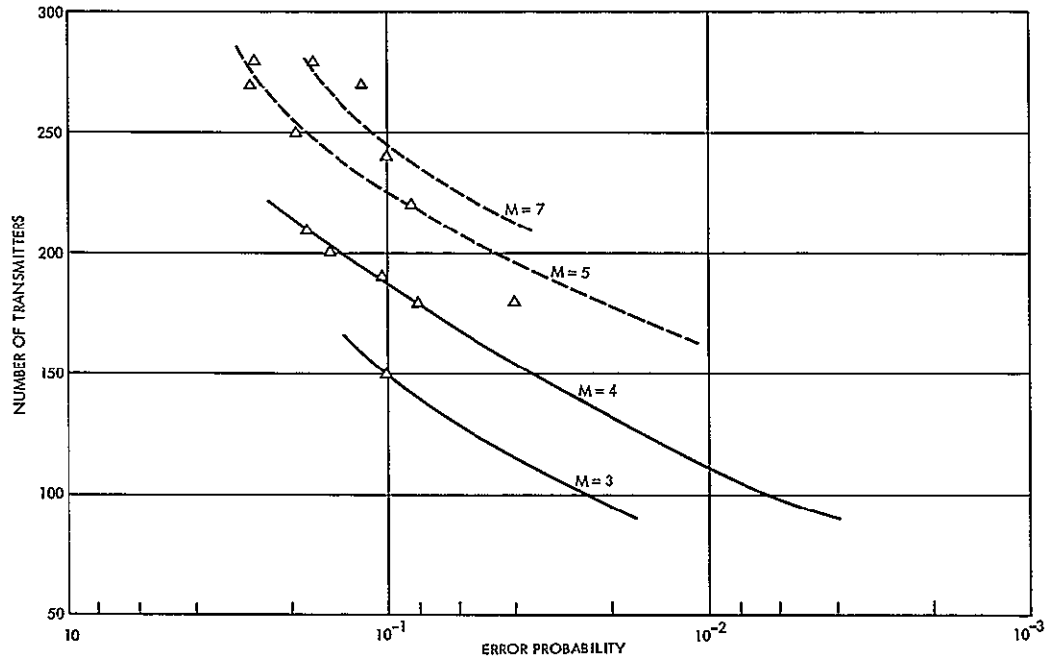


Figure 4-10  
T-REMA SYSTEM SIMULATION RESULTS

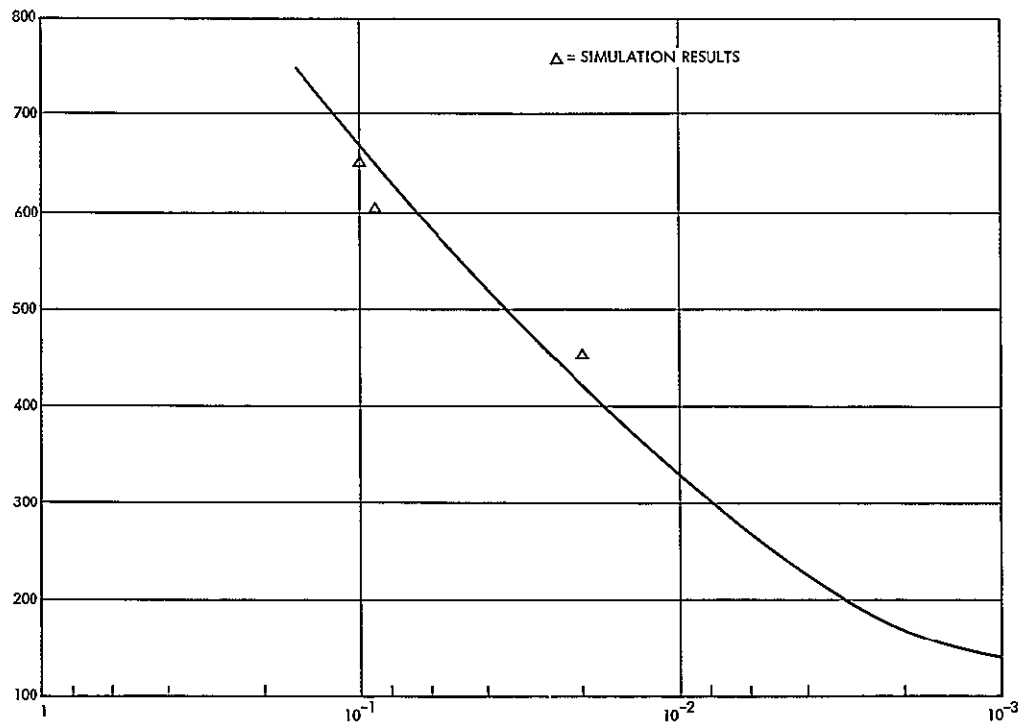


Figure 4-12  
TIME-FREQUENCY REMA SYSTEM SIMULATION RESULTS,  $M = 2$

## CONTENTS

	Page
5 DATA TRANSMISSION TO GSFC	5-1

## 5 DATA TRANSMISSION TO GSFC

As will be discussed in considerable detail in the volumes of this report to be submitted in April, in transferring data to the ground data handling subsystem, the two principal constraints are the specialized nature of equipment needed for separation of the signals in the 120-kHz IF bandwidth and the underirability of locating such equipment at remote stations. It is assumed that all ground stations will have 1.024 MHz sub-carrier demodulators and adequate record/reproduction capability.

It is desirable that the GDHS receive data in a unified form, therefore an acceptable goal appears to be to make all data collection system data enter the GDHS at the undemodulated IF level. Figure 5-1 indicates how this might be achieved. Of the three ground stations, GSFC/NTTF, Alaska, and Texas, the GSFC/NTTF station is probably the only source from which a 120-kHz IF bandwidth can be received in real time. At the present time a microwave link is being considered for this purpose along with the transmission of video data. In view of the short distance involved, a cable is equally feasible for DCS data transmission.

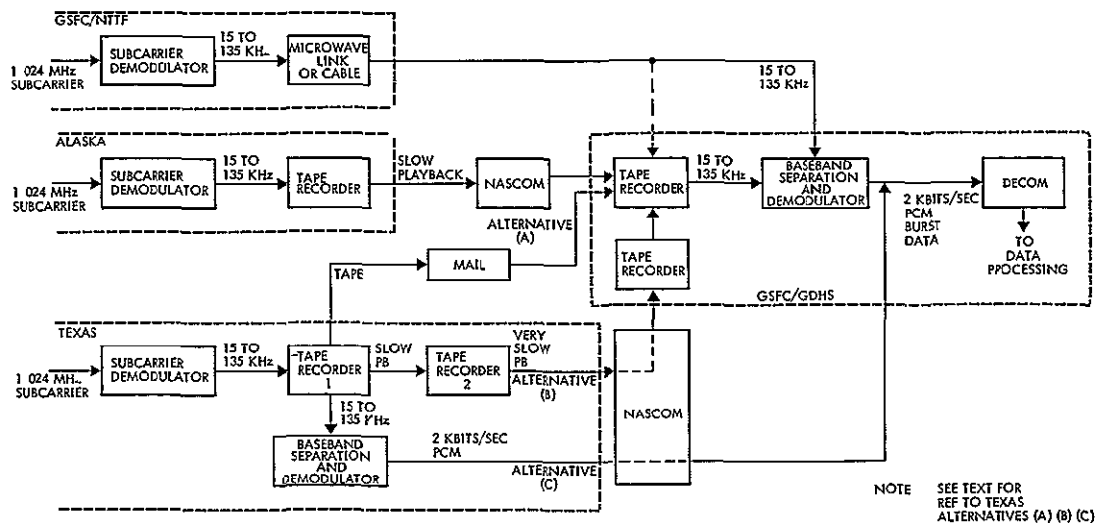


Figure 5-1

### DATA COLLECTION SYSTEM DATA FLOW DIAGRAM

The capability between Alaska and GSFC is rated at 16 kbits/sec maximum on a 48 kHz circuit. There appears to be no reason why a

near real-time transmission of the intermediate frequency cannot be achieved by a slow playback technique at perhaps a 4:1 record/playback ratio. This method could result in approximately two hours of delay from the data collection system to the NDPF computer output.

The Corpus Christi, Texas, station presents the greatest problem because of the limitations of available NASCOM line bandwidth, permitting a maximum of 2.4 kbits/sec. Unfortunately the slow playback technique is not practical because of the playback ratios. The alternatives appear to be as follows:

- a) Mail, since the distance is not great the time delay may be acceptable.
- b) A double record/playback sequence to achieve an acceptable playback ratio. Although slight degradation of data can be expected, such a sequence might suffice for quick-look data if backed up by mail. In any case, such a double sequence would take longer than the normal slow playback method and is cumbersome when viewed in terms of tape-run times. However, there are plans to improve line capabilities so that a normal slow playback may become practical.
- c) Complete reduction to PCM at 2 kbits/sec with normal transmission to GSFC. This obviously violates the concept of providing no specialized demodulation equipment at remote stations. Here it may be worth noting that separation of the signals on the 120-kHz IF bandwidth would almost certainly involve a multitrack (five-channel) recording of PCM since there could be time collisions of burst data which can only be separated in terms of band location. Then each track would be played back in turn to develop a single-channel of PCM for overland transmission.
- d) It is also understood that a tariffed line with a bandwidth of 300 Hz to 20 kHz may be available, thus, playback could be one-eighth the rate.



# APPENDIX A

## DERIVATION OF $P(K = \text{ODD})$

This appendix shows the derivation of an approximation to the probability that exactly an odd number of  $K$  messages are lost. To illustrate the counting procedure used in this section, consider the five ordered messages, 1, 2, 3, 4, and 5, to be lost. As an example, assume that these five messages are lost because of the following interferences:

1 & 2, 3 & 5, 4 & 5

where  $N$  is assumed to be at least as large as five.

The probability of this particular event (1 & 2, 3 & 5, 4 & 5) is

$$P\left(\begin{matrix} 3 \text{ particular pairs} \\ \text{interfere} \end{matrix}\right) \cdot P\left(\begin{matrix} \binom{N}{2} - 3 \text{ pairs are free} \\ \text{of interference} \end{matrix}\right) = (d/T)^3 \cdot (1 - d/T) \binom{N}{2}^{-3} \quad (\text{A-1})$$

In obtaining Equation A-1, the basic assumptions presented in Section 4 were used; i. e., whether or not one pair interferes in independent of what happens to other pairs.

The next step is to determine the total number of ways three pairs can be chosen and five messages can be lost. Without proof, the most likely way to lose five messages is to have interference of two distinct pairs and one nondistinct pair. This can be proven regorously. To find the number of ways to choose two distinct and one nondistinct pairs, the  $\binom{N}{2}$  pairs are drawn as follows:

1-2,	1-3,	1-4,	1-5,	1-6, .....	1-N
	2-3,	2-4,	2-5,	2-6, .....	2-N
		3-4,	3-5,	3-6,	
			4-5,	4-6, 4-7,	4-7
				5-6, 5-7,	5-N
				6-7, 6-8, .....	6-N
				7-8, .....	
					N-1, N



To illustrate this counting procedure, assume that interferences between 1 and 2, and 3 and 4 have occurred. Therefore, the only way to have a loss of five messages with three pairs of interferences is to have an interference among any of the following pairs:

1 & 5,	1 & 6,	1 & N
2 & 5,	2 & 6,	2 & N
⋮	⋮	⋮
4 & 5,	4 & 6,	4 & N

Five messages are lost if the third pair is any one in the shaded region of the triangle matrix shown in the previous paragraph. Of course, the pairs can be 1&2, 3&4, 1&3, 4&7 and five messages can still be lost, but the probability of such an event is smaller than one being considered.

After choosing two distinct pairs (1&2, 3&4), four (N-4) pairs remain from which to choose the third pair. Suppose the first two pairs chosen are 2&4, 1&5; then the triangle can be made again with  $\binom{N}{2}$  pairs as follows:

2-4,	2-5,	2-1,	2-3,	2-6, 2-7, 2-8,	2-N
	4-5,	4-1,	4-3,	4-6, 4-7, 4-8,	4-N
		5-1,	5-3,	5-6, 5-7, 5-8,	5-N
			1-3,	1-6, 1-7, 1-8,	1-N
				3-6, 3-7, 3-8, .....	3-N
				6-7, 6-8, .....	

Again, there are four (N-4) pairs from which to choose the third pair, and the shaded region shows the possible pairs from which the third pair can be chosen.

The important point in this counting procedure is that once two distinct pairs are chosen, then there are always four (N-4) pairs to choose from for the third. The number of ways two distinct pairs can be chosen is given by

$$\binom{N}{2} \binom{N-2}{2} 1/2!$$

There are  $\binom{N}{2}$  pairs from which to choose the first pair,  $\binom{N-2}{2}$  pairs from which to choose the second after the first is chosen, and a  $2^1$  term is needed to eliminate the redundancy in counting

Recalling that there are four  $(N-4)$  pairs from which to choose the third pair, the number of ways to select two distinct pairs and one nondistinct pair can be written as

$$\binom{N}{2} \binom{N-2}{2} \frac{4(N-4)}{2^1} \quad (A-2)$$

However, the counting is not quite finished. Consider the example,  $(1\&2, 3\&5)$  and  $5\&4$ , where  $(1\&2, 3\&5)$  are the first two distinct pairs. Just as likely, this three-pair combination can be rewritten as  $(1\&2, 5\&4)$  and  $3\&5$ . Therefore, the three-pair combination is counted twice in obtaining (A-2). So it is concluded that the total number of combinations of choosing two distinct pairs and one nondistinct pair is given by

$$\binom{N}{2} \binom{N-2}{2} \frac{1}{2^1} \frac{1}{2} 4 (N-4)$$

and that

$$P(K=5) \approx \binom{N}{2} \binom{N-2}{2} \frac{1}{2^1} \frac{1}{2} 4 (N-4) \left(\frac{d^1}{T}\right)^3 \left(1 - \frac{d^1}{T}\right) \binom{N}{2}^{-3}$$

$$\approx P(K=4) \frac{2}{2} (N-4) \frac{d^1}{T} \quad (A-3)$$

The next task is to extend the counting procedure to a more general case where  $K$  is an arbitrary odd number. If  $K = 7$ , then  $P(K=7)$  is given by approximately  $P$  (three distinct pairs and one nondistinct pair interfere). The number of ways to choose three distinct pairs and one nondistinct pair is given by

$$\frac{1}{3^1} \binom{N}{2} \binom{N-2}{2} \binom{N-4}{2} \frac{1}{2} \cdot 6 (N-6) \quad (A-4)$$

where  $6(N-6)$  is the number of ways of choosing the nondistinct pair once three distinct pairs are picked, and  $1/3! \binom{N}{2} \binom{N-2}{2} \binom{N-4}{2}$  is the number of ways of choosing the three distinct pairs. The factor of  $1/2$  stems from double-counting the combination twice. For example,  $((1&2, 3&4, 5&6) \text{ and } 6&9)$  and  $((1&2, 3&4, 6&9) \text{ and } 5&6)$  are identical combinations.

Using Equation (A-4), this equation can be written

$$\underline{P}(K=7) \approx \frac{1}{3!} \binom{N}{2} \binom{N-2}{2} \binom{N-4}{2} \frac{1}{2} 6(N-6) \cdot \left(\frac{d'}{T}\right)^4 \left(1 - \frac{d'}{T}\right)^{\binom{N}{2} - 4}$$

or

$$\approx \underline{P}(K=6) 6 \frac{(N-6)}{2} \left(\frac{d'}{T}\right) \quad (\text{A-5})$$

In general, it can be shown that

$\underline{P}(K = \text{odd number of messages are lost})$

$$\approx \frac{1}{\binom{K-1}{2}}, \binom{N}{2} \binom{N-2}{2} \dots \binom{N-K+2}{2} \left\{ \frac{(K-1)}{2} (N-K+1) \right\} \left(\frac{d'}{T}\right)^{\frac{K+1}{2}} \left(1 - \frac{d'}{T}\right)^{\binom{N}{2} - \binom{K+1}{2}} \quad (\text{A-6})$$

or

$$\approx \underline{P}(K-1) \left\{ \frac{1}{2} (K-1) (N-K+1) \right\} \frac{d'}{T}$$

## APPENDIX B

### SECOND-ORDER TERMS OF $P(K = \text{EVEN})$

When even  $K$  messages are lost, then it can be assumed that, most likely, they are lost because  $K/2$  distinct pairs interfere. However, this assumption breaks down when  $\binom{N}{2} d^1/t \gtrsim 1$  where  $d^1 = Md$ . If  $\binom{N}{2} d^1 \gtrsim 1$ , other kinds of interferences that give rise to a loss of an even number of messages must be sought. Among them, there are two kinds that contribute more significantly than others to a loss of an even number of messages.

Case A: Loss of  $K-4$  messages due to  $(K-2)/2$  distinct pair interferences and a loss of two messages due to two nondistinct pair interferences. A nondistinct pair interference is an interference between two messages, one of which is a member of  $(K-2)/2$  distinct pairs. Example:  $\{(1\&2, 3\&5), (3\&7)\}$ , where  $(3\&7)$  is a nondistinct pair, if  $\{1\&2, 3\&5\}$  is considered as the two distinct pairs.

Case B: Loss of  $K$  messages due to  $K/2$  distinct pair interferences and one interference among the  $K$  messages that had already interfered by  $K/2$  distinct pair interferences.

The following examples illustrate these cases:

- $(1\&2, 3\&4, 5\&6), 5\&9, 2\&21$  where  $(1\&2, 3\&4, 5\&6)$  are the three distinct pairs
- $(1\&2, 3\&5, 6\&8, 4\&7), 2\&8$  where  $(1\&2, 3\&5, 4\&7, 6\&8)$  are four distinct pairs.

The second case becomes significant only when  $K$  is large. Section 4 shows that when  $\binom{N}{2} d^1/t \gtrsim 1$ , an interference occurs almost with a probability of one. In such a situation, the number of messages most likely to be lost may amount to 20 or more, and Case B is no longer negligible. It is emphasized that these two second-order terms are usually one order less in magnitude in comparison to the first-order terms discussed in Section 4. However, the sum of the two second-order terms becomes significant when  $\binom{N}{2} d^1/t \gtrsim 1$  and  $N \gg 1$ .



# 1. CASE B

Since Case B is simpler than Case A, it will be discussed first. To compute the probability of Case B, a specific example of Case B will be considered, its probability computed, and the probability multiplied by the number of ways such a combination can occur.

Assume that four pairs interfered: 1 & 2, 3 & 5, 6 & 8, and 1 & 8. The probability of such an event is given by

$$(d^1/t)^4 (1 - d^1/t) \exp\left(\frac{N}{2}\right) - 4 \quad (B-1)$$

Consider the triangle matrix below. After counting carefully, it can be seen that the last pair (1 & 8) can be chosen from any one of  $\binom{6}{2} - 3$  pairs. In general, once  $K/2$  distinct pairs are chosen, there are

K-1=5					N-K=N-6				
1-2,	1-3,	1-5,	1-6,	1-8,	1-4,	1-7,	1-9,	1-10,	... , 1-N
	2-3,	2-5,	2-6,	2-8,	2-4,	2-7,	2-9,	2-10,	... , 2-N
		3-5,	3-6,	3-8,	3-4,	3-7,	3-9,	3-10,	... , 3-N
			5-6,	5-8,	5-4,	5-7,	5-9,	5-10,	... , 5-N
				6-8,	6-4,	6-7,	6-9,	6-10,	... , 6-N
					8-4,	8-7,	8-9,	8-10,	... , 8-N
						4-7,	4-9,	4-10,	... , 4-N
							7-9,	7-10,	... , 7-N
								9-10,	... , 9-N
									.
									.
									.
									(N-1)-N

K = 6

$\left[\binom{K}{2} - \frac{K}{2}\right]$  pairs to choose the last pair. There are

$$\left[\binom{N}{2} \binom{N-2}{2} \binom{N-4}{2} \frac{1}{3!}\right] \left[\binom{6}{2} - \frac{6}{2}\right]$$

ways to choose three distinct pairs and another pair which is made up of any two of the six messages (from the three distinct pairs). So, the P (losing six messages, Case B)

$$\approx \left[ \binom{N}{2} \binom{N-2}{2} \binom{N-4}{2} \frac{1}{3!} \right] \left[ \binom{6}{2} - 6 \right] \left( \frac{d^1}{T} \right)^4 \left( 1 - \frac{d^1}{T} \right) \exp \binom{N}{2} - 4$$

In general, there are

$$\frac{1}{\left( \frac{K}{2} \right)!} \binom{N}{2} \binom{N-2}{2} \binom{N-4}{2} \cdot \cdot \cdot \binom{N-K+2}{2}$$

ways to choose the  $K/2$  distinct pairs, and  $\binom{K}{2} - \frac{K}{2}$  ways to choose the last pair. Using these expressions, the following is derived:

P (losing K messages, Case B)

$$\approx \frac{1}{\left( \frac{K}{2} \right)!} \binom{N}{2} \binom{N-2}{2} \cdot \cdot \cdot \binom{N-K+2}{2} \left[ \binom{K}{2} - \frac{K}{2} \right] \left( \frac{d^1}{T} \right)^{K+1} \left( 1 - \frac{d^1}{T} \right) \exp \binom{N}{2} - K-1 \quad (B-2)$$

## 2. CASE A

Case A is a little more complicated than Case B. Consider the example 1&2, 3&5, 6&8, 1&7, 3&9 where eight messages are lost and (1&2, 3&5, 6&8) are the three distinct pairs. The probability of this particular event is

$$\left( \frac{d^1}{T} \right)^5 \left( 1 - \frac{d^1}{T} \right) \exp \binom{N}{2} - 5 \quad (B-3)$$

The next task is to find how many such combinations as (1&2, 3&5, 6&8, 1&7, 3&9) exist. There are  $\binom{N}{2} \binom{N-2}{2} \binom{N-4}{2} \frac{1}{3!}$  ways to select three distinct pairs (e.g., 1 2, 3 5, 6 8).

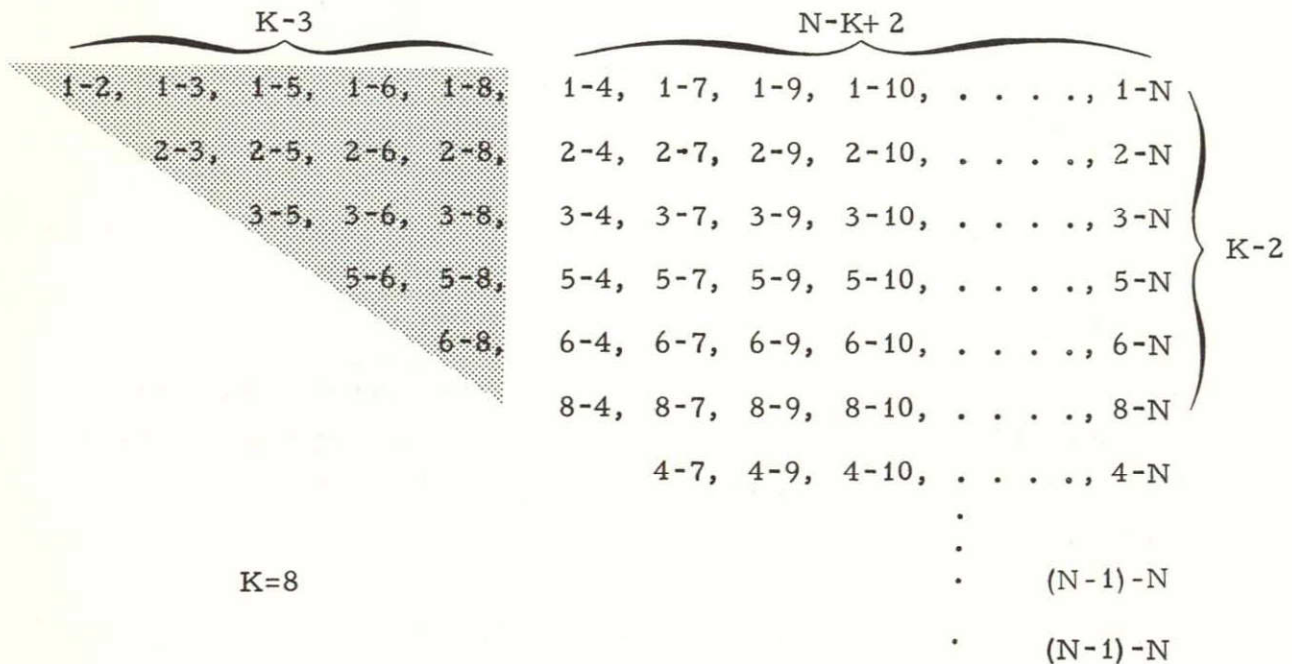
The number of ways to choose the last two pairs must be determined. These two can be chosen from the (N-6), i.e., six pairs in the rectangle of the matrix:

1-4, 1-7, 1-9, 1-10, . . . . , 1-N  
 2-4, 2-7, 2-9, . . . . . , 2-N  
 .  
 .  
 8-4, 8-7, 8-9, . . . . . , 8-N

If multiplying  $(N-6)6$  and  $\binom{N}{2} \binom{N-2}{2} \binom{N-4}{2} \frac{1}{3!}$  and using

$$(N-6)6 \binom{N}{2} \binom{N-2}{2} \binom{N-4}{2} \frac{1}{3!} \quad (B-4)$$

as the number of combinations, then redundancy is incorporated into the counting procedure. To uncover this redundancy, consider the example ( (1&2, 3&5, 6&8) and (1&7), (3&9) ).



By using Equation (B-4), the following

( (1&2, 3&5, 6&8), and (1&7), (3&9) )

( (1&7, 3&5, 6&8), and (1&2), (3&9) )

( (3&9, 1&2, 6&8), and (3&5), (1&7) )

and

( (1&7, 3&9, 6&8), and (1&2), (3&5) )

are counted as four different combinations. Clearly, this is not true. Therefore, the factor of redundancy is four. The number of combinations to choose three distinct pairs and two nondistinct pairs is given by

$$\frac{1}{4} \left[ \binom{N}{2} \binom{N-2}{2} \binom{N-4}{2} \frac{1}{3!} \right] \left[ \frac{1}{2} (N-7)(N-6) 6 \cdot 5 \right]$$

where  $\frac{1}{2} (N-7)^2 6 \cdot 5$  is the number of ways to choose the last two non-distinct pairs.

In general, there are

$$\frac{1}{4} \left[ \binom{N}{2} \binom{N-K+4}{2} \frac{1}{\left(\frac{K-2}{2}\right)!} \right] \left[ \frac{1}{2} (N-K+2)(N-K+1)(K-2)(K-3) \right] \quad (B-5)$$

ways to choose  $(K-2)/2$  distinct pairs and two nondistinct pairs.

Unfortunately, counting is not finished because such combinations as

$$\{(1\&2, 3\&5, 6\&8), (1\&7, 1\&9)\}$$

and

$$\{(1\&2, 3\&5, 6\&8), (1\&4, 2\&4)\} \quad (B-6)$$

have not been considered. These examples were not included in the counting of Equation (B-5) in which the last two pairs involving four different messages were not considered. In Equation (B-6), the last two pairs are made of only three messages.

The number of ways to select the last two pairs of Equation (B-6) is given by

$$(N-1)(N-2)/2$$

Next, the redundancy observed is 3 if the number of ways to select three distinct pairs is multiplied by  $(N-1)(N-2)/2$ . This conclusion follows when  $(1\&2, 3\&5, 6\&8)$ ,  $(1\&7, 1\&9)$  may be written as  $(1\&7, 3\&5, 6\&8)$ ,  $(1\&2, 1\&9)$  and  $(1\&9, 3\&5, 6\&8)$ ,  $(1\&2, 1\&7)$ . Therefore, the number of ways to select combinations of Equation (B-6) is

$$\frac{1}{6} \left[ (N-1)(N-2) \right] \left[ \binom{N}{2} \binom{N-2}{2} \binom{N-4}{2} \frac{1}{3!} \right]$$



In general, there are

$$\frac{1}{6} \left\{ (N-1) (N-2) \binom{N}{2} \binom{N-2}{2} \cdot \cdot \cdot \binom{N-K+4}{2} \left( \frac{1}{\binom{K-2}{2}} \right) \right\} \quad (B-7)$$

Using Equations (B-5) and (B-7),

$$\begin{aligned} \underline{P} (K = \text{even, Case A}) = & \left[ \binom{N}{2} \binom{N-2}{2} \binom{N-K+4}{2} \left( \frac{1}{\binom{K-2}{2}} \right) \right] \\ & \left\{ \frac{1}{8} (N-K+2) (N-K+1) (K-2) (K-3) \right. \\ & \left. + \frac{1}{6} (N-1) (N-2) \right\} \quad (B-8) \end{aligned}$$

for  $K > 4$ .

As a final remark, if  $K = 4$ , the above equation is not valid. Consider an example ((1 & 2), 1 & 7, 3 & 9). The redundancy is not four, but is three, so the special case of  $K = 4$

$\underline{P} (K = 4, \text{Case B})$

$$\left[ \binom{N}{2} \right] \left\{ \frac{1}{6} (N-2) (N-3) (2) + \frac{1}{6} (N-1) (N-2) \right\}$$

There are other terms, of course, which can improve the accuracy in estimating  $P(K)$ 's. However, for the examples considered, at least 93 out of 100 percent was obtained by summing up these second-order terms and the primary contribution due to distinct pair interferences. This result is enough to use in the subsequent analysis of the probability of error when there is  $M$  replication. Of course, the need of these second-order terms becomes more urgent as  $M$  increases. If  $M$  increases and  $N$  remains constant, the subinterval gets smaller and closer to one and may be even greater than one. Then these second-order terms are needed to compute  $P(K)$  in the subinterval.

RUN 2 3H 01/14/70

C-1

000003		PROGRAM MAIN (INPUT, OUTPUT, TAPE60=INPUT)	2
000003		DIMENSION T(500), F(500), S(500), S2(500), C1(500), C2(500)	3
000003		INTEGER A2, A5	4
000011		READ (60.25) NCASE	5
000013		DO 10 LOOP=1, NCASE	6
000014		S1=0.	7
000034		READ (60.20) IFREQ, A1, IREPL, A2, FQBAND, A5	8
000036		FQBAND=FQBAND/100	85
000041		A7=A1*IREPL/(983040 )	9
000042		LF=1	10
000066		PRINT 91 , IFREQ, A2, IREPL, A5, A1, A7, FQBAND, FQBAND	105
000067		ECOUNT=0	11
000071		KK=A2-1	21
000073		CALL UPRI(LF, RINI)	22
000075		DO 1120 I=1, A2	23
000102	1120	S(I)=S2(I)=C1(I)=C2(I)=0.	24
000104		CONTINUE	25
000106		I5=A5-1	27
000110		DO 1150 ICOUNT=1, I5	28
000111		SPRIME=0.	29
000113		DO 1180 L=1, A2	30
000115	1180	CALL UPRI (LF, T(L))	32
000120		CONTINUE	33
000121		DO 1250 IL=1, KK	34
000123		KK1=IL+1	35
000124		DO 1249 N=KK1, A2	36
000130		A=ABS(T(IL)-T(N))	37
000133		IF (A.GE. A7) GO TO 1249	41
000135		IF (IFREQ NE 1) TO TO 1235	42
000142		IF (C1(IL) NE 1) CALL UPRI(LF, F(IL))	43
000147		IF (C1(N) NE 1) CALL UPRI(LF, F(N))	44
000153		AF=ABS(F(IL)-F(N))	45
000156		IF (AF, .LT. FQBAND) GO TO 1235	46
000161		S(IL)=S(N)=0	47
000165		C1(IL)=C1(N)=1.	48
000165	1235	GO TO 1249	
		S(IL)=S(N)=C1(IL)=C1(N)=1.	

FORTRAN IV MONTE CARLO PROGRAM

APPENDIX C

RUN 2.3H 01/14/70

MAIN

000174	1249	CONTINUE	49
000177	1250	CONTINUE	50
000201		IF(IREPL .EQ. 1) GO TO 2275	51
000203		DO 1253 JOINT=2, IREPL	
000205		DO 1255 L=1, A2	52
000206		CALL UPRI(LF, T(L))	53
000210	1255	CONTINUE	54
000213		DO 1268 IL=1, KK	61
000214		KK1=IL+1	62
000216		DO 1267 N=KK1, A2	63
000217		A=ABS(T(IL)-T(N))	64
000223		IF(A .GT. A7) GO TO 1267	65
000227		IF(IFREQ. NE. 1) GO TO 3235	66
000231		IF(C2(IL) .NE. 1) CALL UPRI(LF, F(IL))	67
000236		IF(C2(N) .NE. 1) CALL UPRI(LF, F(N))	68
000244		AF=ABS (F(IL)-F(N))	69
000250		IF(AF .LT. FQBAND) GO TO 3235	70
000253		S2(IL)=S2(N)=0.	71
000256		C2(IL)=C2(N)=1.	72
000262		GO TO 1267	73
000262	3235	S2(IL)=S2(N)=C2(IL)=C2(N)=1.	74
000271	1267	CONTINUE	75
000274	1268	CONTINUE	76
000276		DO 1277 I=1, A2	80
000300		IF(S(I) .NE. 1. .OR. S2(I) .NE. 1.) S(I)=0.	
000313	1277	CONTINUE	25
000316		DO 1282 I=1, A2	86
000317		S2(I)=C1(I)=C2(I)=0.	87
000323	1282	CONTINUE	88
000325	1253	CONTINUE	89
000327	2275	DO 2300 I=1, A2	90
000331		SPRIME=SPRIME+S(I)	91
000333		S(I)=S2(I)=0.	92
000336	2300	CONTINUE	93
000340		IF (SPRIME .EQ. 0) GO TO 1150	94
000341		S1=S1+SPRIME	95

RUN 2.3H 01/14/70

MAIN

000343		ECOUNT=ECOUNT+1.	96
000345	1150	CONTINUE	97
000350		SPRIME= S1/A5	990
000352		ECOUNT=ECOUNT/A5	1000
000354		PRINT 3372, SPRIME, ECOUNT	1010
000364	10	CONTINUE	
000367	20	FORMAT (I3, F10. 5, 2I3, F10 6, I5)	200
000367	25	FORMAT (I5)	201
000367	91	FORMAT (5X, 39HTHIS RUN WITH BOTH TIME+FREQ IF	202
		*IREPL=1, I5/5X, 16HNUMBER OF USERS=, I5/5X, 14HNBR OF	203
		*REPLIC=, I5/5X, 27HNUMBER OF TRIALS TO BE MADE I5/5X,	204
		*22HMESSAGE LENGTH IN BITS, 5X, F10 3/5X, 34HRATIO OF ON	205
		*E MES LEGT TO TOTAL TM=, F10. 6/5X, 15HFREQ. BANDWIDTH=,	206
		*F10. 6/5X, 29HRATIO OF BANDWIDTH TO 100 KHZ=, F10. 6)	
000367	101	FORMAT (5X, 13HMESSAGE LOST=, I5, I10)	207
000367	3372	FORMAT (1X, F10. 3, 5X, 15HFRAC OF INTERF=, F10 3)	2080
000367		STOP	1020
000371		END	10000



APPENDIX D



ONE SPACE PARK REDONDO BEACH CALIFORNIA

CODE IDENT 11982

TITLE	
SYSTEM SPECIFICATION	
DATA COLLECTION SYSTEM	
FOR	
EARTH RESOURCES TECHNOLOGY SATELLITES	
A AND B	
DATE 1/28/70	NO D-13590

SUPERSEDING \_\_\_\_\_  
\_\_\_\_\_

PREPARED BY S. Spiegel

APPROVAL SIGNATURES

Stanley B. Clark 2 FEB 70 W. W. Winkler 2 FEB 70  
DATE DATE

E. B. Bradford 2 FEB 70 \_\_\_\_\_  
DATE DATE

John E. Tiller 2 Feb 70 \_\_\_\_\_  
DATE DATE



ONE SPACE PARK REDONDO BEACH CALIFORNIA

AS OF \_\_\_\_\_

SUPERSEDING \_\_\_\_\_

# SPECIFICATION CHANGE RECORD

SCN/REV	SCN/SPEC DATE	AUTHORIZATION		PRODUCTION EFFECTIVITY	PAGES AFFECTED
		ECP/CCN	OTHER		
Basic				Original Issue	

## 1 0 SCOPE

1 1 This specification establishes the requirements for the performance, design, and test of a Data Collection System for the ERTS Satellites A and B

## 2 0 APPLICABLE DOCUMENTS

2 1 The following documents of the exact issue shown, form a part of this specification to the extent specified herein. In the case of TRW Systems documents, the latest issue shall apply. In case of conflict between documents referenced herein and the detail content of Sections 3, 4, 5, and 10, the detailed requirements of sections 3, 4, 5, and 10 shall be considered superseding requirements.

## SPECIFICATIONS

Military

MIL-D-1000  
01 March 1965

Engineering Drawings and Associated  
Lists

TRW Systems

D-13351

Environmental Design Qual Test-  
Electronic and Mechanical Flight  
Assemblies

D-13352

Environmental Acceptance Test-  
Electronic and Mechanical Test Assembly

D-13353

Environmental Design Qualification  
Test-Earth Resources Technological  
Satellite

D-13354

Environmental Acceptance Test  
Earth Resources Technological  
Satellite

PK4-10

Packaging Spec, Commercial Packaging  
of Parts and Assemblies

PR12-1

Identification and Marking



STANDARDS

Military

MIL-STD-143A	Specifications and Standards, Order of Precedence for the Selection of
MIL-STD-803A Part 1 27 January 1964	Human Engineering Criteria for Aircraft, Missile and Space Systems Ground Support Equipment
MS 33486A 16 December 1958	Metals, Definitions of Dissimilar

### 3 0 REQUIREMENTS

#### 3.1 Performance

3.1 1 Mission The Data Collection System, herein after referred to as the System, shall serve as a low cost telemetry link for agricultural water resource and allied monitoring on a national scale. Low cost, self-contained data collection platforms, distributed throughout the United States, shall transmit data to a polar orbiting Earth Resources Technology Satellite. The satellite will then relay this data to one of any MSFN ground tracking station on the Unified S Band downlink.

#### 3.1.2 System Definition

3.1 2 1 General Design Concept The System shall have the same basic design although the housing may differ because of the area of operation. A primary objective shall be to achieve a standardized design with a high degree of flexibility for accomodating many types of sensors.

3.1 2 2 System List The system shall contain the following sub-systems

##### a) Flight Subsystem

- (1) Receiver
- (2) Antenna

##### b) Ground Subsystem (Data Collection Platform)

- (1) Transmitter
- (2) Antenna
- (3) Power Supply
- (4) Analog Signal Conditioner
- (5) A/D Converter and Programmer
- (6) Sensors (Government Furnished Equipment)

3.1 2 3 Data Collection System Specification Tree The System Specification tree is shown in Figure D-1

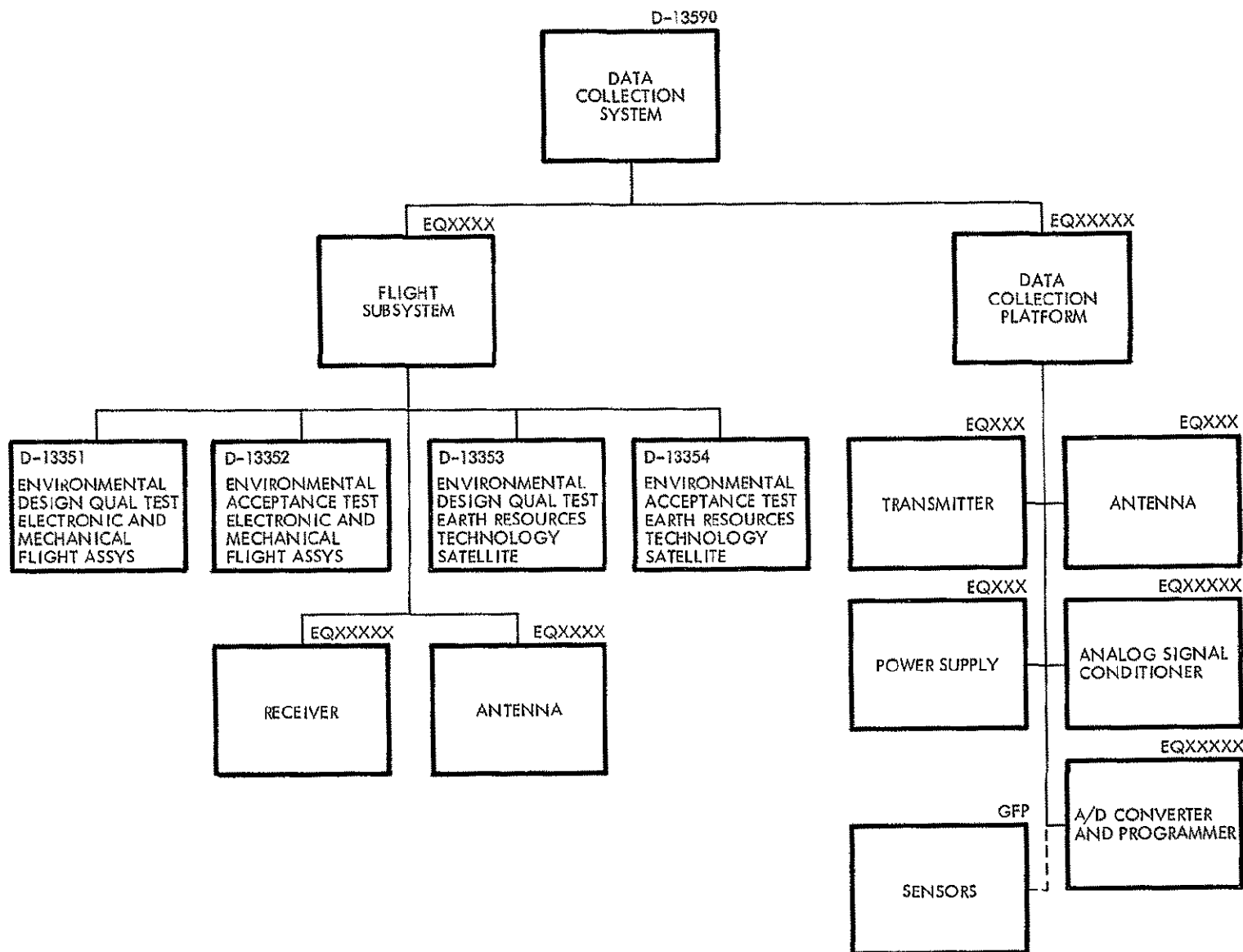


Figure D-1

3 1 3 Operability

3 1.3 1 Reliability As a design goal, the ground portion of the System (Data Collection Platform) shall be capable of sustained unattended performance in any combination of extreme earth environment for a period of six months, minimum. The flight portion of the System shall have a minimum operational lifetime of one year in orbit.

3 1 3 1 1 Reception Probability As a design goal, the probability of successfully receiving at least one transmission from each data collection platform during any 12 hour interval will be greater than 0.95 with a probability of failure to recognize the occurrence of errors in the decoded message of less than 0.01.

3 1 3 2 Maintainability The System shall be designed to give consideration to accessibility and interchangeability. The design goal for mean time to repair any flight subsystem function or failure at the launch base shall be a maximum of 12 hours. The design goal for mean time to repair any ground subsystem function or failure at the installation site shall be one day.

3 1 3 2 1 Maintenance and Repair Cycles Field maintenance shall be limited to checkout, removal, and replacement of equipment at the component level.

3 1 3 2 2 Service and Access The System shall be designed for ease of service with access doors to enable the removal and replacement of all significant components with normally available tools and fixtures. Batteries, if used, shall be installed so that they can be changed and checked without difficulty.

3 1 3 3 Environmental The System shall be designed to withstand or shall be protected against climatic conditions as defined in Table I, except for the flight subsystem which shall meet the requirements of TRW Specifications D-13353 and D-13354, and shall operate as specified herein without performance degradation Where presently existing, or planned, facilities are, or will be available for use and will afford adequate protection under all factory to field conditions, such facilities may be considered as "protection against "

TABLE I

Temperature	minus 40° to plus 104°F
Humidity	80% Continuous

3 1 3 5 Transportability The system shall be designed to be transported by common carrier with a minimum of protection. Special packaging will be used as necessary to assure that transportation methods do not impose design penalties TRW Systems Specification PK-10 shall apply for packaging of parts and assemblies (components)

3 1 3 6 Human Performance The design of the System shall use MIL-STD-803A, Part I as a guide for man/machine interfaces \_\_\_\_\_

### 3 2 System Design and Construction Standards

#### 3.2 1 General Design and Construction Requirements

3 2 1 1 Selection of Specifications and Standards Selection of specifications and standards for necessary commodities and services not specified herein shall be in accordance with the provisions of MIL-STD-143A Engineering Drawings and associated lists shall be in accordance with the provisions of MIL-D-1000

#### 3 2 1 2 Materials, Parts, and Processes

3 2 1 2 1 Electronic Parts Electronic parts shall be as specified in the TRW Systems DCS Reliability Plan

3 2 1 2 2 Screening Tests. Screening tests shall be as specified in the TRW Systems DCS Reliability Plan

3.2.1.2.3 Derating Derating shall be as specified in the TRW Systems DCS Reliability Plan

3.2.1.3 Fungus and Moisture Resistance Materials that are not nutrients for fungus shall be used whenever possible. Where the use of fungus nutrients cannot be avoided, treating, packing, or other protective means shall be employed to ensure no degradation in system performance.

3.2.1.4 Corrosion of Metal Parts System parts, including spares, shall be protected against corrosion. To avoid electrolytic corrosion, dissimilar metals, as defined in MS-33486A, shall not be used in direct contact.

3.2.1.5 Protective Treatment Any materials used in the construction of the System that may be subject to deterioration when exposed to climatic and environmental conditions likely to occur during operational service, shall be protected against such deterioration in a manner that will in no way prevent compliance with the performance requirements specified herein. The use of any protective coating that will crack, chip, or scale when exposed to extremes of climatic and environmental exposure shall be avoided.

3.2.1.6 Interchangeability and Replaceability The ERTS A and B design shall meet the requirements of MIL-STD-100 for interchangeability and replaceability.

### 3.1.7 Workmanship

3.2.1.7.1 Workmanship Standards Workmanship shall conform to the requirements of the applicable process specifications relating to fabrication and assembly as invoked by the particular assembly drawing. Critical steps of fabrication that are item-peculiar shall be detailed in drawing notes which shall include appropriate criteria of workmanship. Workmanship relating to all other aspects of fabrication, general handling, and storage shall be deemed to be adequately covered by the quality control program.

3 2 1 7 2 Personnel Certification Personnel involved in assembly, soldering, welding, or other activity requiring special technical skills shall be certified as to their capability to perform such duties effectively

3.2 1 8 Identification and Marking System components shall be identified in accordance with the provisions of TRW Systems Specification No PR12-1 Electrical connectors on the data collection platforms shall be identified by permanent markings as to function

3 2 1 9 Storage The System, with the exception of batteries, shall be designed to be stored for a period of one year without requiring major repair, maintenance, or retesting at the end of storage

### 3 2 2 Design Disciplines

3 2 2 1 Mechanical The ground subsystem shall be housed in an appropriate weatherproof, protective casing, with a carrying handle The case shall have provision for quick, secure attachment to and removal from the antenna mast, the sensor and power cables The case shall be sealed, to prevent moisture ingress, and equipped with a lock to prevent tampering When the case is unlocked, the following adjustments shall be accessible

- (a) Sensor conditioning
- (b) Multiplexing Format
- (c) A/D Quantizing
- (d) Address code
- (e) Crystal
- (f) PRF Control

### 3 3 System Performance Allocations

#### 3.3 1 Overall System Performance

3 3 1 1 Mode of Operation The System shall operate in a random mode to eliminate the use of a timing signal or interrogation command by the data collection platforms, and allow a finite number of message collisions

3 3.1 1.1 Error Detection The structure of the messages used shall ensure that not more than one percent of the messages received contain undetected erroneous data

3 3.1 2 Bandwidth The System parameters shall be optimized to accommodate 1000 data collection platforms within the 100 KHz total special width allocation for the UHF uplink from the data collection platform to the spacecraft

### 3 3 2 Flight Subsystem

3 3 2 1 Receiver The receiver shall be a double frequency conversion, superhetrodyne design The receiver characteristics shall be as shown in TABLE I

TABLE I

Frequency	400 to 406 MHz
Output Signal	75 KHz broadband IF signal delivered into a 600 ohms impedance at a one volt, peak, level
Noise Figure	Two db, maximum
Frequency Stability	Plus or minus 5 ppm referenced to the 400 MHz input signal

3 3 2 1 1 Weight The receiver shall have a maximum weight of 2 5 pounds

3 3 2 1 2 Size The dimensions shall be 2 inches by 6 inches by 6 inches (Maximum volume of 72 cubic inches)

3 3 2 2 Antenna The receiver antenna shall have the following functional characteristics

- |                 |   |
|-----------------|---|
| a) Frequency    | 402 $\pm$ 1 0 MHz   |
| b) Polarization | Right hand circular   |
| c) Peak Gain    | 2.5 dbi, minimum with respect to right hand circular polarization at 60 degree off axis |



d) Minimum Gain Minus 7.5 db, minimum with respect to right hand circular polarization on axis

e) Axial Ratio Six db, maximum, over the hemisphere to within 60 degrees off axis

3.3.3 Ground Subsystem (Data Collection Platform) The subsystem shall process eight input sensor signals of analog format. The analog data shall be converted to digital form, combined with other message elements and transmitted in a 110 bit format. There shall be no internal storage capability in the subsystem.

3.3.3.1 Sensor Capacity Each subsystem shall accommodate eight sensor inputs, and provide the requisite signal conditioning.

3.3.3.1.1 Encoding Eight bits analog to digital conversion, and eight channel multiplexing shall be incorporated. Means of increasing the input resolution by using more than one 8 bit word for a sensor shall be provided if feasible. The multiplexer shall permit simple re-arrangement of the sampling pattern to suit different numbers of sensors, from 1 to 8 and differing frequencies of sampling each. Error detection coding shall be incorporated using an eight bit BCH block code.

3.3.3.1.2 Message Structure The desired message structure for the subsystem emissions shall be as follows:

a) Preamble	-25 Bits
b) B/W Synch	- 3
c) Sensor Data	-64
d) DCP Address	-10
e) Error Detection	- 8

---

TOTAL      110 Bits

3.3 3.2 Transmitter The transmitter design shall provide a minimum of 5 watts RF output, at 401.9 MHz. It shall provide for bi-phase carrier modulation with the 110 bit quantized data message using differential phase shift keying. The transmitter shall be equipped with a crystal controlled oscillator of such stability that it shall remain within the allocated 100 KHz bandwidth under all conditions of temperature and voltage excursions. The crystal shall be a plug-in replaceable item.

3.3 3.2 1 Timing The subsystem transmitter shall be provided with a PRF timing circuit which shall allow the subsystem to transmit at a rate of approximately one message every two minutes.

3.3 3.3 Prime Power The subsystem shall be furnished with both line and battery power supplies. The line supply shall provide for continuous operation from the domestic 117 vac 60 Hz single phase supply. The battery supply shall provide for a minimum of six months of unattended operation.

3.3 3.4 Antenna The subsystem antenna shall have the following functional characteristics:

- |                 |  |
|-----------------|--|
| a) Frequency    | 402 MHz $\pm$ 1.0 MHz  |
| b) Power Input  | 10 watts, cw   |
| c) Polarization | Right hand circular  |
| d) Minimum Gain | One dbi with respect to the right hand circular polarization at any point over the hemisphere to within 7 1/2 degrees of the horizon |
| e) Axial Ratio  | Five db, maximum over the hemisphere to within 7 1/2 degrees of the horizon  |

#### 3.4 Interfaces

3.4 1 Flight Subsystem/Spacecraft No signal detection shall be performed on the subsystem signals within the spacecraft, with the exception of that frequency translation necessary to allow retransmission via the Unified S Band down link.

3.4.1.1 Power Input Power input to the subsystem shall be  $28 \pm 5$  vdc from the spacecraft payload bus.

3.4.1.2 Input Bandwidth The input bandwidth to the receiver of the subsystem shall be 117 KHz

3.4.1.3 Antenna The antenna shall have an input impedance of 50 ohms with a VSWR of less than 2 to 1

#### 4 QUALITY ASSURANCE PROVISIONS

4.1 Responsibility for Inspection and Test Unless otherwise specified in the contract or purchase order, the supplier is responsible for the performance of all test requirements as specified herein. Except as otherwise specified, the supplier may utilize his own facilities or any commercial laboratory acceptable to TRW Systems. TRW Systems reserves the right to perform any of the tests set forth in this specification when such tests are deemed necessary to assure that supplies and services conform to prescribed requirements. Subsystem qualification shall be performed at the observatory level only.

4.2 Inspection Inspection of the System shall be accomplished in accordance with the applicable portions of TRW Systems Group Quality Requirements.

4.3 Design Qualification Testing Formal qualification testing and test conditions of the flight subsystem shall be accomplished in accordance with TRW Systems Specification D-13353.

4.4 Acceptance Tests. Formal acceptance testing of the flight subsystem shall be accomplished in accordance with TRW Systems Specification D-13354.

4.4.1 Acceptance and Qualification Testing Ground Subsystem Acceptance and Qualification testing shall be as specified in the individual equipment specifications.

4.5 Rejection and Retest If a failure, malfunction, or out of tolerance performance degradation occurs during or after a test, testing shall be discontinued until the failure, malfunction, or out of tolerance condition (including design defects) is corrected. The pertinent test procedure shall be repeated until completed successfully. If the corrective action substantially affects the significance of results of previously completed tests, such tests shall also be repeated.

## ROAD MAP

### REVISIONS AND ADDITIONS TO FEBRUARY SUBMITTAL

This material is an addendum to be bound in at the back of Volume 5 of the final report. It represents further studies on the data collection system covering the areas of (1) visibility, message collision and system capacity, (2) baseband signal definition and link analysis, and (3) extension of the system's environmental performance.

EARTH RESOURCES TECHNOLOGY SATELLITE

FINAL REPORT

Volume 5 Data Collection System

April 17, 1970

prepared for  
National Aeronautics and Space Administration  
Goddard Space Flight Center

Contract NAS5-11260

item 5a

TRW Systems Group  
One Space Park Redondo Beach  
Los Angeles County  
California 90278

# CONTENTS

	Page
1. INTRODUCTION	1-1
2 COVERAGE AND VISIBILITY TIMES	2-1
2 1 Manual Analysis	2-1
2 2 Computer Analysis	2-5
2 3 Equations Development	2-6
2 4 Results	2-10
2 5 Computer Program Description	2-21
3 SYSTEM CAPACITY, RANDOM T AND F MODE	3-1
4 SIGNAL CHARACTERISTICS	4-1
4 1 Statistics For Simultaneous Signals	4-1
4 2 Signal Amplitude Distribution	4-6
4 3 DCS Data and Ranging Code Mutual Interference Analysis	4-14
5 DCS COMMUNICATION LINK DESCRIPTION AND ANALYSIS	5-1
5 1 Link Description	5-1
5.2 Overall Link Analysis	5-3
5 3 Downlink Analysis	5-5
5 4 Limiter Performance Analysis	5-12
6 PERFORMANCE UNDER EXTREME TEMPERATURE CONDITIONS	6-1
6 1 High Temperature Operation	6-1
6 2 Low Temperature Operation	6-3

## 1 INTRODUCTION

Since issuing the ERTS data collection system final report on February 11, TRW has continued to investigate a number of important aspects related to the DCS. In this addendum to the DCS final report, we have taken the opportunity to assemble the results of a number of analytical studies. These activities have been pursued to extend our understanding of the problem of providing optimum data transmission with a low cost, simple platform and cover the areas of (1) visibility, message collisions, and system capacity, (2) baseband signal definition and link analysis, and (3) extension of the system's environmental performance.

Specifically, the supplemental work performed is as follows:

- A comprehensive computer based analysis of the visibility times available for both North America and Alaska was completed.
- Detailed quantitative data was prepared which supports and supplements the message collision data provided in the final report and proposal.
- The system capacity of 1000 platforms was validated and an adequate margin shown for degradation, using a message replication factor of 3.
- An analysis was made of the mutual interference effects of the DCS data and the ranging code.
- The analyses for the number of signals simultaneously present in the DCS baseband and their probable signal amplitudes were revised and supplemented by a comprehensive overall communication link analysis.
- System performance margins were computed and the overall end-to-end DCS link SNR verified.
- The TRW proposal described a spacecraft receiver design incorporating a limiter. The performance of such a limiter, under the actual multiple signal environment of 1000 platforms was examined in depth.
- A computer analysis of the magnitude of the intermodulation products and signal suppression effects was completed. Results are presented for a representative variety of signal combinations.



- A multichannel configuration of 1st IF amplifiers, each equipped with independent fast AGC loops, was examined as an alternative to a limiter for the spacecraft receiver
- The data collection platform proposed was specified for operation over a limited temperature range. Battery performance is the limiting factor. TRW calculations on high temperature self discharge effects and on low temperature operation are presented. The use of thermal insulation and electrical heating was analyzed.

## 2 COVERAGE AND VISIBILITY TIMES

Our earlier visibility analyses were based on the use of a magnetic tape recorder for DCS data storage in the observatory. For the phase B/C study, this concept was superseded by one in which the spacecraft serves only to repeat the DCS signals, without processing or storing. For this new mode, signals are received at a NASA ground station only during mutual visibility. The platform must be in view of the satellite and the satellite in view of the ground station.

This new mode of operation changes the values of visibility times used in earlier analyses, and it became necessary to develop a new geometric model and accumulate new visibility time data. The approach was to make an initial simplified manual analysis, while perfecting a new geometric model, and then devise a computer program that would yield a sufficient volume of test data for message collision calculations.

### 2.1 MANUAL ANALYSIS

The initial manual analysis of mutual visibility was performed to obtain an idea of the order of magnitude of the minimum times involved. The procedure consisted of laying down limit visibility curves on a map of the United States. The initial work used Mercator projections, but these were replaced by conical projections for all later analyses, since they allow the antenna coverage to be represented by circular patterns, which eases the geometry. Copies of the new figures (all of which assume a 7.5 degree communications cut-off angle) are presented to show the basic antenna patterns for the DCP and USB stations. Figure 2-1 illustrates the coverage region for a DCP centrally located in the United States. The ERTS ascending and descending node ground traces are superimposed as dashed lines. Figure 2-2 shows the coverage patterns associated with the three NASA ground stations at Fairbanks, Goddard and Corpus Christi.

The mutual visibility times obtained for various regions of CONUS are shown as map entries in Figures 2-3 and 2-4. It is important to appreciate that these times are approximate values and relate to a single orbit. Obtaining the total time for all useful orbits in a 12-hour period is too complex to handle manually and was pursued using our Tymshare computer facilities.

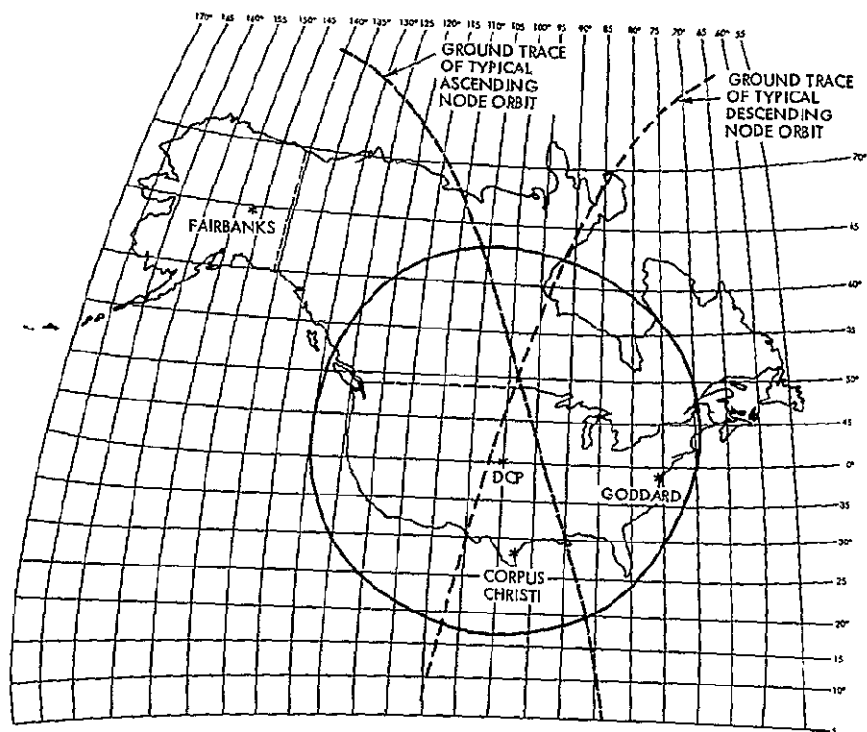


Figure 2-1

VISIBILITY COVERAGE FOR A SINGLE DCP CENTRALLY LOCATED IN CONUS

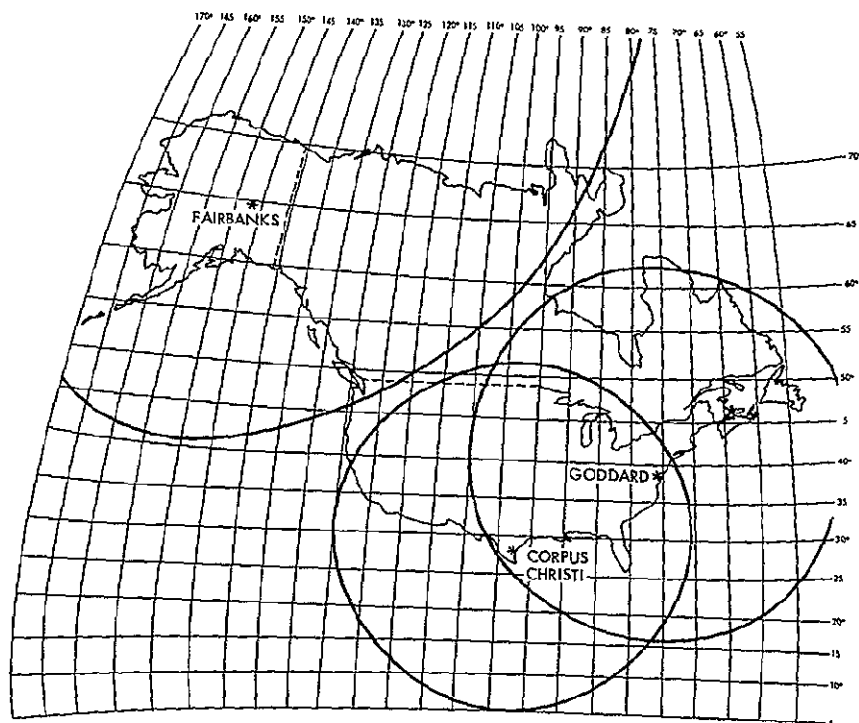


Figure 2-2

COVERAGE CURVES FOR THREE USB SITES (7.5 DEGREE CUTOFF)

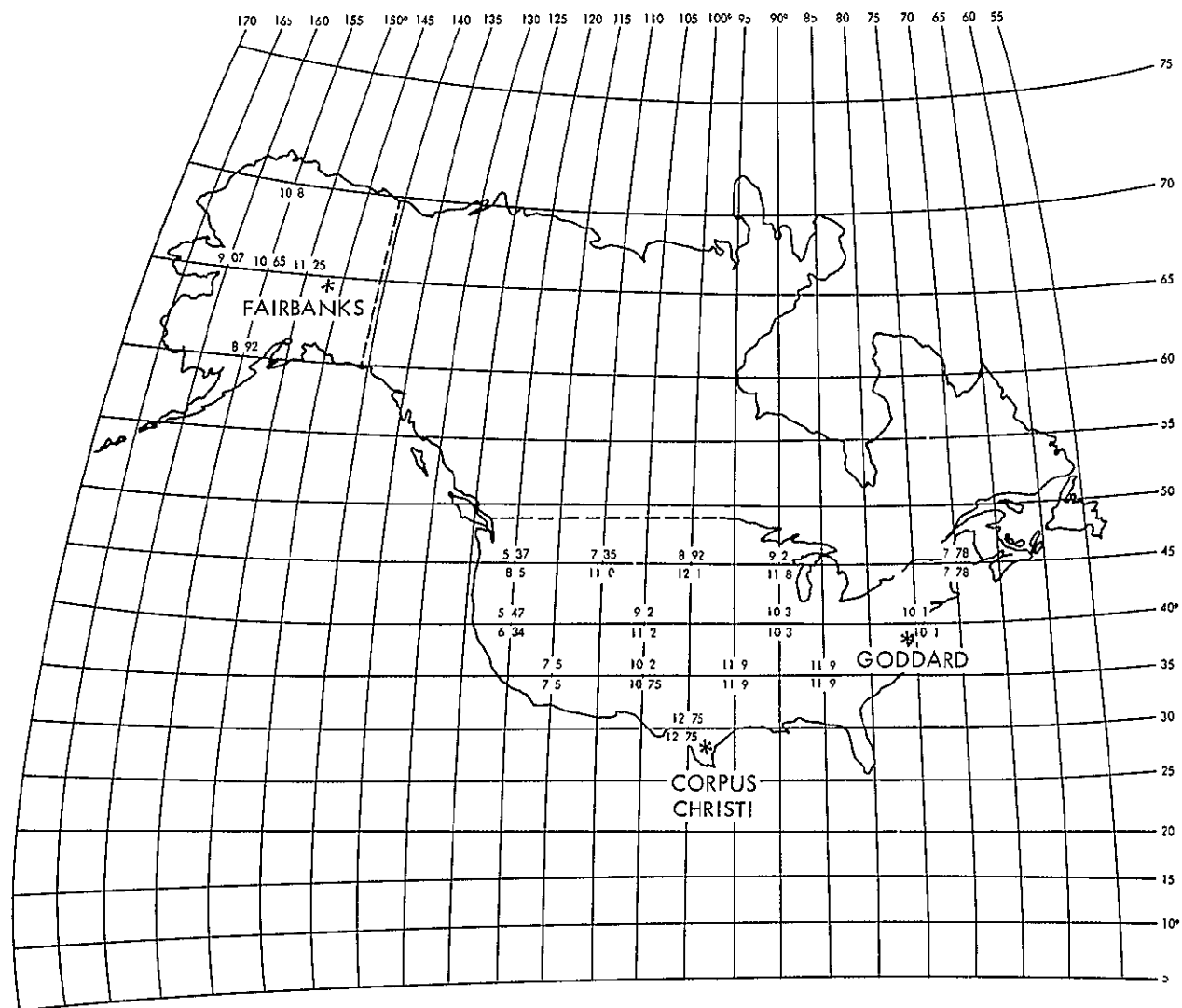


Figure 2-3

MUTUAL VISIBILITY TIME BETWEEN DCP's AND GROUP RECEIVE STATIONS (ASCENDING)  
 Upper figures are for Fairbanks and the lower figures are for all three stations

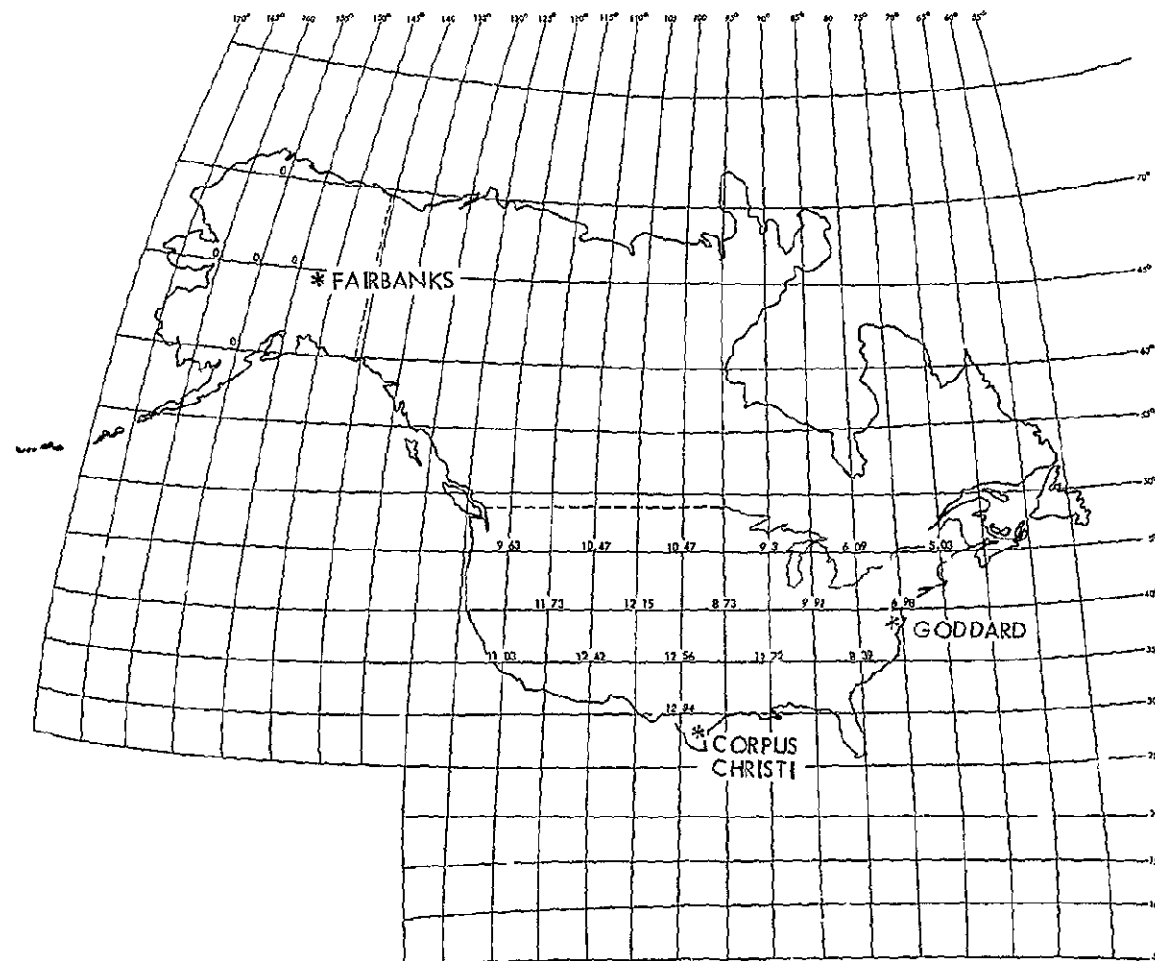


Figure 2-4  
 COMBINED MUTUAL VISIBILITY TIME BETWEEN DCP's AND ALL GROUND RECEIVING  
 STATIONS (DESCENDING)

## 2 2 COMPUTER ANALYSIS

The first step of the computer based approach was to develop a geometric analysis which would allow the mutual visibility time to be expressed as a function of the DCP location and orbit. Two such models are required, one for ascending orbits and the other for descending. A computer algorithm was written to mechanize the iterative solution of the visibility time models. The visibility time to each of the three ground stations was computed separately for one DCP location, while the orbit subtrack was iterated, thereby generating a set of visibility times. The DCP location was then incremented and the process repeated to derive a second set of visibility times.

Since we had no basis for presuming particular geographic preferences for platforms, a uniform (chess board) array over CONUS was used. The set of visibility times corresponding to each location (a matrix of positions) was accumulated for each station and as a mutually exclusive sum. The set was calculated for all three stations and for many different 12-hour subtrack combinations, the initial collection of visibility values by DCP location permits locations to be statistically weighted later if deployment data becomes available. The separation of visibility times by ground station allows the effect of the station not in sight to be evaluated, and the potential cost benefit of each station to be computed.

The mutually exclusive sum of visibility times was subjected to a rudimentary statistical analysis subroutine, within the same computer program, to yield the mean value of time and the distribution.

The following ground rules were used:

- The satellite has a circular orbit around the earth in a plane that has a fixed 99 degree inclination (9 degrees west of the north pole).
- The satellite altitude is a fixed 496 n mi.
- The period of the orbit is 103.28 minutes.
- The earth is a perfect sphere with a radius of 3443.93 n mi.
- The Fairbanks station is at  $0^{\circ}\text{N}$ ,  $147.51478^{\circ}\text{W}$ .

- The Corpus Christi station is at  $27^{\circ} 65' 37.5''$ N,  $97^{\circ} 27' 46.9''$ W
- The Goddard station is at  $39^{\circ} 03' 33.3''$ N,  $76^{\circ} 8' 25''$ W

It was mathematically convenient to use a three-dimensional reference such that the satellite subtrack on this reference would be fixed. This reference was taken as a sphere of zero shell thickness, exactly enveloping the earth (with the same radius). The earth rotates within this fixed non-rotating reference sphere.

A latitude and longitude angular scale was placed on this reference sphere such that the latitude of a point on earth was fixed relative to this reference and the longitude of this point varied linearly with time relative to the reference sphere. In other words, for a point on earth, the normal latitude of that point is also equal to the latitude on the reference sphere and the longitude (degrees) of this point relative to the reference sphere equals  $360/(24 \times 60)$  times the time in minutes after that point passes the zero reference longitude.

The computer assisted analysis provides results on the time that an ERTS sensor platform is receivable by the three stations and the total system, or the accumulated time that any one or more stations is able to receive transmissions from this platform. The DCP locations utilized are the intercept points of a grid whose lines are separated 5 degrees in both longitude and latitude. The area covered is the entire United States. The times are those found in a 12-hour spacecraft orbital period. Since all time positions or phasing of a 12-hour period are equally likely, the times are variables dependent on equally likely conditions. The time parameters selected for output are the average, minimum, and maximum values.

Section 2.3 gives the geometrical model and derives the basic equations used in the computer analysis. Section 2.3 gives the results of the computer analysis and Section 2.4 the developed computer program and its descriptive explanation.

## 2.3 EQUATIONS DEVELOPMENT

The following analysis derives the sine of the angle between a plane tangent at earth and a line from the point of tangency to the spacecraft.

This point on earth represents the sensor platform or either of the three ground stations. The derivation is in two parts, with the first using the geometry of Figure 2-5, for which

$\alpha(t)$  = angle between plane tangent at earth point and line-of-sight to satellite

$E$  = earth radius

$A_s$  = satellite altitude

$A(t)$  = distance between earth point and earth crossing of line between satellite and earth center

Using the law of cosines,

$$(E + A_s)^2 = R^2(t) + E^2 - 2ER(t) \cos(\alpha(t) + \pi/2) \quad (2-1)$$

and

$$R^2(t) = E^2 + (E + A_s)^2 - 2E(E + A_s) \cos \beta(t) \quad (2-2)$$

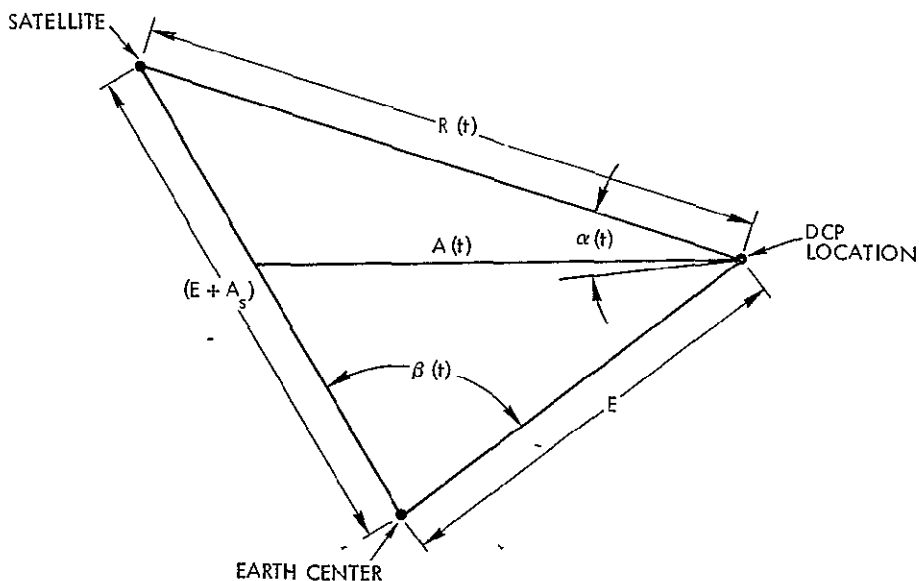


Figure 2-5

GEOMETRIC RELATIONSHIP OF EARTH POINTS AND SATELLITE



Noting that  $\cos (A + \pi / 2) = -\sin A$  and solving for  $\sin \alpha (t)$

$$\sin \alpha (t) = \frac{(E + A_s)^2 - E^2 - R^2 (t)}{2 E R (t)} . \quad (2-3)$$

Substituting (2-2) into (2-3),

$$\sin \alpha (t) = \frac{(E + A_s) \cos \beta (t) - E}{[E^2 + (E + A_s)^2 - 2E(E + A_s) \cos \beta (t)]^{1/2}} .$$

Simplifying,

$$\sin \alpha (t) = \frac{\cos \beta (t) - G}{[G^2 + 1 - 2G \cos \beta (t)]^{1/2}} \quad (2-4)$$

for

$$G = E/(E + A_s) .$$

Using the law of cosines,

$$A^2(t) = 2E^2 (1 - \cos \beta (t))$$

and

$$\cos \beta (t) = 1 - A^2(t)/2E^2 \quad (2-5)$$

Substituting (2-5) into (2-4),

$$\sin \alpha (t) = \frac{(1-G) - A^2(t)/2E^2}{[(1-G)^2 + GA^2(t)/E^2]^{1/2}} \quad (2-6)$$

The second derivation will determine  $A^2(t)$  as the square of a vector magnitude, using Figure 2-6, where

$\bar{N}$  = vector from earth center to earth surface point

$\bar{S}$  = vector from earth center to point where line of sight from satellite to earth center reaches earth surface

$\theta_e$  = latitude (not a function of time)

$L_e(t)$  = longitude which is positive when  $\bar{N}$  is in the positive "X" space

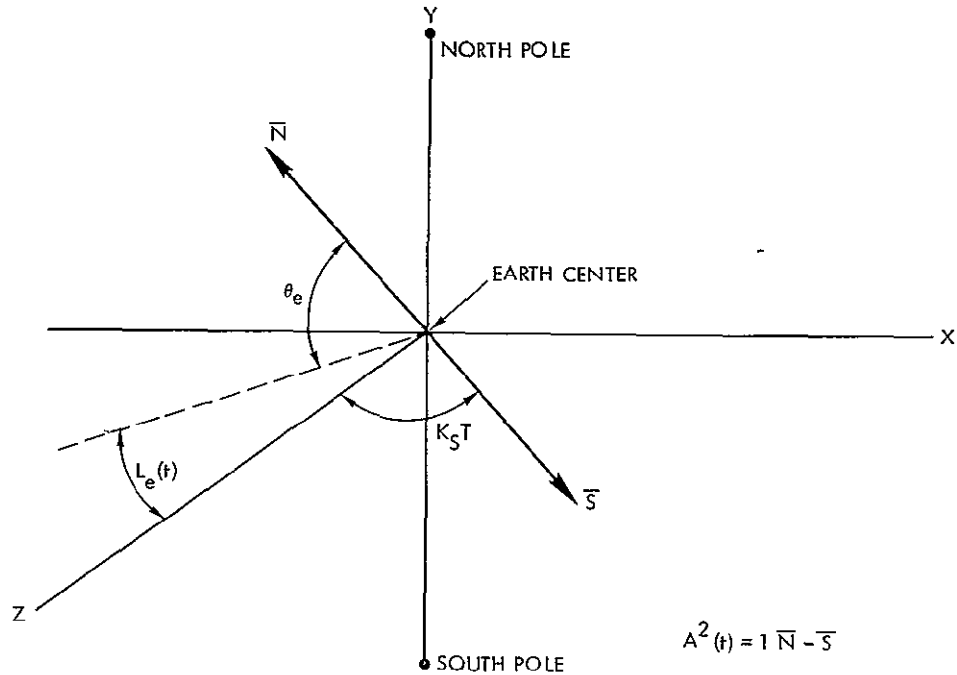


Figure 2-6  
DERIVATION OF  $A^2(t)$

'  $K_s t$  = angle between  $\bar{S}$  vector and Z axis (which  $\bar{S}$  lies on at  $t = 0$ ), where the angle is negative when  $\bar{S}$  is below X-Z plane

NOTE X-Z plane has equatorial circle on it

Z-axis hits equatorial crossing of satellite earth subtrack where time is taken as zero

Y-axis includes north and south poles

Solving for  $\overline{A(t)}$ ,

$$\begin{aligned}\overline{A(t)} = \overline{N} \cdot \overline{S} = & E(\cos \theta_e \sin L_e(t) \overline{X} + \cos \theta_e \cos L_e(t) \\ & + \sin \theta_e \overline{Y}) - E(-\cos(81^\circ) \sin K_s t \overline{X} \\ & + \cos K_s t \overline{Z} + \sin(81^\circ) \sin K_s t \overline{Y})\end{aligned}$$

where  $\overline{X}$ ,  $\overline{Y}$ ,  $\overline{Z}$  are unit vectors on the coordinate axis

Solving for  $A^2(t)$ ,

$$\begin{aligned} A^2(t)/E^2 = \left| \overline{N} - \overline{S} \right|^2 / E^2 = & (\cos \theta_e \sin L_e(t) + \cos(81^\circ) \sin K_s(t))^2 \\ & + (\cos \theta_e \cos L_e(t) - \cos K_s(t))^2 \\ & + (\sin G_e - \sin(81^\circ) \sin K_s(t))^2 \end{aligned} \quad (2-7)$$

where

$$L_e(t) = L_e + K_e t, \quad K_e = 2\pi / (23 \times 60), \quad "t" \text{ in minutes.}$$

Therefore,  $\sin \alpha(t)$  is derived by substituting (2-7) into (2-6).

## 2.4 RESULTS

The results are presented in two forms. The first presents useful data derived in the computer program development. The second presents the final results, which are plots of average and minimum-maximum values of the time that each of the sensors is receivable by the station and by the total system (one or more stations).

### 2.4.1 Developmental Results

Figure 2-7 gives the results of a set of computer runs, one for each orbit. The orbits were stepped 10 degrees in longitude, while the actual progression of sequential orbits due to earth revolution is approximately  $25.6^\circ$ . This then was a check on the single orbit part of the overall computer program. The sensor platform position was in Montana at  $40^\circ$  longitude east of Fairbanks and at  $45^\circ$  latitude.

The time that Fairbanks could receive the sensor during one orbit peaked at 4.7 minutes when the orbit started  $40^\circ$  east of Fairbanks. This time decreased to zero when the orbit started  $90^\circ$  east of Fairbanks. Corpus Christi realized a higher peak value of 7.25 minutes. Goddard realized an even higher peak value of 8.0 minutes. Goddard, however, was more sensitive to orbit positions and had a narrower range for non-zero time values.

Figure 2-8 gives the results for different 12-hour period start longitudes, for the time within 12 hours during which one or more stations can receive a sensor in Nebraska at  $100^\circ W$  longitude and  $40^\circ N$  latitude.

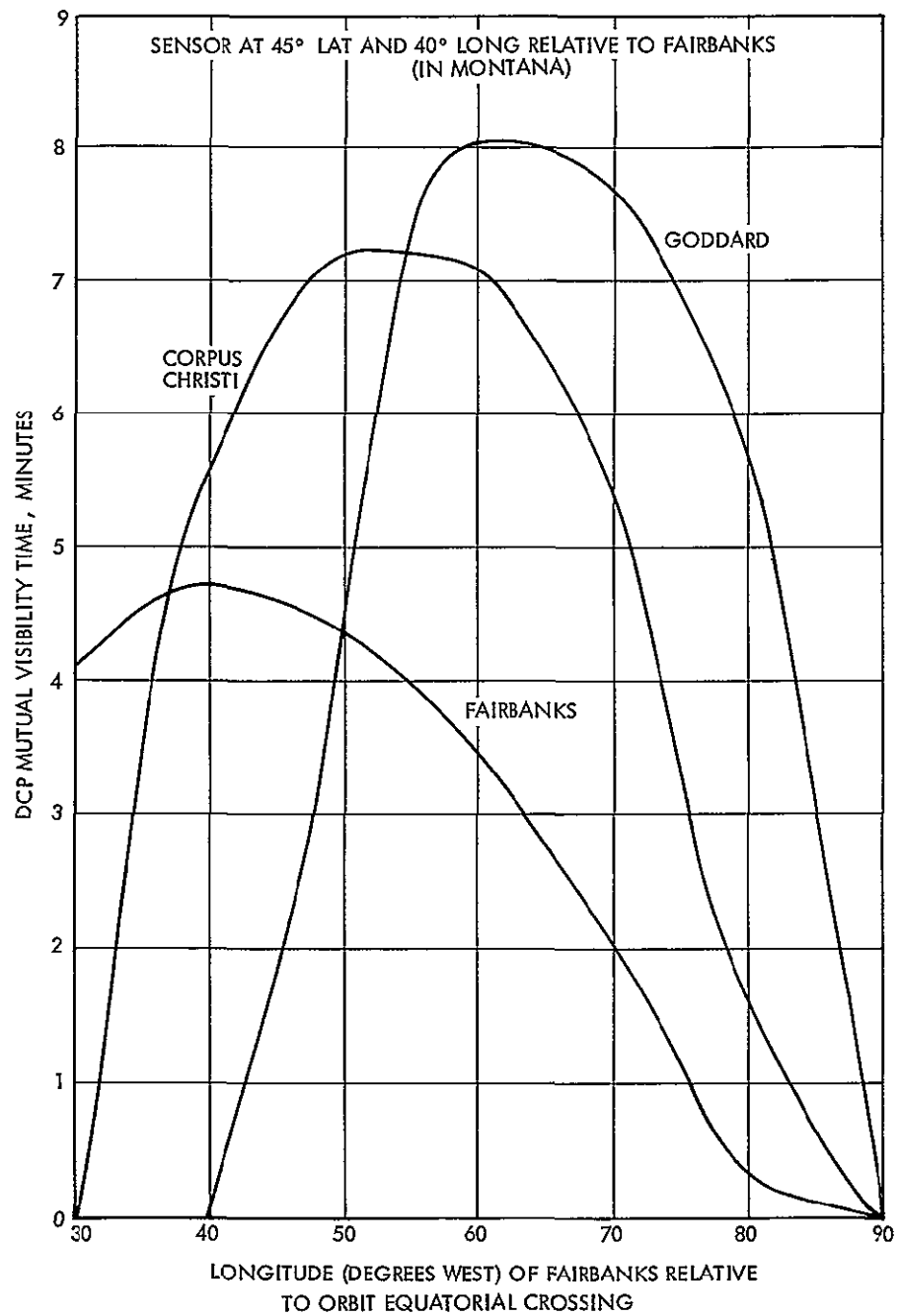
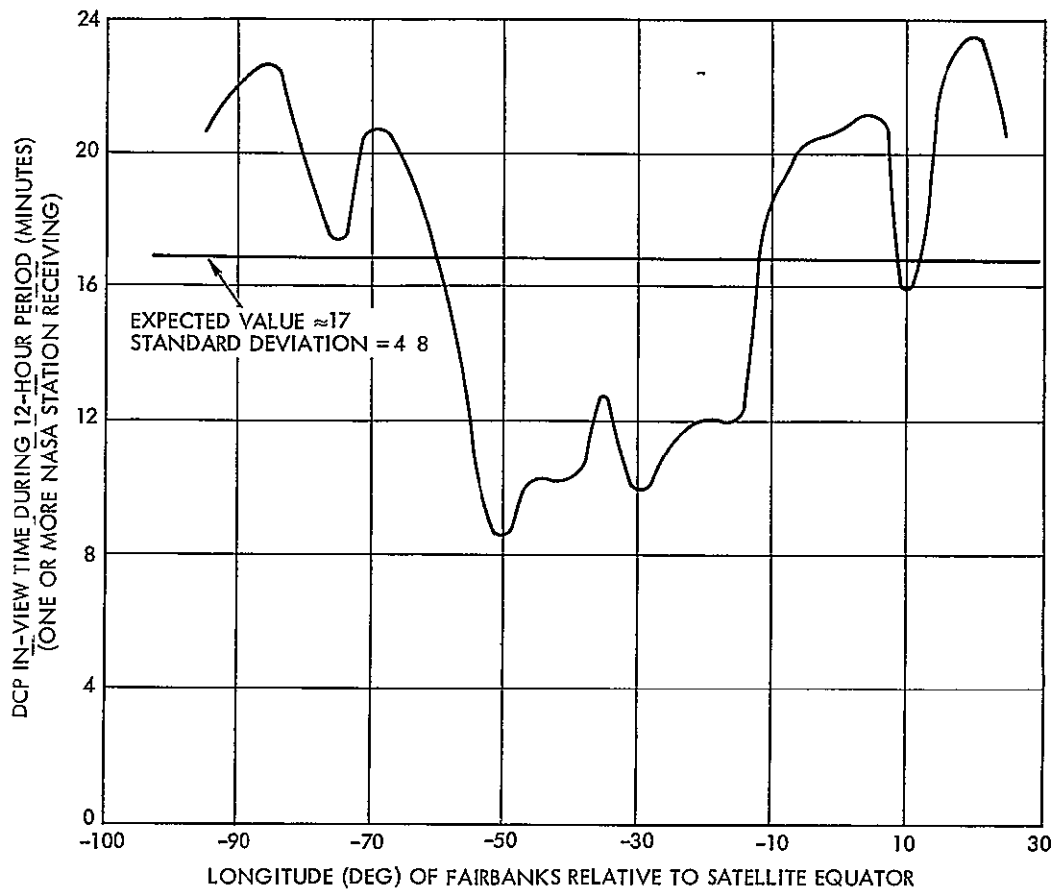


Figure 2-7

ORBITAL EFFECT ON VISIBILITY TIME FOR REPRESENTATIVE  
PCP LOCATION



Since with the normal orbit longitudinal separation (around  $25.6^\circ$ ) there is typically for one sensor only two orbits with non-zero times, the times for each orbit were added (7 orbits in 12 hours) to give the accumulated time in the total 12-hour period. In other words, an orbital distribution essentially does not exist, while a distribution in terms of 12-hour period phasing certainly does. The resulting odd distribution plus the fact that the standard deviation is close to the maximum deviation from the average leads to a primary interest in average values plus minimum-maximum values. These values for the system time (one or more stations) and the above platform location are 16.7, and 8.6 to 23.4 minutes. The cumulative distribution, assuming equally likely 12-hour period phasing, is given in Figure 2-9.

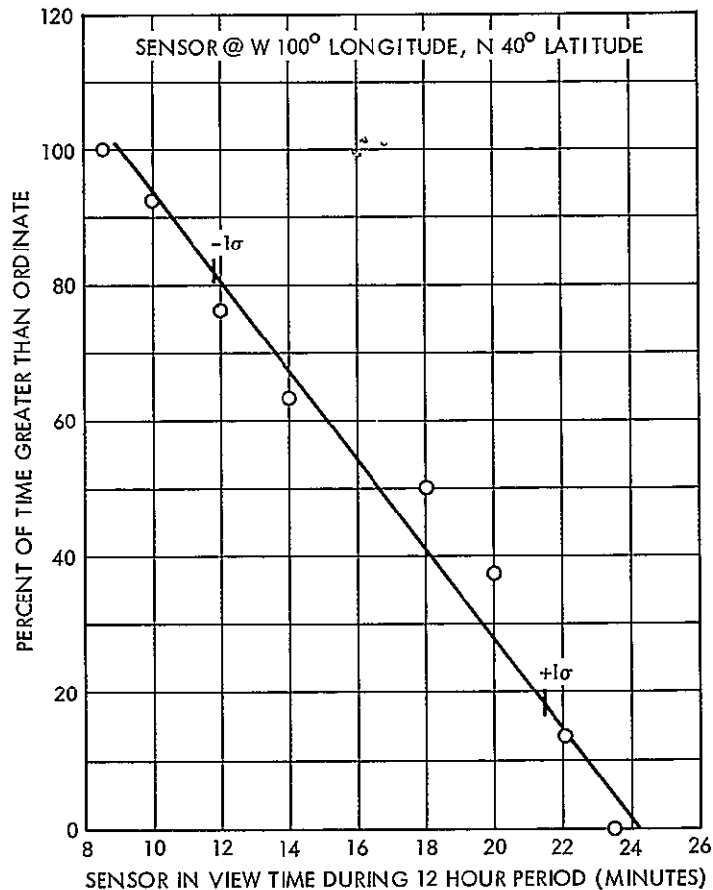


Figure 2-9

CUMMULATIVE DISTRIBUTION FOR ONE OR MORE NASA STATIONS RECEIVING

Actually, the longitude variable should have been taken to 40 degrees instead of just 25 degrees, since the distribution repeats after 40 degrees

Figure 2-10 is for Fairbanks, Figure 2-11 for Corpus Christi, and Figure 2-12 for Goddard. The pronounced dip in all these curves, with high values on both sides results when the contributing orbit sections for the left side are all south to north pole and the right side all north to south pole.

The total visibility time available to a DCP is obtained by combining the time available for each of the ground stations (without duplication). This is presented in Figure 2-8

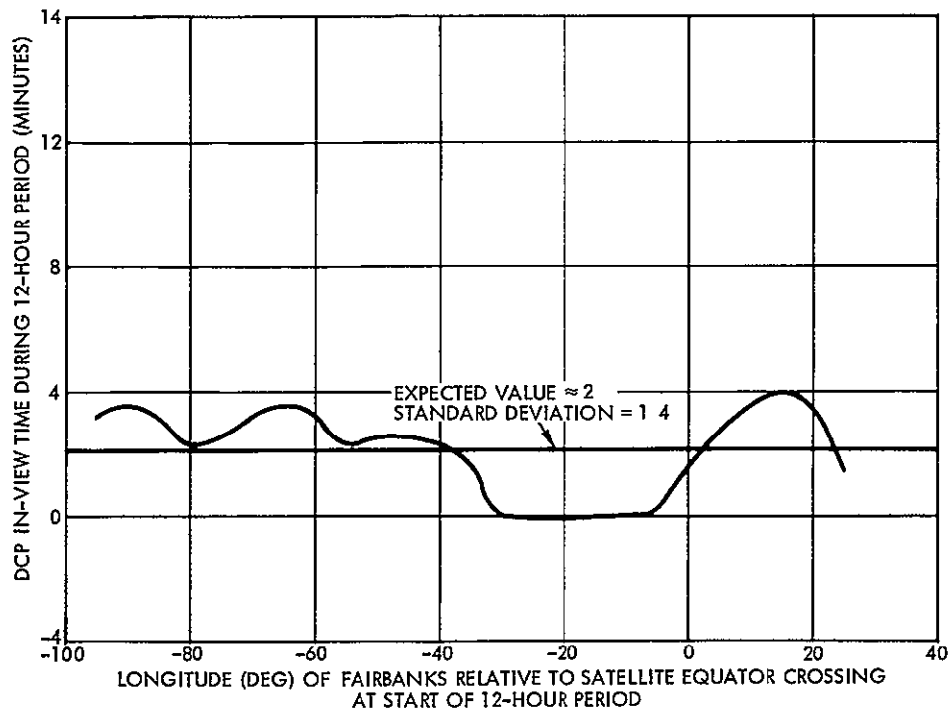


Figure 2-10

VISIBILITY TIME FOR DCP LOCATED AT 100°W LONGITUDE AND 40°N LATITUDE, STATE OF NEBRASKA

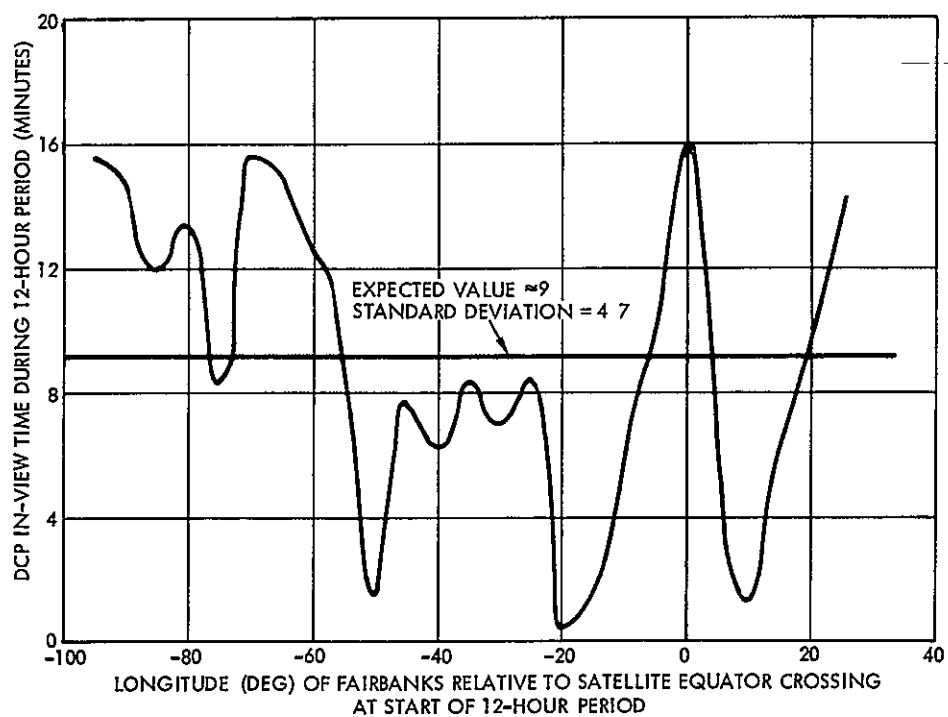


Figure 2-11

CORPUS CHRISTI VISIBILITY TIME FOR DCP LOCATED AT 100°W LONGITUDE AND 40°N LATITUDE, STATE OF NEBRASKA

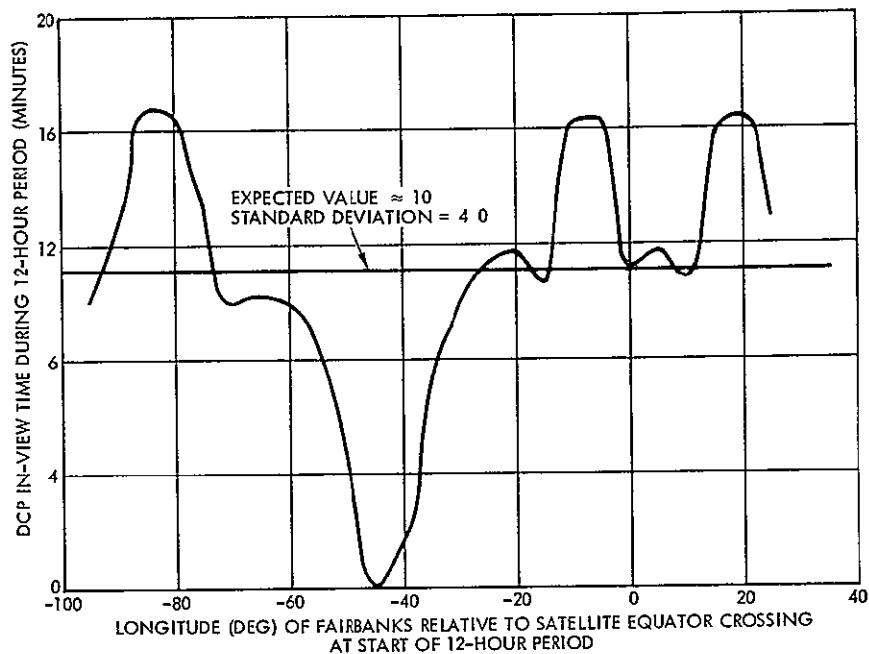


Figure 2-12  
GODDARD VISIBILITY TIME FOR DCP LOCATED AT 100°W  
LONGITUDE AND 40°W LATITUDE, STATE OF NEBRASKA

#### 2.4.2 Final Results

The final results were sequentially-determined time parameters for sensors placed at grid points, with grid lines separated by 5 degrees longitude and latitude. Figure 2-13 is a map of the United States with time parameters listed at each analyzed sensor site. These parameters are the average and minimum-maximum values for the accumulated time that one or more stations can receive acceptable sensor transmission in a 12-hour period. Acceptable transmission implies that the DCP to spacecraft angle is above the 7.5-degree limit. The grid points at latitudes 30 and 50 degrees had not been analyzed when this final addendum was published. The grid points for 40 degrees latitude have 4-degree steps.

Figure 2-14 gives the results for the same platforms for Fairbanks only, Figure 2-15 for Corpus Christi, and Figure 2-16 for Goddard.

Assuming that all DCP positions are equally likely, an unknown DCP has an expected mutual visibility time of 16 minutes, with minimum and maximum times of 11 and 21 minutes.



AVERAGE AND MINIMUM-MAXIMUM VISIBILITY TIMES at a DCP position for a successfully relayed DCP transmission with one or more NASA successfully receiving.

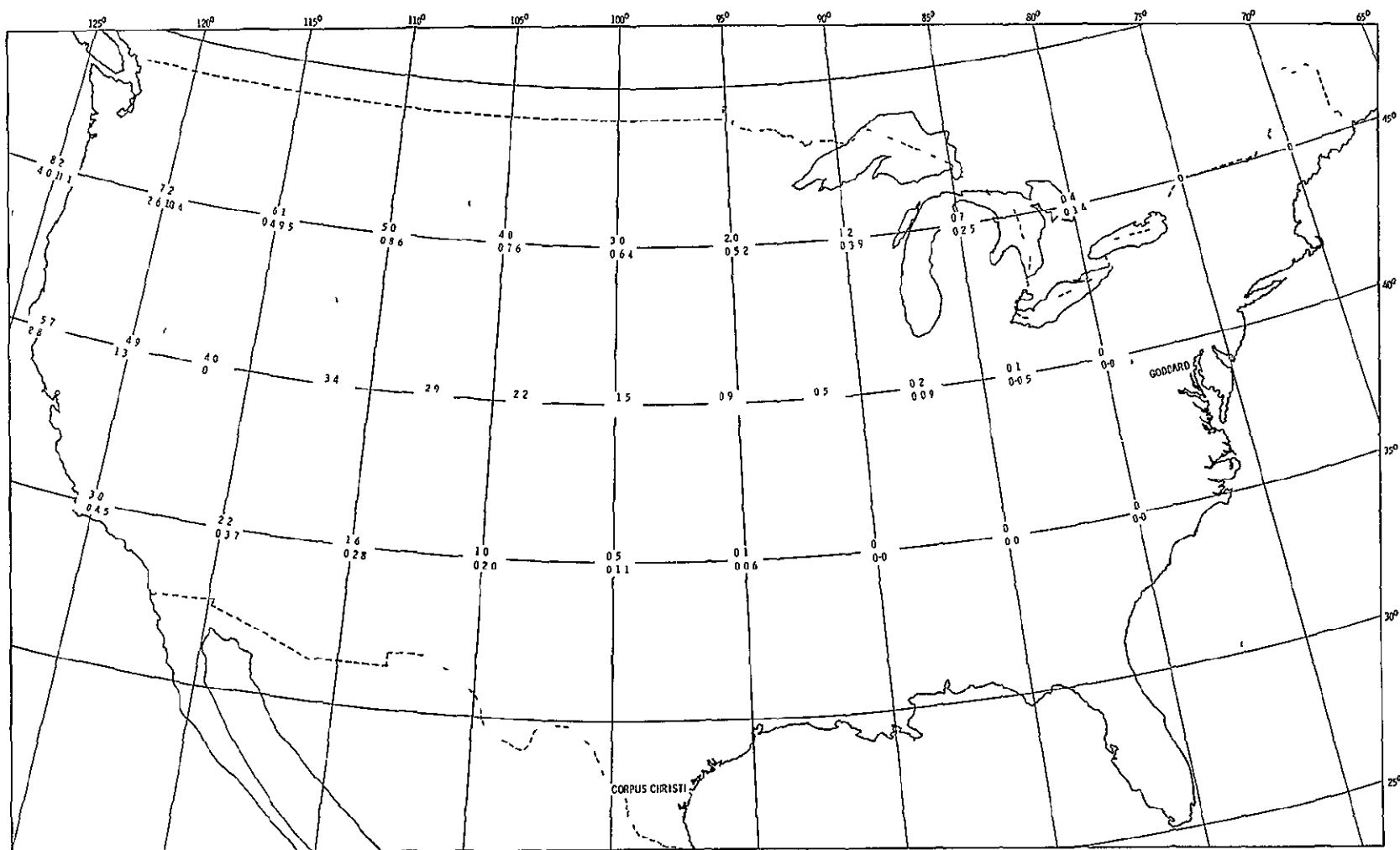


Figure 2-14

AVERAGE AND MINIMUM-MAXIMUM VISIBILITY TIMES at a DCP position for a successfully relayed DCP transmission with the Fairbanks station successfully receiving

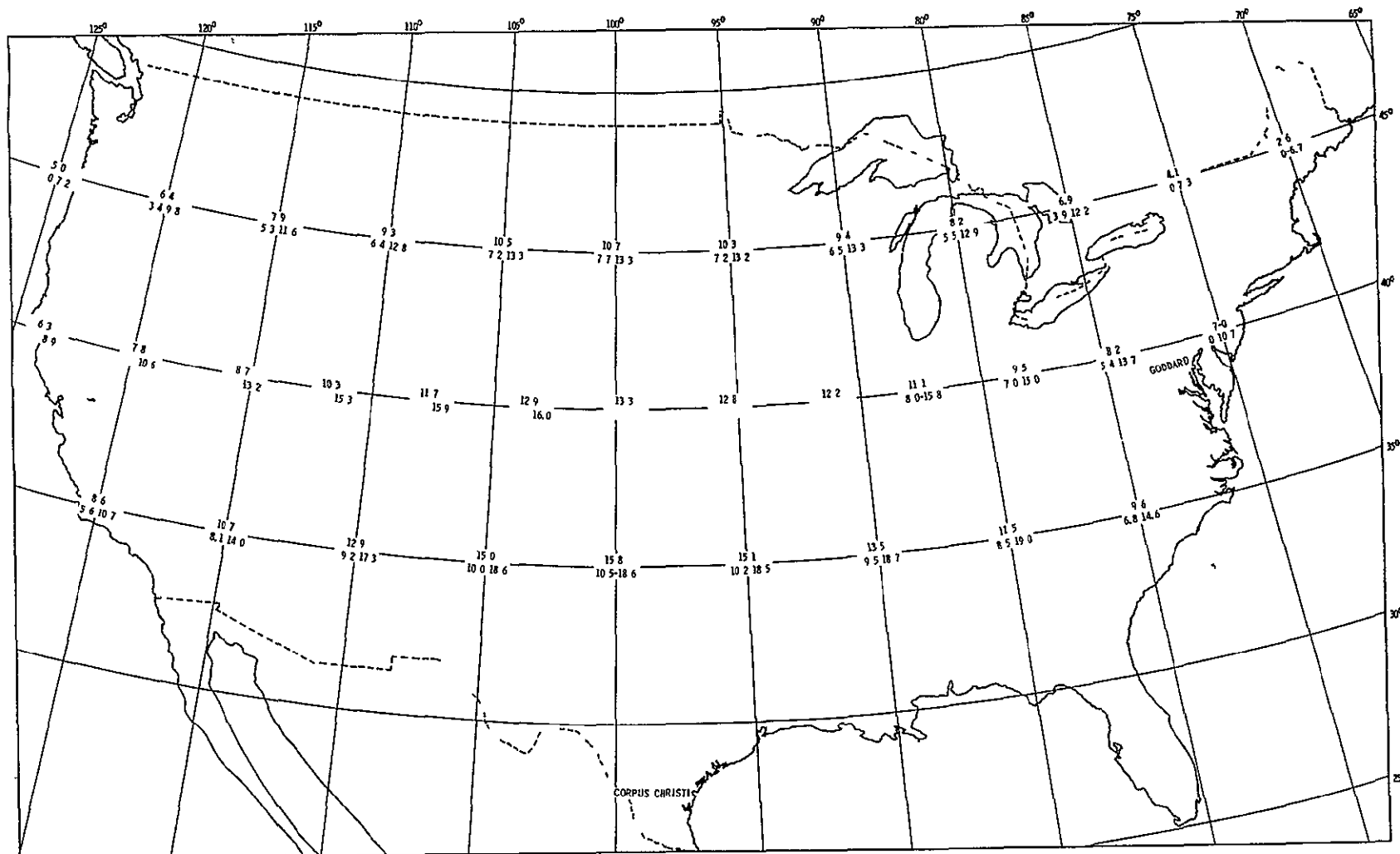


Figure 2-15

AVERAGE AND MINIMUM-MAXIMUM VISIBILITY TIMES at a DCP position for a successfully relayed DCP transmission with Corpus Christi station successfully receiving.

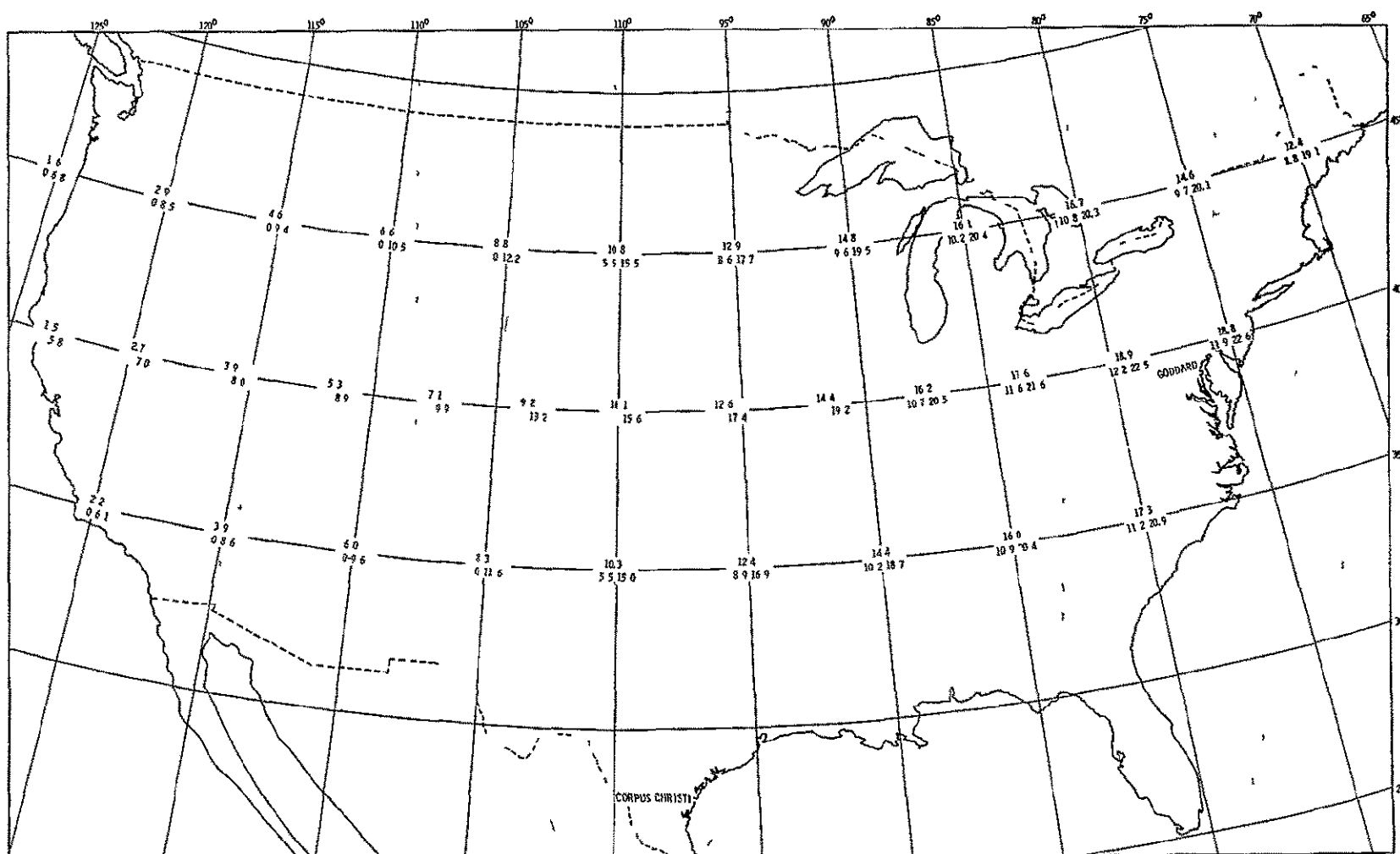


Figure 2-16

AVERAGE AND MINIMUM-MAXIMUM VISIBILITY TIMES at a DCP position for a successfully relayed DCP transmission with Goddard station successfully receiving.

TRW has also prepared a map for the visibility times in Alaska. This is presented as Figure 2-17, and the computer results are listed in Table 2-1. From these data, it is apparent that the worst value for minimum time is 10-1/2 minutes. This assumes excellent DCS performance. Neither Corpus Christi nor Goddard contribute to the coverage times listed.

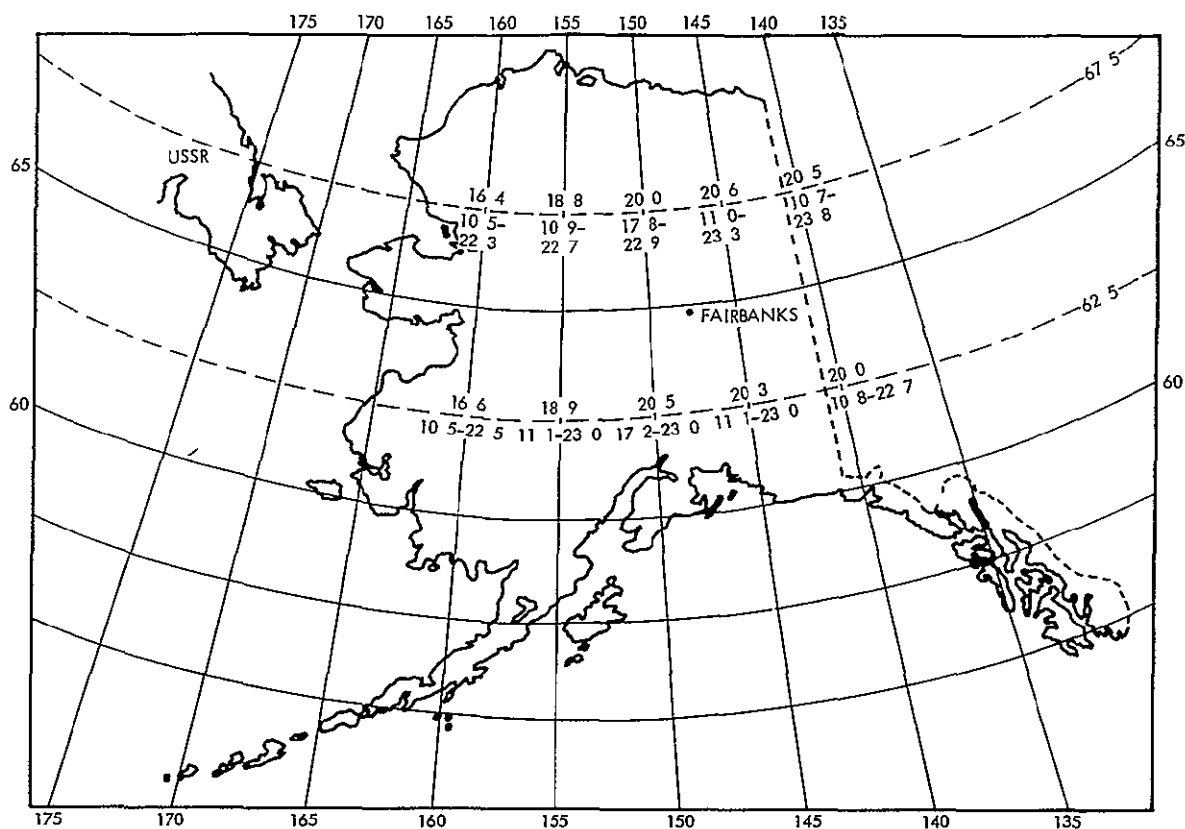


Figure 2-17

AVERAGE AND MINIMUM-MAXIMUM MUTUAL VISIBILITY TIMES FOR THE STATE OF ALASKA TO FAIRBANKS

Table 2-1 Mutual Visibility Time Data for Alaskan Platforms

Latitude (Degrees North)	Longitude (Degrees West)	(Visibility) Time (Minutes)		
		(Average)	(Minimum)	(Maximum)
62 5	160	16 6	10 5	22 5
62 5	155	18 9	11 1	23 0
62 5	150	20 5	17 2	23 1
62 5	145	20 3	11 1	23 0
62 5	140	20 0	10 8	22 7
67 5	160	16 4	10 5	22 3
67 5	155	18 8	10 9	22 7
67 5	150	20 6	17 8	22 9
67 5	145	20 6	11 0	23 3
67 5	140	20 5	10 7	23 8

## 2.5 COMPUTER PROGRAM DESCRIPTION

The computer program sequentially analyzes platforms whose positions are stepped 5 degrees in longitude at a fixed latitude. For each sensor position, the start of the 12-hour orbiting period is stepped 5 degrees in longitude at the satellite equator crossing. A range of 135 degrees (28 steps) is covered. The time zero for each orbit is the time that the spacecraft crosses the equator. The different DCP in-view times are determined for each 12-hour period and an average value for each is obtained, as well as the minimum and maximum.

For each DCP and 12-hour period, there are seven orbits. Since in almost all cases there are only two orbits that give in-view times greater than zero, a distribution over the orbits is not feasible. Therefore, the times are added over all orbits to give the total viewing time during the 12-hour period. For each orbit, the time is determined that the DCP is receivable by Fairbanks, Corpus Christi, and Goddard, also the accumulated time when one or more stations can receive. (That is, if two stations receive simultaneously for 5 minutes, then 5 minutes is accumulated, not 10 minutes.)

For each DCP, 12-hour period and orbit, the time of orbit is stepped one-tenth minute over the interval that the spacecraft is in view of any of the ground stations. The limit angle, or the minimum value of  $\alpha(t)$  under which communication is considered unreliable, is taken as 7.5 degrees. The accumulation of time for each station starts when both the DCP and station have  $\alpha(t)$  angles greater than 7.5 degrees. The time for a station stops when either the station  $\alpha(t)$  is below the limit angle or the DCP  $\alpha(t)$  is below the limit angle.

#### 2.5.1 Explanation of Computer Program Statements

- 1) Statements 20 and 22 establish the sensor platform latitude
- 2) Statement 24 creates a constant which is later used to place the sensors at integer degrees on the normal map. This is required since the program longitude variables were related to the longitude of Fairbanks, which is not at integer degrees in the normal map.
- 3) Statement 25 gives the sequential orbital step, in radians, at the equator, due to earth revolution.
- 4) Statement 27 gives a constant which is used only when the earth has revolved to the point where the satellite crosses the earth from north to south and the longitude of the next equator crossing after time zero is increased 180 degrees ( $\pi$  - radians) minus that from earth revolution in one half orbit.
- 5) Statements 30-39, 52-67. For equation (2-7),  $K_e = K1$ ,  $K_s = K2$ ,  $K3$  = longitudinal difference between Fairbanks and Corpus Christi, which in itself is part of  $L_e$  for Corpus Christi,  $K7$  = this difference for Goddard,  $A1$  and  $C1$  are  $\cos \theta_e$  and  $\sin \theta_e$  for Fairbanks,  $A2$ ,  $C2$  for the sensor,  $A3$ ,  $C3$  for Corpus Christi,  $A4$ ,  $C4$  for Goddard,  $A5$ ,  $C5$  are  $\cos(81^\circ)$  and  $\sin(81^\circ)$ . For equation (2-6),  $G = G1$ ,  $1-G = G1$ ,  $(1-G)^2 = G2$ .
- 6) Statements 68, 69 move the sensor longitudinal positions in 5 degree steps from west coast to east coast (different numbers used for Alaska sensors).
- 7) Statements 70, 72 move the 12-hour period first orbit time zero equatorial longitudinal position in 5-degree steps over a range outside of which the geometrical pattern repeats.
- 8) Statement 80 derives a constant which is later used to determine whether the direction of the present orbit over the United States is south to north or north to south.

- 9) Statement 85 sets up the seven orbits
- 10) Statements 90-105 derive the longitude at time zero for each orbit for the sensor and NASA stations
- 11) Statements 110, 115 are reset functions between orbits
- 12) Statement 120 creates the time variable
- 13) Statement 125 determines whether the orbit over the United States is south to north or north to south
- 14) Statements 130-160 set up the conditions unique for the north to south orbit
- 15) Statements 147, 148 and 167, 169 are used to abort analysis of orbits that cannot receive the sensor
- 16) Statements 170-205 solve equation (2-7) for the sensor and NASA stations, while 210-225 solve equation (2-6)
- 17) Statements 230-355 determine the start and stop time pairs between which the sensor is receivable by NASA station for the three stations (325-350 for the case where the sensor drops out before NASA stations).
- 18) Statements 360-370 determine the time that the sensor is receivable by Fairbanks and then Corpus Christi and then Goddard.
- 19) Statements 380-425 determine the time that one or more NASA stations can receive the sensor
- 20) Statements 430-445 accumulate the above times over all orbits in one 12-hour period
- 21) Statements 455-470, 500-515 determine the averages over all 12-hour periods
- 22) Statements 475-491 determine the minimum-maximum values over all 12-hour periods
- 23) Statement 494 is a reset function for independent 12-hour periods and 546, 547 for independent sensors

## 2 5 2 Computer Program Listing

```

2  VAR=ZERO
20  PRINT "TYPE IN PLATFORM LATITUDE (DEG)"
22  INPUT M2
24  A=PI*(2+(30+53.206/60)/60)/180

```



```

25 G3=1540/3443 93
27 I4=G3/2 - PI
30 K1=2*PI/(24*60)
31 K2=2*PI/103 28
32 K3=PI*(147-97 378469+(30+53 206/60)/60)/180
33 K7=PI*(147-76+(30-51+(53.206/45)/60)/60)/180
40 M1,M3,M4,Z3=20
50 OPEN/DATA2/, OUTPUT,1
52 A1=COS(PI*(64+(58+36.582/60)/60)/180)
53 C1=SIN(PI*(64+(58+36 572/60)/60)/180)
54 A3=COS(PI*27.65375/180)
55 C3=SIN(PI*27 65375/180)
56 A4=COS(PI*(39+2/60)/180)
57 C4=SIN(PI*(39+2/60)/180)
58 A5=COS(81*PI/180)
59 C5=SIN(81*PI/180)
65 A2=COS(PI*M2/180)
67 C2=SIN(PI*M2/180)
68 FOR I5=20 TO 70 STEP 5
69 I2=I5*PI/180
70 FOR H1=-95 TO 40 STEP 5
72 I1=H1*PI/180
75 I3=I1 + I4
37 G=3443 93/(3443.93+496)
38 G1=1-G
39 G2=G1+2
80 G5=1 + (0 4-I1)/G3
85 FOR J=1 TO 7
90 L1=I1 + G3*(J-1)
95 L2=L1 + I2 + A
100 L3=K3 + L1
105 L4=K7 + L1
110 T1,T2,T3,T4,T5,T6=0
115 04,05,06=0
120 FOR H=0 TO 26 STEP 1
125 IF J<=G5 THEN 165

```

```

130 T=H - 26
135 K6=- C5*SIN(K2*T)
140 L1=I3 + G3*(J-1)
145 L2=L1 + I2 + A
147 IF L2<-0 36 THEN 450
148 IF L2>0 48 THEN 450
150 L3=K3 + L1
155 L4=K7 + L1
160 GO TO 175
165 T=H
167 IF L2>0 36 THEN 450
169 IF L2<-0 48 THEN 450
170 K6=C5*SIN(K2*T)
175 K4=K1*T
180 K5=A5*SIN(K2*T)
185 J3=COS(K2*T)
190 B1=(A1*SIN(L1+K4)+K5↑2+(A1*COS(L1+K4)-J3)↑2+(C1-K6)↑2
195 B2=(A2*SIN(L2+K4)+K5↑2+(A2*COS(L2+K4)-J3)↑2+(C2-K6)↑2
200 B3=(A3*SIN(L3+K4)+K5↑2+(A3*COS(L3+K4)-J3)↑2+(C3-K6)↑2
205 B4=(A4*SIN(L4+K4)+K5↑2+(A4*COS(L4+K4)-J3)↑2+(C4-K6)↑2
210 S1=(G1-B1/2)/SQR(G2+G*B1)
215 S2=(G1-B2/2)/SQR(G2+G*B2)
220 S3=(G1-B3/2)/SQR(G2+G*B3)
225 S4=(G1-B4/2)/SQR(G2+G*B4)
230 IF S2<S THEN 325
235 IF X1=1 THEN 255
240 IF S1>S THEN X1=1 ELSE 265
245 T1=T
250 GO TO 265
255 IF S1<S THEN X1=0 ELSE 265
260 T2=T
265 IF X3=1 THEN 285
270 IF S3>S THEN X3=1 ELSE 295
275 T3=T
280 GO TO 295
285 IF S3<S THEN X3=0 ELSE 295

```

```

290 T4=T
295 IF X4=1 THEN 315
300 IF S4>S THEN X4=1 ELSE 355
305 T5=T
310 GO TO 355
315 IF S4<S THEN X4=0 ELSE 355
320 T6=T
322 GO TO 355
325 IF X1=0 THEN 335
330 T2=T, X1=0
335 IF X3=0 THEN 345
340 T4=T, X3=0
345 IF X4=0 THEN 355
350 T6=T, X4=0
355 NEXT H
360 O1=T2-T1
365 O2=T4-T3
370 O3=T6-T5
380 IF T1<=T3 THEN IF T3<T2 THEN IF T4>T2 THEN O4=T2-T3
    ELSE O4=O2 ELSE 395 ELSE 390
385 GO TO 395
390 IF T1<T4 THEN IF T2>T4 THEN O4=T4-T1 ELSE O4=O1
395 IF T1<=T5 THEN IF T5<T2 THEN IF T6>T2 THEN O5=T2-T5
    ELSE O5=O3 ELSE 410 ELSE 405
400 GO TO 410
405 IF T1<T6 THEN IF T2>T6 THEN O5=T6-T1 ELSE O5=O1
410 IF T3<=T5 THEN IF T5<T4 THEN IF T6>T4 THEN O6=T4-T5
    ELSE O6=O3 ELSE 425 ELSE 420
415 GO TO 425
420 IF T3<T6 THEN IF T4<T6 THEN O6=T6-T3 ELSE O6=O2
425 Z=O1 + O2 + O3 - O4 - O5 - O6
430 P1=P1 + O1
435 P2=P2 + O2
440 P3=P3 + O3
445 Z1=Z1 + Z
450 NEXT J
455 P4=P1 + P4

```

```

460 P5=P2 + P5
465 P6=P3 + P6
470 Z2=Z1 + Z2
475 IF P1<M1 THEN M1=P1
477 IF P1>N1 THEN N1=P1
480 IF P2<M3 THEN M3=P2
482 IF P2>N3 THEN N3=P2
485 IF P3<M4 THEN M4=P3
487 IF P3>N4 THEN N4=P3
490 IF Z1<Z3 THEN Z3=Z1
491 IF Z1>Z4 THEN Z4=Z1
492 WRITE ON 1,M2,I5,H1,Z2,Z3,Z4,P1,M1,N1,P2,M3,N3,P3,
    M4,N4
493 PRINT H1,Z2,Z3,Z4
494 P1,P2,P3,Z1=0
495 NEXT H1
500 P4=P4/28
505 P5=P5/28
510 P6=P6/28
515 Z2=Z2/28
537 PRINT I5
540 PRINT P4,M1,N1,P5,M3,N3,P6,M4,N4
545 PRINT Z2,Z3,Z4
546 P4,N1,P5,N3,P6,N4,Z2,Z4=0
547 M1,M3,M4,Z3=20
550 NEXT I5
560 CLOSE 1

```

### 3 SYSTEM CAPACITY, RANDOM T AND F MODE

Just before the final DCS briefing we completed the computer synthesis run for system capacity, with combined random time and frequency and a replication factor of 3. These results showed that for a 95% probability of obtaining one good copy of each message in a 12-hour period, the total capacity is approximately 1000 platforms. The data for values of message replication  $M = 1, 2$ , and 3 are presented in Figure 3-1.

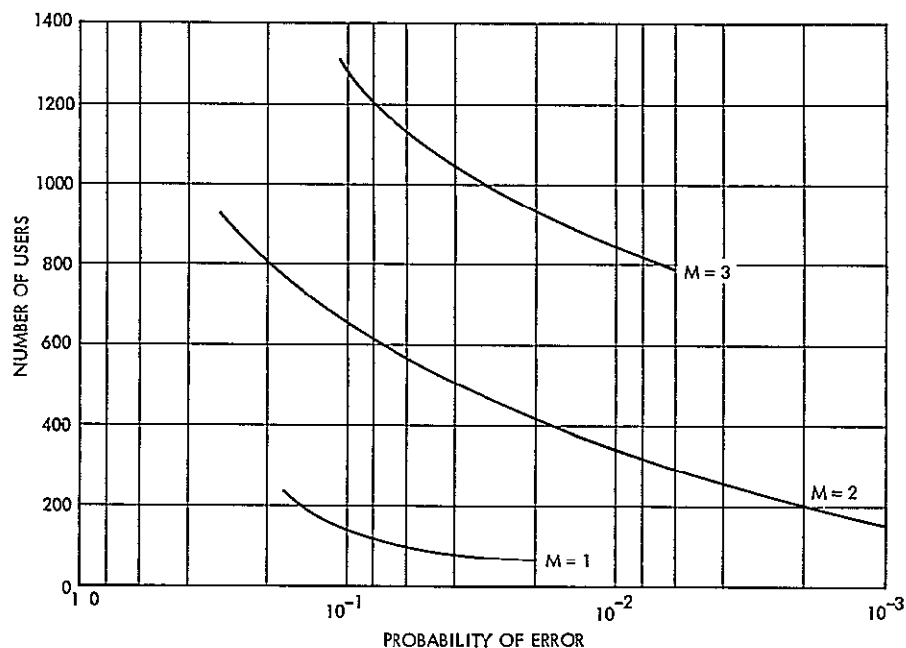


Figure 3-1

PLATFORM CAPACITY VERSUS MESSAGE REPLICATION FACTOR RANDOM TIME AND FREQUENCY MODE

Following the development of these curves, we re-examined the comparative performance of the random T and F mode and the segmented band concept using buried oscillators. Our examination results (Table 3-1) showed that from a gross platform capacity standpoint, the random T and F mode is superior to a segmented random time mode even for (T and F)  $M = 3$ . The  $M = 7$  level for the segmented band concept corresponds to optimal capacity performance, while  $M = 3$ , for the T and F mode has still not exhausted potential improvements. T and F mode capacity performance for  $M$ 's up to 3 is shown in Figure 3-2.

Table 3-1 Comparison of Random Emission DCS Modes

True Random Emission (T and F)		Four Frequency Domain Subgroups	
M	Capacity	M	Capacity
1	90	1	88
2	530	2	260
3	1090	3	480
M = message replication		4	660
		5	800
		7	880

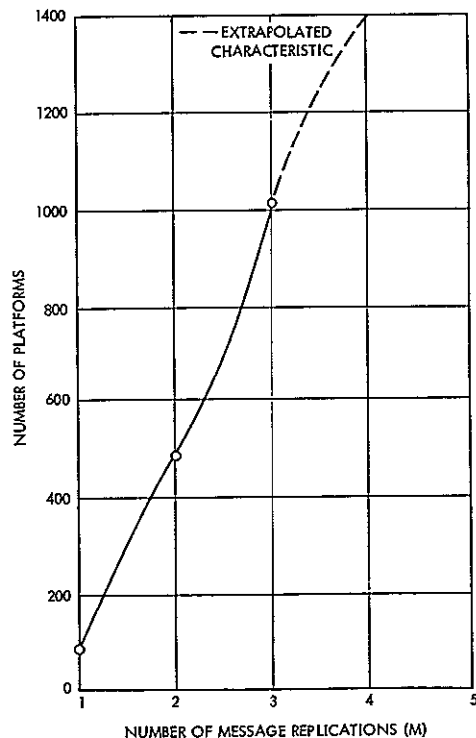


Figure 3-2

T AND F MODE SYSTEM CAPACITY VERSUS REPLICATION FACTOR for 95% probability of one good message from each DCP in 'M' trials (actual Monte Carlo simulation results)

The reserve system capacity at  $M = 3$  plus the fact that all of the 1000 platforms will not be visible at any one time provides an additional degree of assurance that the proposed system will meet the required performance specifications

The further analyses presented, and the actual hardware design proposed by TRW, are all based on a value of  $M = 4$ , ensuring that the system will comfortably meet both the capacity and other performance criteria

## 4 SIGNAL CHARACTERISTICS

### 4.1 STATISTICS FOR SIMULTANEOUS SIGNALS

Since the spacecraft receiver and ground data handling system must be compatible with the received signals, we are interested in the number of messages expected within the baseband. Because of the random mode of operation, the number of simultaneous messages can only be described in statistical terms, as a probability for experiencing one message, two messages, and so forth.

For the purpose of calculation we define simultaneous signals as any period of time during which some portion of a transmitted message overlaps any portion of any other message. This definition encompasses all degrees of overlap from less than 1 message-bit to complete overlap. The limiting condition of overlap clearly occurs when the respective start and finish bits of two messages just coincide. This fact leads to the definition of a message starting time aperture of duration equal to the standard message length.

The system parameters assumed for this analysis are those previously presented.

Number of messages	1000
Message length	110 bits
Data rate	2048 bps
Visibility time	8 minutes
Replication factor	4

These data indicate a message duration of  $\frac{110}{2048}$  second and a time aperture of 0.054 second. Each message can appear anywhere within the sub-interval of 2 minutes. The probability of exactly  $k$  messages will now be computed for a limited set of values for  $k$ .

$k = 1$  The probability of only one message occurring is given by the combined probabilities that (a) one message occurs within the slot time, and (b) all 999 remaining messages fall outside the slot time.

These probabilities are

$$(a) \quad C \binom{1000}{1} \frac{0.054}{120} = 10^3 \times 4.5 \times 10^{-4} = 0.45$$

$$(b) \quad [1 - (4.5 \times 10^{-4})] (1000-1) = 0.636$$

Thus the probability of only one message occurring is 0.286

k = 2 The probability of two messages occurring simultaneously is given by the product of (a) probability that a particular first message falls in the slot, (b) the probability that a particular second message falls within the slot, (c) the number of ways in which those two messages can be derived from the total 1000 available, and (d) the probability that all the remaining 988 messages fall outside the slot

These factors are

$$(a) = (4.5 \times 10^{-4})$$

$$(b) = (4.5 \times 10^{-4})$$

$$(c) = C \binom{1000}{2} \text{ or } \frac{1000 \times 999}{2} \approx \frac{10^6}{2}$$

$$(d) = [1 - (4.5 \times 10^{-4})] 998 \approx [1 - (4.5 \times 10^{-4})] 999 = 0.636$$

Thus the two-message probability  $P_{(2)}$  is

$$\begin{aligned} P_{(2)} &= (4.5 \times 10^{-4}) (4.5 \times 10^{-4}) \times 0.5 \times 10^6 \times 0.636 \\ &= 20.25 \times 10^{-8} \times 0.5 \times 10^6 \times 0.636 \end{aligned}$$

$$\text{i.e. } P_{(2)} = 0.064$$

k = 3 The probability  $P_{(3)}$  of three messages occurring by a similar reasoning involves

$$(a) = (4.5 \times 10^{-4})$$

$$(b) = (4.5 \times 10^{-4})$$

$$(c) = (4.5 \times 10^{-4})$$

$$(d) = C \binom{1000}{3} = \frac{(1000)^3}{6}$$

$$(e) = [1 - (4.5 \times 10^{-4})] 997 \approx 0.636$$



Thus the probability  $P_{(3)}$  is

$$\begin{aligned} P_{(3)} &= (4.5 \times 10^{-4})^3 \times \frac{(1000)^3}{6} \times 0.636 \\ &= 91 \times 10^{-12} \times 10^9 \times 1/6 \times 0.636 \end{aligned}$$

i.e.  $P_{(3)} = 9.54 \times 10^{-3}$

k = 4 The probability  $P_{(4)}$  of four simultaneous messages is given by

$$\begin{aligned} P_{(4)} &= (4.5 \times 10^{-4})^4 \times \frac{(1000)^4}{24} \times 0.636 \\ &= 410 \times 10^{-16} \times 10^{12} \times 1/24 \times 0.636 \end{aligned}$$

i.e.  $P_{(4)} = 1.06 \times 10^{-3}$

k = 5 The probability  $P_{(5)}$  of five simultaneous messages is given by

$$\begin{aligned} P_{(5)} &= (4.5 \times 10^{-4})^5 \times (1000)^5 \times 1/120 \times 0.636 \\ &= 1.845 \times 10^3 \times 10^{-20} \times 10^{15} \times 1/12 \times 0.636 \end{aligned}$$

i.e.  $P_{(5)} = 9.49 \times 10^{-5}$

It is apparent that the probability of more than five messages occurring simultaneously is very small and can be neglected. Since the sum of the probabilities for all eventualities must equal unity, it follows that the probability  $P_{(0)}$  of no signal being present is closely approximated by

$$P_0 = 1 - (P_{(1)} + P_{(2)} + P_{(3)} + P_{(4)} + P_{(5)})$$

$$P_0 = (1 - 0.36090) = 0.6391$$

These statistics are depicted in Figure 4-1 and summarized below

Number of Simultaneous Messages	Expected Probability of Occurrence (% of Time)
None	63.91
1	28.620
2	6.401
3	0.954
4	0.106
5	0.009

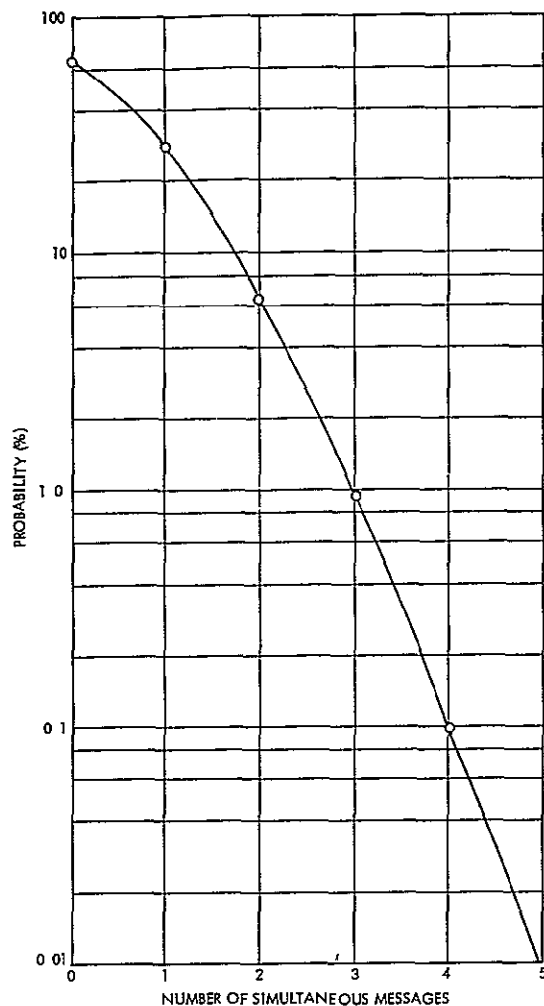


Figure 4-1

ANTICIPATED PROBABILITY FOR OCCURRENCE OF SIMULTANEOUS MESSAGES IN BASEBAND ( $N = 1000$ ,  $M = 4$ )

From the foregoing it is apparent that there will be two or more signals present in the baseband for a significant portion of the time. When more than one signal is present, signal suppression occurs if a limiter is incorporated. Some form of limiting is, however, desirable to ensure constant peak deviation performance of the FM/PM downlink and avoid interference between the DCS signal and other S-band link services. When two or more signals are applied to a limiter, spurious intermodulation and cross modulation components are generated. If such signals have sufficient amplitude and/or fall within the ground data recovery systems phase-lock loop bandwidth, degradation of the lock-up statistics and/or bit error rate may result.

Ideally we would like to tailor the processing gain of each signal to equalize the amplitude and then combine the signals to drive the S-band subcarrier oscillator

If the baseband signals are randomly distributed in the frequency domain, the probability of a signal appearing in any particular segment of that domain is a function only of the fraction which this segment represents of the whole baseband. This finding allows us to develop statistics for simultaneous messages within a typical segment as a function of the number of segments adopted. These results are shown in Table 4-1

Table 4-1 Probability of Simultaneous Messages as a Function of Number of Contiguous IF Channels with AGC in the DCS Spacecraft Receiver

Number of Simultaneous Messages	Number of Channels				
	1	2	3	4	5
0	0 639	0 82	0 88	0 91	0 93
1	0 286	0 143	0 095	0 071	0 0572
2	0 064	0 032	0 021	0 016	0 0128
3	0 009	0 0045	0 003	0 002	0 0018
4	0 001	0 0005	0 0003	0 0002	0 0002
5	0 0001	-	-	-	-

It is apparent that a useful improvement in message processing can be achieved by the simple expedient of dividing the spacecraft 1st IF amplifier into several segments for parallel operation. By providing each segment amplifier with a separate peak detector and AGC loop, the resulting signals can be amplitude equalized and passed through the downlink with least degradation. But the use of more than five segments provides only a small improvement. This mode of operation has the further advantage that it permits ground control over the separate segments allowing any to be disabled for combating RFI or similar problems. It is simple and relatively inexpensive to implement because of the availability of integrated IF amplifier circuit modules and because of the proposed DCS ratio of broad bandwidth to center frequency.

## 4.2 SIGNAL AMPLITUDE DISTRIBUTION

The level of each DCP signal arriving at the spacecraft receiver is an inverse function of its slant range. In order to understand and analyze the signal interactions that occur within the DCS receiver and S-band downlink, we must establish a model for the number of signals involved and the distribution of power.

In Section 2.4 of Volume 5 we presented the basic link analysis calculation and showed that to meet the overall system performance an SNR of more than 11 dB was needed for the optimum modulation mode (PSK) under limit slant range conditions.

The slant range only changes by a factor of  $\approx 3$  between the nadir and the design limit set by the visibility angle (assumed value 7.5 deg). Thus the variation in signal level due to range differences for signals which could be usefully processed is only 10 dB. It is clear that other signals from beyond the limit range will be present within the 100 kHz receiver baseband. Fortunately, there is a relatively rapid reduction for signals near or beyond the horizon. Moreover, the proportion of foliage present in the signal path increases substantially for very low angles close to horizon tangent (see Figure 4-2). We therefore believe that it is reasonable to consider only those signals within the visibility coverage region. The signal level expected as a function of slant range is presented in Figure 4-3.

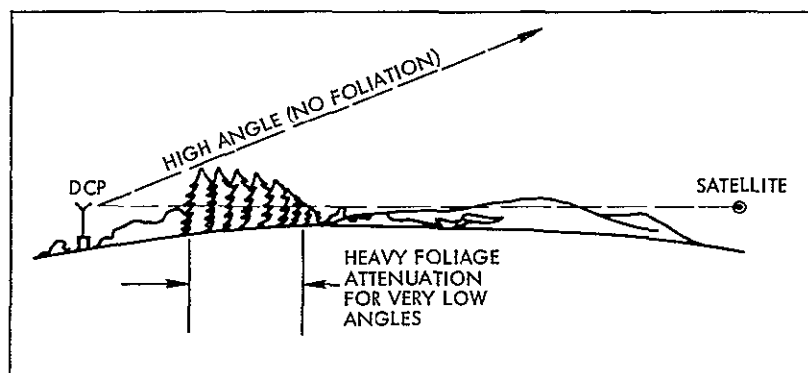


Figure 4-2

SIGNAL ATTENUATION BY FOLIAGE AT LOW ANGLES

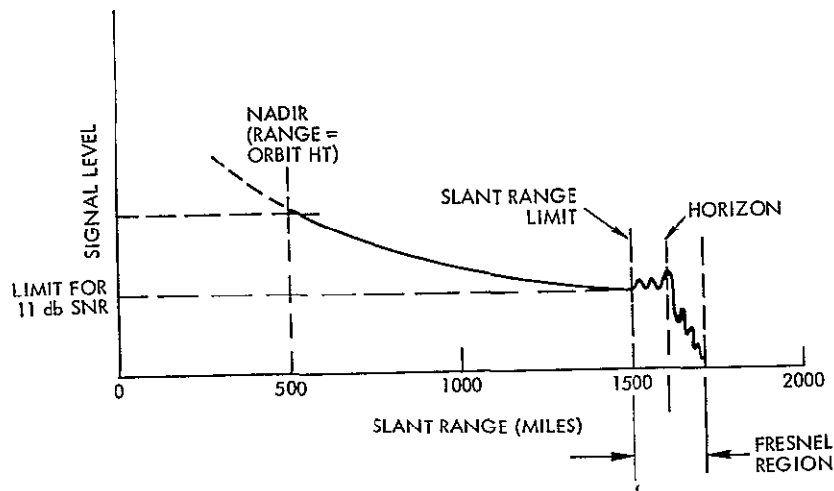


Figure 4-3

### SIGNAL LEVEL AS A FUNCTION OF SLANT RANGE

A simple geometric analysis using concentric annuli shows that the ground area coverage increases as the square of the ground offset from the nadir. It is therefore evident that for uniformly distributed DCP's, the number in-view increases as a square law function of range.

Combining these facts with the power budget from Table 2-3 (p 2-17 in Volume 5), we developed statistical data to describe the received DCP signal power level as a function of the probability signal exhibiting that power level. This was done in the following manner:

#### 4.2.1 Derivation of Geometric Model

The signal power level at the spacecraft is highly dependent on the relative location of a DCP with respect to the spacecraft. Two basic factors must be considered:

- The signal transmission distance between receiving stations and individual DCP
- The look angle of transmitting and receiving antennas, and the effective gain along the signal propagation path

The slant range (relative distance) between a DCP and the spacecraft, a function of elevation angle and the spacecraft altitude, can be determined from

$$D(\phi) = \frac{R + h}{\cos \phi} \cos \left[ \phi + \sin^{-1} \left( \frac{R}{R + h} \cos \phi \right) \right] \quad (4-1)$$

where

$R$  = earth radius

$h$  = spacecraft altitude

$\phi$  = the limit elevation angle for communication ( $= 7.5^\circ$ )

The geometric model for this situation is shown in Figure 4-4

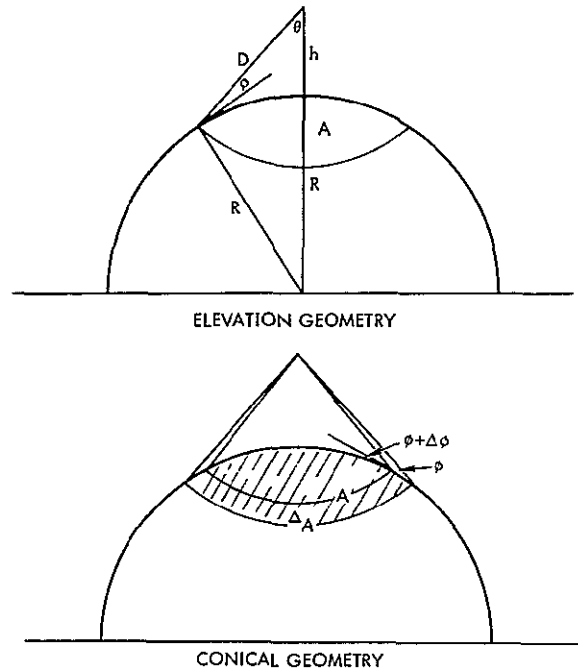


Figure 4-4

#### SATELLITE CONE COVERAGE AT EARTH SURFACE

For any particular fixed value of spacecraft altitude, signals can be successfully received from DCP units located anywhere inside area A. Area A is bounded by the requirement for limit angle  $\phi = 7.5$  degrees.

The magnitude of the area A can be found from

$$A(\phi) = 2\pi R^2 \left[ 1 - \sin \left( \sin^{-1} \frac{R}{R+h} \cos \phi + \phi \right) \right] \quad (4-2)$$

For any increment in  $\phi$ , there is a corresponding decrease in A. Therefore, we have

$$\begin{aligned} \Delta A(\phi, \Delta\phi) = A(\phi) - A(\phi + \Delta\phi) = 2\pi R^2 \left\{ \sin \left[ \sin^{-1} \left( \frac{R}{R+h} \cos \phi \right) + \phi \right] \right. \\ \left. - \sin \left[ \sin^{-1} \left( \frac{R}{R+h} \cos \phi + \Delta\phi \right) + (\phi + \Delta\phi) \right] \right\} \end{aligned} \quad (4-3)$$

Assuming that the data collection platforms are uniformly distributed, then the probability that DCP signals transmitted from inside  $\Delta A$  is given by the ratio of the fractional area increment  $\Delta A$  to the total visibility area  $A$ , i.e.,

$$P = \frac{\Delta A}{A} \quad (4-4)$$

The mean distance between the spacecraft and a DCP located inside  $\Delta A$  is then given by

$$\begin{aligned} D(\Delta A) &= \frac{D(\phi) + D(\phi + \Delta\phi)}{2} \\ &\approx D\left(\phi + \frac{\Delta\phi}{2}\right) \end{aligned} \quad (4-5)$$

#### 4.2.2 Received Power Level

The corresponding power level  $S$  received at the spacecraft, is therefore

$$S = 35 - L_s + G \quad (\text{db}) \quad (4-6)$$

where

transmitter power less transmitting and receiving circuit losses  
 $= 35 \text{ db}$

$L_s$  = space loss  $= 89.88 + 20 \log D \text{ (db)}$

$G$  = platform antenna gain + spacecraft antenna gain minus the polarization loss

Since the full coverage of antenna radiation pattern has not been measured, we assume that the combination of transmitting-receiving antenna gain minus the polarization loss varies linearly with the look angle between the on-axis and off-axis values, i.e.,  $G$  varies linearly between  $-1.5 \text{ db}$  on-axis to  $+0.9 \text{ db}$  off-axis

A computer program was developed to calculate the values, their space loss, and the probability of occurrence as a function  $\phi$ . The results are presented in Table 4-2. The cumulative probability of the received signal level, including antenna gain, is plotted in Figure 4-5

Table 4-2 Space Loss and Associated Probability vs Elevation Angle for DCP Signals Having Estimated SNR Values Above 11.1 db

Elevation Angle $\phi$	Percent Occurrence	CUM PROB	Distance (n mi) $\phi + 2.50$	Space Loss (db)
7.50	0.2860	2861	1406.9	152.8
12.50	0.2003	4864	1219.7	151.6
17.50	0.1407	6272	1069.72	150.5
22.50	9.988E-02	7271	948.8	149.4
27.50	7.191E-02	7990	852.4	148.5
32.50	5.260E-02	8516	774.9	147.7
37.50	3.906E-02	8907	712.5	146.9
42.50	2.939E-02	9201	661.9	146.3
47.50	2.233E-02	9424	621.0	145.7
52.50	1.707E-02	9595	587.8	145.3
57.50	1.304E-02	9725	561.1	144.9
62.50	9.877E-03	9824	539.9	144.5
67.50	7.315E-03	9897	523.4	144.3
72.50	5.170E-03	9949	511.1	144.0
77.50	3.305E-03	9982	502.6	143.9
82.50	1.611E-03	9998	497.6	143.8
87.50	4.685E-07	9998	496.0	143.8

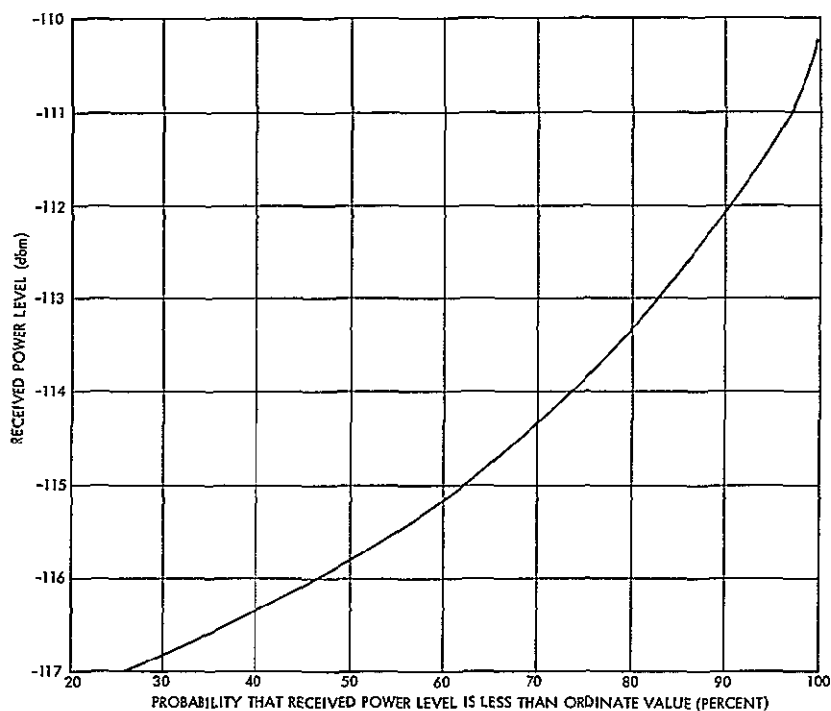


Figure 4-5  
CUMULATIVE PROBABILITY CHARACTERISTICS FOR SIGNAL LEVEL  
RECEIVED AT SPACECRAFT



### 4.2 3 Power Difference Statistics

The probability of any particular signal having a specified power level (for levels within the range of interest) can be obtained by using the space loss values of Table 4-2. From this we derived the signal power vs probability of occurrence data shown in Table 4-3, and Figure 4-5

When multiple signals are simultaneously present in the DCS receiver baseband, we can define their probable difference in power level in statistical terms by a further manipulation of the foregoing analyses. The most serious limiter conditions occur when one signal is much larger than some other signal. For this reason we are interested in establishing statistics which describe the probability of a given power difference occurring

In Section 4.1 we showed that more than four simultaneous signals are statistically unlikely (0.1 percent) for a replication factor of  $M = 4$ , and obviously substantially less for  $M = 3$ . Consequently we have evaluated the signal differences for the specific cases of two, three, and four simultaneous signals

The probability equations related to the worst condition of any two signals (of the total number being considered) having the specified power difference is presented in Table 4-4

Table 4-3 Probability of Occurrence of Various Signal Levels

<u>Signal Level</u>	<u>Probability</u>
-117 db	0.28600
-116	0.20037
-115	0.14081
-114	0.09989
-113	0.12453
-112	0.06848
-111	0.07495
-110	0.00497

Table 4-4 Probability Equations for Specified Power  
Signal Differences (Four Signals Present)

Maximum Power Level Difference	Probability
0 db	$\sum_{n=1}^8 P_n^4$
1 db	$\sum_{n=1}^7 \left[ (P_n + P_{n+1})^4 - (P_n^4 + P_{n+1}^4) \right]$
2 db	$\sum_{n=1}^6 \left[ (P_n + P_{n+2})^4 - (P_n^4 + P_{n+2}^4) + 12 P_n P_{n+1} P_{n+2} \left( \sum_{i=n}^{n+2} P_i \right) \right]$
3 db	$\sum_{n=1}^5 \left[ (P_n + P_{n+3})^4 - (P_n^4 + P_{n+3}^4) + 12 P_n P_{n+3} \left( \sum_{i=n}^{n+3} P_i \right) \left( \sum_{j=n+1}^{n+2} P_j \right) \right]$
4 db	$\sum_{n=1}^4 \left[ (P_n + P_{n+4})^4 - (P_n^4 + P_{n+4}^4) + 12 P_n P_{n+4} \left( \sum_{i=n}^{n+4} P_i \right) \left( \sum_{j=n+1}^{n+3} P_j \right) \right]$
5 db	$\sum_{n=1}^3 \left[ (P_n + P_{n+5})^4 - (P_n^4 + P_{n+5}^4) + 12 P_n P_{n+5} \left( \sum_{i=n}^{n+5} P_i \right) \left( \sum_{j=n+1}^{n+4} P_j \right) \right]$
6 db	$\sum_{n=1}^2 \left[ (P_n + P_{n+6})^4 - (P_n^4 + P_{n+6}^4) + 12 P_n P_{n+6} \left( \sum_{i=n}^{n+6} P_i \right) \left( \sum_{j=n+1}^{n+5} P_j \right) \right]$
7 db	$(P_1 + P_8)^4 - (P_1^4 + P_8^4) + 12 P_1 P_8 \left[ \sum_{n=1}^8 P_n \right] \left[ \sum_{m=2}^7 P_m \right]$

A similar procedure was used to derive equations appropriate to the cases of two and three simultaneous signals. The results of all these calculations were combined and presented in Table 4-5 and Figure 4-6

Table 4-5 Signal Difference Statistics for Simultaneous Messages

Signal Power Difference (db)	Two-Signal Case		Three-Signal Case		Four-Signal Case	
	Probability of Event $P(\Delta)$	Cumulative Probability of Event Less Than Ordinate	Probability of Event $P(\Delta)$	Cumulative Probability of Event Less Than Ordinate	Probability of Event $P(\Delta)$	Cumulative Probability of Event Less Than Ordinate
7	0028	9972	0073	9927	0126	9874
6	0449	9523	1084	8843	1771	8103
5	0706	8817	1406	7437	1924	6179
4	1208	7609	2056	5381	2449	3730
3	1425	6184	1843	3538	1708	2022
2	1887	4297	1776	1762	1273	0749
1	2521	1776	1383	0379	0658	0091
0	1776	$\approx 0$	0379	$\approx 0$	0091	$\approx 0$

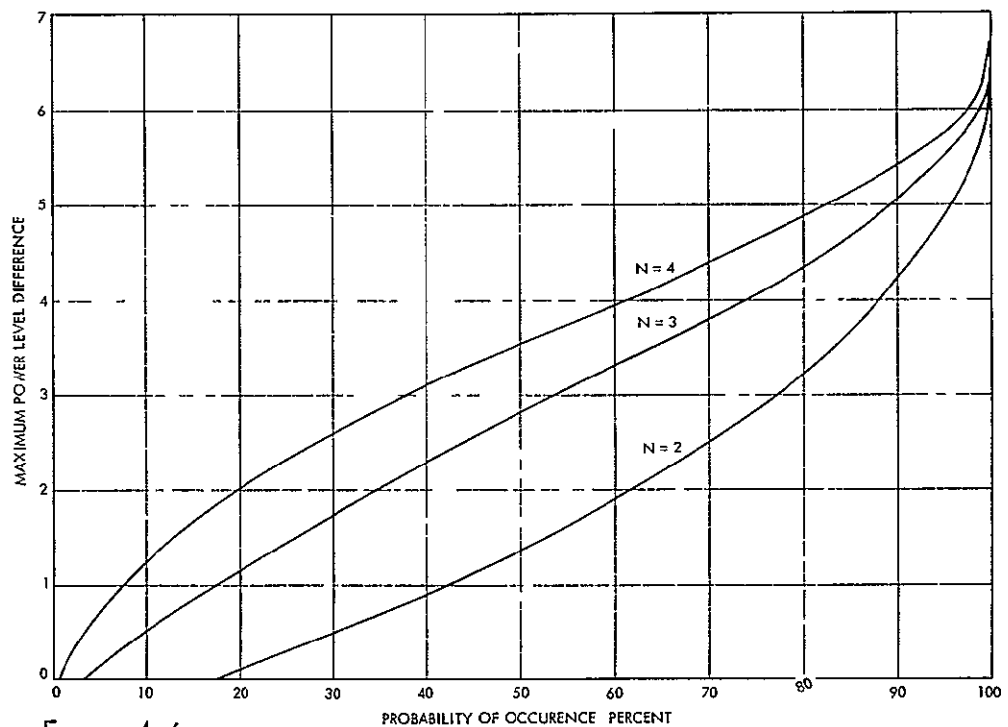


Figure 4-6

MAXIMUM SIGNAL DIFFERENCE VS PROBABILITY OF OCCURRENCE FOR WORST SIGNAL PAIR

### 4.3 DCS DATA AND RANGING CODE MUTUAL INTERFERENCE ANALYSIS

The following analysis is addressed to the effects of the DCS data upon the ranging code and vice versa. The assumed division of power between the downlink services is that given in the power budgets of Table 9-11 in Volume 4 of the final report

First we consider the interference caused by the DCS data on the ranging code. Our main interest is with the power that the DCS data introduces within 120 kHz of the USB carrier. To this end we assume that a single tone FM-modulates the DCS 1.024 MHz subcarrier oscillator since this leads to the worst case. Let the S-band downlink signal with just the DCS subcarrier phase modulating the carrier be described by

$$V(t) = E \sin \left( \omega_c t + \beta \cos \left( \omega_1 t + 2\pi\Delta F \int^t x(\tau) d\tau \right) \right) \quad (4-7)$$

where

$E$  = amplitude scale factor

$\frac{\omega_c}{2\pi}$  = downlink carrier frequency

$\frac{\omega_1}{2\pi}$  = DCS data subcarrier frequency

$\beta$  = DCS data subcarrier modulation index

$\Delta F$  = DCS FM frequency deviation

$x(\tau)$  = DCS data

The above waveform is passed to a phase detector that essentially multiplies it by  $\sqrt{2} \cos(\omega_c t)$  to yield

$$z(t) = \frac{E}{\sqrt{2}} \sin \left( \beta \cos \left( \omega_1 t + 2\pi\Delta F \int^t x(\tau) d\tau \right) \right) \quad (4-8)$$

Using a well known trigonometric expansion<sup>3</sup> in (4-8) yields

$$Z(t) = \frac{2E}{\sqrt{2}} \sum_{L=1}^{\infty} (-1)^{L+1} J_{2L-1}(\beta) \cos \left[ (2L-1) \left( \omega_1 t + 2\pi \Delta F \int x(\tau) d\tau \right) \right] \quad (4-9)$$

where  $J_k(x)$  = kth order Bessel function of the first kind. Further manipulation of (4-9) is impossible without specifying the form of DCS modulation. We assume that one DCP signal is received and that it can be represented as a tone. This assumption is valid since we are interested in the total interference power caused by the tone rather than spectral shape. Hence,

$$X(t) = \cos \omega_m t \quad (4-10)$$

where

$$\frac{\omega_m}{2\pi} = \text{received DCP carrier frequency as measured at the spacecraft receiver output}$$

Using the same trigonometric series for

$$\cos \left[ (2L-1) \left( \omega_1 t + \frac{\Delta F}{f_m} \sin \omega_m t \right) \right]$$

used in (4-8) reduces (4-9) to

$$\begin{aligned} Z(t) = & \frac{2E}{\sqrt{2}} \sum_{L=1}^{\infty} (-1)^{L+1} J_{2L-1}(\beta) \left[ J_0(2L-1) \left( \frac{\Delta F}{f_m} \right) \cos [(2L-1) (\omega_1 t)] \right. \\ & + \sum_{k=1}^{\infty} (-1)^k J_k \left[ (2L-1) \left( \frac{\Delta F}{f_m} \right) \right] \cos \left[ (2L-1) \omega_1 t - k \omega_m t \right] \\ & \left. + \cos \left[ (2L-1) \omega_1 t + k \omega_m t \right] \right] \quad (4-11) \end{aligned}$$

---

<sup>3</sup>M. Schwartz, "Information Transmission Modulation and Noise," McGraw-Hill, New York, 1959.

The power in the interference tone located at  $(2L-1)\omega_1 \pm k\omega_m$  is therefore

$$P_{Lk} = E^2 J_{2L-1}^2(\beta) J_k^2 \left( (2L-1) \left( \frac{\Delta F}{f_m} \right) \right) \quad (4-12)$$

For purposes of evaluation  $P_{Lk}$  is normalized by the total power in the ranging code. The total power in the ranging code is<sup>\*</sup>

$$P_r = \frac{E^2}{2} M_r \quad (4-13)$$

where  $M_r$  = code ranging modulation loss

The final result is obtained by dividing (4-12) by (4-13)

$$P_1 = \frac{P_{Lk}}{P_r} = 2 \frac{J_{2L-1}^2(\beta) J_k^2 \left[ (2L-1) \left( \frac{\Delta F}{f_m} \right) \right]}{M_r} \quad (4-14)$$

Our goal is to choose  $L$ ,  $k$ , and  $f_m$  to yield the largest interference below 120 kHz. Thus we require that

$$(2L-1)\omega_1 - k\omega_m \leq 120 \text{ kHz} \quad (4-15)$$

Using (4-15) in conjunction with (4-14) yields as a worst case

$$L = 1, k = 7, f_m = \Delta F \text{ for } f_1 = 1.024 \text{ MHz}$$

The values were obtained by satisfying (4-15) with the smallest values of  $L$  and  $k$  and largest value of  $\omega_m$ , since, for the range of arguments we are considering, the Bessel function magnitudes in (4-14) decrease rapidly as their order increases.

Using the values given above along with  $\beta = 1.04$  radians,  $M_r = -25$  dB, and  $\Delta F = 136$  kHz (derived in Addendum No 1 to Volume 5) yields

$$P_1 \cong -95 \text{ dB} \quad (4-16)$$

From this it is clear that the effects of the DCS data upon the ranging code can be neglected

---

\*TRW Systems, "Final Design Report Space-Ground Link Subsystem," Volume III, Document 4300-7500-022, February 1967.

We next consider the effect of the ranging code on the DCS data. Since the spectrum of the ranging code is extremely complex, we approximate it by

$$S_c(f) = P_r t_o \frac{\sin^2 \pi f t_o}{(\pi f t_o)^2} \quad (4-17)$$

where

$P_r$  = power in the ranging signal

$t_o$  = bit rate of the digits comprising the code

For this analysis we assume\*  $t_o = 1 \mu\text{sec}$ . Then the total power falling within the bandwidth of the DCS subcarrier discriminator normalized by the total power in the DCS subcarrier is

$$P = \frac{2P_r}{P_{\text{DCS}}} \int_{f_1 - \frac{B_D}{2}}^{f_1 + \frac{B_D}{2}} t_o \frac{\sin^2 \pi f t_o}{(\pi f t_o)^2} df \quad (4-18)$$

where

$P_{\text{DCS}}$  = total power allotted to the DCS subcarrier

$f_1$  = DCS subcarrier frequency (1 024 MHz)

$B_D$  = DCS subcarrier discriminator bandwidth (600 kHz)

Substituting the system parameters in the integral of (4-18) yields

$$P = \frac{2P_r}{P_{\text{DCS}}} \left( \frac{1}{\pi} \int_{.724\pi}^{1.32\pi} \frac{\sin^2 z}{z^2} dz \right) \quad (4-19)$$

Using the values of  $P_r$  and  $P_{\text{DCS}}$  as given in Table 9-12 of Volume 4 yields

$$P = -33.7 \text{ dB}$$

Hence, it can be concluded that the ranging code has a negligible effect upon the DCS signal

---

\* TRW Systems, "Preliminary Analysis of the LM and CSM Antenna Tracking Systems," Document 05952-H320-R0-00, 24 October 1967

## 5 DCS COMMUNICATION LINK DESCRIPTION AND ANALYSIS

### 5.1 LINK DESCRIPTION

The purpose of the DCS communication link is to collect information from a large number of platforms and relay this data to the three ground stations for processing and recovery of sensor information. The proposed link configuration (Figure 5-1), consists of three main subsystems the DCP transmitters which transmit data collected by the platform sensors to the spacecraft, the spacecraft receiver that downconverts and amplifies the received data, and the S-band downlink which serves as the final transmission link from satellite to the ground

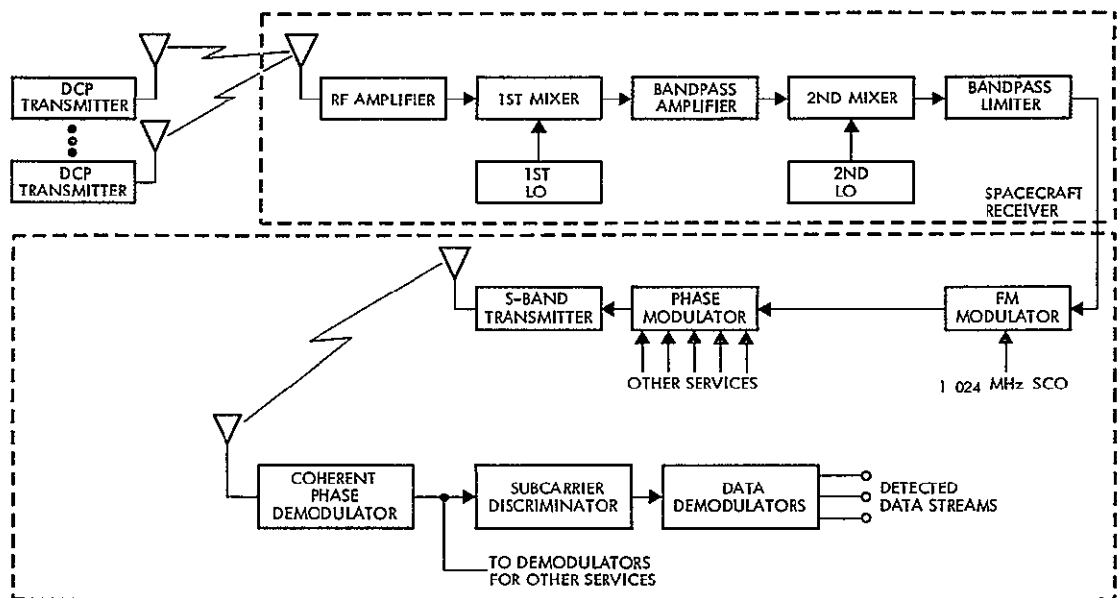


Figure 5-1

DCS COMMUNICATION LINK BLOCK DIAGRAM

The information collected by the various platforms is transmitted to the spacecraft using PSK modulation. The system data rate is about 2 kbits/sec and the message consists of 110 bits. Because the environment of the various platforms differ as well as their distance to the spacecraft and their basic carrier frequencies, the frequency of the signals received by the spacecraft are spread out over a 100 kHz bandwidth



centered about the nominal DCP transmitter frequency of 401.9 MHz. In a given period, a random number of the DCP signals will fall within the spacecraft's field of view. This type of operation, referred to as random emission multiple access, was discussed in Section 3. For the discussion of link performance, we can assume that the input to the spacecraft DCP antenna consists of a random number of PSK signals, each having a different frequency (and periodically two or more will coincide).

The spacecraft portion of the DCS link consists of a UHF antenna, and its associated hardware, a dual conversion receiver, and one service of the S-band downlink. The data processed by the receiver FM-modulates the 1.024 MHz subcarrier oscillator of the spacecraft baseband assembly. As a means of controlling the peak frequency deviation of this oscillator, the receiver data is bandpass limited prior to being passed to the FM modulator. In the design proposed by TRW, the nominal limiter output value is 1 volt rms. The S-band downlink consists of an S-band transmitter, a phase modulator, and various subcarrier oscillators. The broadband signal from the DCS, and other users signals to be transmitted to the ground, are first FM-modulated onto their separate subcarriers, and the resultant outputs are combined and used to phase modulate the S-band transmitter. The phase deviation index chosen for the DCS data is 1.04 radians. This value, in conjunction with the indices of the other five services which modulate a common transmitter, was chosen to provide an optimum power division between the five services and the S-band carrier component. The particular division of power is a direct function of the needs of the various services. The overall system constraint is that enough power be assigned to the DCS subcarrier to ensure that the DCS demodulator on the ground operates above threshold.

On the ground, the downlink signal is first coherently demodulated and the resultant passed to subcarrier detectors. In this operation the downlink doppler is tracked out. It should be noted that this is not the case for the doppler components on the uplinks. The DCS signal is recovered from its subcarrier by a discriminator having a center frequency of 1.024 MHz and a bandwidth of 600 kHz. The individual DCP signals are recovered from the composite baseband at the discriminator.

output by a combination of filters and multiple phase-lock loops in the GDHS

## 5.2 OVERALL LINK ANALYSIS

This section is devoted to a general signal processing analysis of the DCS communication link. The results of this discussion are used in Sections 5.3 and 5.4 on the effects of the downlink on DCS overall performance, and the response of the limiter to a multi-carrier input.

The system depicted in Figure 5-1 is modeled in Figure 5-2

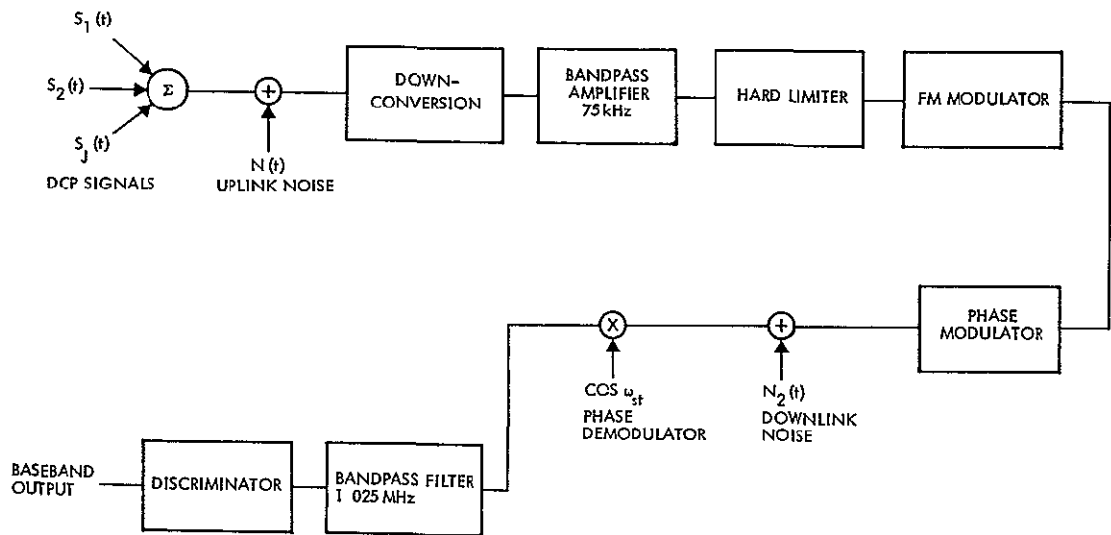


Figure 5-2  
OVERALL DCS COMMUNICATIONS LINK MODEL

A DCP signal is described by

$$s_j(t) = A_j \sin [\omega_j t + \pi/2 U_j(t) + \theta] \quad (5-1)$$

where

$A_j$  = amplitude scale factor

$\theta$  = unknown carrier phase

$\omega_j/2\pi$  = received carrier frequency for the  $j^{\text{th}}$  platform

$U_j(t)$  = a rectangular pulse train consisting of pulses of duration  $T$  (the bit time) and height +1 or -1 representing the data stream

A random number of these signals and noise are added together to form the input to the system. After ideal frequency translation, the input to the limiter is

$$I(t) = \sum_{j=1}^{j=k} s_j(t) + N_1(t) \quad (5-2)$$

where  $k$  is the number of DCP signals received by the spacecraft and  $N_1(t)$  the bandlimited Gaussian noise having a spectral density of  $\phi_1/2$

After limiting, the resultant signal FM-modulates a 1 024 MHz subcarrier oscillator. Denoting the limiter output by  $V(t)$ , the FM-modulated subcarrier takes the form of

$$\cos \left[ \left( \omega_{sco} t + 2\pi\Delta F \int_0^t V(\tau) d\tau \right) \right] \quad (5-3)$$

where

$\omega_{sco}/2\pi$  = DCS subcarrier oscillator frequency

$\Delta F$  = peak frequency deviation

The output of this SCO is phase modulated onto an S-band transmitter carrier and transmitted to the ground. Thus, one can describe the overall S-band downlink signal by combining the previous expressions

$$Z(t) = B \sin \left[ \omega_s t + D \cos \left( \omega_{sco} t + 2\pi\Delta F \int_0^t V(\tau) d\tau \right) + H(t) + \psi \right] \quad (5-4)$$

where

$B$  = transmitted carrier amplitude

$\omega_s/2\pi$  = carrier frequency

$D$  = peak phase deviation for the DCS subcarrier

$H(t)$  = other downlink services

$\psi$  = unknown phase angle

Downlink noise can be described as a Gaussian process that has flat spectral density across the RF band. The above noise is added to the  $Z(t)$  signal, and the resultant coherently demodulated. Thus the input to the DCS subcarrier discriminator is

$$D(t) = BL \cos \left( \omega_{sco} t + 2\pi\Delta F \int_0^t V(\tau) d\tau \right) + N_3(t) \quad (5-5)$$

where

$$\frac{B^2 L^2}{2} = \text{effective subcarrier power as measured in the filter preceding the discriminator}$$

The factor  $L^2$  denotes the modulation loss relative to the carrier that arises due to phase modulation of the carrier by the six services.  $N_3(t)$  is additive Gaussian noise having flat spectral density equal to  $\phi_3/2$

$$N_3(t) = \sqrt{2} [x(t) \cos \omega_{sco} t - y(t) \sin \omega_{sco} t] \quad (5-6)$$

where  $x(t)$  and  $y(t)$  are Gaussian processes whose spectral densities are identical to  $N_3(t)$ . Assuming the discriminator is operating above threshold, its output is\*\*

$$A(t) = 2\pi\Delta F(t) + \frac{1}{BL} \frac{d}{dt} [\sqrt{2}x(t)] \quad (5-7)$$

The desired DCP signals are contained in the first term of the above equation. The last term of the equation indicates the noise added to the system by the downlink.

### 5.3 DOWNLINK ANALYSIS

The downlink when viewed as a separate entity is another source of additive noise, and thus tends to degrade overall system performance. We first consider the case when only one DCP signal is received. This following discussion indicates the way the overall DCS performance varies as a function of the efficiency of the downlink, and further indicates

---

\*A. J. Viterbi, Principles of Coherent Communication, McGraw-Hill, New York, 1966.

\*\*M. Schwartz, Information Transmission, Modulation, and Noise, McGraw-Hill, New York, 1959.

the system parameters involved. By considering the most pessimistic case with regard to the downlink, a lower bound on performance is obtained. Thus, in the ensuing discussion we choose the uplink signal frequency so that it falls where the downlink noise spectral density has a maximum value. Since the spectrum of this noise is parabolic,\* the region of maximum noise density occurs at the high end of the band. We then assess the degradation introduced by the downlink for a multicarrier input. It is shown that proper choice of frequency deviation ensures that the degradation added by the downlink is negligible. The selected value of modulation index is also shown to be consistent with the analysis for a single input tone.

For the single DCS signal, our analysis is concerned with total output power ratios so that the particular form of phase modulation need not be considered. Hence, for purposes of analysis, we describe the DCP input signal by an unmodulated tone. For such a condition, the limiter output can be expressed in the following form\*\*

$$V(t) = \sqrt{2}\alpha \sin(\omega_j t) + N_\ell(t) \quad (5-8)$$

where

$\alpha$  = limiter suppression factor

$\omega_j$  = signal carrier frequency as referenced to the spacecraft receiver IF

$N_\ell(t)$  = is the noise appearing at the limiter output

The SNR at the bandpass limiter output,  $SNR_L$ , is related to the input SNR,  $SNR_1$ , by the relationship

$$SNR_L = \frac{\alpha^2}{1 - \alpha^2} SNR_1 \quad (5-9)$$

From (5-7), we have as the discriminator output

---

\* M. Schwartz, op cit

\*\* J. C. Springett "Signal-to-Noise and Signal-to-Noise Spectral Density Ratios at the Output of a Filter-Limiter Combination" Jet Propulsion Laboratory, Tech Summary 3341-65-2, July 15, 1965

$$Q(t) = 2\pi\Delta F [\sqrt{2} \alpha \sin \omega_t + N_\ell(t)] + \frac{1}{BL} \frac{d}{dt} (\sqrt{2}x(t)) \quad (5-10)$$

We then define the overall system SNR as

$$SNR = \frac{[E(Q)]^2}{\sigma_Q^2} \quad (5-11)$$

where  $E$  denotes expected value and  $\sigma_Q^2$  the variance of the discriminator output. The indicated operation yields

$$SNR = \frac{1}{\frac{1}{SNR_L} + \frac{1}{SNR_D}} \quad (5-12)$$

where  $SNR_D$ , the downlink SNR, is given by

$$SNR_D = \frac{\alpha^2 (2\pi\Delta F)^2}{\left(\frac{1}{BL}\right)^2 E\left[\frac{d}{dt} \sqrt{2} x(t)\right]^2} \quad (5-13)$$

Evaluating the denominator of (5-13) yields

$$\begin{aligned} E\left[\frac{d}{dt} \sqrt{2} x(t)\right]^2 &= 2\phi_3 \int_{f_J - \frac{B_m}{2}}^{f_J + \frac{B_m}{2}} (2\pi)^2 f^2 df \\ &= 2\phi_3 (2\pi)^2 \frac{\left[\left(f_J + \frac{B_m}{2}\right)^3 - \left(f_J - \frac{B_m}{2}\right)^3\right]}{3} \end{aligned} \quad (5-14)$$

where  $B_m$  indicates the bandwidth within which the SNR is to be calculated. For our analysis,  $B_m$  is taken as the nominal data bandwidth, 2.4 kHz, and  $f_J$  as 136 kHz since this is the highest frequency a DCP signal could have and still be totally in band (as indicated above, this corresponds to the worst case for the parabolic noise spectrum). For these particular choices  $f_J \gg B_m$  and thus (5-14) reduces to the simplified form

$$E \left( \frac{d}{dt} \sqrt{Z} (t)^2 \right) \approx 2\phi_3 (2\pi)^2 f_j^2 B_m \quad (5-15)$$

Substitution into (5-13) yields

$$SNR_D = \frac{\alpha^2 \Delta F^2 (BL)^2}{2\phi_3 f_j^2 B_m} \quad (5-16)$$

This equation can be put into a more recognizable form by introducing the following quantities

$B_D$  = bandwidth of the filter preceding the discriminator

$\frac{C}{N} = \frac{(B^2/2) L^2}{\phi_3 B_D} =$  effective subcarrier S/N ratio as measured at the discriminator input

$\beta_j = \Delta F/f_j =$  deviation index

Then (5-16) becomes

$$SNR_D \approx \alpha^2 \beta_j^2 C/N \left( \frac{B_D}{B_m} \right) \quad (5-17)$$

We are now in a position to assess link performance numerically. Our previous study indicated that the SNR required to recover the DCP signals with an acceptably low probability of error was 11.1 dB. Thus, we are constrained to choose the frequency deviation  $\Delta f$  so that the uplink does not degrade the input SNR below this value. In Table 5-1, we list the parameters used in our calculations.

Table 5-1 DCS Link Parameters

Parameter	Value
$B_D$	600 Hz
$C/N$	10 dB
$F_j$	136 kHz
$B_m$	2.4 kHz
$F_u$	137.5 kHz
$F_L$	15 kHz

Using these data in conjunction with the several equations derived above allows us to develop the performance curves shown in Figure 5-3 where we have plotted the downlink degradation  $SNR_D$  for  $\beta_j = 0.5$  and  $\beta_j = 1.0$ . Also shown is  $SNR_L$  in 2.4 kHz, the function of  $SNR_1$  over the range indicated by Table 2-3. This curve was obtained by combining (5-9) with curves from "Signal-to-Noise Ratios in Bandpass Limiters," J Appl Phys 24 (June 1953) pp 720-27. The calculations must first be performed in a 125 kHz bandwidth and the resulting value converted to 2.4 kHz. This is done by simply scaling by the bandwidth factor, the error resulting from this simplification is negligible. Finally, the overall SNR given by (5-12) is shown for the two values of  $\beta_j$ . As one can see, the downlink has its greatest effect for large values of SNR. Furthermore, for the two values of modulation index chosen, the minimum overall SNR requirement is satisfied.

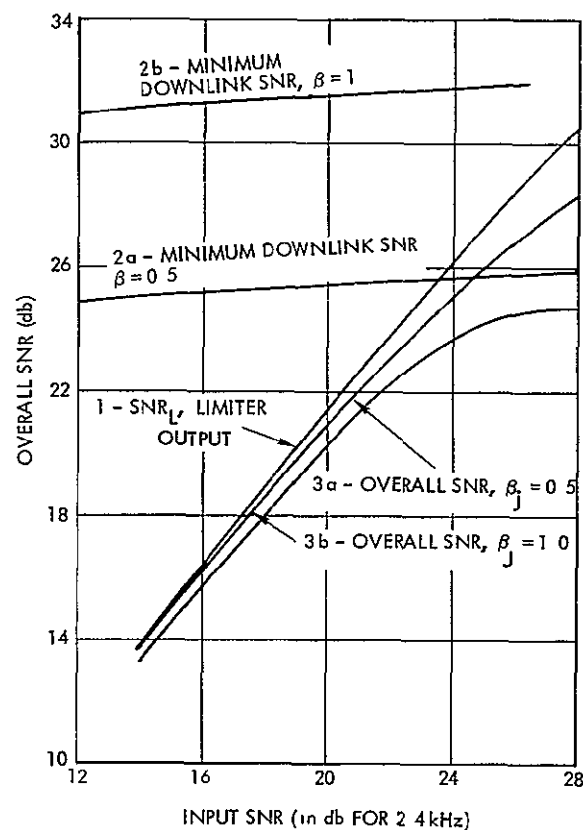


Figure 5-3

DCS COMMUNICATIONS LINK PERFORMANCE as measured by overall signal-to-noise ratio for two values of subcarrier oscillator modulation index



Thus, the conclusion to be drawn from this data is that for a single DCP signal input, a modulation index of at least 0.5 is required. The analysis presented thus far cannot be extended directly to cover the multicarrier signal condition. However, the effect of the downlink for this situation can be ascertained as follows. Let us describe the input to the modulator as a random process of known total power and not attempt to identify the DCP signals individually and the uplink noise within the composite spectrum. As far as the downlink is concerned, this is the desired "signal" and we need only concern ourselves with the effect of the added downlink noise on the fidelity of transmission. Our goal is to show that by a proper choice of peak frequency deviation, the downlink noise will be small enough in relation to the signal portion of the discriminator output so it may be neglected without significant error. We use as our starting point equation (5-7), and define the overall SNR ratio at the discriminator output as

$$\text{SNR} \triangleq \frac{(2\pi\Delta F)^2 E[V^2(t)]}{\left(\frac{1}{BL}\right)^2 E\left[\frac{d}{dt}\sqrt{Z}x(t)\right]^2} \quad (5-18)$$

Values for  $E[V^2(t)]$  and

$$E\left[\frac{d}{dt}\sqrt{Z}x(t)\right]^2$$

were established for the DCS earlier (see (5-13) and (5-14)). Performing the indicated operations yields

$$\text{SNR} = \frac{3}{2} \frac{\Delta F^2 \left(\frac{C}{N}\right) B_D}{\left[F_\mu^3 - F_L^3\right]} \approx \frac{3}{2} \left(\frac{\Delta F}{F_\mu}\right)^2 \frac{C}{N} \left(\frac{B_D}{F_\mu}\right) \quad (5-19)$$

where  $F_\mu$  denotes the upper and  $F_L$  the lower discriminator output band edge.

Substituting data from Table 5-1 yields

$$\text{SNR (in db)} \approx 16.4 + 10 \log_{10} \left(\frac{\Delta F}{F_u}\right)^2$$

From the same table, we have  $F_u = 137.5$  kHz. If we choose the frequency deviation  $\Delta F$  to be 125 kHz or a modulation index of 1.0, we find that the downlink noise is a factor of 40 below the signal at the discriminator output and hence can be neglected. This modulation index also relates conveniently to the above case for a single DCP signal input. An additional increase in the modulation index can reduce the significance of the downlink noise on the overall DCS performance. However, the increase in frequency deviation results in bandwidth widening and consequent overlap of the signal into adjacent signal bands carrying other non-DCS services, causing undesirable crosstalk of the S-band downlink signals. Hence a modulation index of 1.0 appears a satisfactory compromise.

The foregoing analysis has been based on calculating the total signal and noise power ratios in the band. It ignores the distribution of noise in the band. The actual noise spectrum is shown in Figure 5-4. The noise due to the uplink is uniform across the band, but that incurred in the downlink due to the discriminator action is not uniform, and is a square law function of frequency, referred to as  $f^2$  noise. When we assume that the signal tones occur uniformly across the signal band, the results cited above hold for the average SNR. The deviation of the true noise from the average value determines how good an assumption it was to ignore the downlink noise term (with the  $f^2$  shape). Taking the  $f^2$  noise and uniformly distributing it between  $f_1$  and  $f_w$ , we find that 71 percent of the  $f^2$  noise is below the crossover point and 29 percent is above. The worst

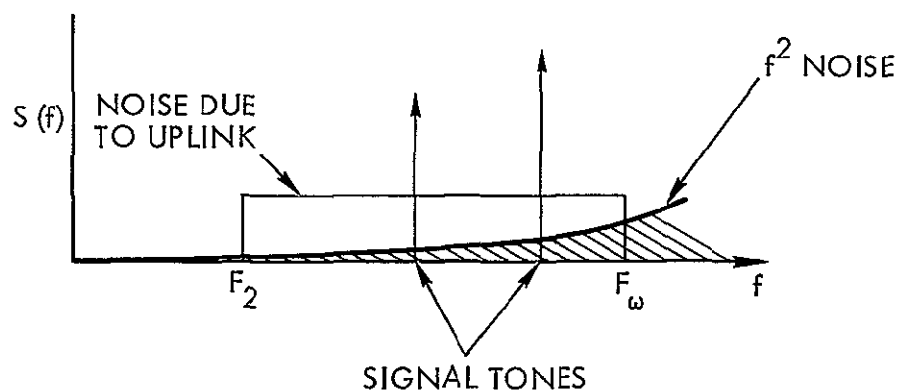


Figure 5-4  
NOISE SPECTRUM FOR DOWNLINK DISCRIMINATOR

case is, of course, for a signal at the upper frequency band edge, where the  $f^2$  noise power is 4.8 db above its equivalent uniform noise. Our calculations show that even for this case, the downlink noise is over an order of magnitude less than the uplink noise, and consequently can be ignored in making first order approximations of the overall performance. On this basis, we conclude that we need concern ourselves only with the uplink noise.

## 5.4 LIMITER PERFORMANCE ANALYSIS

### 5.4.1 Approach

This section analyzes the signal suppression due to two, three, or four signals passed through an ideal bandpass limiter in the spacecraft receiver. For the case of two signals, the results of J. J. Jones\* are used. The magnitude of the limiter output products are established for the four-signal case and degenerated for the three-signal case. Sample signal combinations are analyzed and the results are discussed.

The bandpass limiter considered in this section consists of an ideal hard limiter followed by a zonal filter. The characteristics of the limiter are given as

$$y(t) = \begin{cases} +1 & x(t) > 0 \\ -1 & x(t) < 0 \end{cases} \quad (5-20)$$

where

$x(t)$  = input signal to the limiter

$$= \sum_{i=1}^N S_i(t) + N(t) \quad (5-21)$$

$y(t)$  = output signal from the limiter

$$= S_o(t) + N_l(t) \quad (5-22)$$

---

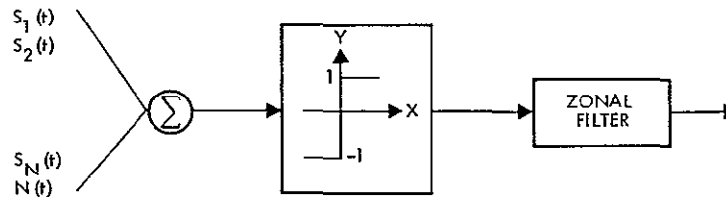
\* J. J. Jones, "Hard-Limiting of Two Signals in Random Noise," IEEE Trans Infor Theory, January 1963

$S_1(t) = 1^{\text{th}}$  input tone

$N(t) =$  input thermal noise

$S_o(t) =$  fundamental and crosstalk output

$N_o(t) =$  output thermal noise



Since we are concerned with total power, the  $N$  signals can be represented by  $N$  tones with the power in the tone equal to the signal power. J. L. Sevy has shown\* that although the autocorrelation and spectral density functions for the CW signal and angle-modulated signal differ in appearance, if a wide enough bandpass filter follows the limiter, the average signal and noise powers will be equal. Thus, for a bandpass limiter, the output SNR and input SNR for an angle modulated signal will be the same as for a CW signal.

The amplitude of the output signal from the limiter is (for four input tones) given by\*\*

$$h_{m_1 m_2 m_3 m_4} = \frac{(-1)^{(m_1 + m_2 + m_3 + m_4 - 1)/2}}{\pi} \int_{-\infty}^{\infty} \frac{J_{m_1}(A_1 X) J_{m_2}(A_2 X) J_{m_3}(A_3 X) J_{m_4}(A_4 X)}{X} \cdot \exp \left[ \frac{-\sigma^2 X^2}{2} \right] dX$$

\* J. L. Sevy "The Effect of Hard Limiting on Single-Modulated Signal Plus Noise," IEEE Trans Aer. Elec Sys, Jan 1968

\*\* W. B. Davenport, Jr and W. L. Root, An Introduction to the Theory of Random Signals and Noise, McGraw-Hill, New York, 1958

where

$A_1$  = amplitude of 1<sup>th</sup> signal

$m_1$  = integer multipliers which determine the specific inter-modulation product

$$\pm m_1 \omega_1 \pm m_2 \omega_2 \pm m_3 \omega_3 \pm m_4 \omega_4$$

$\sigma^2$  = noise power

Let  $x = Z/\sigma$ ,

$$C_1 = \frac{(-1)^{(m_1 + m_2 + m_3 + m_4 - 1)/2}}{\pi}$$

Then

$$h_{m_1 m_2 m_3 m_4} = C_1 \int_{-\infty}^{\infty} J_{m_1} \left( \frac{A_1}{\sigma} Z \right) J_{m_2} \left( \frac{A_2}{\sigma} Z \right) J_{m_3} \left( \frac{A_3}{\sigma} Z \right) J_{m_4} \left( \frac{A_4}{\sigma} Z \right) \exp \left[ -\frac{Z^2}{2} \right] \frac{dZ}{Z} \quad (5-24)$$

Since  $J_m(x)$  is an odd function if  $m$  is odd and an even function if  $m$  is even

$$|m_1| + |m_2| + |m_3| + |m_4| = \text{odd}$$

in order to produce a non-zero result Therefore

$$(-1)^{(m_1 + m_2 + m_3 + m_4 - 1)/2} = 1$$

and

$$C_1 = \frac{1}{\pi}$$

The magnitude of any term is given by\*

$$\text{MAG}_{m_1 m_2 m_3 m_4} = 2h_{m_1 m_2 m_3 m_4}^2$$

---

\*P. D. Shaft, "Limiting of Several Signals and Its Effect on Communication System Performance," IEEE Trans. Com. Tech, Dec 1966

$$\text{MAG}_{m_1 m_2 m_3 m_4} = \frac{8}{\pi^2} \left\{ \int_0^{\infty} J_{m_1} \left( \frac{A_1}{\sigma} Z \right) J_{m_2} \left( \frac{A_2}{\sigma} Z \right) J_{m_3} \left( \frac{A_3}{\sigma} Z \right) \cdot J_{m_4} \left( \frac{A_4}{\sigma} Z \right) \exp \left[ -\frac{Z^2}{2} \right] \frac{dZ}{Z} \right\}^2 \quad (5-25)$$

The signal power for the 1<sup>th</sup> signal is

$$S_1 = \frac{A_1^2}{2}$$

and the noise power =  $\sigma^2$  so that

$$(\text{SNR})_1 = \frac{A_1^2}{2\sigma^2} \quad (5-26)$$

Substituting into (5-25)

$$\begin{aligned} \text{MAG}_{m_1 m_2 m_3 m_4} &= \frac{8}{\pi^2} \left\{ \int_0^{\infty} J_{m_1} (\sqrt{2 \text{SNR}_1} Z) J_{m_2} (\sqrt{2 \text{SNR}_2} Z) \right. \\ &\quad \cdot J_{m_3} (\sqrt{2 \text{SNR}_3} Z) J_{m_4} (\sqrt{2 \text{SNR}_4} Z) \\ &\quad \left. \cdot \exp [-Z^2/2] \frac{dZ}{Z} \right\}^2 \quad (5-27) \\ |m_1| + |m_2| + |m_3| + |m_4| &= \text{odd} \end{aligned}$$

The limiter output is a square wave of unit magnitude. When followed by a zonal filter around the first zone, the total output power in the zone is  $8/\pi^2$ . Thus, MAG can be normalized by dividing it by  $8/\pi^2$ .

For three signals, the magnitude can be obtained in an analogous manner from the relationship

$$\text{MAG}_{m_1 m_2 m_3} = \frac{8}{\pi^2} \left\{ \int_0^{\infty} J_{m_1}(\sqrt{2 \text{SNR}_1} Z) J_{m_2}(\sqrt{2 \text{SNR}_2} Z) J_{m_3}(\sqrt{2 \text{SNR}_3} Z) \exp \left[ -\frac{Z^2}{2} \right] \frac{dZ}{Z} \right\}^2 \quad (5-28)$$

$$|m_1| + |m_2| + |m_3| = \text{odd}$$

To determine the output noise power, it must be remembered that the total power out of a bandpass limiter is a constant equal to  $8/\pi^2$ . If the desired signal is one of the fundamental components, the noise includes the thermal noise and all intermodulation products. Thus, the output noise power is given by

$$N = \frac{8}{\pi^2} - \sum S_j(t) \quad (5-29)$$

where

$S_j(t)$  = The output power of the  $j^{\text{th}}$  signal

From Section 4.2, the maximum input SNR at the limiter in a 125 kHz bandwidth is 9.6 db. From Table 4-4, the largest difference between the smallest signal and the largest signal is 7.0 db. Thus, the minimum input SNR at the limiter is 2.6 db.

The amplitude of various cross-product terms was investigated for the case of four signals with equal input SNR's of 9.6 db. It was found that the largest cross-product term was 13.1 db below the output signal amplitude. The next largest IM term was 20.3 db below the signal. Since the amplitude of IM terms decreases rapidly for decreasing SNR, and the probability of one of the IM products falling within the 3 kHz filter bandwidth is small, it can be concluded that the intermodulation terms are negligible.

#### 5.4.2 Results

Using the curves of Figure 5-5, the output SNR can be found. Two cases are considered here, and the results are shown in Table 5-2. The first case considers the two largest signals into the limiter, while the second considers the two smallest signals into the limiter.

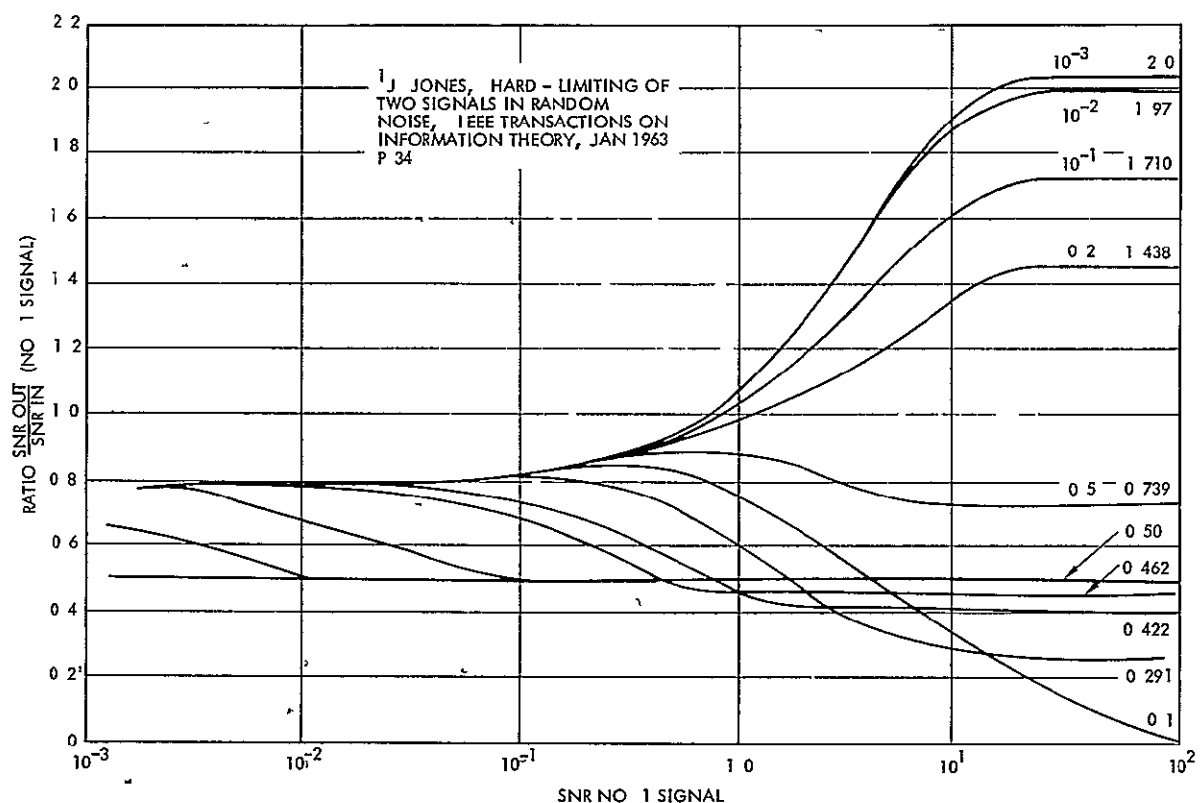


Figure 5-5

RATIO OF THE OUTPUT SNR TO THE INPUT SNR as a function of the latter for the ideal bandpass limiter. Each curve is a ratio of signal No. 1 to signal No. 2.

Table 5-2 Limiter Performance for Two DLP Signals as Input

	SNR <sub>1</sub> (db) BW = 125 kHz	SNR <sub>L</sub> (db) BW = 125 kHz	SNR <sub>L</sub> (db) BW = 2.4 kHz
Case 1	9.6	5.0	22.2
	9.6	5.0	22.2
Case 2	2.6	1.1	18.3
	2.6	1.1	18.3

As can be seen from Table 5-2, the worst case of two weak signals is still 7.2 db above the minimum system requirement of 11.1 db.



### 5 4 3 Computer Results and Discussion

The three and four-signal cases were analyzed by the use of the computer program described in Section 5 4.4. Various input SNR combinations were chosen to illustrate worst case situations. Although the particular situations occur with a low probability, they provide data that set lower bounds to system performance. Three and four-signal sets of equal SNR corresponding to the largest (9.6, 9.6, 9.6, (9.6) dB) and smallest (2.6, 2.6, 2.6, (2.6) dB) values were selected. Each calculation also used a set ((9.6, 8.6, 7.6, 6.6) dB) equal to a cumulative probability of occurrence equal to one sigma. In addition, a calculation was made that included an RFI signal of 19.6 dB along with the system signals of (2.6, 2.6, 2.6 dB) and (9.6, 9.6 dB). Various other cases are shown which include the worst case bounds.

The results are shown in Tables 5-3 and 5-4. As can be seen for the three-signal case, all combinations meet the minimum system requirement of 11.1 dB except for the case of two signals and RFI. It is apparent that the stronger signal will suppress the weaker signal, but the system can still operate above the minimum requirement.

For the case of four signals, once again the RFI signal severely suppresses the desired signal. Also three large signals (9.6 dB) suppress a weak signal (2.6 dB) 2.8 dB below the minimum system requirement of 11.1 dB. For the case of four signals with input SNR's equally spaced between 9.6 dB and 2.6 dB, the weak signal is suppressed 0.3 dB below the required 11.1 dB. The results of all other cases are above the minimum level.

As shown in Section 5 3, the downlink does not contribute any significant degradation to the system. Thus, the output SNR of the limiter determines the system performance

To determine the suppression effect between one RFI signal and three desired signals, the SNR of the RFI signal was increased in 1 db intervals from 9.6 db to 19.6 db. The SNR of the desired signals was chosen to be 2.6 db which is the minimum desired signal SNR, thus causing a worst case situation. The results are shown in Table 5-5. From

the results it can be seen that a single RFI signal which has a SNR  $\geq 11.6$  db at the limiter input will not result in a degradation of the desired signals below the minimum system output SNR of 11.1 db. Under normal conditions, the input SNR's of the desired signals will be larger and the RFI signal will not have as strong of a suppression effect on the desired signals.

Table 5-3. Input and Output S/N for Three Signals Through an Ideal Bandpass Limiter. Shading indicates unacceptably degraded SNR.

	SNR <sub>i</sub> (dB) BW = 125 kHz	SNR <sub>L</sub> (dB) BW = 125 kHz	SNR <sub>L</sub> (dB) BW = 2.4 kHz
Case One	2.6	0.17	17.37
	2.6	0.17	17.37
	2.6	0.17	17.37
Case Two	9.6	1.35	18.55
	9.6	1.35	18.55
	2.6	-4.58	12.62
Case Three	2.6	-3.52	13.68
	2.6	-3.52	13.68
	9.6	6.93	24.13
Case Four	9.6	-0.34	16.86
	9.6	-0.34	16.86
	9.6	-0.34	16.86
Case Five	9.6	1.07	18.27
	8.7	-0.13	17.07
	7.6	-1.15	16.05
Case Six	19.6	2.68	19.88
	9.6	-14.9	2.30
	9.6	-14.9	2.30



Table 5-4. Input and Output S/N for Four Signals Through an Ideal Bandpass Limiter. Shading indicates unacceptably degraded SNR.

	SNR <sub>i</sub> (dB) BW = 125 kHz	SNR <sub>L</sub> (dB) BW = 125 kHz	SNR <sub>L</sub> (dB) BW = 2.4 kHz
Case One	9.6	-2.5	14.5
	9.6	-2.5	14.5
	9.6	-2.5	14.5
	9.6	-2.5	14.5
Case Two	2.6	-1.14	16.06
	2.6	-1.14	16.06
	2.6	-1.14	16.06
	2.6	-1.14	16.06
Case Three	9.6	1.79	18.99
	7.6	-0.97	16.23
	5.6	-3.04	14.16
	2.6	-6.40	10.80
Case Four	9.6	-0.91	16.29
	9.6	-0.91	16.29
	9.6	-0.91	16.29
	2.6	-8.96	8.24
Case Five	9.6	5.14	22.34
	2.6	-4.32	12.88
	2.6	-4.32	12.88
	2.6	-4.32	12.88
Case Six	19.6	3.94	21.14
	2.6	-21.0	-3.8
	2.6	-21.0	-3.8
	2.6	-21.0	-3.8
Case Seven	9.8	-0.24	16.96
	8.6	-1.55	15.65
	7.6	-2.76	14.44
	6.6	-3.98	13.22



Table 5-5. Input and Output S/N for Four Signals Through an Ideal Bandpass Limiter: One RFI Signal and Three Desired Signals. Shading indicates unacceptably degraded SNR.

	SNR <sub>i</sub> (dB) BW = 125 kHz	SNR <sub>L</sub> (dB) BW = 125 kHz	SNR <sub>L</sub> (dB) BW = 2.4 kHz
Case One	2.6	-4.51	12.69
	2.6	-4.51	12.69
	2.6	-4.51	12.69
	9.6	4.93	22.13
Case Two	2.6	-5.2	12.0
	2.6	-5.2	12.0
	2.6	-5.2	12.0
	10.6	5.95	23.15
Case Three	2.6	-6.13	11.07
	2.6	-6.13	11.07
	2.6	-6.13	11.07
	11.6	6.7	23.90
Case Four	2.6	-7.6	9.6
	2.6	-7.6	9.6
	2.6	-7.6	9.6
	12.6	7.16	24.36
Case Five	2.6	-8.93	8.27
	2.6	-8.93	8.27
	2.6	-8.93	8.27
	13.6	7.45	24.65
Case Six	2.6	-10.9	6.3
	2.6	-10.9	6.3
	2.6	-10.9	6.3
	14.6	7.29	24.49
Case Seven	2.6	-12.8	4.4
	2.6	-12.8	4.4
	2.6	-12.8	4.4
	15.6	6.9	24.1



Table 5-5. Input and Output S/N for Four Signals Through an Ideal Bandpass Limiter: One RFI Signal and Three Desired Signals (Continued)

	SNR <sub>i</sub> (dB) BW = 125 kHz	SNR <sub>L</sub> (dB) BW = 125 kHz	SNR <sub>L</sub> (dB) BW = 2.4 kHz
Case Eight	2.6	-14.8	2.4
	2.6	-14.8	2.4
	2.6	-14.8	2.4
	16.6	6.31	23.51
Case Nine	2.6	-16.35	0.85
	2.6	-16.35	0.85
	2.6	-16.35	0.85
	17.6	5.6	22.8
Case Ten	2.6	-20.1	-2.9
	2.6	-20.1	-2.9
	2.6	-20.1	-2.9
	18.6	4.73	21.93
Case Eleven	2.6	-21.0	-3.8
	2.6	-21.0	-3.8
	2.6	-21.0	-3.8
	19.6	3.94	21.14

#### 5.4.4 Description of Computer Program

Using a CDC 6400, our computer program solves the equation

$$\begin{aligned}
 \text{MAG}_{m_1 m_2 m_3 m_4} &= \int_0^{\infty} J_{m_1}(\sqrt{2 \text{SNR}_1} Z) J_{m_2}(\sqrt{2 \text{SNR}_2} Z) \\
 &\quad J_{m_3}(\sqrt{2 \text{SNR}_3} Z) J_{m_4}(\sqrt{2 \text{SNR}_4} Z) \\
 &\quad \cdot \exp \frac{-Z^2}{2} \frac{dZ}{Z}
 \end{aligned}$$

The inputs consist of SNR<sub>1</sub>, SNR<sub>2</sub>, SNR<sub>3</sub>, SNR<sub>4</sub>, M<sub>1</sub>, M<sub>2</sub>, M<sub>3</sub>, M<sub>4</sub>. The output is SNR<sub>1</sub>, SNR<sub>2</sub>, SNR<sub>3</sub>, SNR<sub>4</sub>, all of which are in db, M<sub>1</sub>, M<sub>2</sub>, M<sub>3</sub>, M<sub>4</sub>, and MAG<sub>m<sub>1</sub>m<sub>2</sub>m<sub>3</sub>m<sub>4</sub></sub>.

The program generates the integrand using a function subroutine which calculates  $J_0(x)$ ,  $J_1(x)$ , or  $J_2(x)$ . To numerically integrate the integrand over the range  $(0, \infty)$ , the second degree Simpson's rule formula was used. Basically, it is

$$\int_{X_0}^{X_n} f(x) dx = \frac{h}{3} [y_0 + y_n + 4(y_1 + y_3 + \dots + y_{n-1}) + 2(y_2 + y_4 + \dots + y_{n-2})]$$

where

$h$  = interval spacing between the  $X_i$ 's

$y_i = f(X_i)$

Geometrically, it gives the value of the sum of areas under the second-degree parabolas that have been passed through points  $(X_{2i}, y_{2i})$ ,  $(X_{2i+1}, y_{2i+1})$ , and  $(X_{2i+2}, y_{2i+2})$  where  $i = 0, 1, 2, \dots, (n-2)/2$ . The interval of numerical integration was chosen to be  $(0, 30)$  since  $\exp(-30/2) \approx 0$  and this bounds the integral. The number of points chosen was 301 with a spacing factor  $h = 0.1$ .

The function subroutine which generates the Bessel functions is based on the polynomial approximations for  $J_0(x)$  and  $J_1(x)$  in the Handbook of Mathematical Functions by Abramowitz and Stegun. The Bessel functions generated by these polynomials are accurate to within  $10^{-8}$ .

RUN 2.3I 03/13/70

PROGRAM IM (INPUT,OUTPUT)

```

000003      DIMENSION Y(305)
000003      REAL MAG
000003      40 READ 42,SNR1,SNR2,SNR3,SNR4 ← Input the four S/N ratios
000017      42 FORMAT(4F7.2)
000017      50 READ 52,M1,M2,M3,M4,JK ← Input the four indices
000035      52 FORMAT(5I1)
000035      Y(1)=0.
000036      DO 100 I=1,300
000040      Z=I/10.
000042      X=Z*SQR(2.*SNR1)*$N =M1 } Jm1(√2 SNR1 Z)
000051      BES1=WW(N,X)
000053      X=Z*SQR(2.*SNR2)*$N =M2 } Jm2(√2 SNR2 Z)
000062      BES2=WW(N,X)
000064      X=Z*SQR(2.*SNR3)*$N =M3 } Jm3(√2 SNR3 Z)
000073      BES3=WW(N,X)
000075      X=Z*SQR(2.*SNR4)*$N =M4 } Jm4(√2 SNR4 Z)
000104      BES4=WW(N,X)
000106      RECP=1./Z
000110      EXPZ=EXP(-(Z**2)/2.)
000115      Y(I+1)=BES1*BES2*BES3*BES4*RECP*EXPZ Jm1(√2 SNR1 Z)Jm2(√2 SNR2 Z)Jm3(√2 SNR3 Z)Jm4(√2 SNR4 Z)
000124      100 CONTINUE
000126      SUM=C.
000127      DO 200 K=2,300,2
000130      SUM=SUM+Y(K)
000132      200 CONTINUE
000134      TOTAL=0.
000135      DO 300 J=3,299,2
000137      TOTAL=TOTAL+Y(J)
000141      300 CONTINUE
000143      H=(4.*SUM+2.*TOTAL+Y(1)+Y(301))*0.1/3. — hm1m2m3m4
000151      MAG=H — Magnitude of output signal component
000152      S1=1C.*ALOG10(SNR1)
000155      S2=1C.*ALOG10(SNR2)
000160      S3=1C.*ALOG10(SNR3)
000163      S4=1C.*ALOG10(SNR4)
000167      PRINT 500,S1,S2,S3,S4,M1,M2,M3,M4,MAG Output
000214      500 FORMAT(4(2X,F6.1),4(2X,I2),4X,E15.8)
000214      IF(JK.EQ.1) GO TO 50
000216      IF(JK.EQ.2) GO TO 40
000220      RETURN
000222      END

```

RUN 2.3I 03/13/70

	REAL FUNCTION WW(N,X)	Generates $J_0(x)$ , $J_1(x)$ , $J_2(x)$ according to the polynomial approximations in "Handbook of Mathematical Functions" by Abramowitz and Stegun
000005	REAL J0,J1,J2	
000005	IF(X.GT.3) GO TO 40	
000011	IF (N.EQ.0) GO TO 5	
000011	IF (N.EQ.1) GO TO 20	
000013	IF (N.EQ.2) GO TO 5	
000015	5 J0=1.-2.2499997*(X/3)**2+1.2656208*(X/3)**4-.3163866*(X/3)**6+	
	1.0444479*(X/3)**8-.0039444*(X/3)**10+.00021*(X/3)**12	
000047	WW=J0	
000051	IF(N.EQ.0) GO TO 90	
000052	20 J1=X*(.5-.56249985*(X/3)**2+.21093573*(X/3)**4-.03954289*(X/3)**6	
	1+.00443319*(X/3)**8-.00031761*(X/3)**10+.00001109*(X/3)**12)	
000105	WW=J1	
000106	IF(N.EQ.1) GO TO 90	
000111	J2=J1*2./X-J0	
000114	WW=J2	
000116	GO TO 90	
000116	40 IF (N.EQ.0) GO TO 45	
000117	IF (N.EQ.1) GO TO 60	
000121	IF (N.EQ.2) GO TO 45	
000123	45 F0=.79788456-.00000077*(3/X)-.0055274*(3/X)**2-.00009512*(3/X)**3	
	1+.00137237*(3/X)**4-.00072805*(3/X)**5+.00014476*(3/X)**6	
000152	THET0=X-.78539816-.04166397*(3/X)-.00003954*(3/X)**2+.00262573*	
	1(3/X)**3-.00054125*(3/X)**4-.00029333*(3/X)**5+.00013558*(3/X)**6	
000202	J0=FC*COS(THET0)/SQRT(X)	
000213	WW=J0	
000215	IF (N.EQ.0) GO TO 90	
000216	60 F1=.79788456+.00000156*(3/X)+.01659667*(3/X)**2+.00017105*(3/X)*	
	1*3-.00249511*(3/X)**4+.00113653*(3/X)**5-.00020033*(3/X)**6	
000245	THET1=X-2.35619449+.12499612*(3/X)+.0000565*(3/X)**2-.00637879*(	
	13/X)**3+.00074348*(3/X)**4+.00079824*(3/X)**5-.00029166*(3/X)**6	
000275	J1=F1*COS(THET1)/SQRT(X)	
000306	WW=J1	
000310	IF (N.EQ.1) GO TO 90	
000312	J2=J1*2/X-J0	
000315	WW=J2	
000317	90 CONTINUE	
000317	RETURN	
000321	END	



## 6 PERFORMANCE UNDER EXTREME TEMPERATURE CONDITIONS

### 6 1 HIGH TEMPERATURE OPERATION

The type of battery proposed by TRW for the data collection platform is a calcium lead acid storage unit. In the previous Volume 5 we listed the 15-day self discharge rates for such a battery operating at 77°F (25°C) and 92°F (33°C). The actual degradation represents the fraction of stored energy lost due to internal circulating currents. These result in resistive heating and actual dissipation of energy. This situation is quite different at low temperatures, where the greatly increased internal resistance limits the rate of energy withdrawal, but does not result in energy loss.

The latest data indicates that the percent capacity loss per month due to self discharge are as follows:

Temperature	Percent Loss
77°F	1.5
95°F	3.0
113°F	6.0
131°F	12.0

Thus the total available capacity ( $C_a$ ) at the end of an  $n$  month period is given by

$$C_a = (1 - k)^n$$

where  $k$  is the percent loss per month. The levels of capacity available for four representative elevated temperatures over use spans of six and nine months are presented in Figure 6-1 and as follows:

Period of Use	Temperature (°F)			
	77	95	113	131
6 months	91.3%	83.3%	69%	46.4%
9 months	87.3%	76%	57.3%	31.6%

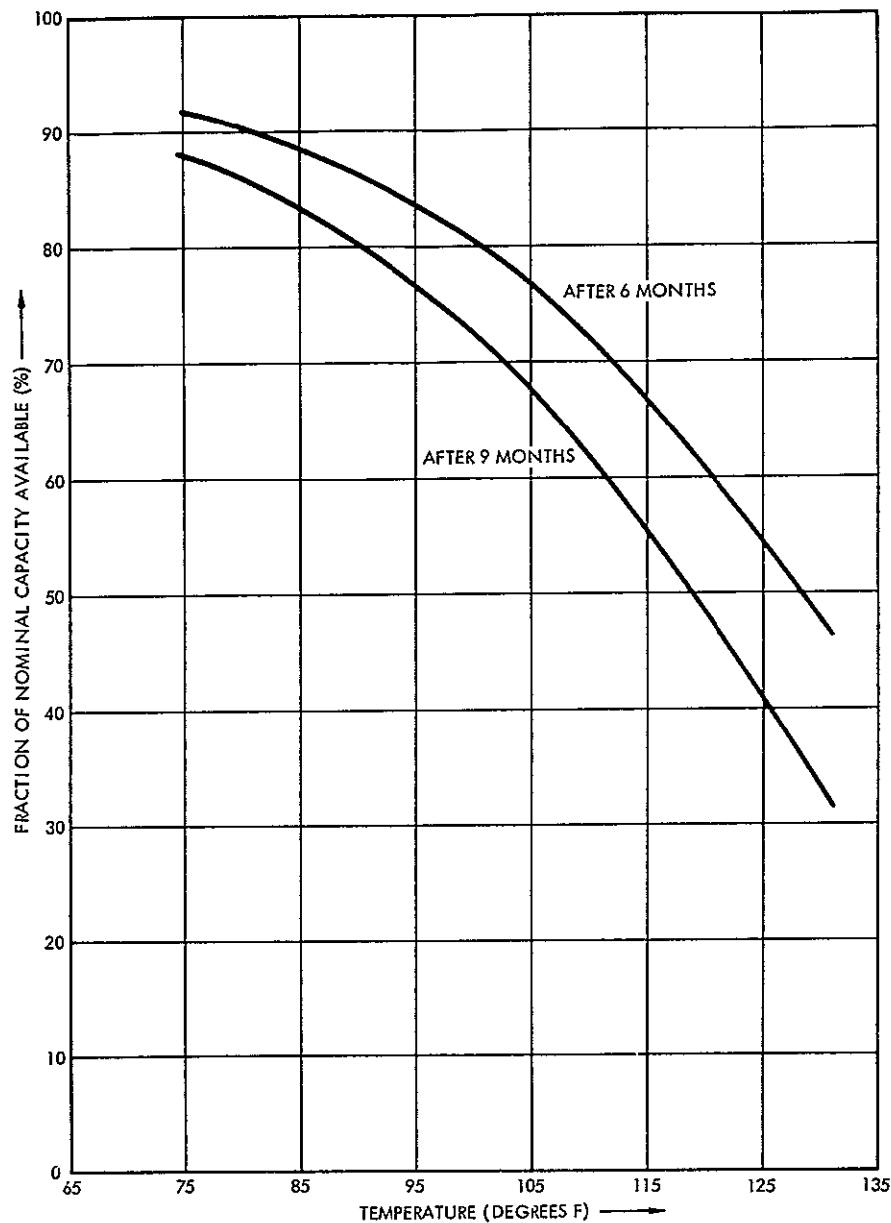


Figure 6-1

LEVELS OF BATTERY CAPACITY available for representative elevated temperatures over use spans of 6 and 9 months

The magnitude of allowance necessary at any location depends on the particular high temperature profile expected at that site. Although burial of the battery is primarily attractive for alleviating the large increase in internal resistance at low temperatures, it is also helpful in limiting the upper temperature excursion and holding down the self discharge effect.

## 6 2 LOW TEMPERATURE OPERATION

The performance of any conventional battery can be extended by the use of a suitable combination of electrical heating and thermal insulation. Insulation materials have a very low value of thermal conductivity and thus drastically reduce the heat flow between the battery and external environment. The actual heat energy lost must be supplied by a resistive heating element which uses a portion of the battery chemical energy. The art, in designing such a system involves balancing the conflicting factors of

- Insulation thickness
- Heater power
- Stabilized battery temperature

The limitations on increasing the insulation thickness involve avoiding excessive size, weight, cost and assembly difficulty. Heater power is parasitic. The smaller the heater used the smaller fraction of the battery capacity that needs to be allocated to thermal control and lower the battery cost.

As stated, the lower the battery temperature the higher its internal resistance. The internal resistance increases exponentially near the electrolyte freezing temperature. The colder we can operate the battery the smaller the temperature differential across the insulation and the lower the heat flow. Freezing of the electrolyte forms a lower bound to cold temperature operation. Figure 6-2 shows the internal resistance of the selected lead-calcium acid cell versus temperature for the cold region.

The freezing temperature is a function of the specific gravity of the electrolyte. A typical value of  $+15^{\circ}\text{C}$  specific gravity is 1.2, for which the freezing temperature is  $-27^{\circ}\text{C}$ . As the battery discharges, the specific gravity falls and with it the corresponding freezing temperature.

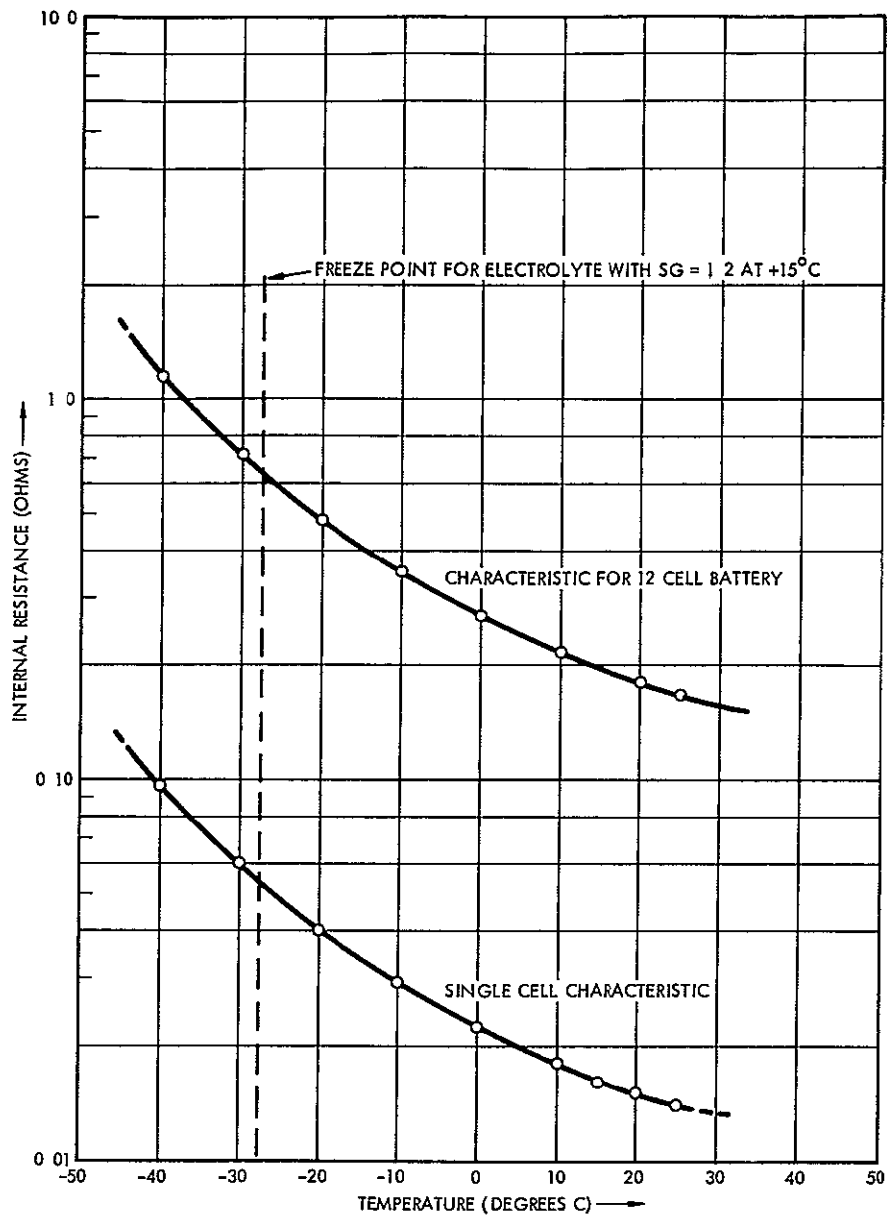


Figure 6-2

INTERNAL RESISTANCE VS TEMPERATURE FOR CALCIUM-LEAD  
ACID BATTERY TYPE 3AC-10 BATTERY

The relationship between the  $+15^{\circ}\text{C}$  value of SG and freeze point is shown in Figure 6-3

By employing a battery of appreciably larger capacity than is required for the electrical load energy storage, we can prevent deep discharge of the battery and ensure an acceptable value for the "end of use" specific gravity.

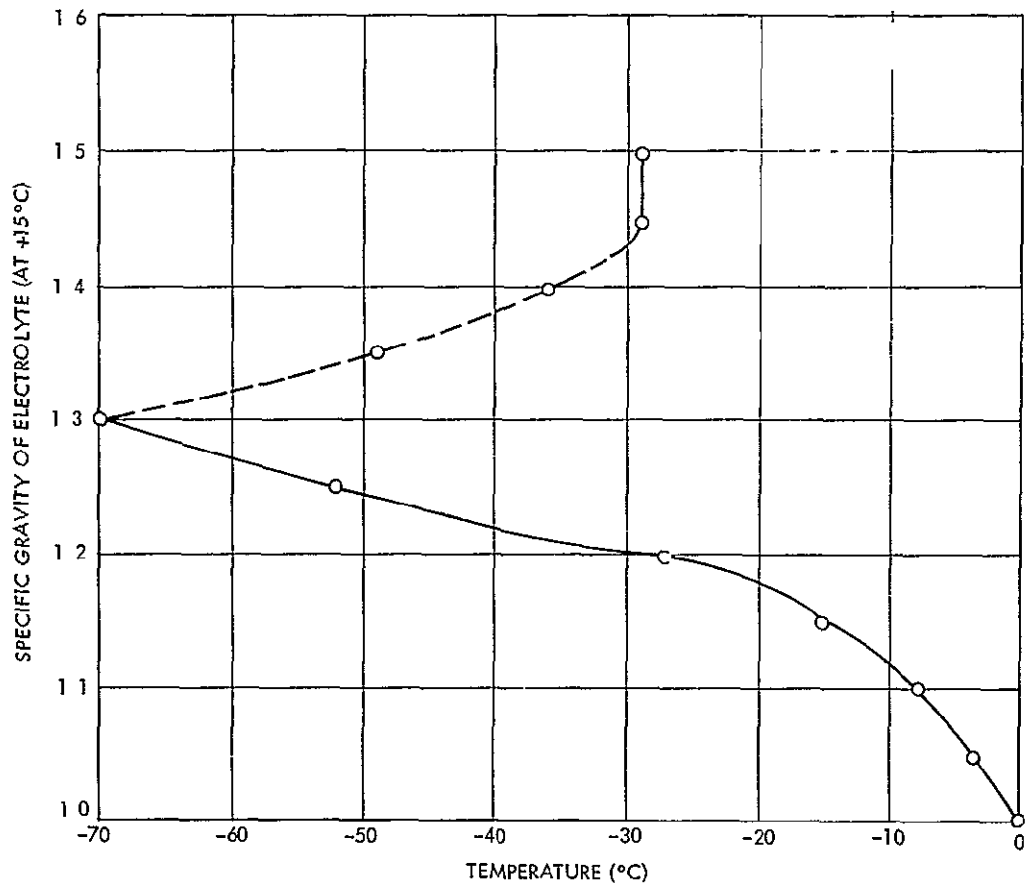


Figure 6-3

ELECTROLYTE FREEZING TEMPERATURES VS SPECIFIC GRAVITY  
(MEASURED AT +15°C) FOR SULPHURIC ACID AND WATER MIXTURE

The freeze temperature can also be raised by increasing the basic specific gravity of the electrolyte mixture by the simple expedient of increasing the acid to water ratio. Unfortunately, this increases the high temperature self-discharge so the technique is only relevant to DCP locations where the temperatures are always very low to moderate. This is not a valid assumption even in Canada, but might be relevant for DCPS in high elevation mountain sites.

When such a battery supplies the only DCP electronics load of  $\approx 0.7$  amperes peak, the voltage drop due to this self-resistance down to a temperature of  $-30^{\circ}\text{C}$  is only 2% ( $\approx 0.5$  volts). Even with very poor

thermal insulation ( $\approx 1$  inch) the continuous heater demand would not exceed about 0.5 amperes, thus the DCP electronics peak demand is the major factor to be considered in determining the maximum value of self-resistance permissible.

Of the available thermal insulation materials, the most promising for this application is a closed cell plastic foam manufactured by the CPR division of Upjohn, and designated as type 9005-2. The salient details of this foam, which is sold in board form, are as follows:

Thermal conductivity	0.11 Btu/sq ft/hour/deg F/inch thick
Density	2 lbs/cu ft
Approximate cost	\$0.19/board foot (12" wide, 1" thick)
Range of thickness available	0.25 to 5 inches

For a preliminary appraisal of the possibilities of this material, we considered the situation for a single battery assembly capable of operating the DCP electronics only, but including an ample safety margin. Such a battery was featured in the TRW proposal. The example used was the C and D Battery Corporation, Type 3 AC-10, comprising a cell assembly of AC-10 size units (see Figure 6-4). The overall size of this unit is 12" long x 7" wide x 7-3/4" high.

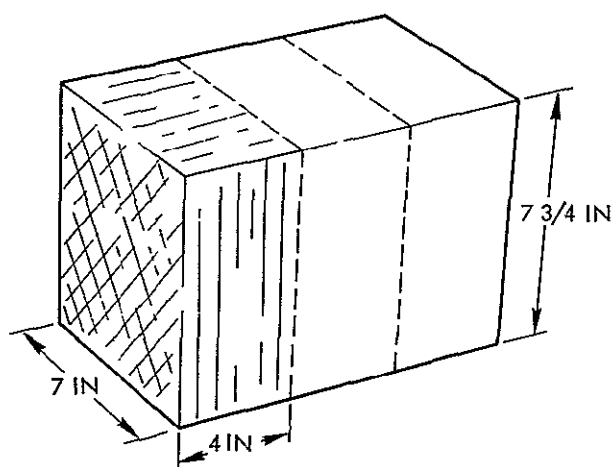


Figure 6-4

#### CONFIGURATION OF BASIC 3 CELL BATTERY

We assume an external temperature of  $-70^{\circ}\text{F}$  and a lower limit battery temperature of  $-15^{\circ}\text{F}$  ( $\approx -25^{\circ}\text{C}$ ), i.e. a temperature differential of  $55^{\circ}\text{F}$ . The total surface area (A) of the battery unit is

$$\begin{aligned} A &= 2(12 \times 7\text{-}3/4) + 2(7 \times 7\text{-}3/4) + 2(7 \times 12) \\ &= 462 \text{ sq inches} \\ &= 3.2 \text{ sq feet} \end{aligned}$$

The heat transferred (H) through a thin continuous skin of the suggested foam insulant, enclosing a Type 3 AC-10 battery is

$$\begin{aligned} H &= 0.11 \times (70 - 15) \times 3.2 \\ &= 19.4 \text{ Btu/hour/inch of insulant} \end{aligned}$$

1 Btu = 0.3 watt hours, so we can rewrite the expression for heat lost in terms of electrical energy as

$$H = 19.4 \times 0.3$$

$$\text{i.e. } H = 5.81 \text{ watts/inch of insulant}$$

Assuming that the full voltage of the DCP battery is applied to the heater, the heating current demand will be simply  $5.81/24$  or  $0.242$  amperes

The total amp hour stored energy penalty (Eh) due to the use of electrical heating is simply nine months of operation, 6,750 hours, at the appropriate current

For  $0.242$  ampere current value, this amounts to

$$E(h) = \frac{0.242 \times 6.57 \times 10^3}{t} = \frac{1590}{t} \text{ amp hours}$$

where  $t$  = the insulation thickness in inches

It will be obvious that when the insulation layer thickness dimension approaches the magnitude of the linear dimensions of the battery, the surface area exposed to the outside environment becomes appreciably larger than that of the battery surfaces. Under these conditions, heat spreading occurs and the heat flow problem must be treated with differential equations exactly analogous to current flow in a conductive surface

For a quick look at the order of magnitudes involved, we simply extend the thin skin approach as follows

If 6 inches of foam were used all around the battery, the maximum heat energy required would be

$$E(h) \approx \frac{1590}{6} = 265 \text{ amp hours}$$

Since the estimated DCP electronics requirement is 55 amp hours, the addition of heating entails a 50% increase in battery capacity

The practical limitation on the amount of insulant is principally the inconvenience of excessive volume from the standpoint of transportation and field commissioning

A suggested upper bound for a single DCP, delivered by a rough terrain vehicle, is probably 300 cubic feet, or a finished battery module size of 6-1/2 x 7 x 6-1/2 feet. Such an arrangement would afford a minimum foam path length of 36 inches between battery and environment. This material can be very easily assembled into any desired shape from large 'building blocks' using the type PR4-18 type I cement and the process outlined in TRW Specification No. DWG 121176. A gross estimate for the related heater energy storage needs for this case is

$$E(h) = \frac{1590}{36} \approx 44 \text{ amp hours}$$

Since the existing battery has a nominal capacity of 10 amp hours, we can conjecture that five such batteries would probably allow satisfactory operation at -70°F. A more rigorous treatment of this problem is necessary but this simplified approach does give a good approximation.